PERFORMANCE EVALUATION OF STORM WATER TREATMENT CONTROLS AT AN INDUSTRIAL SITE

by

VIJAY KUMAR EPPAKAYALA

ROBERT E. PITT, COMMITTEE CHAIR

S. ROCKY DURRANS
ANDREW ERNEST
GLENN TOOTLE
SHIRLEY E. CLARK

A DISSERTATION

Submitted in partial fulfillment of the requirements
for the degree of Doctor of Philosophy
in the Department of Civil, Construction, and Environmental Engineering
in the Graduate School of
The University of Alabama

TUSCALOOSA, ALABAMA

2015

ABSTRACT

Discharges from industrial activities may contain various hazardous pollutants including metals, oils and grease, organic toxicants, chemical oxygen demand, nutrients and suspended sediment. Limited information is available on the characteristics of the pollutant constituents that affect treatment and treatment technologies that can effectively treat the runoff from industrial activities. Understanding the association of contaminants with different particle sizes is important for determining suitable treatment controls. The primary objective of this research was to evaluate the performance of treatment controls (a pre-treatment hydrodynamic separator device followed by a dry infiltration pond) at a heavy industrial site and describe the pollutant characteristics that affect stormwater treatability for different flow conditions.

Water quality monitoring through a seven month monitoring period showed that suspended sediment concentrations (SSC), COD, nutrients, and heavy metals were commonly found in the industrial runoff. Multivariate analyses were performed to identify the correlations between site hydrological and water quality parameters. The calculations showed strong correlations between hydrological parameters. Strong correlations were also observed between suspended sediment and metal concentrations. Treatment performance was evaluated based on the particle size distributions using several data exploratory methods. These showed that the hydrodynamic separator device had low to moderate reductions for SSC and low reductions for metals. The Hydrodynamic separator device also showed moderate reductions for particle sizes greater than 12 μm.

The dry infiltration pond showed very high removals for particulate solids concentrations and mass, medium to high removals for heavy metal concentrations and high removals for masses of the metals. Significant moderate to high reductions in concentration and mass were observed for particle sizes greater than 3μm. The dry pond also showed high runoff reductions (75 to 100%) for storm events smaller than 1.5 inches and associated high removals of pollutant masses for all constituents and moderate runoff reductions (about 50%) for events greater than 1.5 inches.

As part of this research, groundwater contamination potential was evaluated based on measured metal concentrations in the soil profile under the dry infiltration pond and by using a water chemistry vadose zone fate model. The results indicated high retention capacity of both particulate-bound and filtered metals in the surface soils in the pond. Vadose zone chemical fate modeling showed retention of metals to the soils at depths well above the water table. However, the increased runoff entering the pond greatly accelerates the pollutant migration in the subsurface, with metals potential reaching about a meter below the ground surface during a 50 year operational period. Other pollutants having greater mobility (such as nitrates) could reach the several meter deep water table quickly and, if present in problematic concentrations, result in potential groundwater contamination.

DEDICATION

To

My advisor Dr. Robert E. Pitt

My beloved parents Balaiah Eppakayala and Sujatha Dasari

LIST OF ABBREVIATIONS AND SYMBOLS

µg/L	Micrograms per Liter
µm	Micrometer
cm^2	square centimeter
cm/s	centimeters per second
g/cc	grams per cubic centimeter
in/hr	Inch per Hour
m/s	meters per second
mg/L	Milligrams per Liter
mg/kg	Milligrams per Kilogram
%	Percentage
<	Less Than
>	Greater Than
ANOVA	Analysis of Variance
ac	Acre
Al	Aluminum
As	Arsenic
ASTM	American Society for Testing and Materials
BDL	Below Detection Limit
BOD	Biochemical Oxygen Demand

C	Carbon
Ca	Calcium
Cd	Cadmium
CEC	Cation Exchange Capacity
cf	cubic-feet
cfs	cubic feet per second
COD	Chemical Oxygen Demand
COV	Coefficient of Variation
Cu	Copper
DL	Detection Limit
Eff	Effluent
Fe	Iron
f_o	Initial infiltration rate
f_c	Final (constant) infiltration rate
ft	Feet
ft^2	Square feet
ft^3	Cubic feet
HDD	Hydrodynamic Separator Device
hr	Hour
in	inch
Inf	Influent
K	Potassium
L	Liter

lbs	Pounds
LOD	Limit of Detection
MDL	Method Detection Limit
mg	milligram
Mg	Magnesium
Mn	Manganese
MPCA	Minnesota Pollution Control Agency
N	Nitrogen
NA	Not Available
n/a	not applicable
NH_3	Ammonia
Ni	Nickel
NO_3	Nitrate
NPDES	National Pollutant Discharge Elimination System
NRCS	Natural Resources Conservation Service
NSQD	National Stormwater Quality Database
OM	Organic Matter
PAHs	Polycyclic Aromatic Hydrocarbons
PCA	Principal Component Analyses
P	Phosphorous
Pb	Lead
PO_4	Phosphate
PSD	Particle Size Distribution

PSH	Penn State Harrisburg
sd	Standard Deviation
S	Sulfur
SESOIL	Seasonal Soil compartment model
SOR	Surface Overflow Rate
SS	Suspended Solids
SSC	Suspended Solids Concentration
SWPP	Stormwater Pollution Prevention Plan
TDS	Total Dissolved Solids
TN	Total Nitrogen
TP	Total Phosphorous
TSS	Total Suspended Solids
UA	The University of Alabama
US	United States
U.S. EPA	United States Environmental Protection Agency
Zn	Zinc

ACKNOWLEDGMENTS

I would like to thank my advisor and committee chairman Dr. Robert E. Pitt for his continuous guidance, advice, and support during this research.

I also would like to thank Dr. Shirley E. Clark, Dr. S. Rocky Durrans, Dr. Andrew Ernest, and Dr. Glenn Tootle for serving on my dissertation committee, for their advice suggestions, and comments.

I am grateful to Jejal Bathi and Alex Maestre for their help during the sampling and field visits. I am thankful to my fellow research mates Cai Yezhao, Leyla Talebi, and Redahegn Sileshi for their continuous encouragement.

I would like to thank my friends Kofi Adanu, Xiaoyin Zhang, Peng Wei, Philip Grammer, Majeed Abdulai, Abhishek Srivastava, Kuldeep Saxena and Anurag Chaturvedi for their support and encouragement.

Finally, I would like to thank (XXX) for their financial support of this research.

TABLE OF CONTENTS

LIST OF TABLES

LIST OF FIGURES

CHAPTER 1 INTRODUCTION AND HYPOTHESES

Stormwater runoff from industrial activities is of increasing concern in the U.S. Most industrial facilities have activities involving material handling, storage and recycling, often expose materials to stormwater, and the stormwater that is discharged at these facilities may cause significant environmental problems. Pollutant types, concentrations, and loads from industrial activities are dependent on several factors, such as type of industrial activity, precipitation characteristics, and stormwater management used at the facility. Discharges from industrial activities may contain various hazardous pollutants including metals, oil and grease, organic toxicants (such as PAHs), chemical oxygen demand, nutrients, and suspended sediment (Line, et al. 1996, Line, et al. 1997, Duke, et al. 1998, Marques, et al. 2001, Chys, et al. 2013). However, limited information is available on the characteristics of the pollutant constituents that affect treatment and treatment technologies that can effectively treat the runoff from industrial activities. As part of the NPDES Storm Water Multi- Sector General permit for Industrial Activities, facility operators develop a site-specific Storm Water Pollution Prevention Plan (SWPPP) with treatment technologies designed specifically for their facility (US EPA 1995).

Control of stormwater pollutants from industrial activity can be achieved by implementing suitable treatment control practices such as better site material handling, detention ponds, hydrodynamic devices, oil-water separators, constructed wetlands, and filtration devices. The main goal of this research is to evaluate the performance of treatment control devices at an industrial site and describe the pollutant characteristics that affect stormwater treatability

(particle size distributions, pollutants associated with different particle sizes, and filterable fraction of the pollutants) for different flow conditions.

As part of this research, runoff samples were collected from an industrial site in the southeastern United States (the site is client confidential). Rainfall patterns and intensities, flow rates and runoff volumes were continuously monitored at the site using rain gauges and area-velocity flow sensors. Runoff samples were collected from the influent and effluent locations of a pre-treatment unit and from a dry infiltration pond (having significant infiltration potential). The runoff samples were analyzed to study the removal efficiencies of suspended sediment, pollutant mass reductions by sediment size, nutrients and metals. Also, the heavy metal concentrations in the soil profile of the dry infiltration pond, and sediment accumulated in the pre-treatment unit, were also monitored as pollutants accumulations in soils can pose a significant threat to ground waters (Ipeaiyeda, et al. 2007, Nwachukwu, et al. 2011). Water chemistry and vadose zone modeling was also conducted to predict long-term groundwater contamination potential. Detailed site surveys, including soil characteristics and impervious cover characteristics were also conducted.

1.1 Need for Research

Limited information is available for pollutant monitoring and treatment at industrial facilities. Pre-treatment (typically using sedimentation in small units), filtration, and infiltration practices are some of the control methods that have been used for industrial area stormwater runoff treatment to remove particulate solids and associated contaminants including metals and nutrients. Quantifying the performance of some of these treatment controls provide a better application of how these practices can achieve the numeric effluent limits of industrial stormwater discharges.

1.2 Dissertation Research

This dissertation research included monitoring and data evaluations to examine:

1) Treatment performance of a dry infiltration pond for runoff volume control along with a hydrodynamic separator for pre-treatment
2) Treatability based on particle size distribution, and other pollutant characteristics (concentrations associated with different particle size categories)
3) Quantifying the pollutant concentration and mass reductions under different rainfall conditions
4) Evaluate the concentrations of pollutants captured in soils in a dry infiltration pond
5) Particle size distribution and metal concentrations in the sediment deposited in treatment control devices
6) Determination if runoff characteristics and performance controls can be applied to similar industrial activities and controls located elsewhere

1.3 Hypothesis and Experimental Design

The objective of this dissertation research work was to evaluate the performance of treatment control devices at an industrial site and relate performance to site and environmental conditions. The literature review assessed the common pollutants of concern and different treatment technologies to achieve pollutant reductions. The monitoring results showed that pre-treatment (hydrodynamic device) is effective in removing the larger particles, but is less effective for the removal of the smaller particles. The infiltration control is very efficient in reducing the runoff volumes (>80%) for all the monitored storm events along with associated pollutant mass reductions. Pollutant concentrations associated with different particle sizes and filtered forms of

pollutants were also determined to evaluate the treatability of the runoff using different stormwater unit treatment processes. Pollutant concentrations in the soils lining the dry pond were also evaluated to investigate concentrations of metals associated with the soils with depth under the infiltration pond. Site hydrology was also being examined, especially considering site development characteristics including soil compaction and associated infiltration rates in different areas on the site. The following hypotheses statements for this dissertation research are based on the literature review, need for research, and preliminary analyses.

1.4 Hypothesis 1:

Pre-treatment hydrodynamic devices are effective in removing larger particles, but less effective for smaller particles.

Prediction1: Pre-treatment devices are the first step in a stormwater treatment train and are usually designed to remove gross solids, floatables, debris and large solids to decrease maintenance on more effective downstream components.

Research Activities 1:

a) Perform particle size distribution analyses for stormwater samples from the influent and effluent of the hydrodynamic device.
b) Perform suspended sediment concentration analyses and quantify suspended sediment concentrations based on particle size.
c) Perform particle size distribution analysis and a full mass balance for sediment accumulated in the hydrodynamic device.

Critical Tests 1:

a) Particle size distributions for water and sediment were assessed and graphically presented, reflecting the accumulative particle solids percentage and mass percentage distribution by particle size.
b) Performed statistical analyses examining the performance of the hydrodynamic separator in capturing SSC and other constituents by particle size ranges.

1.5 Hypothesis 2:

The dry infiltration pond is very effective in reducing the runoff volumes for monitored storm events, along with associated pollutant mass reductions, along with small to moderate pollutant concentration reductions.

Prediction 2: Infiltration treatment practices are designed to attenuate stormwater runoff as part of the treatment train. Reductions in runoff volumes result in similar reductions of pollutant masses

Research Activities 2:

a) Performed particle size distribution analysis for stormwater samples collected at the dry infiltration pond outlet (the hydrodynamic device outlet is the pond inlet)
b) Assessed the runoff volumes measured by an area-velocity sensor and calculated the associated pollutant loads and conducted full mass balance of pollutant retention
c) Groundwater contamination potential was also examined by measuring the metal content of soils at different depths below the infiltration area and conducted water chemistry and vadose zone modeling.

Critical Tests 2:

a) Hydrographs entering and exiting the dry infiltration pond were assessed reflecting reductions in runoff volumes
b) Accumulative particle solids mass distribution by particle size were calculated and graphically represented quantifying reductions in solids mass
c) Metal content of subsurface soils were examined by depth to calculate retention characteristics and groundwater contamination potential.
d) Performed regression and statistical analyses examining SSC and contaminant performance by particle size ranges.

1.6 Quantifying the performance of stormwater treatment controls

Runoff samples were collected during the storm events from the influent and effluent locations of the two main stormwater treatment controls (hydrodynamic separator and the dry infiltration pond). All the runoff samples were analyzed to study the removal efficiencies of suspended sediment, pollutant mass reductions by sediment size, nutrients and metals for each unit process separately and combined.

The number of samples needed for comparison between two paired data sets, to calculate the removal effects for example, can be calculated by the following equation (Burton and Pitt 2002):

$n = 2[(Z_{1-\alpha} + Z_{1-\beta})/(\mu_1-\mu_2)]^2\sigma^2$

Where, α = false positive rate ($1-\alpha$ is the degree of confidence. A value of α of 0.05 is usually considered statistically significant, corresponding to a $1-\alpha$ degree of confidence of 0.95 or 95%)

β = false negative rate ($1-\beta$ is the power. If used, a value of β of 0.2 is common, but it is frequently ignored, corresponding to a β of 0.5)

$Z_{1-\alpha}$ = Z score (associated with area under normal curve) corresponding to $1-\alpha$

$Z_{1-\beta}$ = Z score corresponding to $1-\beta$ value

μ_1 = mean of data set one

μ_2 = mean of data set two

σ = standard deviation (same for both data sets, same units as μ; both data sets are assumed to be normally distributed)

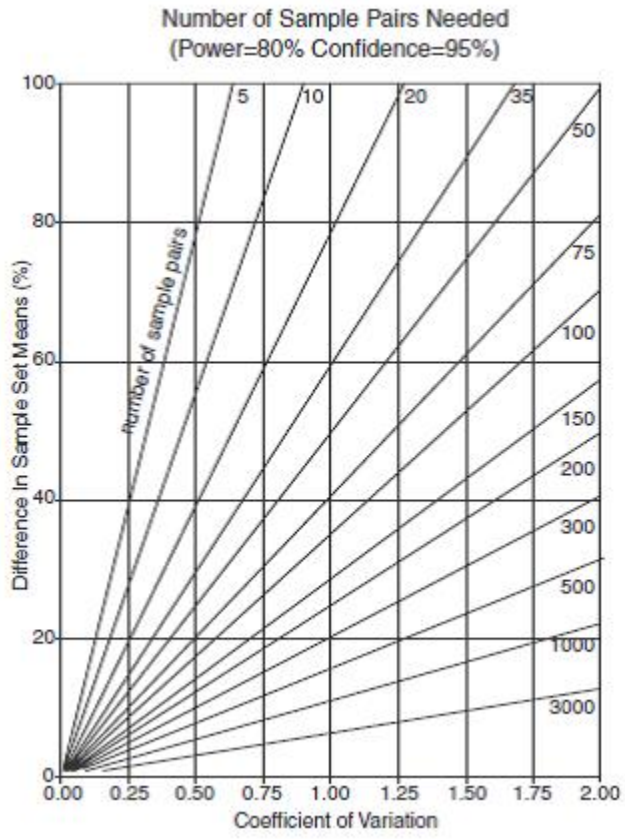

Figure 1-1 Sample effort needed for paired testing (power of 80% and confidence of 95%) (Pitt and Burton 2002)

Figure 1-1 is a plot of the above equation (normalized using COV and differences of sample means) showing the approximate number of sample pairs needed for an α of 0.05 (degree of confidence of 95%), and a β of 0.2 (power of 80%). Assuming the coefficient of variation is no more than about 0.5, the 12 sample pairs collected are sufficient to detect significant differences with at least a 50% difference in the parameter concentration or mass values between the paired data (influent vs. effluent).

Pollutant contamination for each particle size was quantified and described using summary statistics and exploratory data analyses methods, including tools such as box and whisker plots and probability plots. Statistical tests such as ANOVA, followed by Wilcoxon sign ranked tests, were performed to identify significant differences in particle size distributions and contaminant concentrations for each particle size to evaluate the treatability of the runoff and the performance of the treatment processes. Further analyses used included Pearson correlations, Cluster analyses, and Principle Component analyses were also used to identify correlations and relationships between site and rain conditions, with the observed stormwater characteristics.

1.7 Research Objectives

The primary objective of this research was to study the characteristics of the stormwater observed at a heavy industrial site and to evaluate the treatment capabilities for the different stormwater controls employed at the site. The detailed objectives and results are discussed in Chapters 2, 3 and 4 and are presented as individual journal articles.

Chapter 2 presents the descriptions of the site characteristics and pollutants associated with the heavy industrial activity. Specifically, the influent concentrations at the site and correlations between different hydrologic and pollutant constituents are discussed.

Chapter 3 describes the efficiency of the different stormwater treatability controls at the site. Pollutant contamination is quantified based on particle size and filtered fractions and described using summary statistics and exploratory data analyses methods such as box and whisker and probability plots. Statistical tests such as Kruskal-Wallis, followed by Wilcoxon sign ranked tests are performed to identify significant differences in particle size distributions and contaminant

concentrations for each particle size to evaluate the treatability of the runoff and the performance of the treatment processes.

Chapter 4 examines the groundwater contamination potential by presenting the results of the metal concentrations in the soil profile under the infiltration treatment control. The mobility of contaminants in vadose zone was modeled and the results are also discussed to evaluate long-term groundwater contamination potential.

The inter-relationships between the research objectives are then summarized in Chapter 5, representing the overall research as a single body of work.

CHAPTER 2 POLLUTANTS IN STORMWATER RUNOFF FROM A HEAVY INDUSTRIAL SITE: SITE DESCRIPTION AND POLLUTANT CHARACTERISTICS AND ASSOCIATIONS WITH PARTICULATES

2.1 Introduction

Industrial stormwater discharges have been regulated by the USEPA since 1990's with the establishment of NPDES permit requirements for stormwater discharges associated with industrial activities (USEPA, 1995). Many of the activities at industrial facilities can contribute to stormwater contamination. Although a considerable amount of stormwater quality monitoring data exists for runoff from urban area (U.S. EPA 1983b, Marsh, *et al*. 1993, Bannerman, *et al*. 1993, Pitt and Maestre 2005), very limited monitoring data are available on stormwater runoff from specific industrial activities (Line, *et al*. 1997, Golding, *et al*. 2006, Duke, *et al*. 1998, Marques, *et al*. 2001). Due to the wide range of industries involved in the industrial sector and lack of information available on types and concentrations of storm water pollutants, it is very difficult to monitor pollutants from a specific industrial group or sector (Line, *et al*. 1997). The association of stormwater pollutants with particulate and dissolved forms is of great importance in the study of their fate and transport (Morquecho, *et al*. 2005) and to select suitable treatment controls.

Marques, *et al.* (2001) studied runoff quality from a waste management landfill in Sweden. The activities on site comprised of mechanical sorting, slag storage, car parking, wood chipping and storage, industrial and demolition waste storage, and composting. The site was monitored during rainfall events from 1994 to 1998. Suspended sediment and several heavy metals

including zinc, copper and nickel were found in every sample. Suspended sediment concentrations varied from 190 to 1,000 mg/L at different locations on the site, with a mean concentration of 600 mg/L. The measured values of suspended sediment, nutrients, COD and BOD exceeded the discharge limits for the receiving water.

Duke, *et al*. (1998) studied stormwater runoff quality from 130 metal plating facilities in Los Angeles County, California over a three year period that were regulated under California's 1992 General Industrial Storm Water NPDES Permit. Three conventional constituents and nine metals were examined in this study. TSS, zinc, copper, and Oil & Grease were detected in more than 80% of the facility locations, and nickel, chromium, lead and cadmium were commonly detected.

Line, *et al*. (1996) studied concentrations of different pollutants from two North Carolina businesses involving five general industrial groups: auto salvage, metal fabrication, scrap and recycling, vehicle maintenance and wood preserving facilities. First flush samples from a single runoff event and both first flush and composite samples from three consecutive samples were collected and analyzed. Zinc and copper were most prevalent from every site, while silver was the least prevalent. Concentrations of zinc were higher than all the other 12 metals for every industrial group except the wood preserving facilities. Only auto salvage and scrap and recycling group samples showed the presence of rare metals, including selenium, silver and titanium. Higher levels of common metals were found at sites that had significant exposure to metal stored on site. Sample analyses showed that zinc and copper were among the most common metals found in the runoff at concentrations ranging from 5 to 21,000 µg/L.

Golding, *et al*. (2006) studied concentrations of zinc from 28 industrial sites in the state of Washington that had permits under the state's Industrial Stormwater General Permit. The

significant facility areas for sources of zinc were found to be roofs, parking lots, loading docks and paved grounds (truck parking and material storage). Storm events were monitored under conditions as required by the permit with grab samples collected within the first hour after the discharge began. Three out of the five sampled events reported zinc concentrations greater than the ISGP benchmark of 117 µg/L. The mean total recoverable concentrations of zinc from parking and loading dock were 48 and 93 µg/L and the mean dissolved concentrations were 30 and 55 µg/L. Zinc in roof runoff was mostly in dissolved forms. A summary of these concentration data from these studies is shown on Table 2-1.

The analyses of particle size distributions of stormwater runoff along with associations of different pollutants with the different particle sizes plays a key role in understanding the pollutant characteristics of a specific site concerning the contaminant's fate and treatability. Several studies have been conducted to examine the particle size distributions originating from different land use settings. Pitt, *et al*. (1995) studied particle size analyses of 121 stormwater inlets from three different states in the US. Median particle sizes ranged from 0.6 to 38 µm. In a study conducted by House, *et al*. (1993), particle sizes were studied from stormwater routed through the Monroe street detention pond in Madison, Wisconsin, the observed median particle sizes ranged from 2 to 26 µm for a variety of storms. Li, *et al*. (2005) studied particle size distributions originating from highway runoff and showed that 97% of the particles were less than 30 µm and nearly 30-60% of the particle mass is found in particles smaller than 50 µm. None of these studies included heavy industrial facilities.

Pollutants in stormwater runoff can to be separated into particulate-bound or filtered ("dissolved") forms to better understand their treatability (Pitt, *et al*. 1995, Maniquiz-Redillas, *et al*. 2014, Zgheib, *et al*. 2011). Several studies have investigated the associations of pollutants

with stormwater particulates. Zgheib, *et al*. (2011) examined the partitioning of pollutants between dissolved and particulate phases from urban catchments. The results showed that heavy metals (Pb, Zn, Cu, and Cd) were mostly particulate bound with only Zn being observed in mostly filtered phases. Pitt, *et al*. (1998) analyzed 550 samples collected from telecommunication manhole vaults mostly affected by stormwater. Cu and Pb were found to be mostly associated with particulates, whereas Zn was mostly present in dissolved phase. Similar trends were observed in other studies conducted with metals being strongly associated with particulate matter (Harrison, *et al*. 1985, House, *et al*. 1993, NURP 1996, Gromaire-Mertz, *et al*. 1999, Glenn, *et al*. 2001, Hatje, *et al*. 2003, NSQD, Karlsson, *et al*. 2008). Summary of these data on particulate and dissolved bound metal concentrations are listed in Table 2-2.

Vignoles, *et al*. (1995) studied associations of heavy metal concentrations with different particle sizes in stormwater samples from France. The results showed that heavy metals were highly associated with particle sizes less than 10 μm in size. In a study conducted on urban stormwater runoff in Cincinnati, Ohio, Sansalone, *et al*. (1997) observed that concentrations of heavy materials decreased with decreases in particle size. Again, none of these data are from heavy industrial facilities.

As part of this research conducted at The University of Alabama, stormwater pollutant characteristics at a heavy industrial site were examined during a range of rain conditions. A major objective of this research was to characterize influent concentrations along with correlations between different hydrologic and water quality components, along with stormwater treatability (shown in Chapter 3). Pollutant particle strengths associated with different particle size ranges were also determined during this current research.

Table 2-1 Pollutant data from different industrial activities available in literature

Constituent	Marques et al 2001 Mean, (s.d)	Duke et al 1998 Mean, (s.d)			Line et al 1996 Mean, (s.d)		Line et al 1997 Mean, (s.d)	NSQD Industrial Mean, (COV)
SSC (mg/L)	599, (0.43)						522, (868)	160, (1.57)
COD (mg/L)	268, (183)				98, (97)	96, (86)	157, (222)	
N total (mg/L)	0.32, (0.41)				2.39, (2.06)	2.05, (1.59)	2.7, (3.4)	
P Total (mg/L)	0.072, (0.09)				1.03, (1.24)	0.77, (0.83)	0.8, (1.0)	
P Dissolved (mg/L)					0.46, (0.53)	0.39, (0.61)	0.4, (0.5)	
Total Fe (mg/L)	0.49, (0.57)							
Total Mn (mg/L)	0.25, (n.d)							
Total Zn (mg/L)	0.42, (0.25)	1.3, (2.5)	1.4, (1.5)	1.3, (1.7)	1.8, (4.0)		0.6, (0.64)	0.4, (0.003)
Zn Dissolved (mg/L)								0.11, (0.002)
Total Cu (mg/L)	0.78, (0.83)	0.33, (0.28)	0.39, (0.51)	0.39, (0.37)	0.4, (0.9)		0.12, (0.19)	0.04, (0.002)
Cu Dissolved (mg/L)								0.009, (0.001)
Total Ni (mg/L)	0.012, (0.016)	0.16, (0.24)	0.26, (0.33)	0.35, (0.47)	0.08, (0.14)		0.03, (0.05)	0.02, (0.001)
Ni Dissolved (mg/L)								0.009, (0.002)
Total Pb (mg/L)	0.006, (0.004)	0.13, (0.27)	0.2, (0.32)	0.16, (0.25)	0.55, (1.32)		0.08, (0.15)	0.05, (0.002)
Pb Dissolved (mg/L)								0.01, (0.002)
Total Cd (mg/L)	0.004, (0.006)	0.07, (0.15)	0.08, (0.18)	0.12, (0.26)	0.008, (0.02)		0.002, (0.003)	
Total As (mg/L)					0.05, (0.1)		0.02, (0.08)	
NH3 (mg/L)					0.22, (0.29)	0.32, (0.6)	0.6, (1.4)	
Type of Sampling	Composite	Grab Samples			First Flush	Composite	First Flush	
Monitoring Period	1994 - 1998	1993	1994	1995		1993, 1994	1993, 1994	

Table 2-2 Summary of partitioning of heavy metal data available in literature

	Zinc		Copper		Lead		Arsenic		Cadmium		Nickel	
	% Filt	% Part	% Filt	% Part	% Filt	% Part	% Filt	% Part	% Filt	% Part	% Filt	% Part
Pitt et al 1998	70	30	33	67	21	79						
Karlsson et al 2008	1	99	1	99	1	99	7	93	2	98	2	98
Zgheib et al 2011	14	86	17	83	15	85						
House et al 1993	34	66	13	87	4	96						
NURP 1996			16	84	3	97	25	75	18	82		
NSQD (Industrial)	10	90	10	90	12.4	87.6			11	89		

2.2 Site Description

The test site is a heavy industrial facility located in the southeastern United States (specific location and industry is client confidential). The facility is approximately 21 acres in size, mostly covered with concrete, roofs, and severely compacted soils. As per the site survey and the site drainage network, approximately 15 acres is directed to the main treatment system prior to the site outlet. The site is a heavy industrial land use having several buildings (galvanized metal roofs), driveways, loading docks, and highly compacted pervious areas. Almost all of the roofs and impervious areas are directly connected to drains, except for a few roofs draining directly to compacted soils. Land use characteristics of the site are as shown in Table 2-3 and Figure 2-1.

The site has two oil/water separators (one standalone for the metal turnings storage area that is pumped out and not connected to the stormwater system, and the other connected to the drainage network after collecting runoff from a portion of the site), a pre-treatment hydrodynamic device (baffle box with no media), and a dry infiltration pond that has several rock check dams. The dry infiltration pond rarely accumulates standing water for extended periods. Most of the site stormwater drainage inlets have fabric filter bag filters that are replaced as needed (every several weeks).

Table 2-3 Detailed land use characterization of test site

Detailed land cover characterization of the test site	
	Industrial Land use (ac)
Roofs	
Roofs Flat - drains to asphalt/concrete	0.01
Parking/Streets/Sidewalks/Driveways	
Paved concrete parking/storage - smooth - directly connected	0.44
Driveways/loading dock -concrete- directly connected	4.8
Pervious Areas	
Other pervious infiltration areas (compacted soils)	8.13

Open areas (dry pond)	0.72
Special Areas	
Galvanized metal roofs- directly connected	0.23
Galvanized metal roofs - drains to soil	0.43
Other galvanized materials- directly connected to drains	0.2
Total Area (acres)	14.96

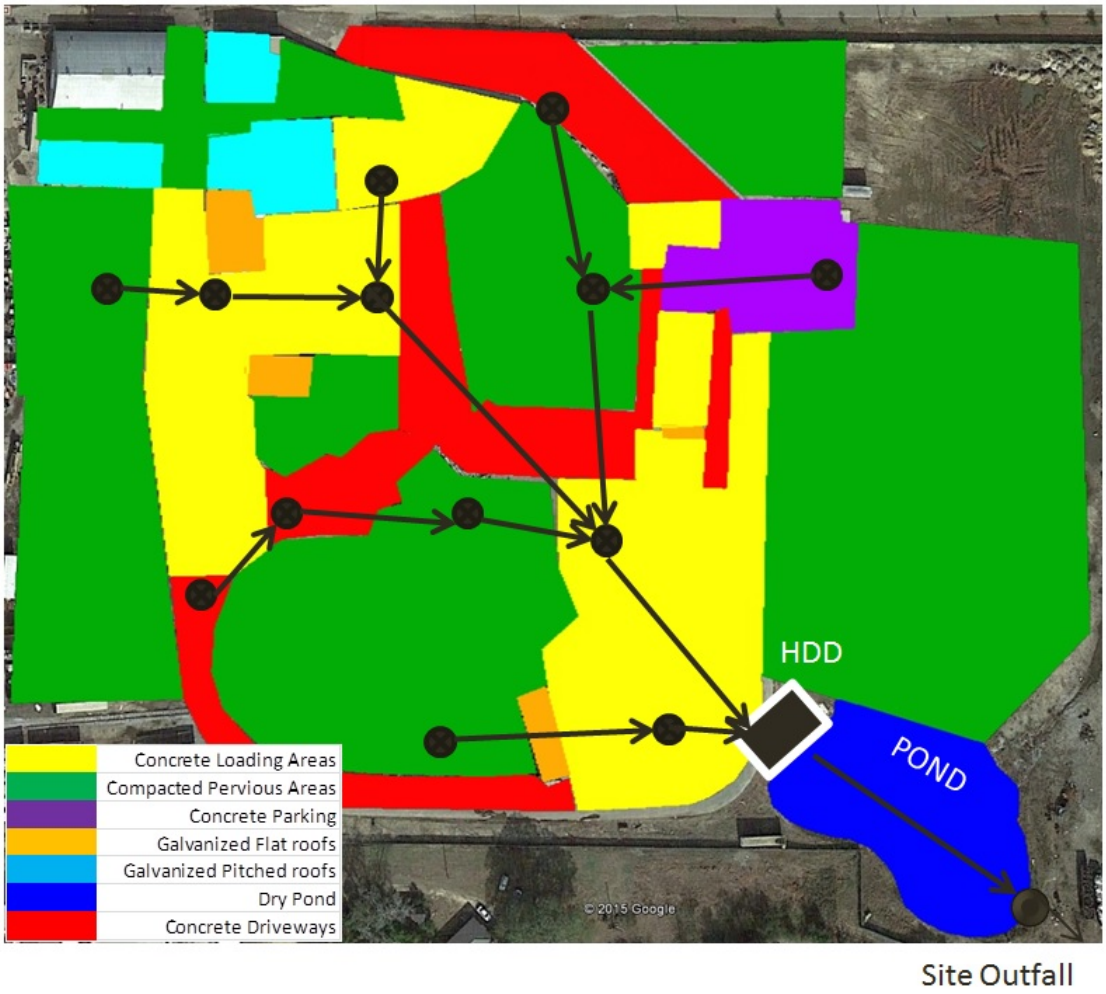

Figure 2-1 Land surface classification and drainage network map for test site

2.2.1 Constituents of Interest

Several categories of constituents were monitored during this research, including solids, metals, and nutrients. The laboratory analytical methods used and limits of detection are listed in Table 2-4.

Table 2-4 Analytes of interest with analytical methods and limits of detection

Analytes	Analytical Methods	Analytical Laboratory	Limit of Detection (LOD)
pH		PSH	0.02 pH units
Aluminum, Total and Dissolved	EPA 200.7	Subcontractor	0.005 mg/L
Arsenic, Total and Dissolved	EPA 200.7	Subcontractor	0.005 mg/L
Cadmium, Total and Dissolved	EPA 200.7	Subcontractor	0.080 mg/L
Copper, Total and Dissolved	EPA 200.7	Subcontractor	0.003 mg/L
Iron, Total and Dissolved	EPA 200.7	Subcontractor	0.041 mg/L
Lead, Total and Dissolved	EPA 200.7	Subcontractor	0.005 mg/L
Manganese, Total and Dissolved	EPA 200.7	Subcontractor	0.003 mg/L
Nickel, Total and Dissolved	EPA 200.7	Subcontractor	0.002 mg/L
Zinc, Total and Dissolved	EPA 200.7	Subcontractor	0.003 mg/L
Total/ Dissolved Nitrogen as N	Method 8075	PSH	1 mg/L
Total/Dissolved Phosphorous as P	Method 8180	PSH	0.06 mg/L
Nitrate as N	Method 10049	PSH	0.1 mg/L
Alkalinity (Carbonate and Bicarbonate) Ions		PSH	0.01 mg/L as $CaCO_3$
Chemical Oxygen Demand		Subcontractor	1 mg/L
Suspended Sediment Concentration	ASTM D3977-97B	UA	5 mg/L
Particle Size Distribution	Coulter Counter/ sieving and filtering	UA	Not Applicable
Specific Gravity (3-250 µm)	Coulter Counter/ Filtering	UA	Not Applicable

2.2.2 Monitoring design and process

Performance monitoring of the treatment control devices used hydrologic and water quality monitoring equipment. ISCO 4250 area-velocity flow meters with flow sensors were used to continuously monitor hydrologic conditions at both the inlet and outlet locations of the pre-treatment unit and the outlet of the dry infiltration pond. ISCO 6712 automatic samplers were used to collect flow-weighted composite samples at the influent and effluent locations of the pre-treatment unit, and time-weighted composite samples were collected at the oil-water separator and dry infiltration pond effluent locations for analyses of the constituents listed in section 1.4. Sediment from the pre-treatment hydrodynamic separator device was collected at the end of the monitoring period for analyses of particle size distribution, nutrients and metals, and total mass retained.

2.2.3 Hydrologic Monitoring

Hydrologic monitoring of the treatment control devices included rain depth and intensity, and runoff flow rates. Both ISCO 4250 area-velocity sensors were used to continuously monitor the flow rates in the effluent pipes at the pre-treatment unit and dry infiltration pond. The internal data logger of the flow meters was setup before each targeted storm event corresponding to the expected runoff conditions. The rain depth and intensity were continuously monitored using an ISCO 674 tipping bucket rain gage installed at the oil-water separator, pre-treatment unit and dry infiltration pond locations. The tipping bucket rain gage was also used as a trigger for the automatic samplers to initiate sampling.

2.2.4 Water Quality Monitoring

The ISCO 674 tipping bucket rain gage was used as a sample trigger to initiate sampling, while the area-velocity sensor in the effluent pipe of hydrodynamic device was used for sample collection pacing during the events. At the beginning of the storm event, both automatic samplers at the pre-treatment unit were initiated when the rain gage registered 0.02 inches of rainfall within 30 minutes. Subsamples from the influent and effluent of pre-treatment unit were obtained based on the programmed sample collection pacing. For the oil-water separator and dry infiltration pond effluent locations, the rain gage was used as a sample trigger. Due to the unavailability of infiltration characteristics of dry pond at the initial stage of monitoring, and very less to no flow observed at the oil-water separator, minimum and maximum discharge volumes required for flow-weighted sampling couldn't be evaluated. Therefore, subsamples at these two locations are collected for each 15 minutes based on time pacing. Based on the hydrographs, the time paced sampling was able to represent 80 – 90% of the flow for all the monitored events. Very few samples were collected at oil-water separator due to very less to no flow observed during the storm events and the samples collected were from the standing water from its inlet and outlet sumps.

2.2.5 Automatic samplers programming design

Historical IDF curves and preliminary runoff modeling for the monitoring locations were studied to develop the sampler programming protocols. The ISCO 6712 automatic samplers used in the research were programmed to meet the different demands of sampling for different rain

conditions. The flow-weighted composite sampling required the samplers to be programmed to cover at least 70% of each storm's duration with a minimum of 10 subsamples collected. A minimum sample volume was needed for the laboratory analyses, and the maximum sample volumes were limited by the maximum volume of composite sample bottle (20 liter). The sampler programming scheme was based on the expected rain depth (and duration), with small rains less than 0.5 inches, moderate rains from 0.4 to 2 inches, and large rains from 1.5 to 8 inches. Table 2-5 shows the sampler programming for these three rain categories.

Table 2-5 Automatic sampler programming for different sized storm events

	Small Size Rain Event	Moderate Size Rain Event	Large Size Rain Event
Precipitation (in)	0.1 – 0.5	0.4 – 2.0	1.5 – 8
Duration (hr)	2-6	4-20	>15
Runoff Volume (ft^3)	4630- 23141	18508-92530	69420-370260
Average Rain Intensity (in/hr)	0.05 – 0.08	0.08 – 0.1	0.1 – 0.33
Programmed Subsample Volume (mL)	200	200	200
Runoff Volume per Subsample (ft^3)	460/2300	1850/9250	6940/37000
Estimated Number of Subsamples	10 -80	10-80	10-80
Sample Volume per Event (L)	2-16	2-16	2-16
Filling Percentage of 20 L Capacity (%)	10-80	10-80	10-80

2.2.6 Stormwater monitoring

Rainfall, runoff volume, and flow rates were continuously monitored at the site, using rain gauges and area-velocity sensors. Automatic samplers and area-velocity samplers were set up at the influent and effluent locations of the treatment controls located on the site. ISCO 6712 automatic samplers were used to collect flow-weighted composite samples at the influent and effluent locations of the treatment controls to meet different demands of sampling. ISCO 4250 area-velocity sensors ware used to continuously monitor the flow rates at the effluent locations of

the treatment controls. ISCO 674 tipping bucket rain-gauges were installed at the oil-water separator, at the hydrodynamic separator device, and at the dry pond to continuously monitor rain depths and intensities. The tipping bucket rain gauges were also used as a trigger to initiate sampling of the automatic samplers at the inlets to the treatment systems. Rainfall data obtained from the rain gage at the hydrodynamic separator device were used for the site rain characteristic descriptions due to the high resolution of data (5 minute interval) obtained (the other two rain gages recorded data at 15 minute intervals). Rainfall depth data from all the three rain gages were compared with no differences observed. Automatic samplers were initiated at the beginning of each rain event when the rain gauge registered at least 0.02 inches of rainfall within 30 minutes. A total of 17 storm events were monitored from November 2013 to June 2014.

2.2.7 Site Precipitation Characteristics

The distribution of rainfall events recorded during the monitoring period are as shown in Figure 2-2. About 65% of the events were less than 0.5 inches, 27% were between 0.5 and 1.5 inches and 8% of the events were greater than 1.5 inches.

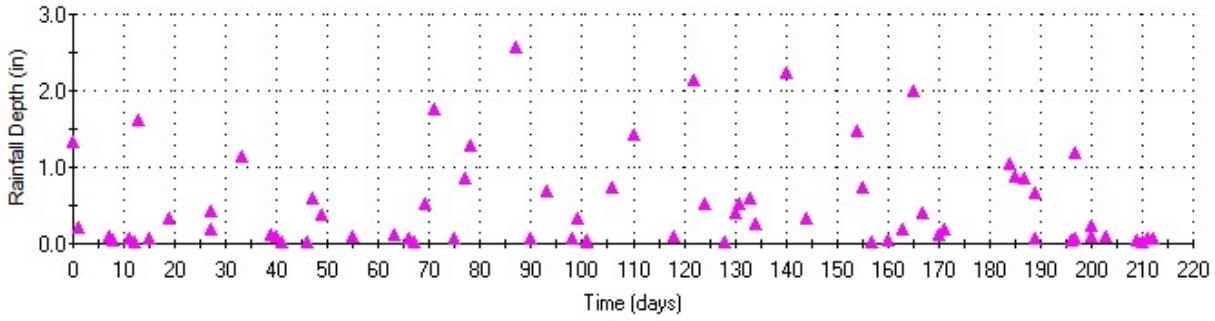

Figure 2-2 Precipitation characteristics for overall monitoring period

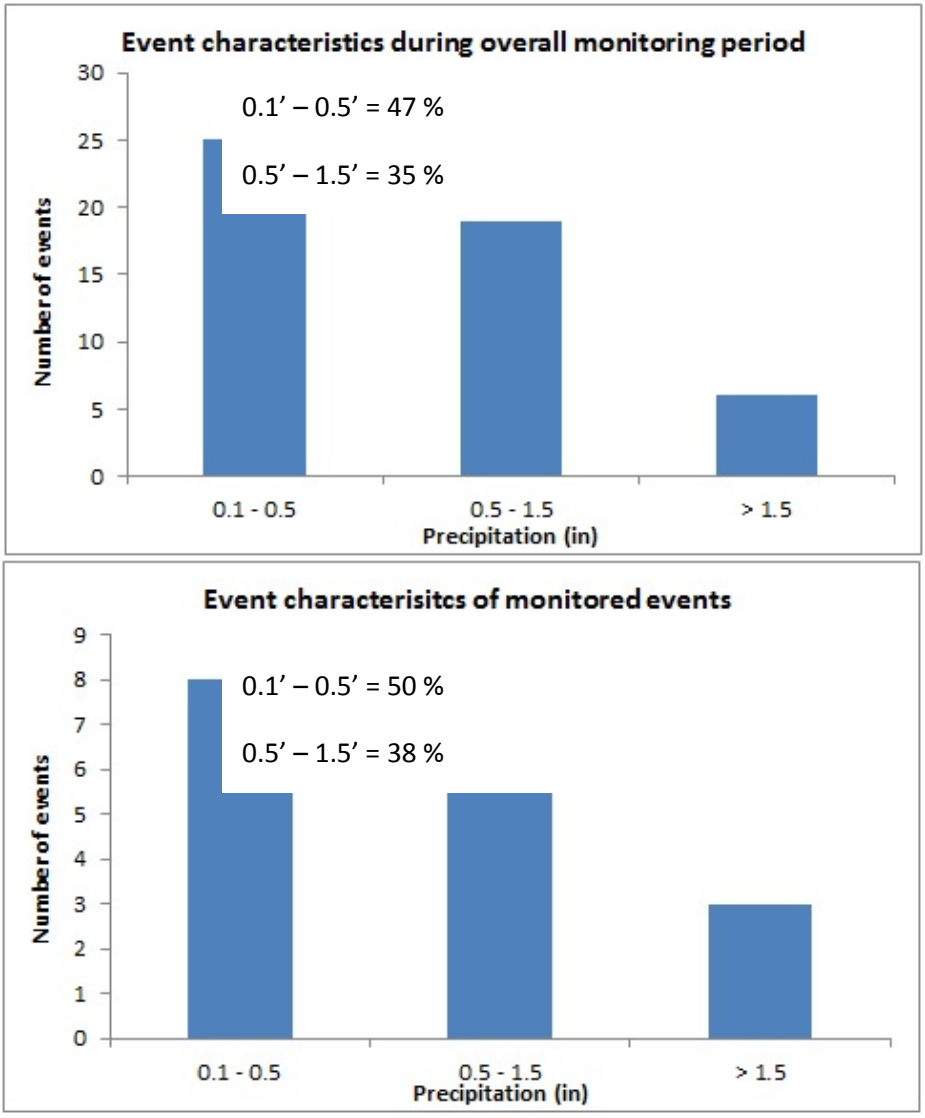

Figure 2-3 Event characteristics for overall and monitored events

During this research, as per the sampling protocol, events greater than 0.1 inches were considered as events of interest. Figure 2-3 compares the rain distribution for all of the events during the monitoring period to those rains that were monitored. The monitored events well-represented the precipitation characteristics of the overall monitoring period.

2.2.8 Sample collection and handling

Automatic samplers were programmed based on the historical IDF curves, site land use conditions, and WinSLAMM modeling to determine flow conditions for a variety of runoff events. The goal of the samplers was to collect samples over at least 70% of each monitored storm event using automatic composite samplers having 20L HDPE bottles. Each monitored event also had at least 10 subsamples collected. The sampler programming was based on the expected rain depth and duration, with the storm events separated into three different categories, as previously shown in Table 2-5.

Composite samples were collected in high-density polyethylene bottles from the influent and effluent locations of the treatment controls. After each targeted storm event, the samples were brought to the UA laboratory as soon as possible and either cooled in a sample refrigerator or immediately processed. Composite samples were split evenly into ten one liter bottles using a USGS/Dekaport Teflon^{TM} cone splitter. Nylon screening material with 1,180 μm openings was placed on top of the cone splitter to capture larger particles and debris to prevent clogging of the cone splitter and to quantify this large material. The different steps involved in the sample processing and water quality analyses were as shown in Figure 2-4. SSC and PSD were analyzed at the UA lab and metals and nutrients were analyzed at the PSH and a commercial lab. Suspended solids concentration was analyzed at the UA laboratory in accordance with the ASTM D 3977-97B testing method. One of the influent sample splits for each event was screened through three different sieves and one filter for analyses of pollutant associations with different particle size ranges. The measured total volume of each subsample was used for the SSC and PSD analyses. Particle size distributions were determined in a multi-step procedure of screening (> 1,180 μm), sieving (250 to 1180 μm) and filtering (0.45-3 μm) followed with

Coulter Counter analyses (3-250 μm). Metals were analyzed at a private lab in accordance with EPA 200.7 method.

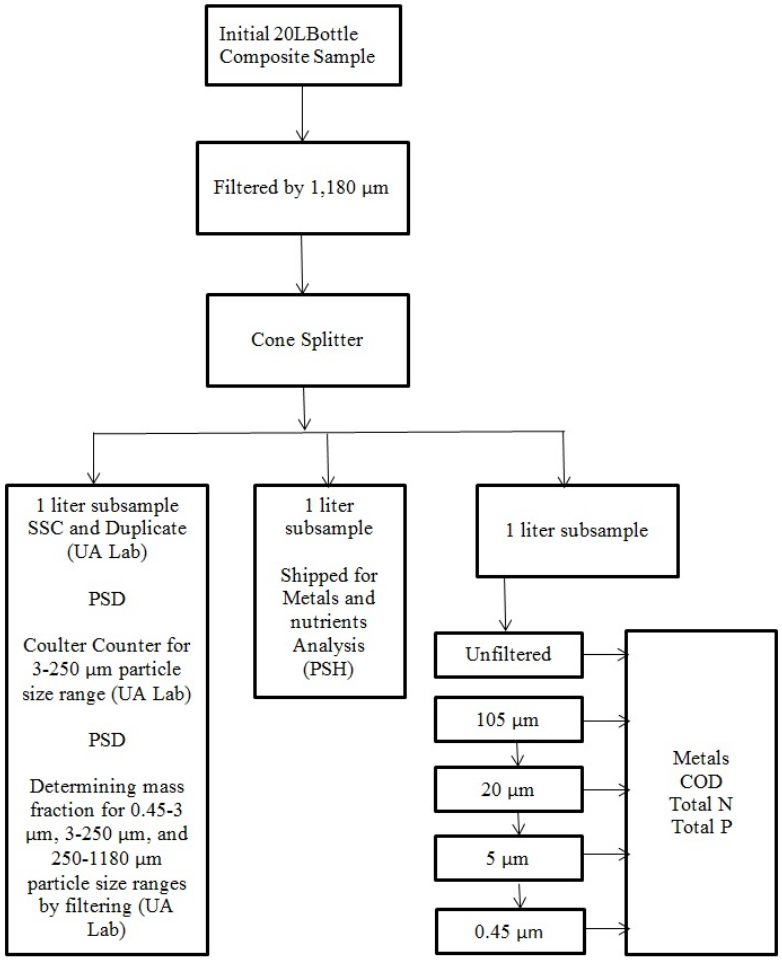

Figure 2-4 Flowchart showing steps of sample processing and water quality analyses

2.2.9 Laboratory Analytical Procedures

Analyses procedures for Suspended Solids Concentration

Suspended solids concentration (SSC) were analyzed at the UA laboratory in accordance with the ASTM D 3977-97B testing method. The steps involved for SSC analyses were as follows:

1) A preserved clean filter (Whatman ® 934-AH™ Glass Fiber Filter) with aluminum weighing dish was weighed in an analytical balance and the initial mass of the filter with the weighing dish was recorded.
2) The filter (with wrinkled side up) was assembled in the cleaned filtration apparatus and vacuum applied
3) Subsample from the previous sample processing was split using the cone splitter and the volume of sub-subsample recorded from the graduated cylinder.
4) The sub-subsample was poured into the filtration apparatus and filtrated. Successive aliquots of DI water were used to wash down the retaining particles. Vacuum was applied until no visible trace of water was seen.
5) The filter was then removed and placed into the previously weighed aluminum weighing dish, and the dish was placed in the drying oven set at 103 to 105^{o}C for at least 24 hours.
6) The filter with the weighing dish were then cooled to room temperature in the desiccator and weighed on analytical balance and the mass of filter with dish recorded.

Suspended Solids Concentration (SSC) was calculated based on the following equation:

Suspended Solids Concentration SSC (mg/L) =

(weight of filter with dish after filtering (mg) – weight of clean filter with dish (mg))/ Sub-subsample volume (L)

Analyses procedures for particle sixe distribution (PSD)

An important evaluation of the treatability of solids was based on the particle size distribution (PSD) analyses. PSD analyses were conducted in a multi-step procedure consisting of sieving and filtering, and then the Coulter Counter analyses.

1) Sieving and Filtering:

i) The mass of clean 1,180 µm opening nylon screening material and clean crucible were measured using the analytical balance. The cleaned screening was placed on the cone splitter and the initial sample was split. A graduate cylinder was used to capture the split sample and to measure the volume of water in each subsample. The nylon screening with the screened debris was then transferred into a previously weighed clean crucible and placed in the drying oven at 103 to 105^{o}C for 24 hours. After that, the crucible along with the nylon mesh was moved into the desiccator and cooled to room temperature. The screening with debris and crucible were then weighed on the analytical balance. The concentration of solids greater than 1,180 µm was determined from the known mass and water volume filtered.

ii) Initial weight of a clean and dried stainless steel sieve with 250 µm openings was measured on the analytical balance. A water subsample from the cone splitter in previous step was selected. The subsample was poured through the 250µm sieve into a graduated cylinder and water volume measured. The sieve was then placed into the drying oven at 103 to 105^{o}C for at least 24 hours. It was then cooled down to room temperature in the desiccator and weighed on the analytical balance. The solids concentration from 250 µm to 1,180 µm was determined by known mass and water volume.

iii) A preserved clean nominal 3 µm MF-Millipore^{TM} membrane filter with aluminum weighing dish was weighed in an analytical balance and the initial mass of the filter with the dish was recorded. The filter was then assembled in the filtration apparatus and vacuum applied. The water subsample that was sieved by the 250 µm sieve was

poured into the filtration apparatus and filtrated. Successive aliquots of DI water were used to wash down the retaining particles. The filter was then removed and placed into the previously weighed aluminum weighing dish, and the dish was placed into the drying oven at 103 to 105^{o}C for at least 24 hours. The filter with the weighing dish was then cooled to room temperature in the desiccator and then weighed on the analytical balance and the mass of filter with dish recorded. The solids concentration from 3μm to 250 μm was determined by known mass and sieving water volume.

iv) A nominal 0.45 μm MF-Millipore^{TM} membrane filter with aluminum weighing dish was weighed in an analytical balance and the initial mass of the filter with the dish recorded. The filter was then assembled in the filtration apparatus and vacuum applied. The water subsample from the filtration flask that was filtered by the 3 μm filter from the previous step was poured into the filtration apparatus. Successive rinses of DI water were used to wash down any retained particles from the filtration flask. The filter was then removed and placed in the drying oven along with the aluminum weighing dish at 103 to 105^{o}C for at least 24 hours. The filter with the weighing dish was then cooled to room temperature in the desiccator and then weighed on the analytical balance and the mass of filter with dish recorded. The solids concentration from 0.45 μm to 3 μm was determined by knows mass and sieving water volume.

2) Coulter Counter Analyses:

A Beckman ® Multi-Sizer III^{TM} with two aperture tubes of 100 μm and 400 μm diameter tube orifices were used for the Coulter Counter analyses of particle sizes. The size range for each aperture tube can be measured over the range of 2% and 60% of the tube orifice diameter, and

the range of measured particle diameters overlap using these two orifice tubes. Therefore a composite high-resolution particle size distribution was obtained from about 2 µm to 250 µm. A subsample from the cone splitter was used for the Coulter Counter analyses. The selected subsample was stirred on the stir plate with a magnetic stir bar and a specific volume pipetted based on expected dilution, at an approximate mid-depth and midway point between the bottle wall and vortex. The pipetted sample was pre-sieved into the beaker to minimize clogging of aperture tube. The selection of the opening size of the pre-filter sieve is based on the smallest size that still exceeds the maximum analytical range of the aperture tube. The opening size of the pre-filtering sieve for the 400 µm aperture tube was 250 µm and for the 100 µm aperture tube was 75µm. The results are reported as particle volume (directly correlated to mass) for each detected particle size. This particle volume along with the previously determined particle concentration in this size range was also used to calculate the particle density. Using a combination of sieving, filtering, and Coulter Counter analyses, the overall particle size distribution (PSD) was integrated from the filtering mass from 0.45 µm to 3 µm, Coulter Counter from 3 to 250 µm, sieving mass from 250 µm to 1180 µm, and screening mass for >1,180 µm.

2.2.10 Quality control and quality assurance

Quality control and quality assurance techniques were used during all portions of the research, from sample collection to laboratory analyses. Field quality assurance methods included pre-storm site setup, monitoring and sampling equipment, calibration, field blanks and samples handling. All the sampling and monitoring equipment was checked by sampling personnel prior to a targeted storm event to make sure it was in good condition and ready to sample. The triggered rain gauge was checked to make sure the funnel was not clogged which would result in sampling failure. Preliminary site inspections were conducted during every site

visit to check for any new activity at the site. The sampler bottles used in the automatic samplers were rinsed with laboratory phosphate-free detergent and air dried and well-sealed before they were brought to the field. Internal sampling tubes of the peristaltic pump of the samplers were inspected for leakage and wearing. Battery status for all the monitoring equipment was checked to ensure sufficient power was available for the period of the sampling event.

After every storm event, the collected samples were transported to the laboratory as soon as possible. The samples were well sealed and cooled in the refrigerator at 4^{o}C until processing. All the equipment used in sample processing and solid analyses including, graduated cylinders, pipettes, HDPE subsample containers, and cone splitters, were washed with laboratory grade non-phosphate detergent and then rinsed with DI water before each use.

2.3 Results

The results from the water quality analyses for the analyzed constituents of interest (SSC, metals, COD and nutrients) are shown in Tables 2-6 through 2-9. These results show the concentrations of the constituents prior to treatment. Chapter 3 describes the effluent concentrations of the constituents after treatment and their removal. Untreated site runoff suspended sediment concentrations ranged between 85 – 493 mg/L with a mean concentration of 253 mg/L. Heavy metals were present in all the samples collected during the monitoring period, except arsenic was only detected in six of the sampled events. Iron and aluminum exhibited higher concentrations compared to other metals. The high concentrations of the metals at the site were associated with exposed metal materials stored on the site. Total nitrogen concentrations ranged from <1 mg/L to 10 mg/L with a mean concentration of 38 mg/L, and the COD concentrations ranged from <1 mg/L to 394 mg/L with a mean concentration of 94 mg/L.

Only copper and zinc were detected in the filtered samples for all of the monitored events. Manganese was detected in the filtered samples for eight of the events, while cadmium and lead were detected in only two of the filtered event samples. Iron was detected in filtered samples from four sampled events. Zinc concentrations in filtered samples ranged from 0.03 mg/L to 0.2 mg/L, with a mean concentration of 0.06 mg/L. This was expected as zinc mostly originates from galvanized metal roofs and other exposed galvanized materials and the literature reports the zinc to be mostly in filtered forms from these sources.

The results obtained from this study were compared to the results from Line, *et al*. (1996) for ten industrial sites in North Carolina, US, and the NSQD. The concentrations of SSC and total and dissolved metals were higher than the industrial runoff concentrations observed in the NSQD, as expected since the data presented in NSQD is a representation of concentrations from outfalls of several light to medium industrial sites throughout the Unites States and do not represent much data from heavy industrial activities.

The mean concentrations of COD were higher than those observed by Line, *et al*. (1996) at ten industrial sites in North Carolina, US. The higher concentrations of COD may be related to the heavy usage of heavy equipment on the study site resulting in elevated oil and grease concentrations and associated high levels of COD at the site. Mean concentrations of ammonia were higher than those reported by Line, *et al*. (1996). This may be related to the use of ammonia-based materials to rinse and wash equipment. The mean concentrations of total metals observed by Line, *et al*. (1996) were higher than those observed at the study site since the samples analyzed for total metals by Line, *et al*. (1996) were first flush samples which are usually are greater than storm composite samples from mostly impervious areas (Maestre, *et al*. 2005. The total nitrogen concentrations reported by Line, et al. (1996) were higher than those

observed in this study. No significant nitrogen sources were observed at the site as non-paved areas had little vegetation and no fertilizers would be used at the site. The mean phosphorous concentrations were also lower than those reported by Line, *et al*. (1996), again for the same reasons as the lower nitrogen values. Overall, different factors such as the nature of the industrial activity, seasonality of precipitation, and amount of exposed material on site and hydrologic transport efficiencies of eroded materials, all affect the characteristics of the chemical runoff constituents from industrial facilities.

Table 2-6 Individual and overall mean concentrations for sediment, COD, and nutrients (total and filtered) for all monitored events

	Rain Depth (in)	SSC (mg/L)	COD (mg/L)	TN (mg/L)	Filtered N (mg/L)	% Filtered N	NO_3 (mg/L)	NH3 (mg/L)	TP (mg/L)	Filtered P (mg/L)	% Filtered P	PO_4 (mg/L)	BiCarb (mg/L)	Carb (mg/L)	Total Alkalinity (mg/L)
Detection Limit			1.0	0.1	0.1				0.01	0.01			0.01	0.01	0.01
1	1.42	121	112	1.2	23.3	1942	0.3	3	0.26	0.01	4	0.06	67.1	0.07	67.2
2	0.55	263	211	<DL	3.5	n/a	0.4	9	0.27	0.16	59	0.59	103.1	0.11	103.2
3	0.16	266	194	3.5	4.4	126	0.2	15	0.13	0.56	431	0.09	153.8	0.43	154.2
4	2.52	493	207	1.3	<DL	<8	0.9	<DL	0.16	<DL	<6	0.1	153.0	0.60	153.6
5	0.75	302	178	8.5	<DL	<0.1	1.1	1	0.27	<DL	<4	0.29	123.6	0.36	124.0
6	0.39	234	175	1.9	<DL	<5	0.9	<DL	0.19	<DL	<5	0.29	168.6	0.38	169.0
7	0.47	303	159	3.3	1.3	39	1	<DL	1.11	0.08	7	<DL	129.3	0.08	129.4
8	0.6	85	<DL	2.7	<DL	<4	<DL	0.03	<DL	<DL	n/a	<DL	97.5	0.07	97.6
9	0.3	282	287	9	2.1	23	0.9	0.11	<DL	0.25	n/a	0.08	170.5	0.09	170.6
10	2.36	275	394	<DL	<DL	n/a	0.6	0.14	0.61	<DL	<2	0.49	116.3	0.09	116.4
11	0.39	91	75	1.3	<DL	<8	0.6	5	0.25	<DL	<4	0.09	121.1	0.34	121.4
14	0.12	234	160	2	n/a	n/a	n/a	n/a**	0.66	n/a	n/a	n/a	n/a	n/a	n/a
15	0.95	323	138	8.8	2.2	25	0.6	1	0.72	<DL	<1	1.17	130.6	0.16	130.8
16	0.23	269	101	10.1	4.2	42	0.3	<DL	<DL	<DL	n/a	<DL	133.3	0.27	133.6
Mean		253	172	3.8	5.9		0.6	2.6	0.331	0.21		0.25	128.3	0.23	128.5
St. Dev		105	98	3.6	7.8		0.34	4.6	0.33	0.21		0.34	29.2	0.17	29.3
COV		0.42	0.56	0.95	1.3		0.57	1.8	1.0	1.01		1.4	0.23	0.74	0.23
Minimum		85	<DL	<DL	<DL		<DL	<DL	<DL	<DL		<DL	67.1	0.07	67.2
Maximum		493	394	10.1	23.3		1.1	15	1.11	0.56		1.17	170.5	0.60	170.6
Percent detected			93	86	54		92	69	79	38		77	100	100	100

*<DL: concentration less than detection limit, ** n/a: sample not available for analyses

Table 2-7 Individual and overall mean concentrations for Al, As, and Cd (total and filtered) for all monitored events

Storm #	Rain Depth (in)	Total Al (mg/L)	Filtered Al (mg/L)	% Filtered Al	Total As (mg/L)	Filtered As (mg/L)	% Filtered As	Total Cd (mg/L)	Filtered Cd (mg/L)	% Filtered Cd
Detection Limit		0.005	0.005		0.005	0.005		0.001	0.001	
1	1.42	1.4	<DL	<0.4	<DL	<DL	n/a	0.0096	0.0039	41
2	0.55	3.7	<DL	<0.1	<DL	<DL	n/a	0.0042	0.0023	55
3	0.16	5.8	<DL	<0.1	0.0059	<DL	<85	0.0047	<DL	<21
4	2.52	8.0	<DL	<0.1	0.0066	<DL	<76	0.0057	<DL	<18
5	0.75	6.6	<DL	<0.1	0.0069	<DL	<72	0.005	<DL	<20
6	0.39	3.7	<DL	<0.1	<DL	<DL	n/a	0.0032	<DL	<31
7	0.47	5.3	<DL	<0.1	0.0054	<DL	<93	0.005	<DL	<20
8	0.6	1.5	<DL	<0.3	<DL	<DL	n/a	0.0014	<DL	<71
9	0.3	6.0	<DL	<0.1	0.0062	<DL	<81	0.0047	<DL	<21
10	2.36	3.7	<DL	<0.1	<DL	<DL	n/a	0.0039	<DL	<26
11	0.39	0.87	<DL	<0.6	<DL	<DL	n/a	0.0011	<DL	<91
14	0.12	4.3	n/a**	n/a	n/a	n/a	n/a	0.0038	n/a	n/a
15	0.95	4.9	<DL	<0.1	0.006	<DL	<83	0.0042	<DL	<24
16	0.23	4.9	<DL	<0.1	<DL	<DL	n/a	0.0038	<DL	<26
Mean		4.3			0.0055			0.004	0.003	
St. Dev		2.1			7.0			0.002	0.001	
COV		0.49			0.13			0.48	0.365	
Minimum		0.87	<DL		<DL	<DL		0.0011	<DL	
Maximum		8.0	<DL		0.0069	<DL		0.0096	0.0039	
Percent Detected		100	0			0		100	15	

*<DL: concentration less than detection limit, ** n/a: sample not available for analyses

Table 2-8 Individual and overall mean concentrations for Fe, Pb, and Mn (total and filtered) for all monitored events

Storm #	Rain Depth (in)	Total Fe (mg/L)	Filtered Fe (mg/L)	% Filtered Fe	Total Pb (mg/L)	Filtered Pb (mg/L)	% Filtered Pb	Total Mn (mg/L)	Filtered Mn (mg/L)	% Filtered Mn
Detection Limit		0.041	0.041		0.005	0.005		0.003	0.003	
1	1.42	5.8	0.06	1	0.14	<DL	<4	0.1	<DL	<3
2	0.55	11.4	0.067	0.6	0.33	0.015	5	0.26	0.01	4
3	0.16	18.1	<DL	<0.2	0.45	<DL	<1	0.32	0.0045	1.4
4	2.52	26.3	<DL	<0.2	0.64	<DL	<0.8	0.63	<DL	<0.5
5	0.75	21.4	<DL	<0.2	0.5	<DL	<1	0.4	0.023	6
6	0.39	12.8	<DL	<0.3	0.25	<DL	<2	0.33	0.15	45
7	0.47	18.7	0.11	0.6	0.57	<DL	<0.9	0.33	0.1	30
8	0.6	5.2	<DL	<0.8	0.12	<DL	<4	0.11	<DL	<3
9	0.3	20.6	<DL	<0.2	0.6	<DL	<0.8	0.3	<DL	<1
10	2.36	13.4	<DL	<0.3	0.42	<DL	<1	0.18	<DL	<2
11	0.39	3.3	<DL	<1.2	0.087	<DL	<6	0.047	0.0025	5
14	0.12	14.9	n/a	n/a	0.39	n/a	n/a	0.26	n/a	n/a
15	0.95	17.5	0.068	0.4	0.54	<DL	<0.9	0.19	0.011	6
16	0.23	17.1	<DL	<0.2	0.56	<DL	<0.9	0.29	0.0027	0.9
Mean		14.8	0.076		0.4	0.015		0.27	0.04	
St. Dev		6.6	0.023		0.19			0.15	0.06	
COV		0.45	0.30		0.49			0.56	1.47	
Minimum		3.3	<DL		0.087	<DL		0.047	<DL	
Maximum		26.3	0.11		0.64	0.015		0.63	0.15	
Percent Detected		100	31		100	8		100	62	

*<DL: concentration less than detection limit, ** n/a: sample not available for analyses

Table 2-9 Individual and overall mean concentrations for Zn, Ni, and Cu (total and filtered) for all monitored events

Storm #	Rain Depth (in)	Total Zn (mg/L)	Filtered Zn (mg/L)	% Filtered Zn	Total Ni (mg/L)	Filtered Ni (mg/L)	% Filtered Ni	Total Cu (mg/L)	Filtered Cu (mg/L)	% Filtered Cu
Detection Limit		0.003	0.003		0.01	0.01		0.003	0.003	
1	1.42	0.34	0.072	21	0.011	<DL	<91	0.22	0.022	10
2	0.55	0.83	0.18	22	0.026	<DL	<38	0.51	0.05	10
3	0.16	1.1	0.083	8	0.031	<DL	<32	0.54	0.073	14
4	2.52	1.2	0.018	2	0.044	<DL	<23	0.79	0.0087	1
5	0.75	1	0.028	3	0.037	<DL	<27	0.55	0.0058	1
6	0.39	0.68	0.07	10	0.022	<DL	<45	0.28	0.0087	3
7	0.47	1.2	0.053	4	0.033	<DL	<30	0.96	0.017	2
8	0.6	0.31	0.052	17	0.011	<DL	<91	0.19	0.028	15
9	0.3	1.2	0.063	5	0.038	<DL	<26	0.87	0.02	2
10	2.36	0.95	0.064	7	0.029	<DL	<34	0.74	0.013	2
11	0.39	0.26	0.053	20	0.01	<DL	<100	0.16	0.19	118
14	0.12	0.94	n/a	n/a	0.025	n/a	n/a	0.64	n/a	n/a
15	0.95	1.1	0.04	4	0.032	<DL	<31	0.85	0.012	1
16	0.23	1	0.056	6	0.03	<DL	<33	0.43	0.034	8
Mean		0.86	0.06		0.030			0.57	0.04	
St. Dev		0.35	0.04		0.012			0.28	0.05	
COV		0.40	0.61		0.35			0.50	1.34	
Minimum		0.26	0.018		0.001	<DL		0.16	0.0058	
Maximum		1.2	0.18		0.044	<DL		0.96	0.19	
Percent Detected		100	100		100	0		100	100	

*<DL: concentration less than detection limit, ** n/a: sample not available for analyses

2.3.1 Multivariate Analyses

Multivariate analyses were conducted to study the relationships between different hydrologic and water quality parameters involved in the study and to predict group memberships. The different analyses performed include Pearson correlation analyses, cluster analyses and principal component analyses. Pearson correlation analyses were performed to determine simple associations between different pairs of parameters, while cluster analyses were performed to identify more complex relationships between the parameters. Principal component analyses were performed to identify groupings of parameters with similar characteristics to explain the variability in the data. The statistical software package XLSTAT 2015 supplement to Excel was used to conduct most of these analyses.

2.3.2 Pearson Correlation Analyses

Correlation techniques are used to investigate linear relationships between two variables. Pearson correlations are one of the most common measures of correlation when examining many constituents. The strength of associations between two variables (stronger or weaker) is measured by Pearson's correlation coefficients (Johnson, et al. 2007). Values of Pearson's correlation coefficients range between –1 (negative correlation) and +1 (positive correlation). A value of 0 indicates no correlation. The linear relationships between variables were analyzed by drawing scatterplots to check for linearity. The strength of association between the variables was assessed by the distance of the scatter of points to a straight line, the nearest the scatter points are to the straight line, the higher is the strength of association between variables. Pearson correlation analyses were performed to investigate relationships between different hydrologic

and water quality parameters. Scatterplots were created to check for linearity between the variables. Parameters examined were rain and runoff depths, average and peak rain intensities, inter-event time, median suspended sediment particle size, SSC, total metal and nutrient concentrations. Figure 2-5 shows example scatterplots illustrating some of the strong and weak correlations, while Appendix XX presents all of the scatterplots for these constituents. Results of the Pearson correlation analyses are shown in Table 2-8 with values highlighted in bold indicating Pearson correlation coefficients with a significance level ≤ 0.05).

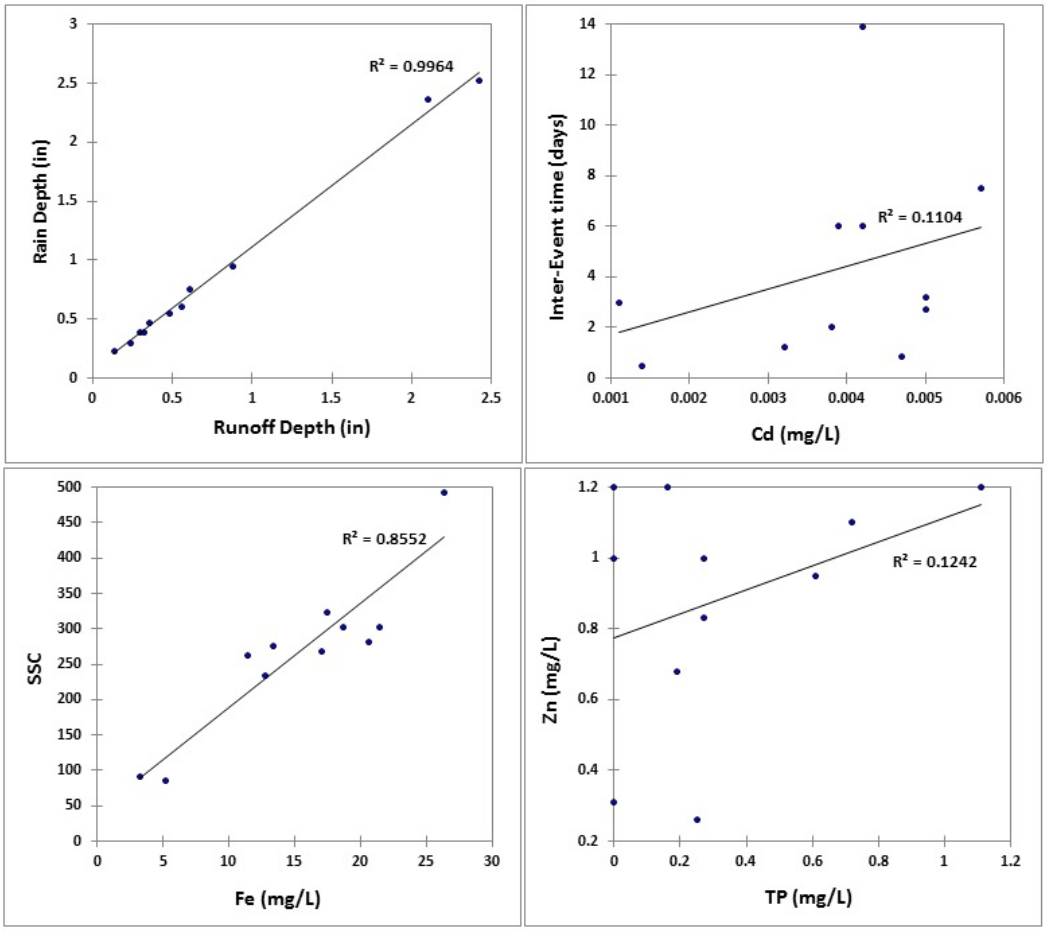

Figure 2-5 Example scatter plots showing strong (left side) and weak (right side) correlations between different parameters

2.3.3 Regression Analyses

Regression analyses are used to determine associations between variables (independent and a dependent variable). Regression analyses help illustrate relationships between variables. Simple linear regression is the most common type and requires that the dependent variable has a linear relationship with the independent variable and for each value of the independent variable. The probability distributions of the independent and dependent variables also need to have the same standard deviation. Linear regression analyses were used to predict the relationships between hydrological and water quality parameters included in the study. The results of the linear regressions were supplemented with ANOVA and residual analyses to ensure that regression assumptions are valid.

2.3.4 Analysis of Variance

ANOVA was conducted to test the significance of the regression coefficients (slope and intercept terms), which are highly dependent on the number of data observations. When an observed data set has only a few observations, it is difficult for the important relationships to have significant calculated coefficients. A high R^2 value does not guarantee by itself that the model has any predicative value, and a low R^2 value does not mean the regression model is useless. An ANOVA table presents the variability of responses and distinguishes what can be explained by regression and what remains as error. The F critical value is the value that would result in a p-value equal to 0.05. A large F value (and correspondingly low p value) suggests that there is a significant linear relationship between the observed and predictor variables. Statistical software Minitab (Version 17) was used to perform these data analyses.

2.3.5 Relationships among hydrologic parameters and suspended sediment

Strong correlations were observed between different hydrologic parameters in reference to the Pearson results (Table 2-10). Rain depth is strongly correlated with runoff depth, as expected. Average and peak rain intensities both showed positive correlations with rain depth, indicating larger intensities as the rain depth increased, again as expected. The strongest correlation was observed between rain depth and runoff depth ($p < 0.05$, $R^2 = 0.997$). SSC showed moderate (but significant) positive correlations with average ($p < 0.05$, $R^2 = 0.40$) and peak rain intensities ($p < 0.05$, $R^2 = 0.45$) and weak linear correlations (not statistically significant) with rain depth ($p > 0.05$, $R^2 = 0.18$), runoff depth and antecedent dry period ($p > 0.05$, $R^2 = 0.22$).

Linear regression analyses were conducted to determine the intercept and slope terms of these parameter relationships. The p-values were checked to determine of the coefficients are significant. The regressions were re-analyzed by forcing the intercept through zero whenever the intercepts were not found to be significant.

Relations between different hydrologic parameters and SSC are shown in Figures 2-6 to 2-9. No strong significant correlations were observed between site hydrology and SSC. This is likely associated with the heavily compacted soils on the site and their lower erosion potential indicating little relationship between the particulate solids and rain energy. Erosion is not a significant factor and SSC and particulate material on the site varies greatly as site activities and materials stored varies throughout the year, making poor relationships between SSC and rain characteristics. The supply of suspended sediment is limited (and variable) on the site and factor most affecting SSC in the runoff is therefore not related to the rainfall.

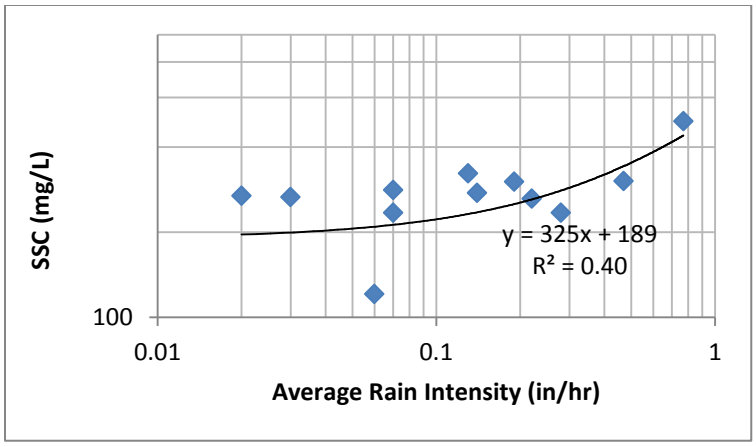

Figure 2-6 Scatter plot of average rain intensity vs SSC (showing significant regression relationship)

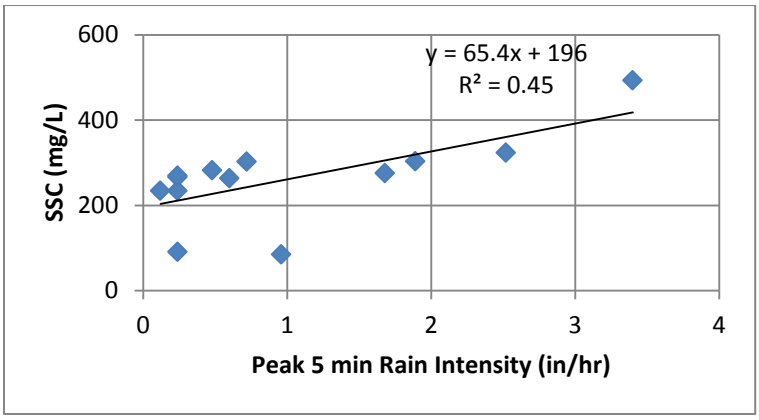

Figure 2-7 Scatter plot of peak rain intensity vs SSC (showing significant regression relationship)

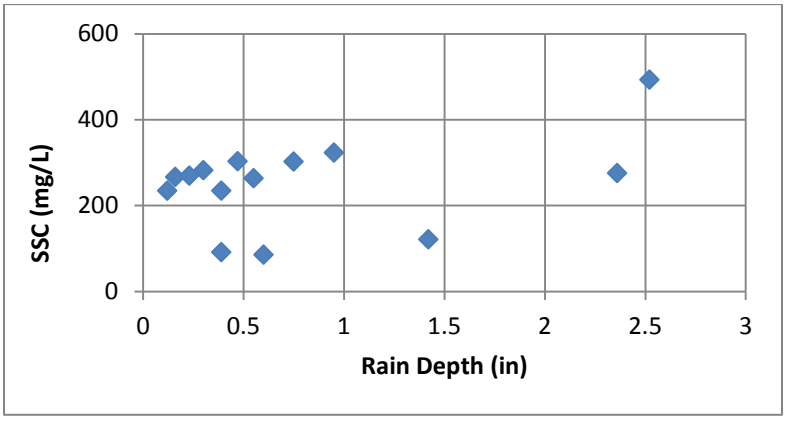

Figure 2-8 Scatter plot of rain depth vs SSC (no significant regression relationship)

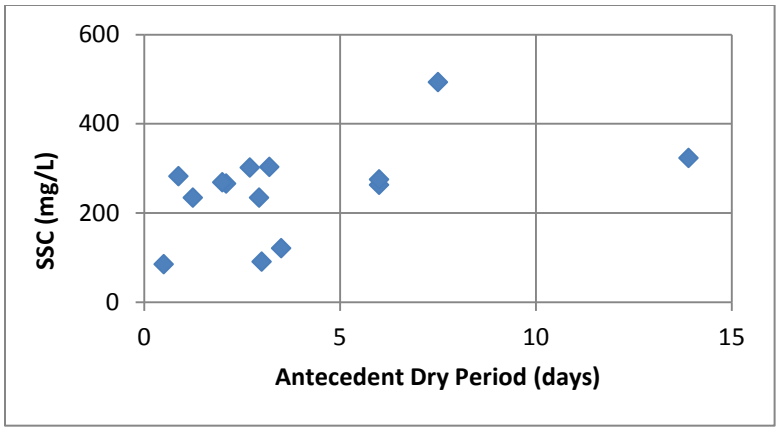

Figure 2-9 Scatter plot of antecedent dry period vs SSC (no significant regression relationship)

Figure 2-9 indicates poor relationships between the antecedent dry period and the SSC concentrations (no obvious build-up and washoff patterns for the paved storage areas at the site).

2.3.6 Relationships among SSC and other pollutants

Pollutants highly correlated with the particulate solids (SSC) can be more readily removed using typical stormwater controls (especially if associated with the larger particles) than those more in the filtered forms. SSC was highly correlated with all the metal constituents (correlation coefficients > 0.7) accounting to increases of total metal concentrations with increased SSC concentrations. This can be related to high affinity of association of metals with particulate matter. All the metals included in the analyses were strongly correlated with each other, while COD, Total N and Total P didn't show any positive correlations with other parameters included in the study. Nitrate showed significant correlations with bicarbonate and total alkalinity. Example scatterplots for some of these constituents are shown in Figures 2-10 to 2-13, while Appendix XX presents all of the scatterplots for all constituents.

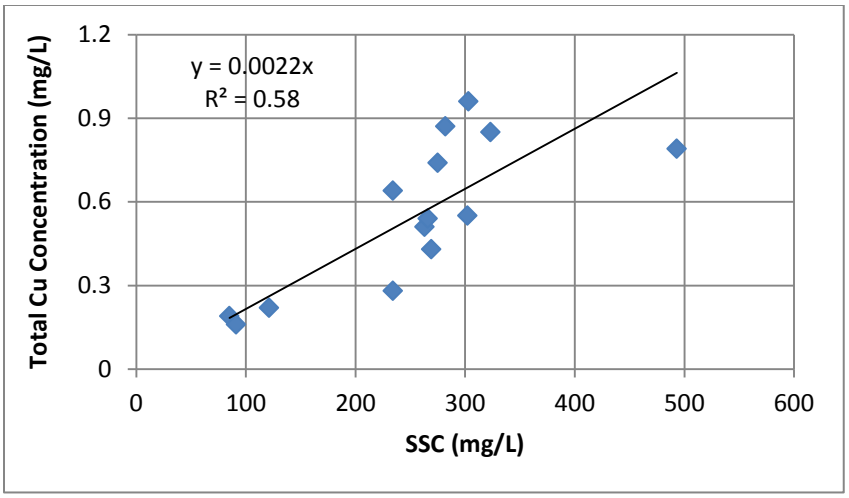

Figure 2-10 Scatterplot of SSC vs Total Cu Concentration (showing significant regression relationship)

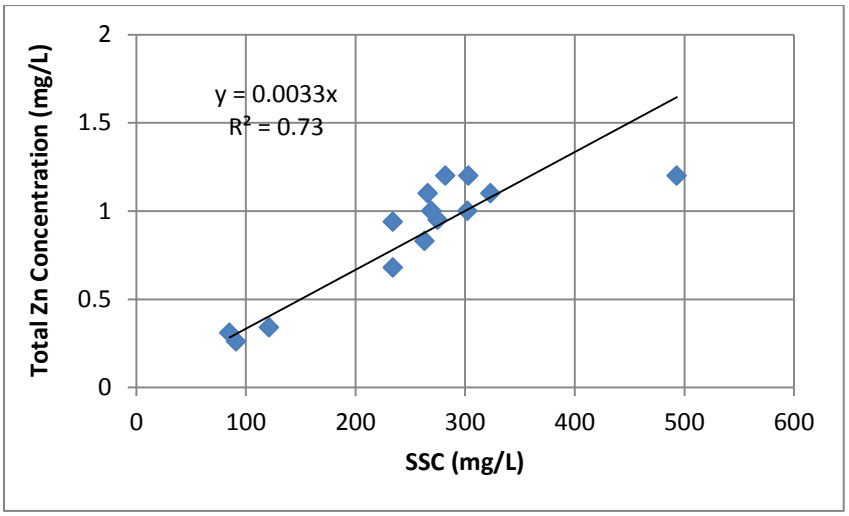

Figure 2-11 Scatterplot of SSC vs Total Zn Concentration (showing significant regression relationship)

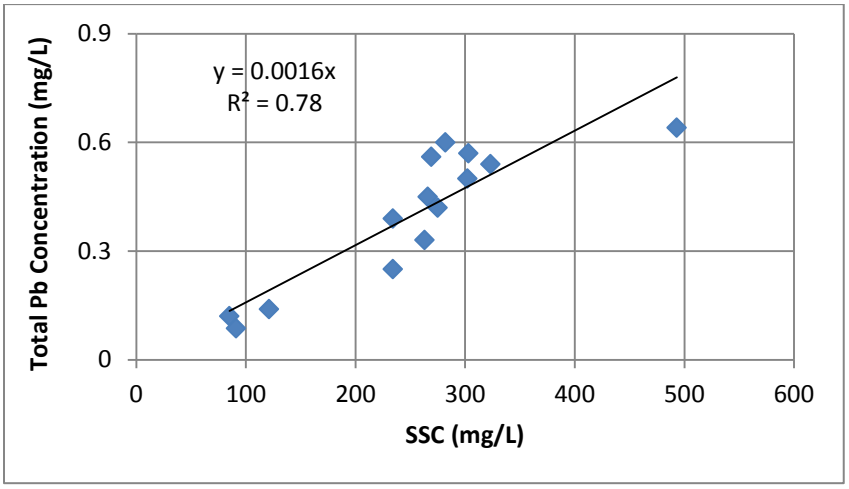

Figure 2-12 Scatterplot of SSC vs Total Pb Concentration (showing significant regression relationship)

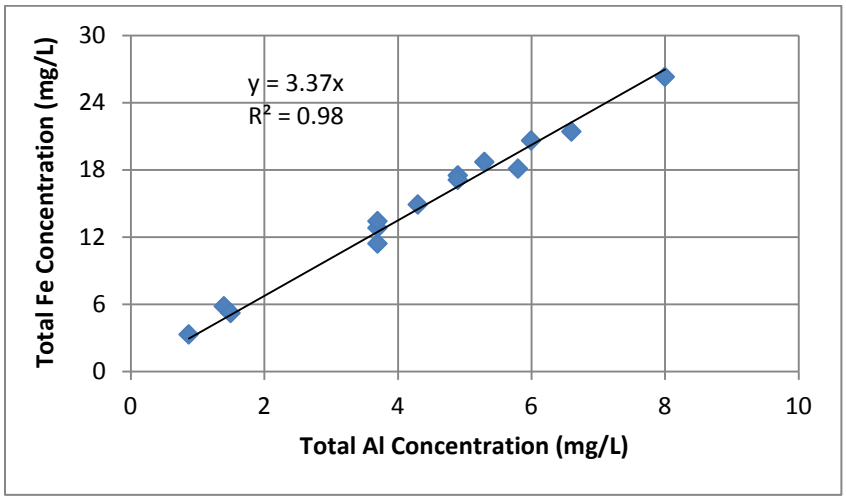

Figure 2-13 Scatterplot of Total Al Concentration vs Total Fe Concentration (showing significant regression relationship)

The median particle sizes were apparently negatively correlated (but not statistically significant) with hydrologic and water quality parameters, indicating smaller median particle sizes as the rain depth and intensities increased, an unexpected result, as increasing rain intensities and flow rates are associated with greater flow energy and should be more capable of eroding and transporting larger particles.

Table 2-10 Pearson correlation matrix for all the parameters included in the study

Variables	Rain Depth (in)	Runoff Depth (in)	Average Rain Intensity (in/hr)	Peak 5 min intensity (in/hr)	Inter-Event time (days)	Median particle size (um)	SSC	Al	Cu	Pb	Fe	Mn	Ni	Zn	Cd	COD	NH3	NO3	PO4	TN	TP	BiCarb	Carb	Total Alk
Rain Depth (in)	1.00	1.00	0.59	0.75	0.48	-0.10	0.57	0.36	0.37	0.29	0.36	0.40	0.39	0.30	0.37	0.53	-0.22	0.14	0.19	-0.41	0.17	-0.02	0.32	-0.02
Runoff Depth (in)	1.00	1.00	0.61	0.77	0.49	-0.12	0.58	0.37	0.37	0.29	0.37	0.42	0.39	0.29	0.37	0.50	-0.22	0.13	0.19	-0.41	0.15	-0.01	0.34	0.00
Average Rain Intensity (in/hr)	0.59	0.61	1.00	0.78	0.26	-0.26	0.65	0.54	0.44	0.40	0.52	0.70	0.46	0.39	0.52	0.07	-0.11	0.34	-0.19	-0.36	0.27	0.07	0.43	0.07
Peak 5 min intensity (in/hr)	0.75	0.77	0.78	1.00	0.70	-0.32	0.69	0.51	0.64	0.51	0.53	0.47	0.52	0.50	0.51	0.20	-0.29	0.20	0.30	-0.14	0.46	0.03	0.22	0.03
Inter-Event time (days)	0.48	0.49	0.26	0.70	1.00	-0.45	0.49	0.25	0.48	0.33	0.27	0.08	0.30	0.36	0.33	0.19	0.15	0.03	0.84	0.01	0.47	-0.11	0.07	-0.11
Median particle size (um)	-0.10	-0.12	-0.26	-0.32	-0.45	1.00	-0.46	-0.38	-0.29	-0.29	-0.35	-0.40	-0.47	-0.38	-0.50	-0.08	-0.15	-0.01	-0.54	0.00	-0.17	0.06	0.04	0.06
SSC	0.57	0.58	0.65	0.69	0.49	-0.46	1.00	0.93	0.75	0.87	0.92	0.87	0.91	0.87	0.92	0.49	-0.25	0.55	0.20	0.15	0.22	0.45	0.43	0.45
Al	0.36	0.37	0.54	0.51	0.25	-0.38	0.93	1.00	0.72	0.92	0.99	0.89	0.96	0.90	0.95	0.41	-0.37	0.64	0.03	0.40	0.09	0.52	0.39	0.52
Cu	0.37	0.37	0.44	0.64	0.48	-0.29	0.75	0.72	1.00	0.86	0.76	0.46	0.81	0.91	0.83	0.59	-0.29	0.51	0.27	0.25	0.57	0.30	-0.18	0.30
Pb	0.29	0.29	0.40	0.51	0.33	-0.29	0.87	0.92	0.86	1.00	0.94	0.69	0.94	0.98	0.91	0.45	-0.40	0.50	0.10	0.52	0.25	0.45	0.12	0.45
Fe	0.36	0.37	0.52	0.53	0.27	-0.35	0.92	0.99	0.76	0.94	1.00	0.87	0.97	0.92	0.94	0.43	-0.43	0.64	0.04	0.43	0.14	0.55	0.36	0.55
Mn	0.40	0.42	0.70	0.47	0.08	-0.40	0.87	0.89	0.46	0.69	0.87	1.00	0.81	0.67	0.81	0.28	-0.29	0.59	-0.17	0.08	-0.06	0.52	0.63	0.52
Ni	0.39	0.39	0.46	0.52	0.30	-0.47	0.91	0.96	0.81	0.94	0.97	0.81	1.00	0.95	0.97	0.54	-0.37	0.55	0.14	0.38	0.17	0.45	0.18	0.45
Zn	0.30	0.29	0.39	0.50	0.36	-0.38	0.87	0.90	0.91	0.98	0.92	0.67	0.95	1.00	0.95	0.56	-0.33	0.56	0.19	0.42	0.35	0.45	0.04	0.45
Cd	0.37	0.37	0.52	0.51	0.33	-0.50	0.92	0.95	0.83	0.91	0.94	0.81	0.97	0.95	1.00	0.56	-0.21	0.63	0.16	0.27	0.29	0.40	0.19	0.40
COD	0.53	0.50	0.07	0.20	0.19	-0.08	0.49	0.41	0.59	0.45	0.43	0.28	0.54	0.56	0.56	1.00	-0.06	0.45	0.24	-0.16	0.22	0.30	-0.11	0.30
NH3	-0.22	-0.22	-0.11	-0.29	0.15	-0.15	-0.25	-0.37	-0.29	-0.40	-0.43	-0.29	-0.37	-0.33	-0.21	-0.06	1.00	-0.24	0.26	-0.39	-0.05	-0.46	-0.11	-0.46
NO3	0.14	0.13	0.34	0.20	0.03	-0.01	0.55	0.64	0.51	0.50	0.64	0.59	0.55	0.56	0.63	0.45	-0.24	1.00	-0.02	0.12	0.34	0.62	0.39	0.62
PO4	0.19	0.19	-0.19	0.30	0.84	-0.54	0.20	0.03	0.27	0.10	0.04	-0.17	0.14	0.19	0.16	0.24	0.26	-0.02	1.00	0.07	0.37	-0.15	-0.18	-0.15
TN	-0.41	-0.41	-0.36	-0.14	0.01	0.00	0.15	0.40	0.25	0.52	0.43	0.08	0.38	0.42	0.27	-0.16	-0.39	0.12	0.07	1.00	-0.15	0.29	-0.06	0.29
TP	0.17	0.15	0.27	0.46	0.47	-0.17	0.22	0.09	0.57	0.25	0.14	-0.06	0.17	0.35	0.29	0.22	-0.05	0.34	0.37	-0.15	1.00	-0.17	-0.31	-0.17
BiCarb	-0.02	-0.01	0.07	0.03	-0.11	0.06	0.45	0.52	0.30	0.45	0.55	0.52	0.45	0.45	0.40	0.30	-0.46	0.62	-0.15	0.29	-0.17	1.00	0.42	1.00
Carb	0.32	0.34	0.43	0.22	0.07	0.04	0.43	0.39	-0.18	0.12	0.36	0.63	0.18	0.04	0.19	-0.11	-0.11	0.39	-0.18	-0.06	-0.31	0.42	1.00	0.43
Total Alk	-0.02	0.00	0.07	0.03	-0.11	0.06	0.45	0.52	0.30	0.45	0.55	0.52	0.45	0.45	0.40	0.30	-0.46	0.62	-0.15	0.29	-0.17	1.00	0.43	1.00

Values in bold are correlations coefficients that are not 0 with a 95% CI ($p<0.05$)

2.3.7 Cluster Analyses

Cluster analysis is a statistical technique used to organize large sets of data into meaningful groups or clusters (Johnson, et al. 2007). Cluster analyses examine the inter-relationships between variables, maximizing the similarity of variables within each cluster. Cluster analyses divide the objects into groups based on their similarity distances. Cluster analyses consider each variable as a separate cluster, and then combines the clusters sequentially, reducing the number of clusters based on distances or dissimilarities. The output of a cluster analysis is presented graphically using a hierarchical tree-like diagram called a dendogram representing the distances at which the clusters are joined. Cluster analyses were performed to examine associations between different parameters included in the study. The analyses included all the hydrologic and water quality parameters. One of the resulting dendogram of this analyses is shown in Figure 2-14.

The analysis resulted in eight different main clusters. All the hydrologic parameters were closely associated. Median particle size was identified as a separate cluster. Phosphate concentrations were associated with inter-event time. Nitrate concentrations were correlated with bicarbonate and total alkalinity. Aluminum concentrations were closely associated with iron. Lead was closely associated with zinc, while nickel was closely associated with cadmium. SSC was strongly associated with metal concentrations (similarity > 0.75).This analysis showed that metals were closely correlated with each other (supporting the findings of the Pearson single pair analyses), indicating possible similar sources of these metals. Ammonia, total N, total P, and carbonate concentrations were identified as separate individual clusters, possibly indicating a different main source for these parameters.

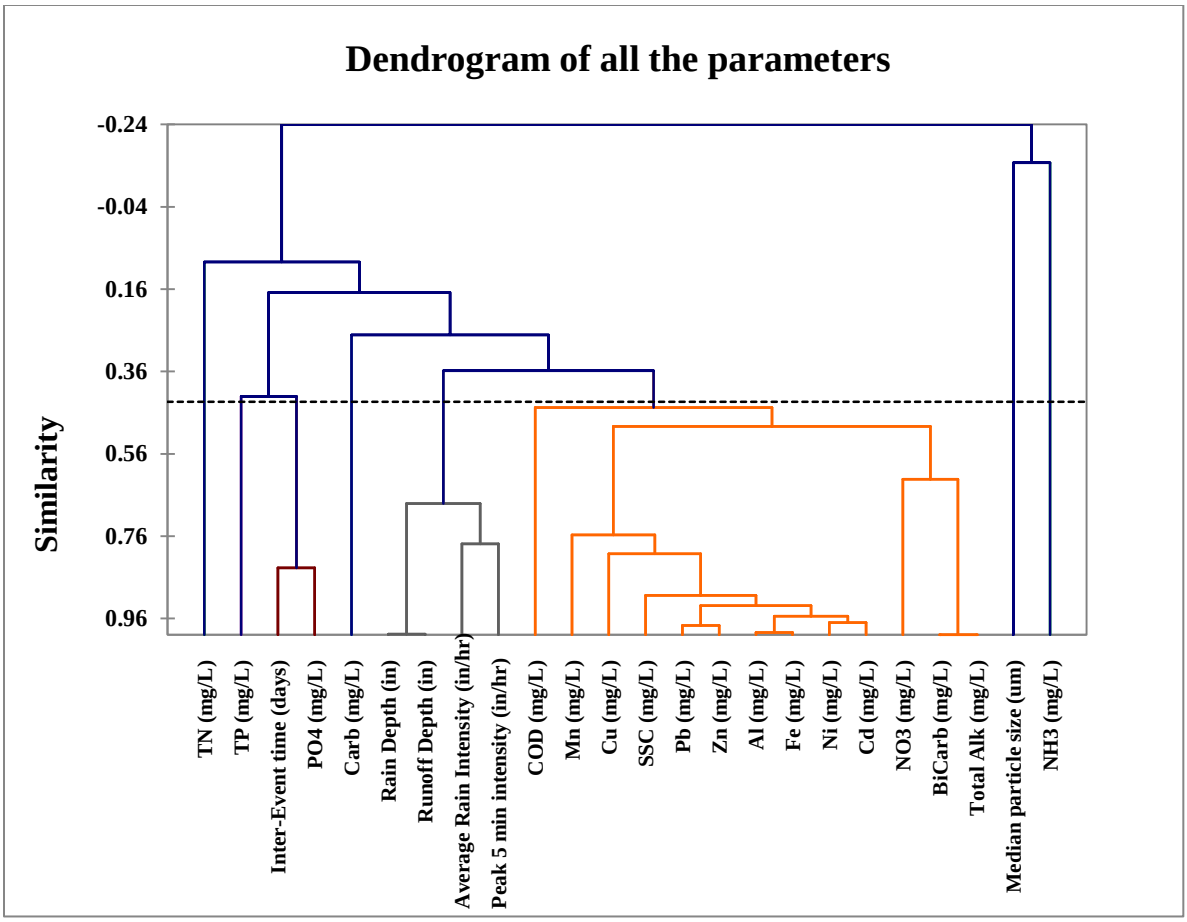

Figure 2-14 Dendogram from Cluster analysis for all the hydrologic and water quality parameters

2.3.8 Principal Component Analyses

Principal Component Analyses (PCA) are a data reduction statistical method which reduces large sets of data variables into smaller sets explaining the variance-covariance structure of the variables through linear combinations (Johnson, et al. 2007). Principal components are derived from the original data sets which retain most of the variance in the data. The maximum amount of variance is usually expressed by the first component with successive components accounting for the remaining amounts of the variance. Variance of data is expressed in terms of eigen vectors and eigenvalues which exist in pairs. Eigen vectors represent the direction of the variance

and eigenvalue represents how much variance is exhibited in that direction. Principal component analyses were performed to identify groupings of parameters with similarities, specifically how they explain the variability in the data. PCA was conducted on all the 24 parameters included in the study. The amounts of the total variance explained by the first six principal component groups are shown in Table 2-11, and the loadings of all the principal components are shown in Table 2-12.

Table 2-11 Percent of total variance explained by first six principal components

Principal Component	Eigenvalue	Variability (%)	Cumulative %
F1	11.064	46.1	46
F2	3.842	16.0	62
F3	2.690	11.2	73
F4	1.581	6.6	80
F5	1.353	5.6	86
F6	1.215	5.1	91

Table 2-12 Loadings of all the principal components

	F1	F2	F3	F4	F5	F6	F7	F8	F9	F10
Rain Depth (in)	0.532	0.561*	0.492	0.232	0.045	-0.196	-0.239	0.029	0.086	0.004
Runoff Depth (in)	0.537	0.560	0.507	0.196	0.047	-0.209	-0.229	0.010	0.053	0.023
Average Rain Intensity (in/hr)	0.609	0.309	0.521	-0.154	-0.313	0.217	0.240	-0.046	-0.162	0.089
Peak 5 min intensity (in/hr)	0.678	0.563	0.198	0.002	-0.200	-0.261	0.212	-0.061	-0.136	0.096
Inter-Event time (days)	0.424	0.687	-0.244	-0.151	0.283	-0.335	0.198	0.137	-0.123	-0.027
Median particle size (um)	-0.399	-0.336	0.302	0.579	-0.139	-0.174	0.067	0.481	-0.127	-0.008
SSC	0.974	0.082	0.079	-0.144	0.061	0.012	-0.033	0.036	-0.048	-0.100
Al (mg/L)	0.951	-0.203	-0.011	-0.170	-0.070	0.034	-0.071	0.081	0.057	0.058
Cu (mg/L)	0.834	0.158	-0.358	0.285	-0.152	0.062	0.061	0.008	-0.180	0.087
Pb (mg/L)	0.910	-0.144	-0.261	-0.005	-0.185	-0.060	-0.088	0.128	-0.095	-0.104
Fe (mg/L)	0.962	-0.211	-0.046	-0.108	-0.085	-0.017	-0.045	0.065	0.046	0.026
Mn (mg/L)	0.838	-0.210	0.349	-0.299	-0.028	0.176	-0.026	-0.069	0.062	-0.028
Ni (mg/L)	0.952	-0.098	-0.163	-0.079	-0.076	0.046	-0.199	-0.026	0.048	0.022
Zn (mg/L)	0.925	-0.079	-0.321	0.057	-0.089	0.060	-0.068	0.035	-0.070	-0.094
Cd (mg/L)	0.949	-0.029	-0.166	-0.082	-0.034	0.229	-0.084	0.037	0.048	-0.020
COD (mg/L)	0.545	0.132	-0.079	0.561	0.352	0.242	-0.423	0.019	0.052	-0.018
NH3 (mg/L)	-0.380	0.361	-0.111	-0.322	0.366	0.543	-0.053	0.334	-0.254	0.027

NO3 (mg/L)	0.647	-0.317	0.059	0.251	0.238	0.292	0.391	0.140	0.264	0.177
PO4 (mg/L)	0.168	0.571	-0.516	-0.130	0.529	-0.252	0.063	-0.026	0.103	0.062
TN (mg/L)	0.230	-0.539	-0.573	-0.204	-0.171	-0.433	-0.039	0.238	0.076	0.075
TP (mg/L)	0.285	0.484	-0.355	0.369	-0.158	0.183	0.559	-0.029	0.149	-0.170
BiCarb (mg/L)	0.510	-0.660	0.118	0.171	0.381	-0.128	0.154	-0.196	-0.193	-0.010
Carb (mg/L)	0.332	-0.218	0.689	-0.354	0.290	-0.145	0.208	0.245	0.139	-0.119
Total Alk (mg/L)	0.511	-0.660	0.123	0.168	0.382	-0.129	0.155	-0.194	-0.192	-0.011

* high-lighted values are the largest loadings for each constituent, indicating their most important component association

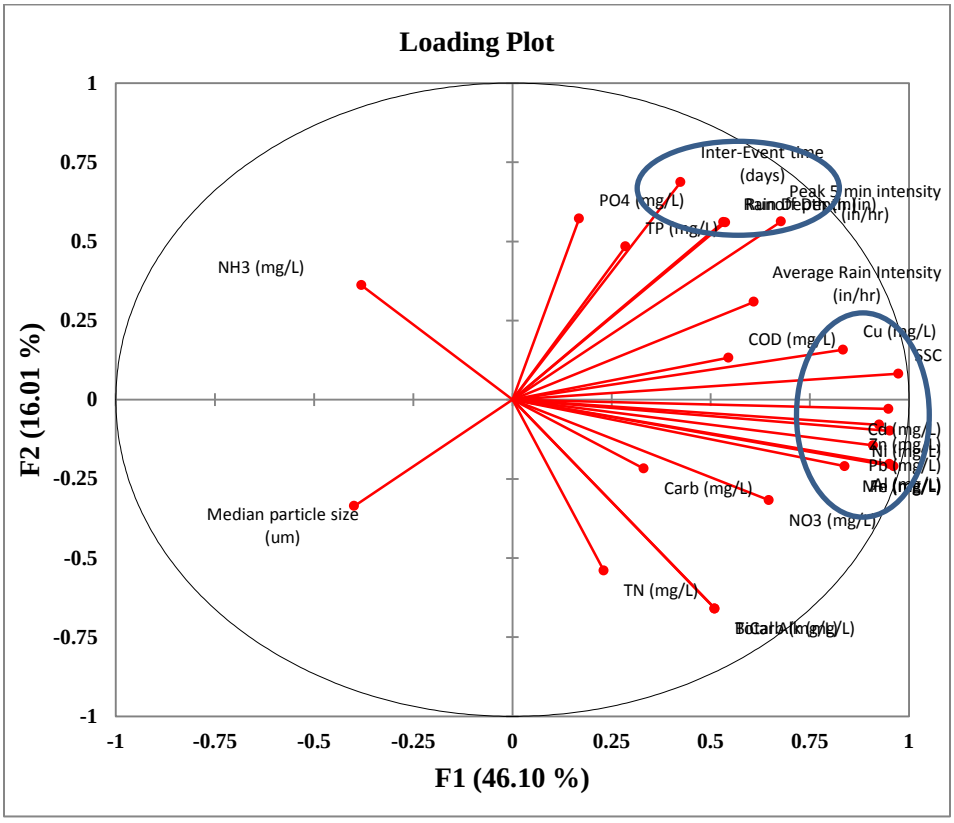

Figure 2-15 Principal component loadings for all the analyzed parameters in first two principal components

The principal component analyses resulted in most of the variance (62%) of the data being contained in the first two principal components F1 and F2. Rain intensity, SSC and metals have high loadings on the first principal component. Rain depth, runoff depth, inter-event time, and phosphate have high loadings on the second component. Runoff depth and average rain intensity

have high loadings on third component, while COD and median particle size have high loadings on the fourth component (Table 2-12).

In the loading plot, the variables that are highly correlated were represented by loadings situated closely to each other. As shown in Figure 2-15 and Table 2-12, loadings in F1 are mostly concerned with SSC and heavy metals, as some researchers have found that heavy metals were strongly associated with particulates (Glenn, *et al*. 2001, Hatje, *et al*. 2003, NSQD, Karlsson, *et al*. 2008). Rain depth and runoff depth have similar loadings on the first three factors.

Based on the principal component analyses, SSC and metal concentrations were identified as a similar group, and the hydrological parameters were identified as a similar group. The principal loadings in the first four principal components account for about 80% of the total variance and should reasonably represent the data.

2.3.9 Full 2^2 Factorial Analyses

Full 2^2 factorial analyses were performed on SSC, median particle size, and metals to examine the effects of rain depth and peak rain intensity, and their interactions on these concentrations to supplement the results obtained from the multivariate analyses. A full factorial analysis (Box, et al 1978) is a tool used for understanding the effect of two or more independent variables on a dependent variable. The factorial design identifies the effects of individual variables and their interaction on the dependent variable of interest (SSC, median particle size, pollutant concentrations, etc.). The effects of different variables are calculated using a table of contrasts, with the averages of the differences between the sums of the pollutant concentrations (or any dependent variable of interest) when the factor is at its maximum value and at its

minimum value. Probability plots of the calculated effects for individual plots and outliers (abnormal points) indicate the most important factors and different factor associations on the dependent variable of interest. Table 2-13 presents the group standard category and interaction of the factors. The high value of a factor is shown by '+' sign and the low value by a '-'sign. High and low values of the factors considered in the design are shown in Table 2-14 for the monitored events. The data were sorted into the four categories corresponding to the rain depth and intensity codes, and the factors for each main factor and interactions were calculated. The significant factors were identified by probability distributions of the results by observing which were not associated with the normal distribution of the calculated values.

Table 2-13 Factorial design showing experimental conditions for 4 runs (Box et al 1978)

Group	A	B	AB
1	+	+	+
2	+	-	-
3	-	+	-
4	-	-	+

A: Rain depth

B: Peak rain intensity

Table 2-14 2^2Full Factorial Design Variable Data

Rain Depth (code)	Peak Rain Intensity (code)
2.52 (high)	3.4 (high)
2.36 (high)	1.68 (high)
1.48 (high)	3.24 (high)
0.95 (high)	2.52 (high)
2.28 (high)	0.6 (low)
0.75 (high)	0.72 (low)
0.47 (low)	1.89 (high)
0.6 (low)	0.96 (high)
0.55 (low)	0.6 (low)
0.16 (low)	0.24 (low)
0.39 (low)	0.12 (low)
0.3 (low)	0.48 (low)
0.39 (low)	0.24 (low)
0.12 (low)	0.24 (low)
0.23 (low)	0.24 (low)
0.1 (low)	0.36 (low)

The effects of rain depth and peak rain intensity on different pollutants are analyzed and the results are shown in Appendix XX. Probability factors of the effects of the factors on SSC, median particle size, lead and copper and shown in Figure 2-16. It is observed that rain depth and peak rain intensity, or their interaction, aren't showing any significant effects on the SSC concentrations (based on the number of available observations). The summarized predicted values for the dependent variable are expressed using a square plot (Figure 2-17) showing the predicted values (SSC in this case) for the two factors (rain depth, and peak rain intensity) at a time. The rain depth appears to have an effect on the SSC concentration (but was shown not to be significant based on the number of data observations), while there is no apparent difference for the peak rain intensity.

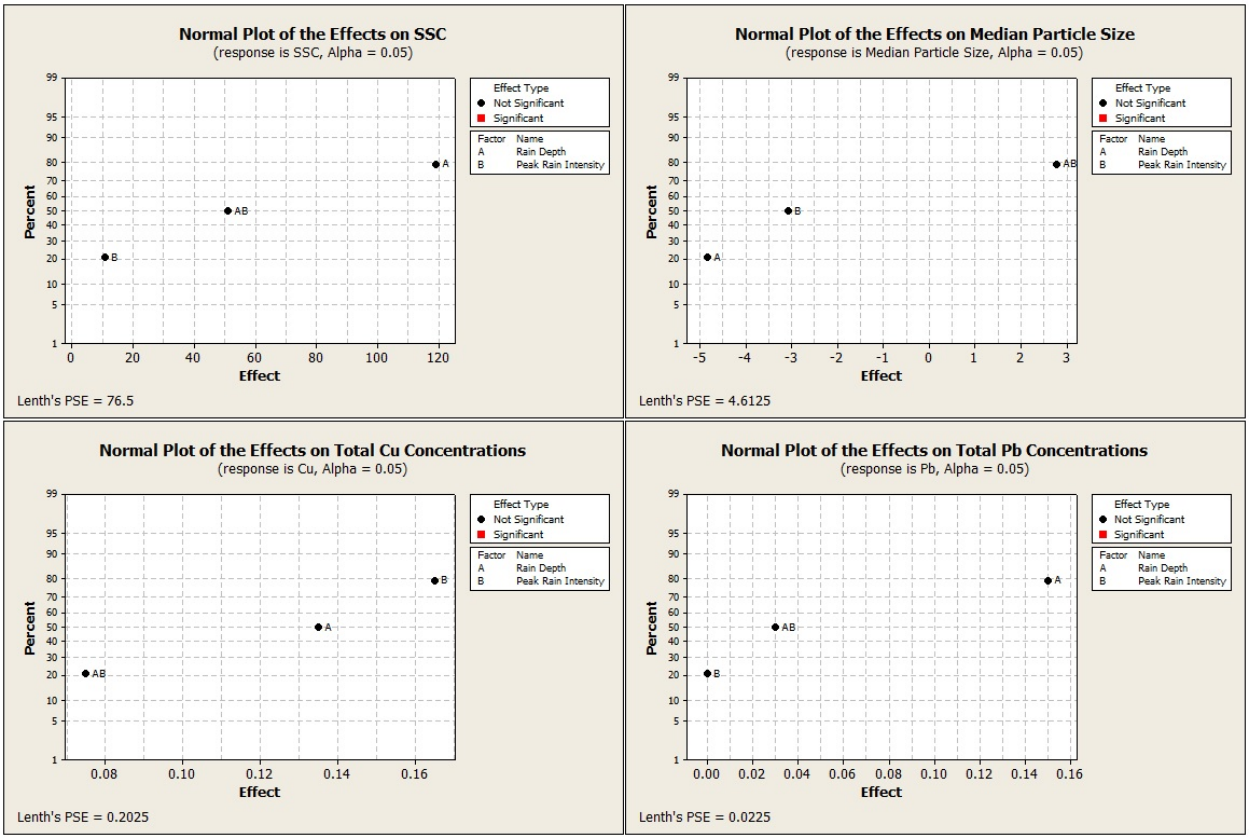

Figure 2-16 Normal plots of effects of rain depth and peak rain intensity on SSC, median particle size, Total Pb and Total Cu

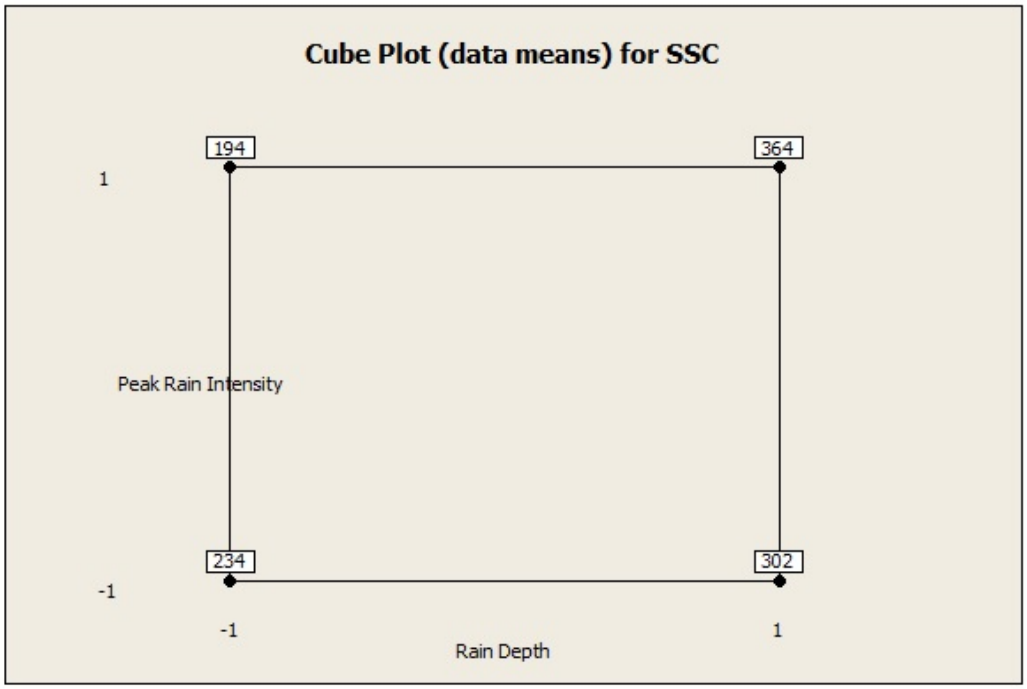

Figure 2-17 Cube plot for data means for SSC

Similar results are found for all the metal constituents and nutrients included in the study. This indicates that the pollutant concentrations are not source limited (associated with pollutants washed off leaving "clean" surfaces with large rains).

2.3.10 Particle size distributions and association of pollutants with particulate matter

The results of particle size distributions for all the analyzed influent samples are shown in Figure 2-18.

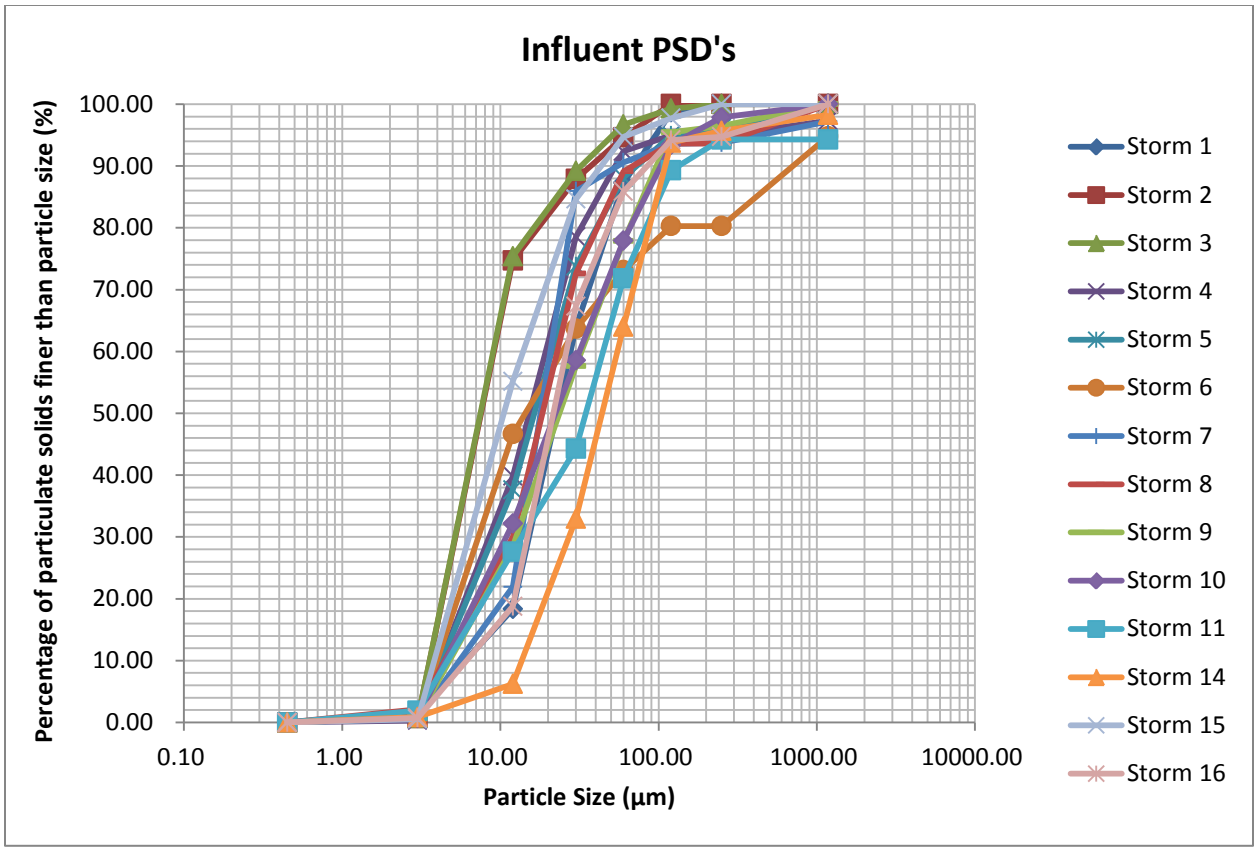

Figure 2-18 Particle Size Distributions for all the monitored influent samples

Median particle sizes for all the monitored events ranged between 7.5 to 45 µm, with an average median particle size of 21 µm. These particle size distributions were similar to previous studies (House, *et al*. 1993, Pitt, *et al*. 1995). Almost all (80+ %) of the suspended sediment is distributed in the particle size range of 3 and 120 µm.

2.3.11 Relationships among median particle size and other parameters

Figures 2-19 to 2-25 represent scatterplots of median particle size with hydrologic parameters, SSC, total Cu, total Pb and total Zn, while the relationships of median particle size with all the parameters included in the study are shown in Appendix XX.

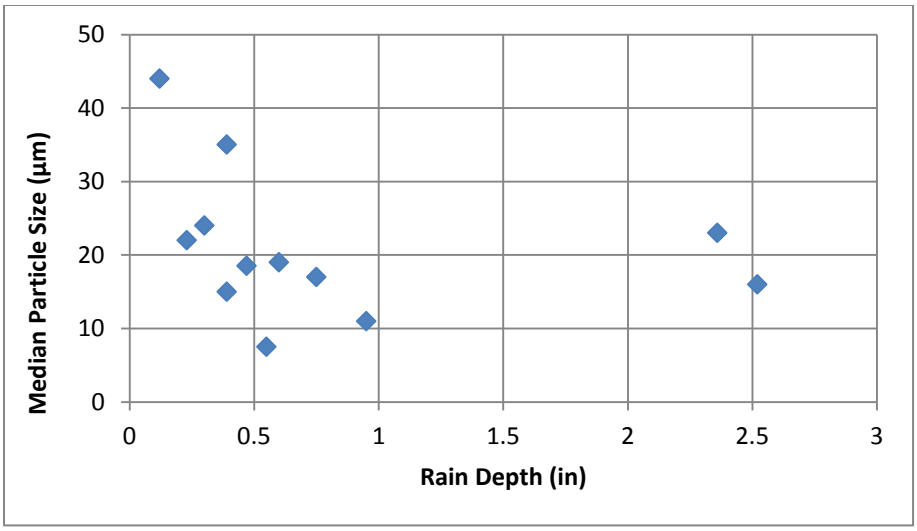

Figure 2-19 Scatterplot of Rain depth vs Median Particle Size (no significant regression relationship)

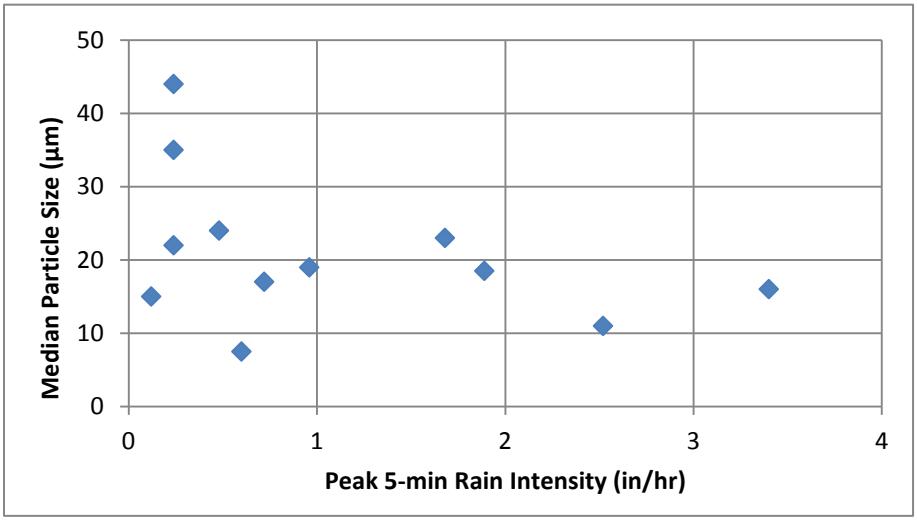

Figure 2-20 Scatterplot of Peak Rain Intensity vs Median Particle Size (no significant regression relationship)

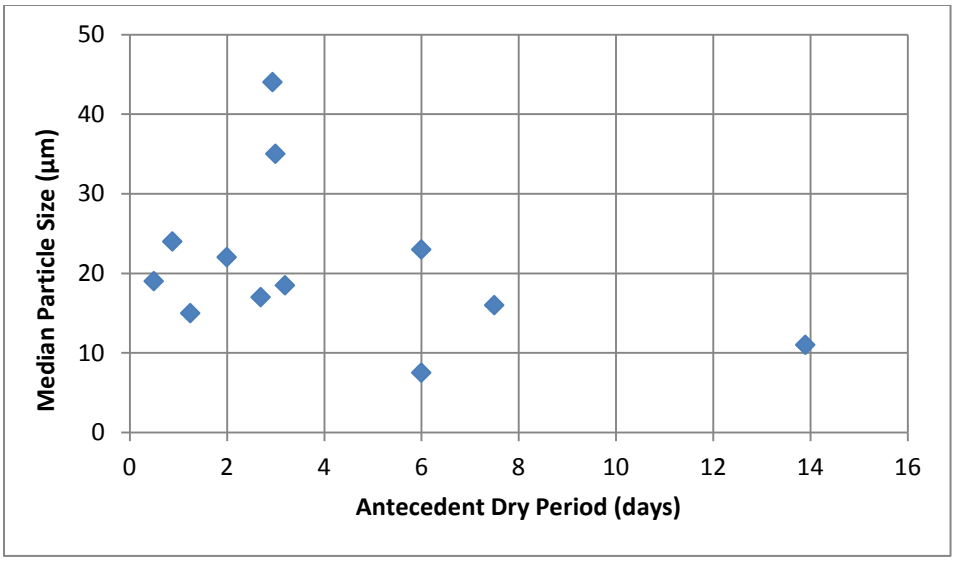

Figure 2-21 Scatterplot of Antecedent Dry Period vs Median Particle Size (no significant regression relationship)

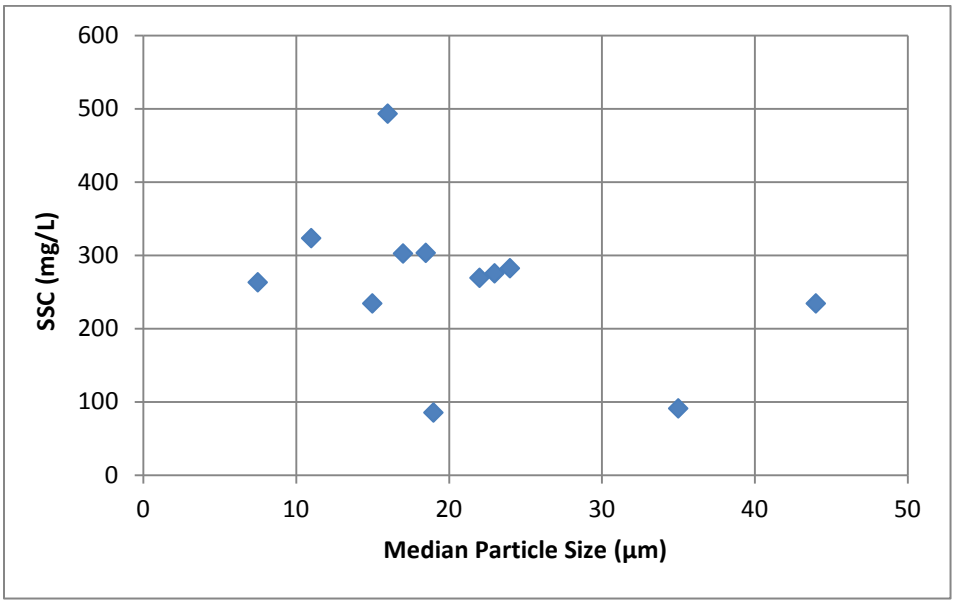

Figure 2-22 Scatterplot of Median Particle Size vs SSC (no significant regression relationship)

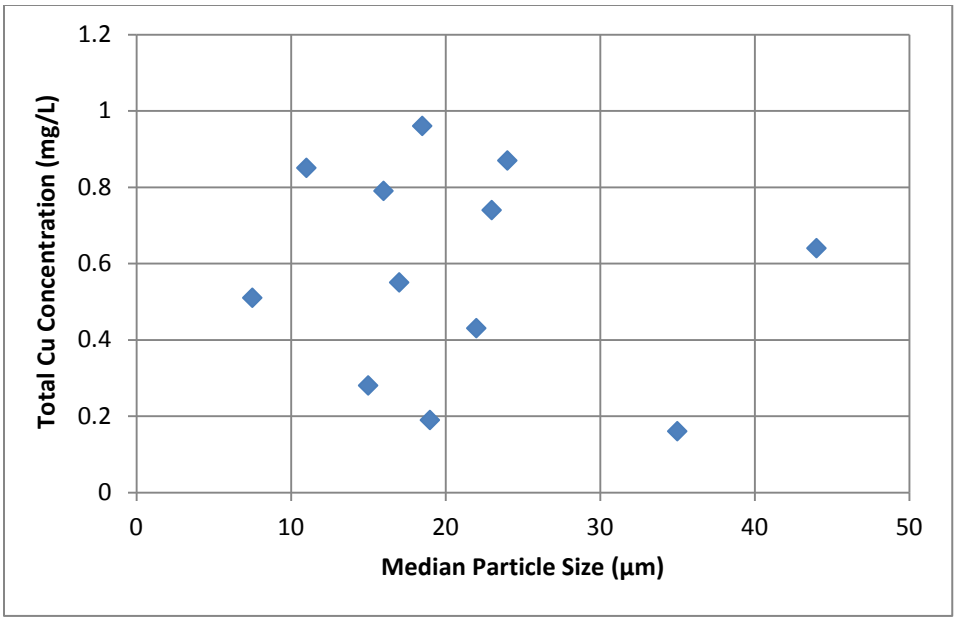

Figure 2-23 Scatterplot of Median Particle Size vs Total Cu Concentration (no significant regression relationship)

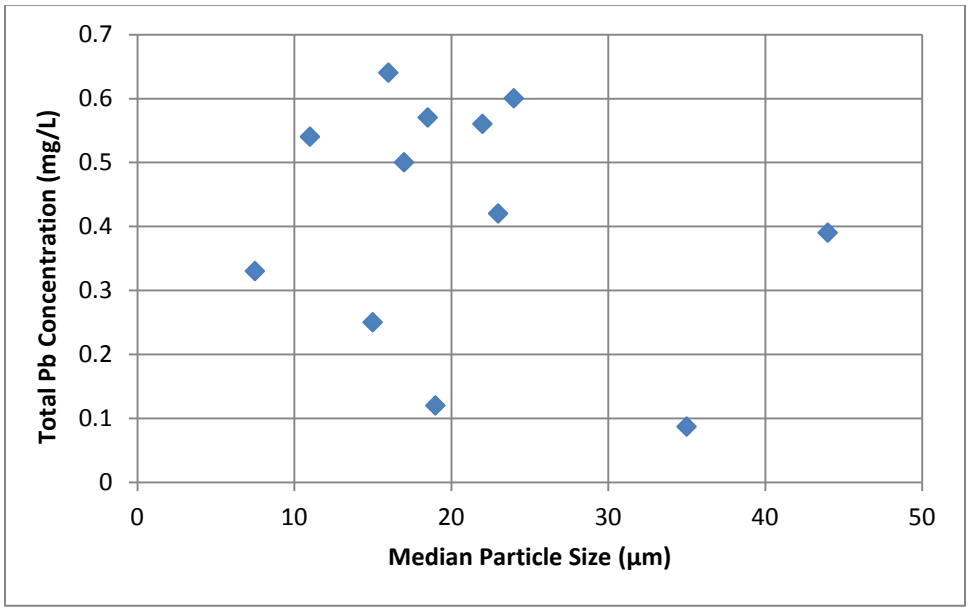

Figure 2-24 Scatterplot of Median Particle Size vs Total Pb Concentration (no significant regression relationship)

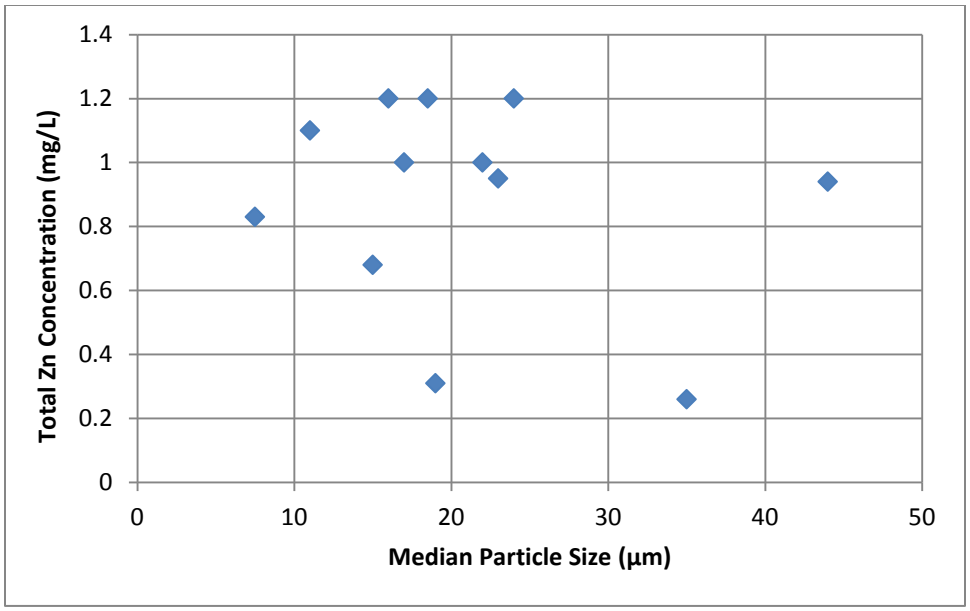

Figure 2-25 Scatterplot of Median Particle Size vs Total Zn Concentration (no significant regression relationship)

Median particle sizes of the influent particulates apparently decreased with increases in rain depth, rain intensity and antecedent dry period, but without any significant relationships. Suspended sediment and total metal concentrations apparently increased with decreases in median particle size, but again with no significant relationships. It was previously observed that median particle size showed apparent negative correlations (not significant) with all the parameters included in the study except for TN, carbonate, bicarbonate and total alkalinity (Table 8). Cluster analysis identified median particle size as a separate cluster in relation to the other parameters. Principal component analysis showed negative loadings of median particle size on the first two principal components and low to moderate loadings on the third and fourth principal components accounting for very little to no variance in the data.

Figures 2-26 through 2-35 show the cumulative concentrations of pollutants for different particle size ranges. The concentrations would decrease with the preferential removal of large particulates, as occurs in sedimentation type devices (both the hydrodynamic separator and the infiltrating dry pond at this site). Small portions of the contaminants are found in the smallest

particles sizes <5 µm. The majority of the pollutant concentrations (and mass) are associated with the 10 to 100 µm particle size range. Pre-treatment sedimentation controls removing only the largest particles (>100 µm for example) would only small effects on the resulting treated water concentrations (about 20% removals). More effective treatment controls that can remove smaller particles would result in better effluent quality (down to about 5 µm, beyond which little additional benefit is possible by sedimentation processes).

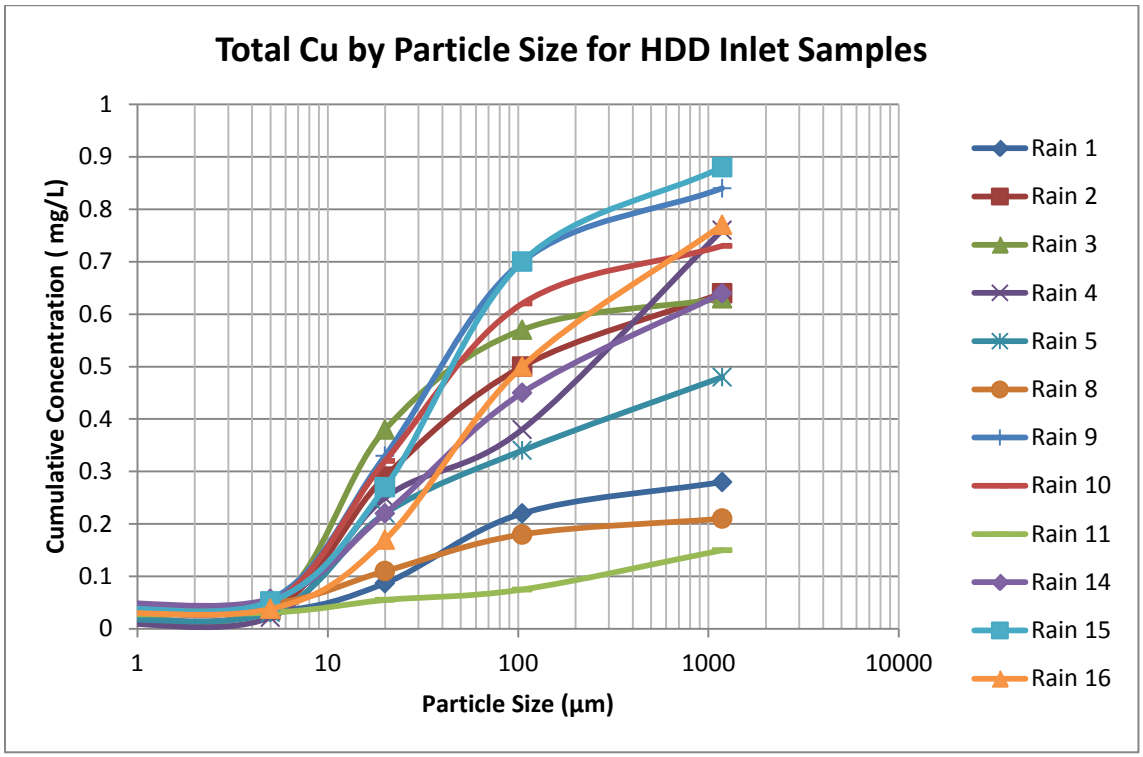

Figure 2-26 Cumulative concentration of Total Copper by Particle Size

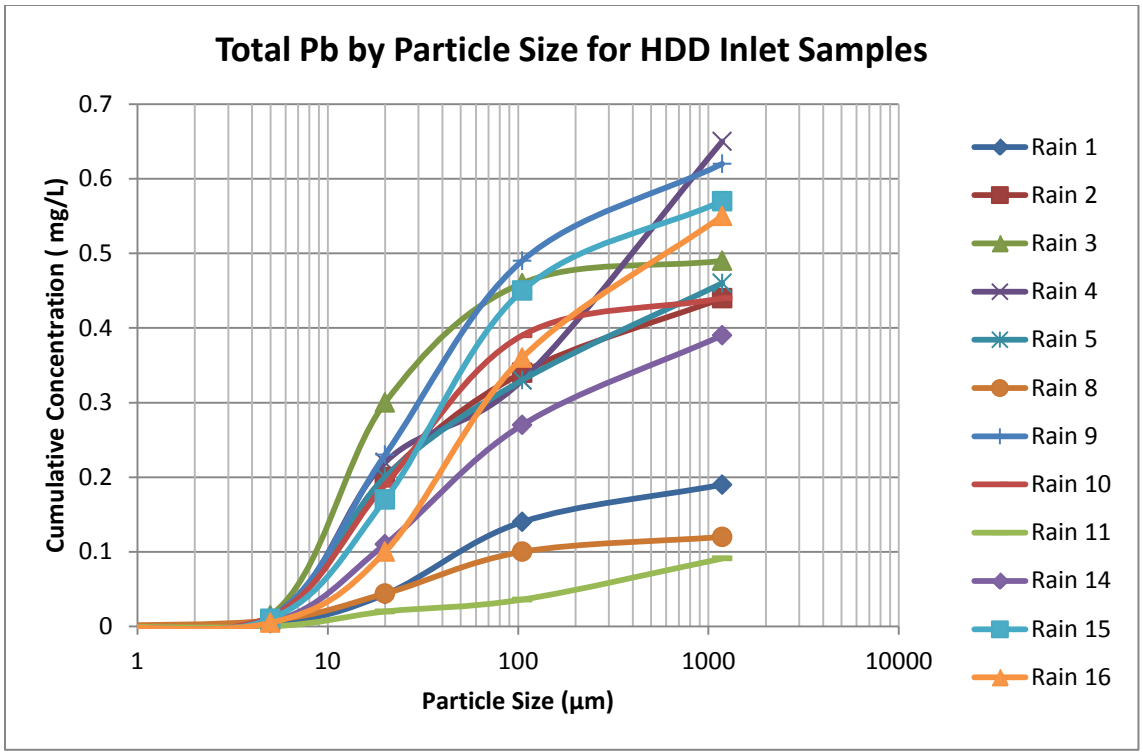

Figure 2-27 Cumulative concentration of Total Lead by Particle Size

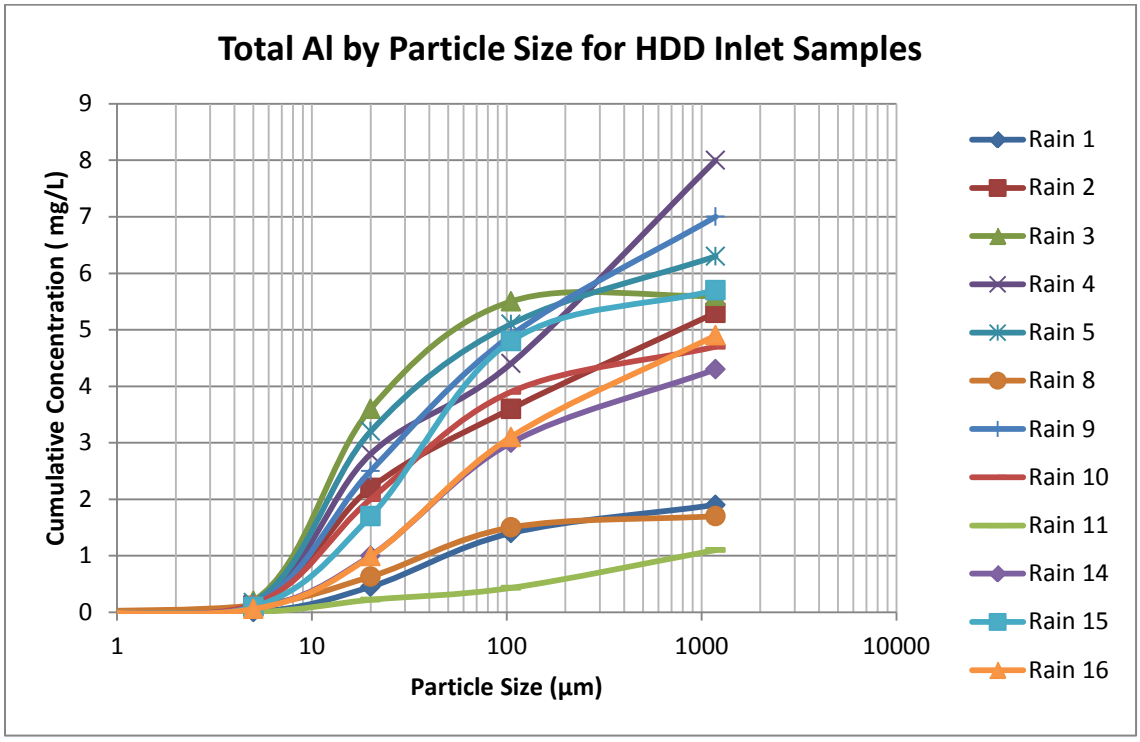

Figure 2-28 Cumulative concentration of Total Aluminum by Particle Size

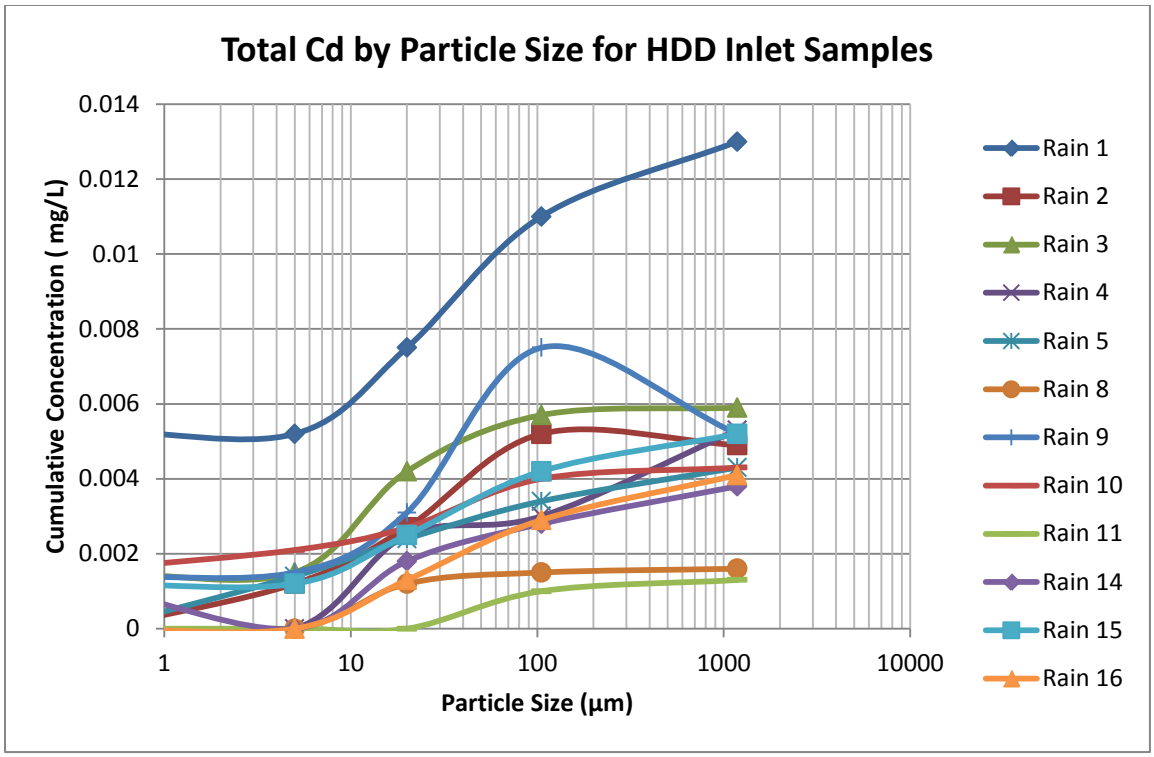

Figure 2-29 Cumulative concentration of Total Cadmium by Particle Size

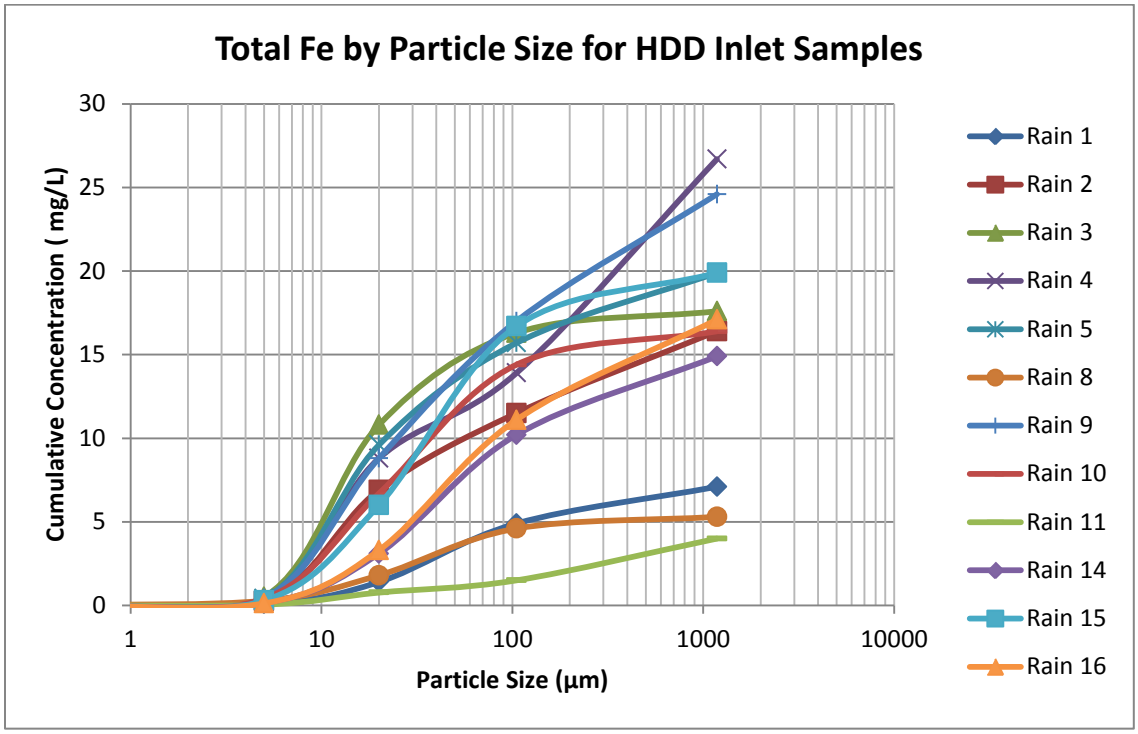

Figure 2-30 Cumulative concentration of Total Iron by Particle Size

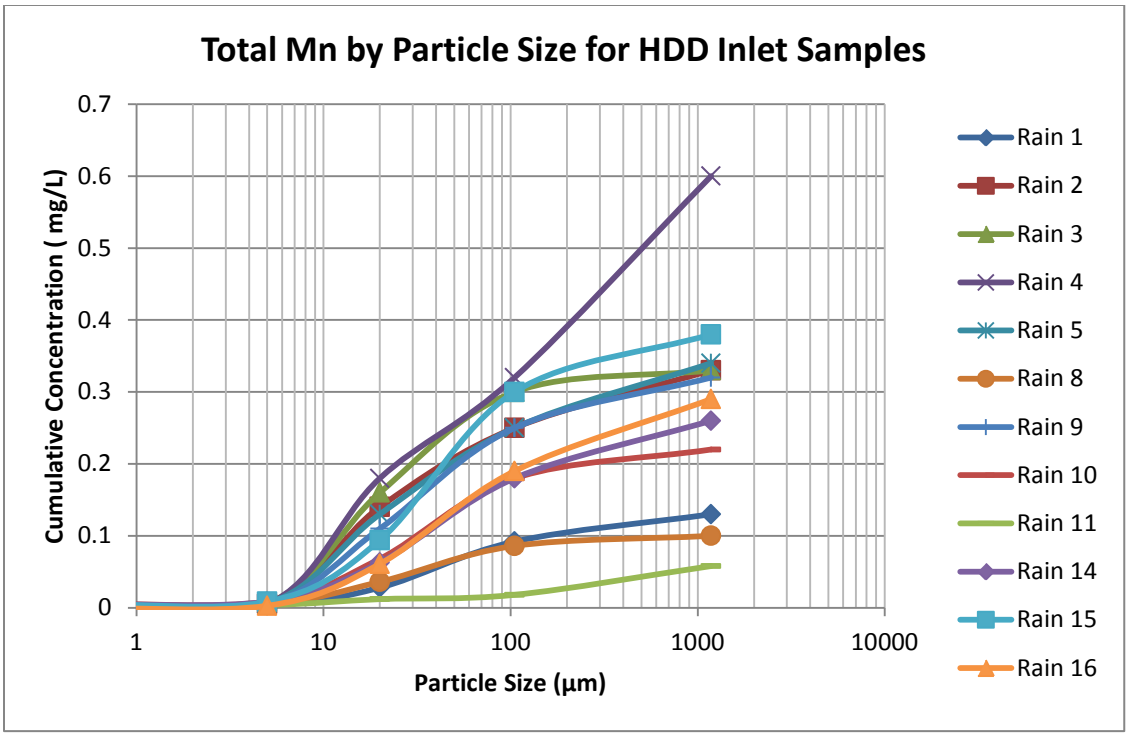

Figure 2-31 Cumulative concentration of Total Manganese by Particle Size

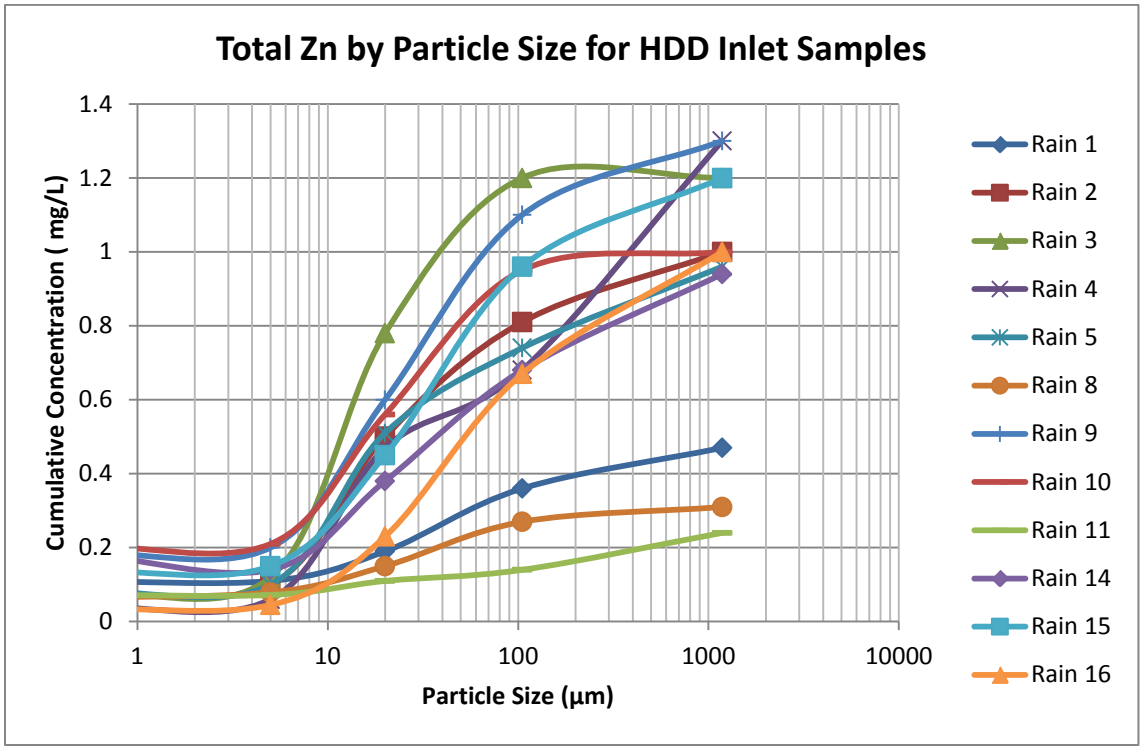

Figure 2-32 Cumulative concentration of Total Zinc by Particle Size

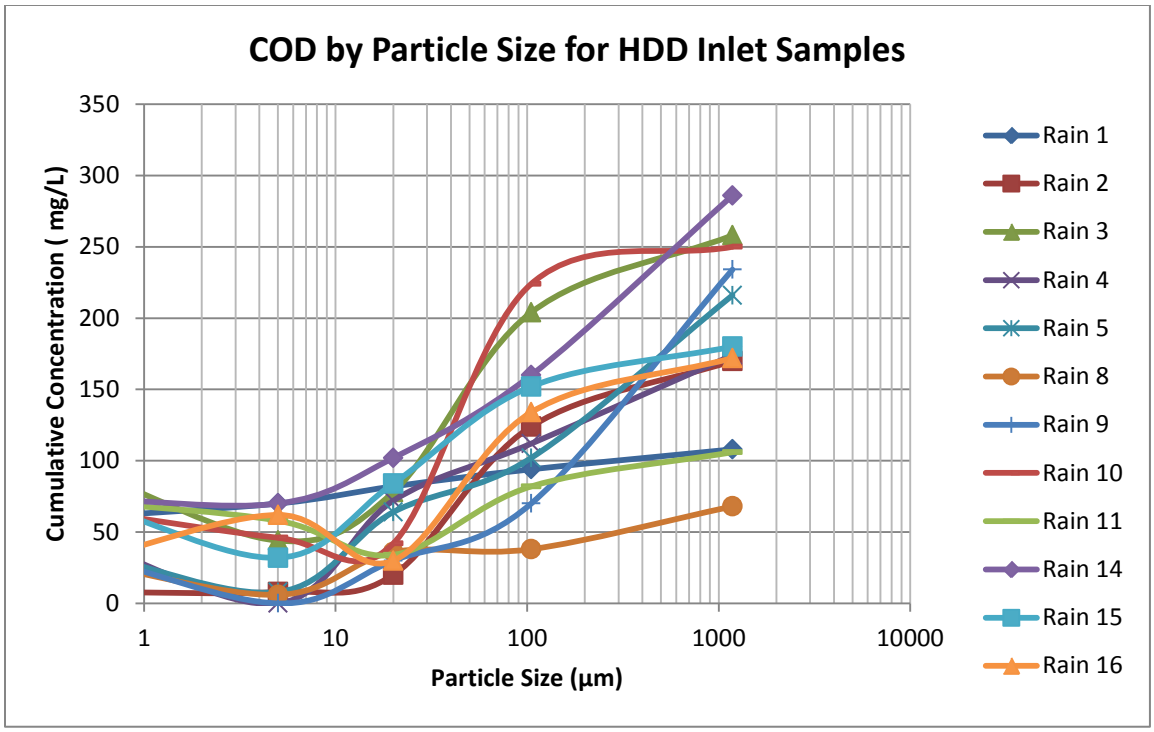

Figure 2-33 Cumulative concentration of COD by Particle Size

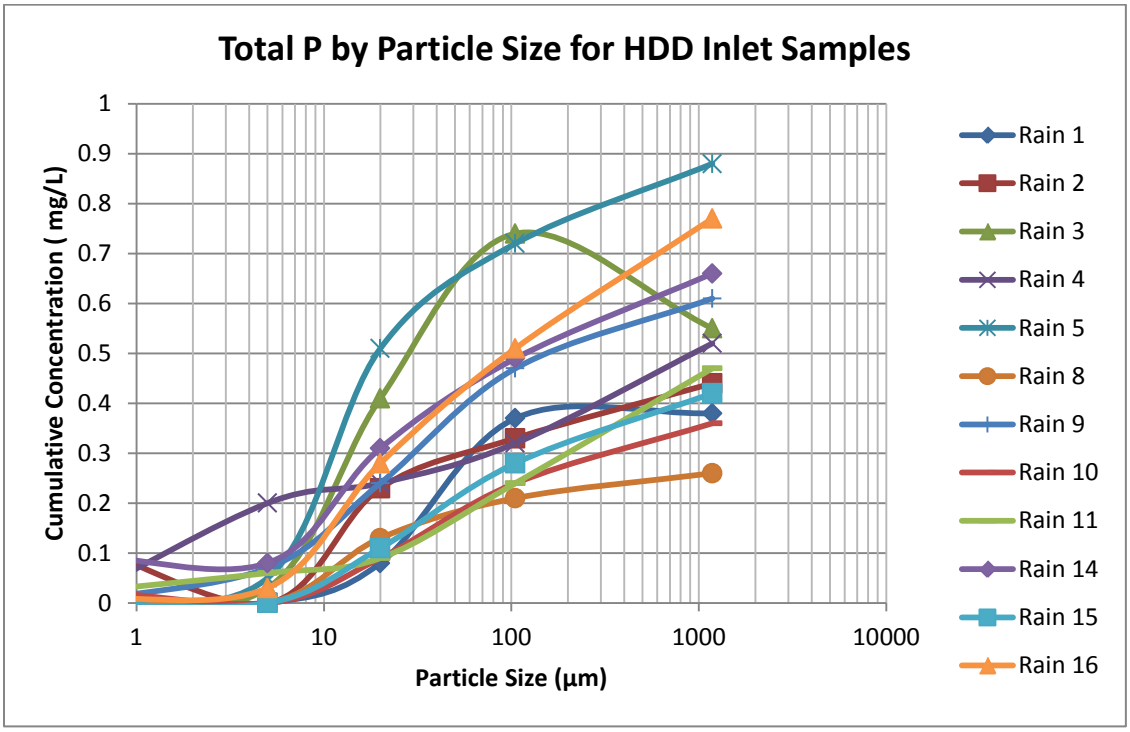

Figure 2-34 Cumulative concentration of Total Phosphorous by Particle Size

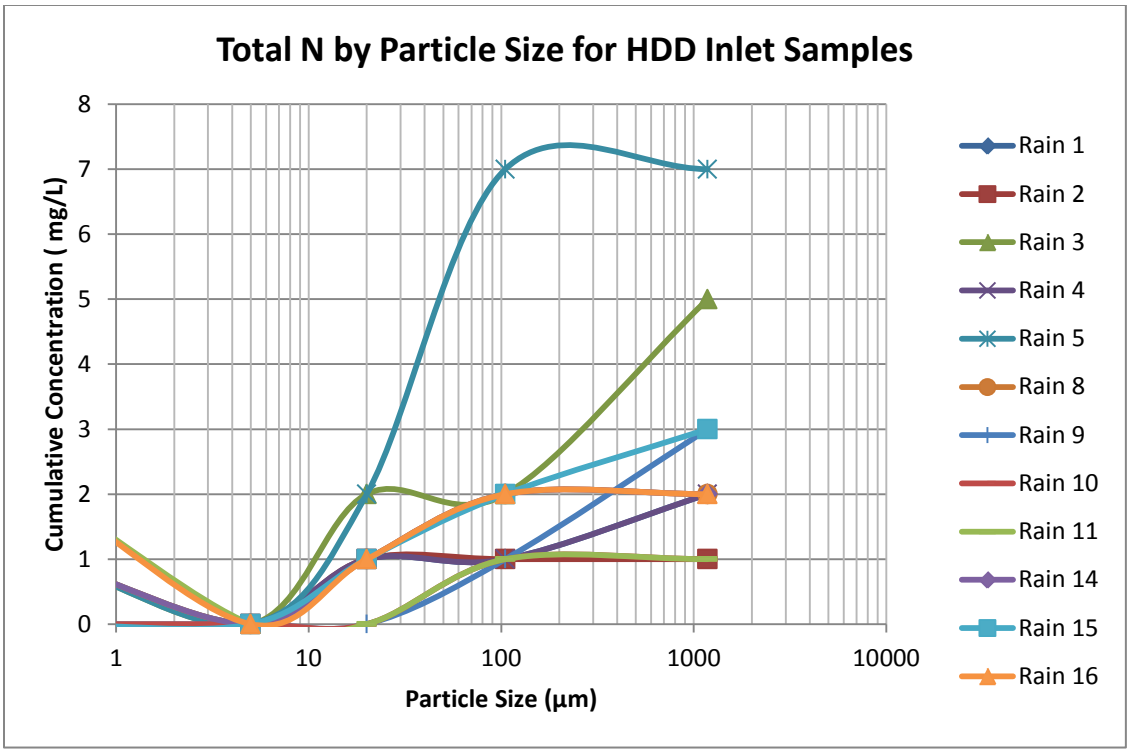

Figure 2-35 Cumulative concentration of Total Nitrogen by Particle Size

2.3.12 Pollutant Particulate Strengths

Associations of pollutants with different particle sizes (pollutant strengths) were calculated as the ratio of a particulate pollutant concentration to the suspended solid concentration, expressed in mg/kg. The strengths of stormwater particulates by particle size were calculated for metals, COD, TN and TP, as shown in Figures 2-36 through 2-47.

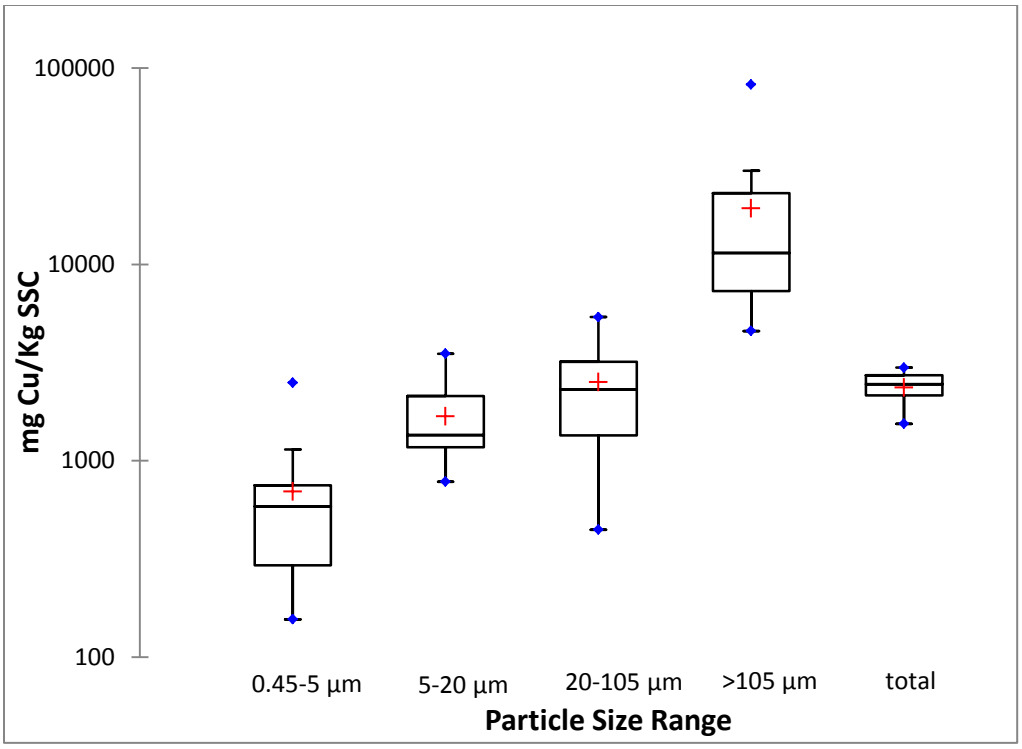

Figure 2-36 Copper Particulate Strengths by Particle Size

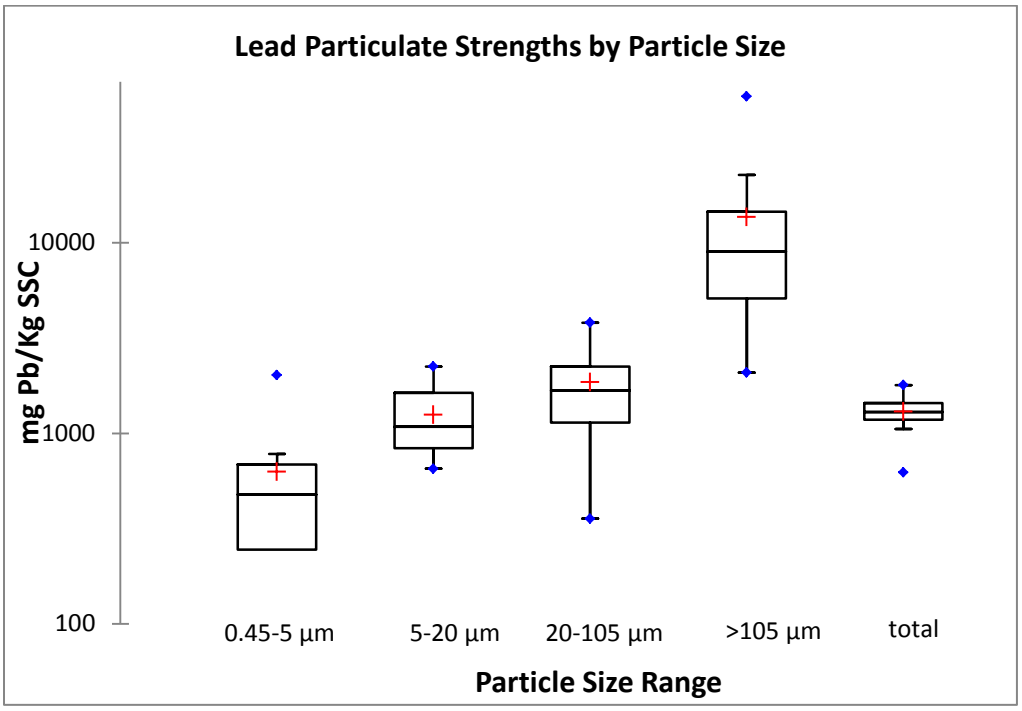

Figure 2-37 Lead Particulate Strengths by Particle Size

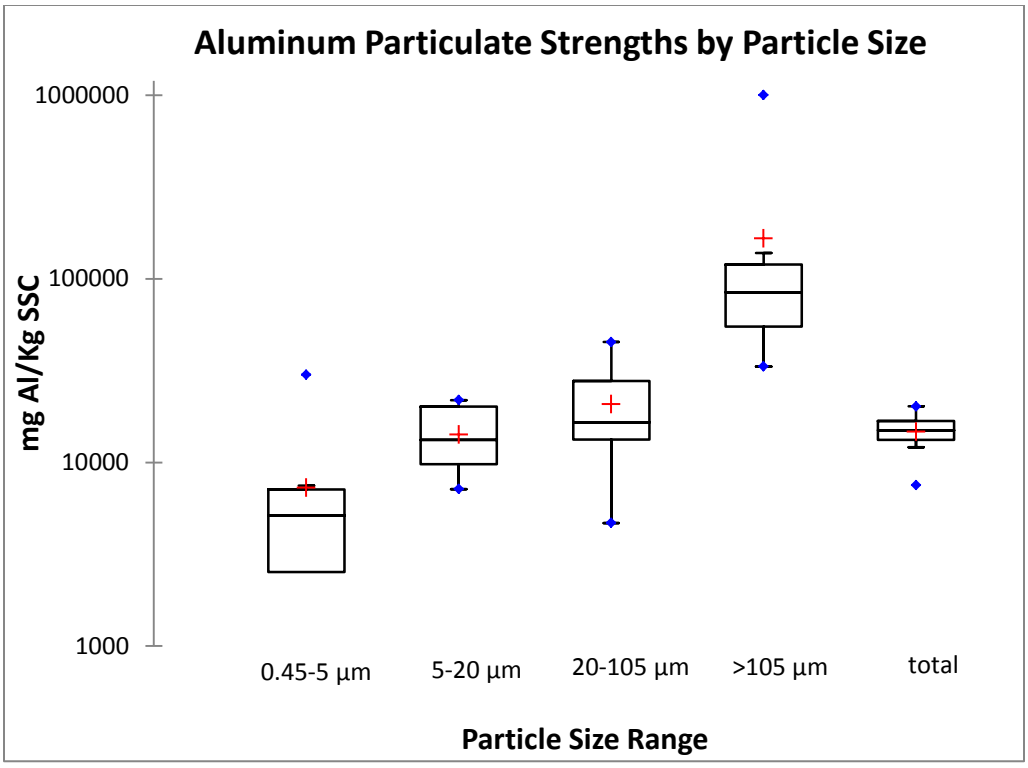

Figure 2-38 Aluminum Particulate Strengths by Particle Size

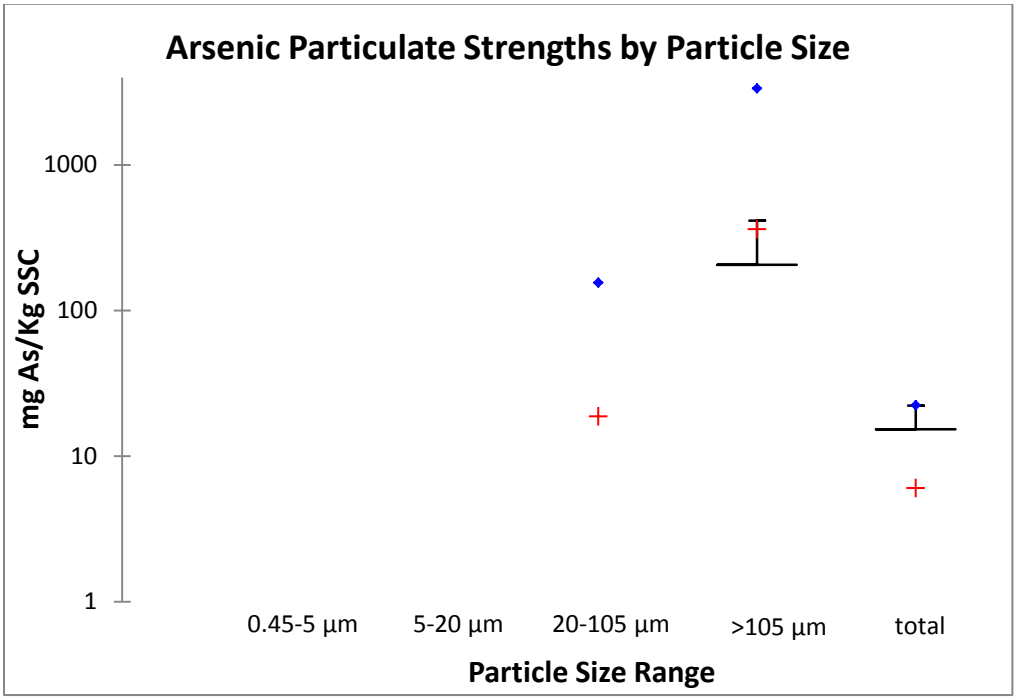

Figure 2-39 Arsenic Particulate Strengths by Particle Size

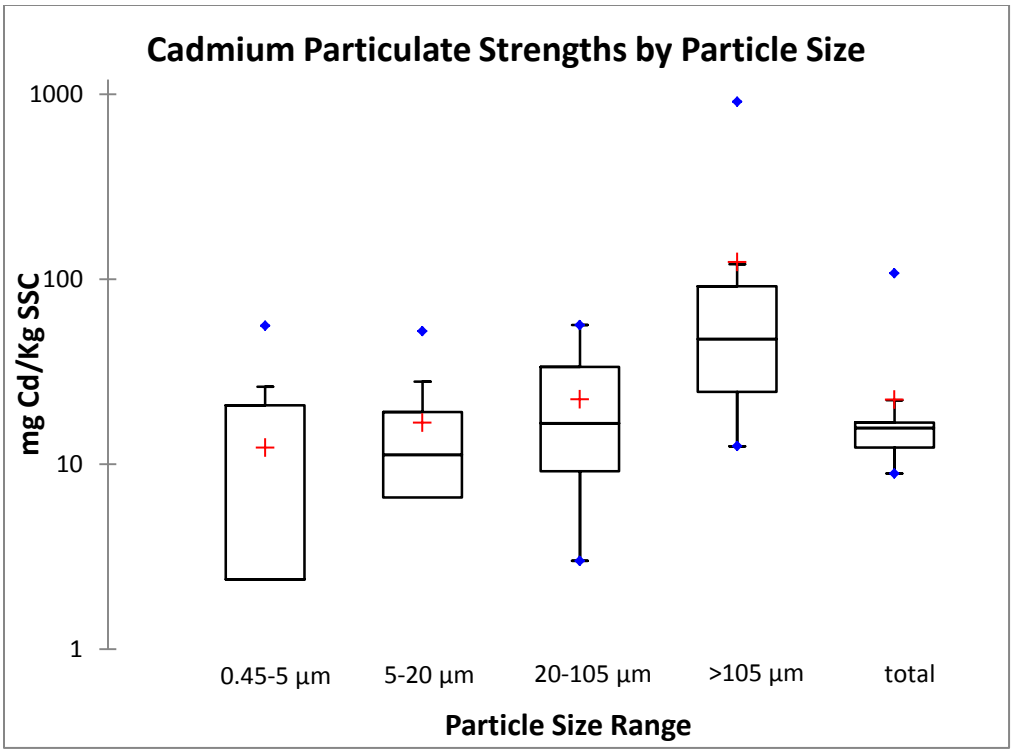

Figure 2-40 Cadmium Particulate Strengths by Particle Size

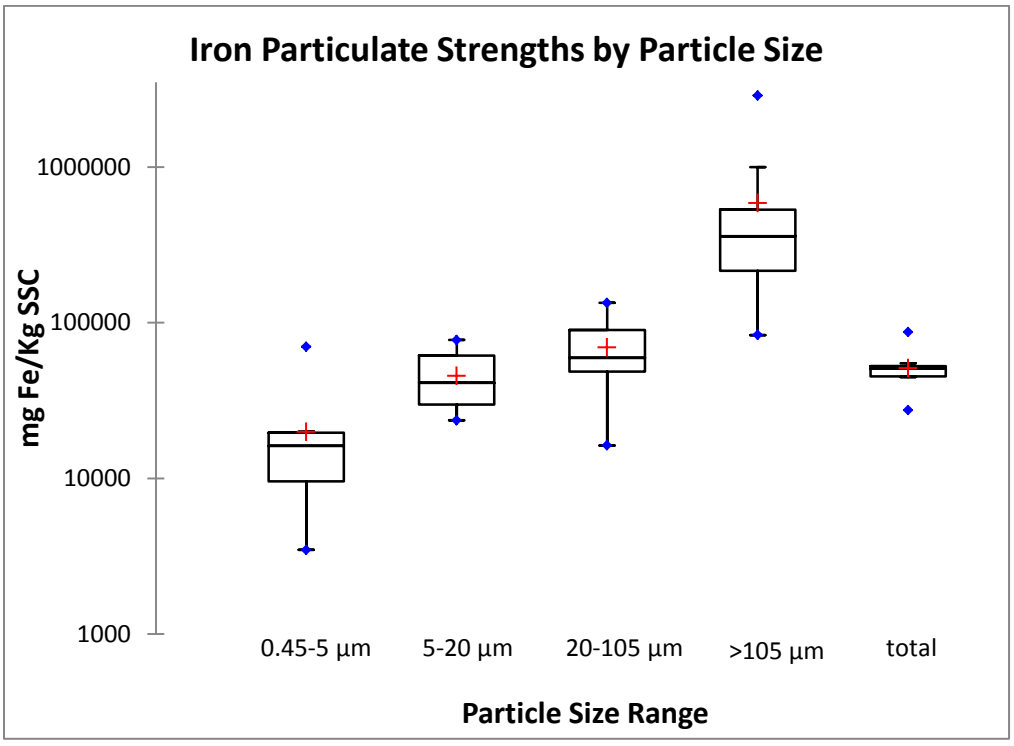

Figure 2-41 Iron Particulate Strengths by Particle Size

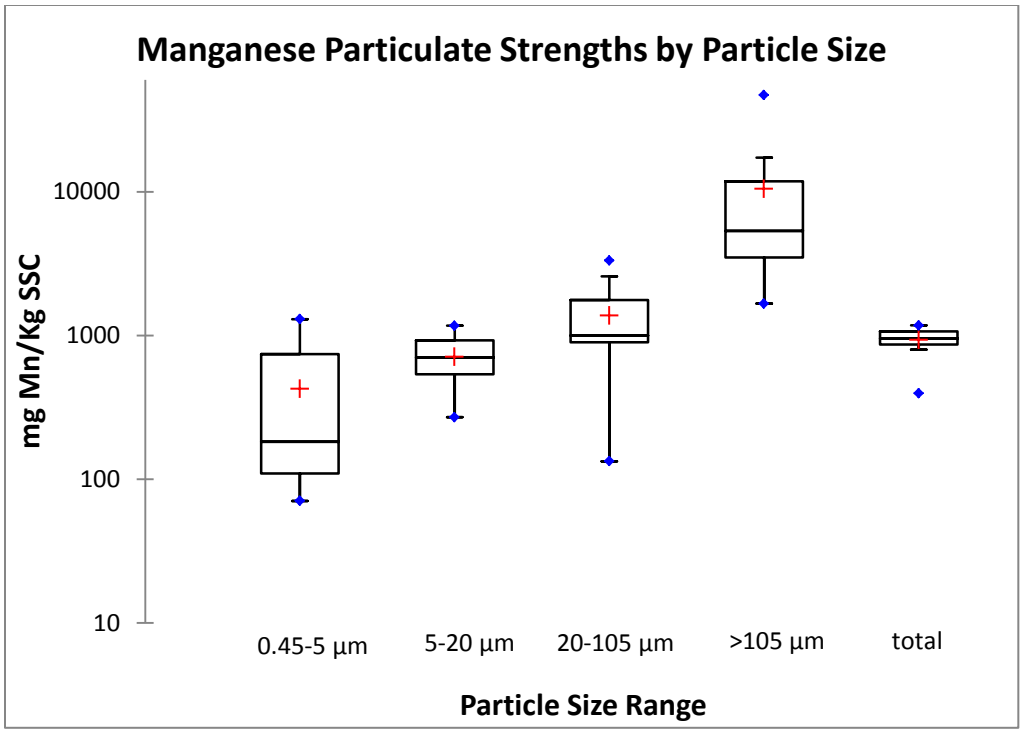

Figure 2-42 Manganese Particulate Strengths by Particle Size

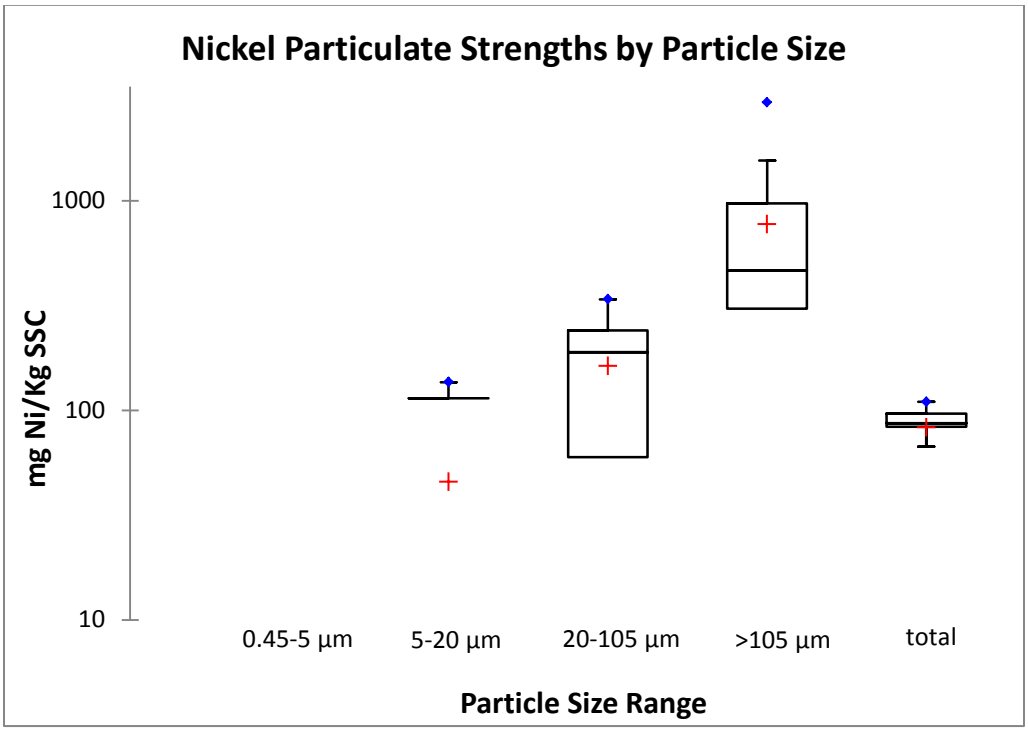

Figure 2-43 Nickel Particulate Strengths by Particle Size

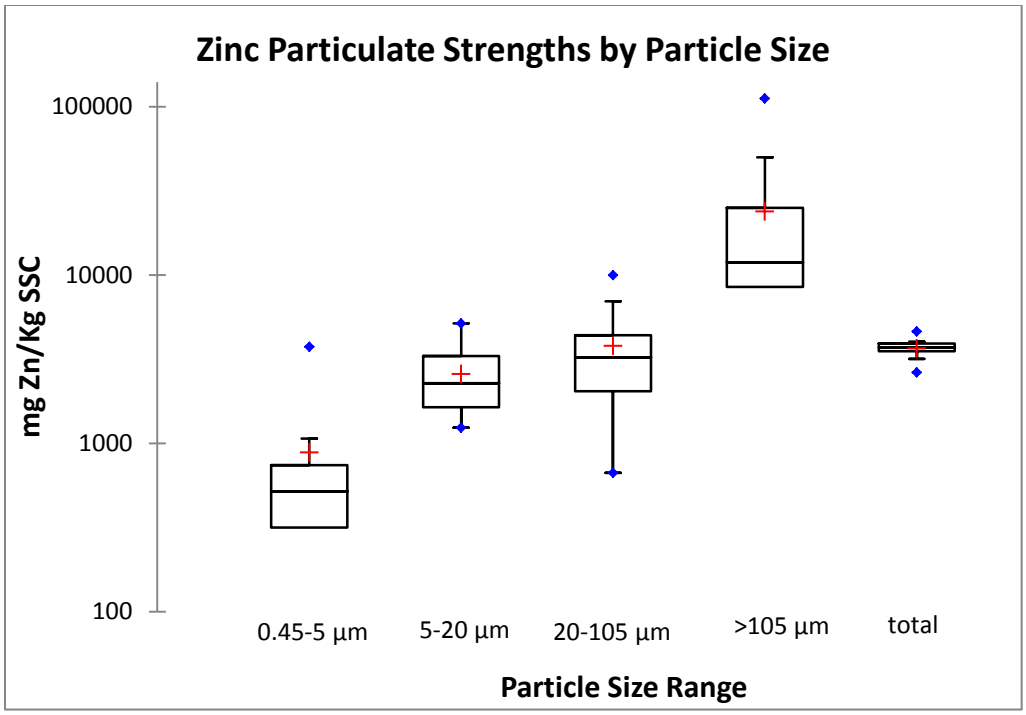

Figure 2-44 Zinc Particulate Strengths by Particle Size

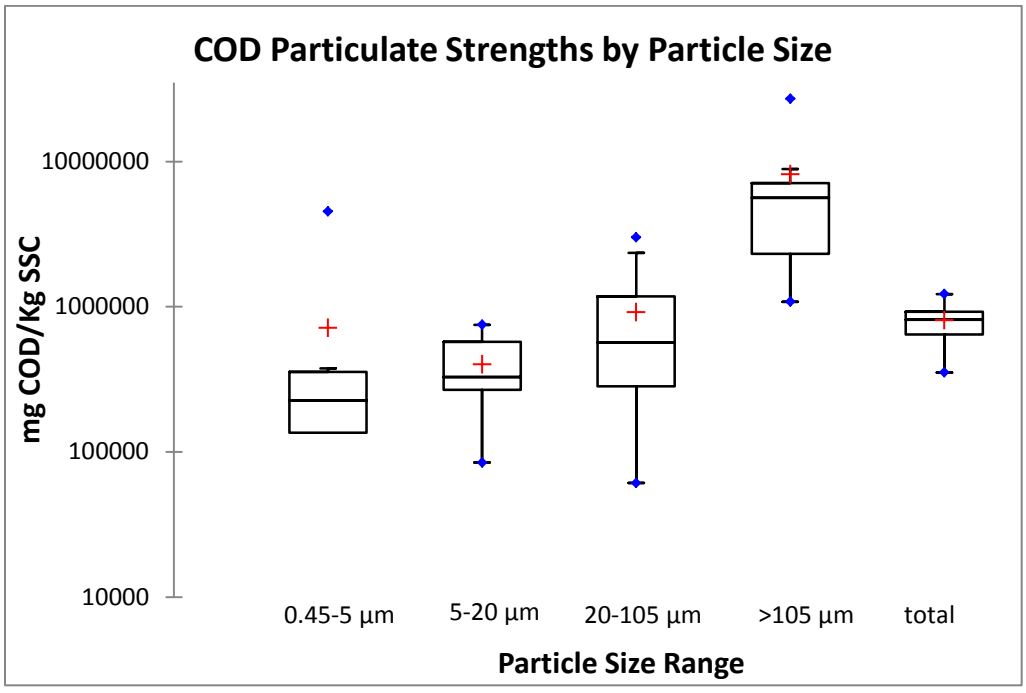

Figure 2-45 COD Particulate Strengths by Particle Size

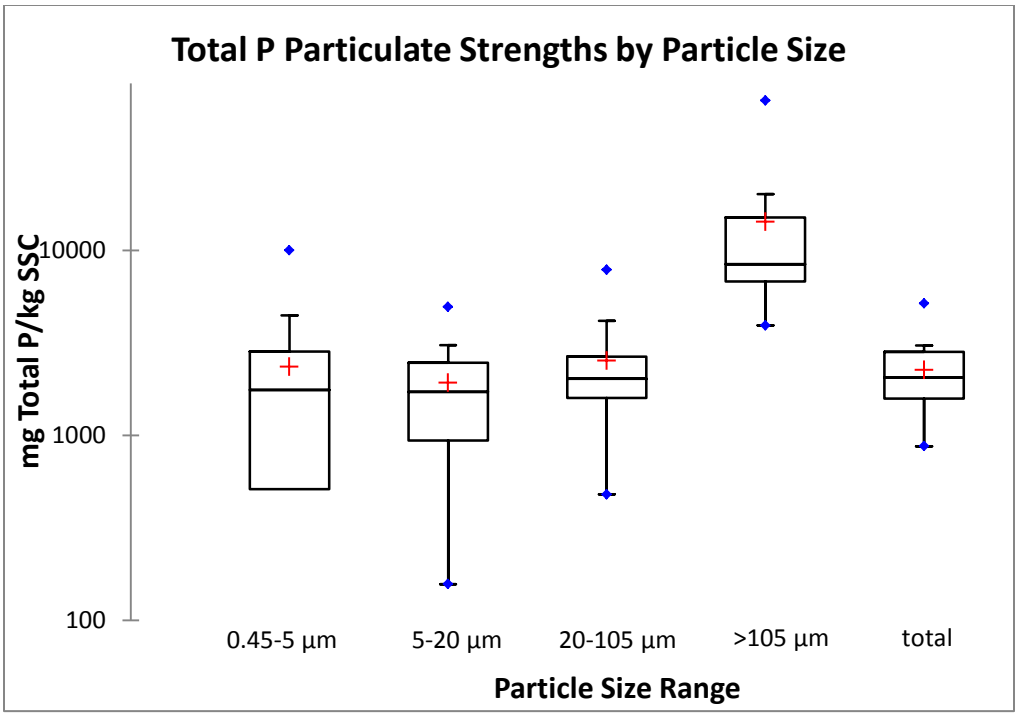

Figure 2-46 Total Phosphorous Particulate Strengths by Particle Size

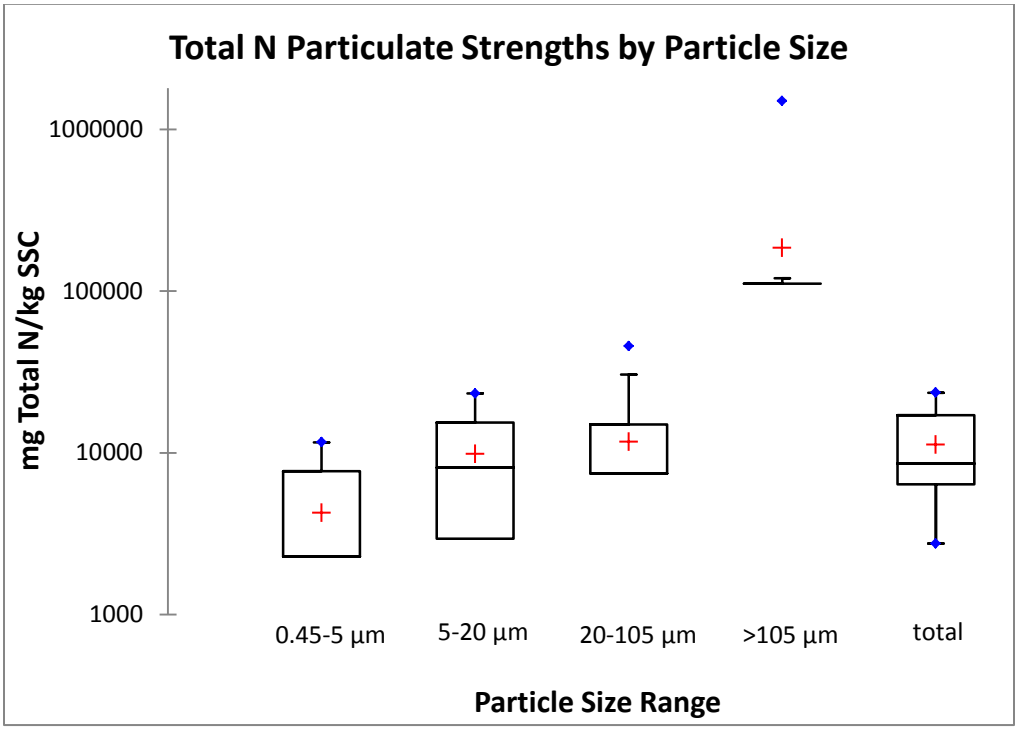

Figure 2-47 Total N Particulate Strengths by Particle Size

At this heavy industrial site, the particulate strengths tended to increase as the particle sizes increase. These results were similar to the results observed by Sansalone, et al. (1997). In general, metals tend to preferentially adsorb to smaller particle sizes due to larger surface areas. In this specific case, the higher particulate strengths associated with larger particle size ranges may be related to the nature of the runoff particulates from the industrial site that has large metal components.

The observed whole sample particulate strength data for Cu, Pb, Ni, and Zn are compared to the data presented in the NSQD for industrial sites as shown in Table 2-15.

Table 2-15 Observed particulate strengths of Cu, Pb, Ni, and Zn in comparison to NSQD industrial outfall observations

	Copper (mg Cu/kg SS)	Lead (mg Pb/kg SS)	Nickel (mg Ni/kg SS)	Zinc (mg Zn/kg SS)
Study Site runoff	2,360 (0.21)*	1,300 (310)	83 (0)	3,666 (0)
NSQD Industrial outfalls	280 (0.6)	664 (0.9)	76 (0.6)	7,147 (1.6)

*Mean (COV)

Copper and lead particulate strengths for this heavy industrial study site are noticeably larger than those observed for NSQD industrial (mostly light to medium industrial) outfalls. Higher copper particulate strengths may be related to the exposure of material such as electrical wiring; roofing, automobile parts etc. on site, and higher lead particulate strengths may reflect exposure to lead materials on the site. Observed nickel particulate strengths were similar to reported values at NSQD industrial outfalls, while the observed zinc particulate strengths were smaller than those for industrial NSQD outfalls. This may be related to a larger large fraction of zinc in dissolved forms at the site (see site particulate and filtered concentration summary above).

2.4 Summary

Stormwater samples were collected from a heavy industrial site in the southeastern US. Metals and COD were present in all the samples while nitrogen and phosphorous were observed in more than 80% of the samples. In addition, copper and zinc were present in all of the filtered samples. Higher concentrations of metals were associated with higher SSC and the presence of large amounts of exposed material stored on the site.

Multivariate analyses indicated no significant relationships between hydrologic and water quality parameters, although SSC and metals showed strong correlations with each other. Suspended solids were predominantly present in particle size ranges < 120 μm. Metals and nutrients showed stronger associations with particulates of larger particle size ranges. Installing stormwater sediment control practices can result in significant reductions of SSC along with associated pollutants, if the appropriate particle sizes are targeted.

References

Box, G. E., Hunter, W. G., & Hunter, J. S. (1978). Statistics for experimenters. John Wiley and Sons. New York.

Duke, L. D., Buffleben, M., & Bauersachs, L. A. (1998). Pollutants in storm water runoff from metal plating facilities, Los Angeles, California. Waste management, 18(1), 25-38

Glenn III, D. W. (2001). *Heavy metal distribution for aqueous and solid phases in Urban Runoff, snowmelt and soils* (Doctoral dissertation, Louisiana State University)

Golding, S. (2006). A Survey of Zinc Concentrations in Industrial Stormwater Runoff. Washington State Department of Ecology

Gromaire-Mertz, M. C., Garnaud, S., Gonzalez, A., & Chebbo, G. (1999). Characterisation of urban runoff pollution in Paris. *Water Science and Technology*, *39*(2), 1-8

Harrison, R. M., & Wilson, S. J. (1985). The chemical composition of highway drainage waters I. Major ions and selected trace metals. *Science of the total environment*, *43*(1), 63-77

Hatje, V., Apte, S. C., Hales, L. T., & Birch, G. F. (2003). Dissolved trace metal distributions in Port Jackson estuary (Sydney Harbour), Australia. *Marine Pollution Bulletin*, *46*(6), 719-730

House, L. B., Waschbusch, R. B., & Hughes, P. E. (1993). Water quality of an urban wet detention pond in Madison, Wisconsin, 1987-88

Johnson, R. A., and Winchern, D. W. (2007). Applied Multivariate Statistical Analysis. 6th Edition. Prentice Hall, Upper Saddle River, NJ

Karlsson, K., & Viklander, M. (2008). Trace metal composition in water and sediment from catch basins. *Journal of Environmental Engineering*, *134*(10), 870-878

Li, Y., Lau, S. L., Kayhanian, M., & Stenstrom, M. K. (2006). Dynamic characteristics of particle size distribution in highway runoff: Implications for settling tank design. *Journal of Environmental Engineering*, *132*(8), 852-861

Line, D. E., Arnold, J. A., Jennings, G. D. and Wu, J. (1996), Water quality of stormwater runoff from ten industrial sites. JAWRA Journal of the American Water Resources Association, 32: 807–816

Line, D. E., Wu, J., Arnold, J. A., Jennings, G. D., & Rubin, A. R. (1997). Water quality of first flush runoff from 20 industrial sites. Water Environment Research, 305-310

Maestre, A. (2005). *Stormwater Characteristics as Described in the National Stormwater Quality Database* (Doctoral dissertation, Ph. D. Dissertation. Department of Civil and Environmental Engineering, University of Alabama. Tuscaloosa, Alabama)

Maniquiz-Redillas, M., & Kim, L. H. (2014). Fractionation of heavy metals in runoff and discharge of a stormwater management system and its implications for treatment. *Journal of Environmental Sciences*, *26*(6), 1214-1222

Marsh, J. M. (1993). Assessment of nonpoint source pollution in stormwater runoff in Louisville, (Jefferson County) Kentucky, USA. Archives of environmental contamination and toxicology, 25(4), 446-455

Marques, M. A. R. C. I. A., & Hogland, W. (2001). Stormwater run-off and pollutant transport related to the activities carried out in a modern waste management park. Waste management & research, 19(1), 20-34

Morquecho, R. E., Pitt, R., & Clark, S. E. (2005). *Pollutant associations with particulates in stormwater* (Doctoral dissertation, University of Alabama)

Pitt, R., Field, R., Lalor, M., & Brown, M. (1995). Urban stormwater toxic pollutants: assessment, sources, and treatability. *Water Environment Research*, *67*(3), 260-275

Pitt, R., Clark, S., Lantrip, J., & Day, J. (1998). Telecommunication manhole water and sediment study. *Special report SR-3841*, *2*

Pitt, R. E., and Maestre, A. (2005, August). Stormwater quality as described in the National Stormwater Quality Database (NSQD). In *Proceedings of the 10th International Conference on Urban Drainage, Copenhagen, Denmark* (pp. 21-26)

Sansalone, J. J., & Buchberger, S. G. (1997). Partitioning and first flush of metals in urban roadway storm water. *Journal of Environmental engineering*,*123*(2), 134-143

Terstriep, M. L., Bender, G. M., & Noel, D. C. (1982). Final Report – NURP Project, Champaign, Illinois: Evaluation of the Effectiveness of Municipal Street Sweeping in the

Control of Urban Storm Runoff Pollution. State Water Survey Division, Illinois Dept. of Energy and Natural Resources, Champaign-Urbana, Illinois

U.S. EPA (1983b) Results of the Nationwide Urban Runoff Program: Volume 1- Final Report. Water Planning Division WH-554. U.S. EPA, Washington, D.C

U.S. EPA (1995). Office of Wastewater Management. NPDES Stormwater Multi-Sector General Permit for Industrial Activities (MSGP)

Vignoles, M., & Herremans, L. (1995, May). Metal pollution of sediments contained in runoff water in the Toulouse city. In *NOVATECH* (Vol. 95, No. 2, pp. 611-614)

Zgheib, S., Moilleron, R., Saad, M., & Chebbo, G. (2011). Partition of pollution between dissolved and particulate phases: what about emerging substances in urban stormwater catchments?. *Water Research*, *45*(2), 913-925

CHAPTER 3 PERFORMANCE EVALUATION OF A HYDRODYNAMIC DEVICE AND A DRY INFILTRATION POND AT AN INDUSTRIAL SITE IN THE SOUTHEASTERN US

3.1 Introduction

Source reduction and prevention is the preferred method of preventing stormwater contamination (MPCA 2011). Materials management practices should be evaluated to determine whether inventories of exposed materials can be reduced or eliminated. Good housekeeping including street sweeping, cleanup of old equipment yards, removal of any contaminated soil, consolidation of materials from many areas to one area, and proper handling and disposal of materials are the first preferred methods (MPCA 2011). If these measures do not provide control of contamination to the adequate level, treatment systems must be installed to remove the pollutants from stormwater prior to discharge in accordance with the discharge limit regulations.

Limited published information is available on the efficiency of treatment control practices for specific industrial activities (Bay, *et al*. 2005, Chys, *et al*. 2013, Kellens, *et al*. 2003, Nelson, *et al*. 2008). However substantial information is available on treatment of stormwater from urban and residential areas (Barrett, *et al*. 2003 , Stanley *et al*. 1996, Birch, *et al*. 2005, Wilson, *et al*. 2009, Guo, *et al*. 2007, and the International BMP Database at BMPdatabase.org).

Pre-treatment is the first step in a typical stormwater treatment train (Wilson, *et al*. 2003). Pre-treatment removes larger sediment, debris, and oil to prevent clogging of the successive treatment devices. Oil water separators, hydrodynamic devices, and sedimentation areas are some of the types of pre-treatment controls commonly used. Sedimentation is the primary

mechanism involved in particulate removal in the pre-treatment devices. Proprietary underground sedimentation devices are attractive options as they are more capable of being sited in dense areas having space constraints. These devices can act as pre-treatment options for other devices such as detentions ponds and infiltration basins. The capture of particles and particulate-associated pollutants in hydrodynamic devices is based on gravitational settling of particles with variations in particle size affecting particle removal processes in these devices. Several studies have been conducted to study the pollutant removal efficiencies from proprietary underground devices (Guo et al 2007, Kim et al 2008, Clark et al 2009, Wilson et al 2009, and the International BMP Database). It is difficult to compare the results from these individual studies because of the differences in site conditions (rainfall patterns, soils, and site activities), experimental criteria, and sampling techniques.

Infiltration, filtration, coagulation/flocculation, and sedimentation facilities are some of the treatment controls that follow pre-treatment. Detention facilities (dry and wet ponds) are commonly used stormwater controls to detain and treat runoff. Sedimentation is the primary pollutant removal mechanism involved with detention ponds. These ponds are usually designed to detain all the runoff from small and intermediate storms, along with some runoff peak flow reductions from larger storms. Sedimentation in ponds affects the particulates and particulate-bound pollutants, with few benefits for filterable pollutants.

This study incorporates performance evaluations of a hydrodynamic separator device and a dry infiltration pond (having substantial infiltration capacity) at a heavy industrial site (site specifics are client confidential). The primary goals of this study are to evaluate pollutant reductions in the treatment train components related to pollutant treatability characteristics associated with the industrial site. Removal efficiencies for SSC, particle size categories of

particulates, total and filterable forms of metals, and nutrients were determined by comparing the concentrations and masses of the constituents entering and leaving the treatment control unit operations. A mass balance was also conducted to quantify the sediment and associated pollutant mass captured in the hydrodynamic device during the monitoring period, and soil profile metal concentrations were examined under the infiltrating dry pond to quantify the mobility of the metal contaminants in the vadose zone (presented in Chapter 4).

3.2 The Study Site

The study site is a heavy industrial facility located in southeastern US. The site is highly impervious and is comprised of parking lots, loading docks, and storage areas. The soils at the site are also highly compacted. The treatment controls at the site include two oil-water separators, a hydrodynamic separator device and a dry pond with infiltration. The oil-water separators are located at two very small subareas to treat runoff from critical locations. No influent was sampled from the one oil-water separator monitored as the drainage area was very small, while some ponded treated effluent was sampled for some of the rains. Runoff from the whole site is pre-treated by a hydrodynamic separator device. The pre-treatment hydrodynamic separator unit at the site is a four chambered treatment system consisting of an inlet chamber where all the drainage from the site is collected, an oil & grit chamber, a settleable solids chamber, and an outlet chamber. The treated effluent from this unit is discharged into a dry infiltration pond with oil sorbent booms across the outlet followed by rock check dams in the channel through the dry pond for velocity attenuation. The treated runoff is then discharged through the site outfall. All of the inlets to the site stormwater collection system have filter fabric barriers to capture large debris. Land surface classification and drainage network of the site

along with the treatment control on the site are as shown in Figure 3-1.The detailed site description can be found in Chapter 2.

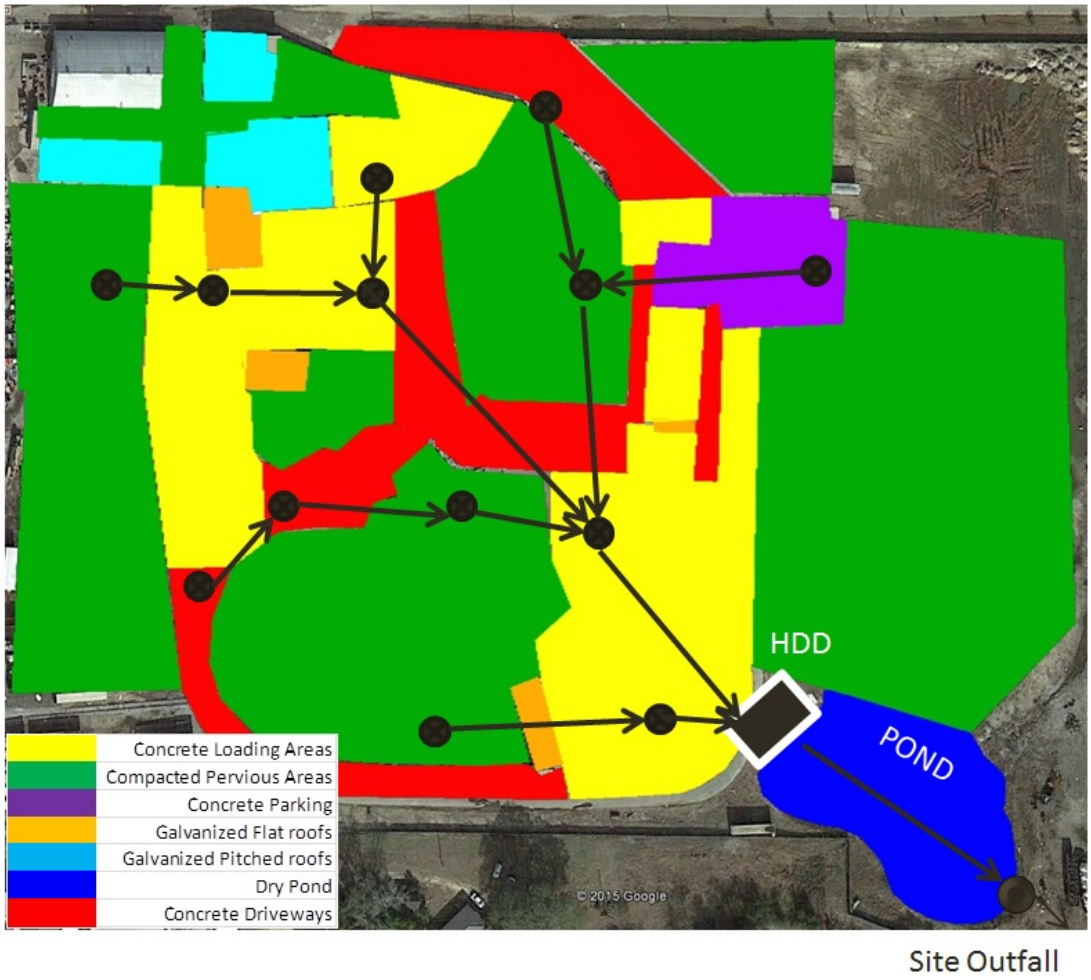

Figure 3-1 Land surface classification and drainage network map for test site

3.2.1 Monitoring and sampling

Hydrologic and water quality monitoring was conducted at the study site from November 2013 to June 2014. Hydrologic monitoring involved data collection on rain depths and intensities and stormwater runoff rates. ISCO 4250 area-velocity sensors were installed at the effluent locations of the hydrodynamic device and the dry infiltration pond. ISCO 674 tipping bucket

rain gages were installed at the treatment control locations for continuous monitoring of rain depths and intensities, and to trigger the water samplers. Water quality monitoring involved collection of samples from the influent and effluent locations of the hydrodynamic separator device and pond. Sampling protocols were developed based on the historical intensity-duration-frequency (IDF) curves for the site location. ISCO 6712 automatic samplers were used for sample collection. Based on flow conditions, flow weighted sampling was conducted at the HDD and time weighted sampling at the dry pond effluent location.

Samples were collected for 17 storm events ranging from 0.1 to 2.5 inches. The composite samples were collected in high-density polyethylene bottles and were brought to the UA laboratory as soon as possible and were refrigerated if no immediate analysis was needed. Suspended sediment concentrations were analyzed using ASTM D3977-97 method, particle size distribution (PSD) using filters and Coulter Counter analysis at the UA laboratory, and subsamples were sent to the PSH lab for analysis of metal and nutrient analyses. Chapter 2 has detailed descriptions on monitoring, sampling, and pollutant analyses.

3.3 Results and Discussion

Several exploratory data analysis techniques were used during this study to represent the behavior of the data, along with other statistical tools.

3.3.1 Probability Plots

Probability plots are used to evaluate the fit of the data to a probability distribution, to estimate percentiles, and compare different sample distributions of data from different sampling locations. A probability plot shows the value of the data distribution against its estimated cumulative probability. Probability plots can display 95% confidence intervals for the percentiles

and the Minitab multiple probability plot tool can compare several data distributions along with calculating the Anderson-Darling test statistic to compare the data set to a normal probability distribution. Probability plots were used to compare the distributions of pollutant concentrations and mass for HDD influent, HDD effluent and pond effluent.

3.3.2 Regression Analyses

Regression analyses are used to determine associations between variables (independent and a dependent variable). Regression analyses help illustrate relationships between variables. Simple linear regression is the most common type and requires that the dependent variable has a linear relationship with the independent variable and for each value of the independent variable, the probability distribution of the dependent variable has the same standard deviation. Linear regression analyses were used to predict the pollutant concentration and mass relationships between HDD influent and effluent, and pond influent and effluent. The results of the linear regression were supplemented by ANOVA and residual analyses to ensure that the regression assumptions were valid.

Residual analyses play a vital role in validating the regression model. Residual analyses help in determining the significance of the regression coefficients. Residuals are calculated as differences between observed and the predicted variable and their examination confirms the validity of the fitted model. The validity of the model is verified based on the error term satisfying the four regression assumptions (the error terms must have constant variance, zero mean, must be independent, and be normally distributed) and should describe a reasonable and sensible relationship between the independent and dependent variables.

3.3.3 Analysis of Variance (ANOVA)

ANOVA is a statistical technique used to evaluate the differences between the means of two sample groups and explain the variabilities within the groups. Typically, one-way ANOVA is used to determine if sub groups of a sample set are significantly different (such as samples collected for different rain categories). One-way ANOVA assumes that the populations are normally distributed with equal variances and the population samples must be independent. The null hypothesis of ANOVA is that the population means are equal. The significant relationships between two groups is evaluated based on the p-value, typically smaller p-values (< 0.05) provide more significant relationship. ANOVA was used to identifying significant relationships between concentrations and also mass of samples between HDD influent and effluent and pond influent and effluent to predict the dependent variable based on the independent variable.

ANOVA was conducted to test the significance of the regression coefficients (slope and intercept terms), which is highly dependent on the number of data observations. When an observed data set has only a few observations, the important relationships may not be shown to be significant. A high R^2 value does not guarantee by itself that the model has any predicative value, and a low R^2 value does not mean the regression model is not significant. An ANOVA table presents the variability of responses and distinguishes what can be explained by regression and what remains as error. The F critical value on the ANOVA table is the value that would result in a p-value equal to 0.05. A large F value resulting from an ANOVA suggests that there is a significant linear relationship between the observed and predictor variables. Statistical software Minitab (Version 17) was used to perform data analyses.

3.3.4 Multiple pairwise comparison tests

Non-parametric pairwise comparison tests were conducted to supplement the ANOVA and regression analyses to evaluate the significance of the observed capture of the contaminants in the HDD and the dry pond.

The Kruskal Wallis test is a nonparametric analysis of variance that can be used to compare several independent samples. It is similar to ANOVA, except that it is used when the data are not normally distributed. This test is used to determine if at least one group is significantly different from other groups included in the comparison. The Kruskal-Wallis test determines whether the medians of the compared groups are different. The null hypothesis is assumed that the population medians are all equal.

Further tests of potential significant differences between the data sets were analyzed using the Wilcoxon signed rank test, if the Kruskal-Wallis indicated a significant result. The Wilcoxon signed rank test is conducted to determine whether the population data distributions are identical without the assumption that the data follows normal distribution. Wilcoxon signed rank test is a non-parametric comparison test similar to a Student's t-test. The null hypothesis assumes that the medians of two samples are identical. The Kruskal Wallis test was initially performed on the data sets and if the compared groups were found to have a significantly different indication, the Wilcoxon signed rank test was then conducted to check the significant differences between the individual groups. MINITAB version 17 was used and multiple comparison tests were conducted to compare the pollutant concentrations and masses for the three data set groups: HDD influent vs, HDD effluent; POND influent vs. pond effluent; and HDD influent vs. pond effluent. The results of these analyses are shown in Table 3-8.

3.3.5 Performance Evaluation of Particulates by Site Stormwater Controls

Analyses of suspended and settleable particulates, along with their particle size distributions, are critical in evaluating treatability and water quality performance of stormwater treatment controls. Many pollutants including metals, nutrients, PAHs, etc., are strongly associated with solids in stormwater (filterable concentrations much smaller than particulate-bound pollutant concentrations). The ability of removing particulates therefore reflects the ability for removing associated particulate-bound pollutants. Performance evaluations if treatment controls in this study examined removals of particulates (TSS and SSC, plus particulates by several particle sizes) along with heavy metals and nutrients.

Evaluations of suspended sediment concentrations (SSC) represent the performance of the overall size range from 0.45 μm to >1180 μm. Figure 3-2 presents line plots illustrating how the particulate concentrations change through the treatment train, through the HDD and dry pond. Table 3-1 is a descriptive performance summary for all of the sampled storms indicating the regression equations of influent vs. effluent concentrations. As shown in the table and plots, the effluent suspended solid concentrations from the HDD and dry pond averaged about 183 mg/L and 58 mg/L, respectively, compared to an average site untreated runoff SSC of 253 mg/L. The SSC concentration reductions averaged about 34% for the HDD and 75% for the pond. Figure 3-3 present the probability and Figures 3-4 through 3-6 show the scatter plots for influent and effluent SSC concentrations. The scatter plots show that the effluent concentrations from HDD effluent and dry pond effluent were always less than the influent concentrations. In Figure 3-3, the pond effluent is normally distributed (Anderson-Darling p value > 0.05), whereas the HDD influent and effluent are not, indicating the need for non-parametric statistical tests in most cases. The probability plot shows some overlaps in HDD influent and effluent concentrations, while the

confidence intervals are separate for pond effluent. The results for the non-parametric pairwise comparison tests for particulate concentration reductions are shown in Table 3-3. The hypothesis testing using the Wilcoxon signed ranked test indicates significant reductions for SSC for the HDD, the dry infiltrating pond and the overall system.

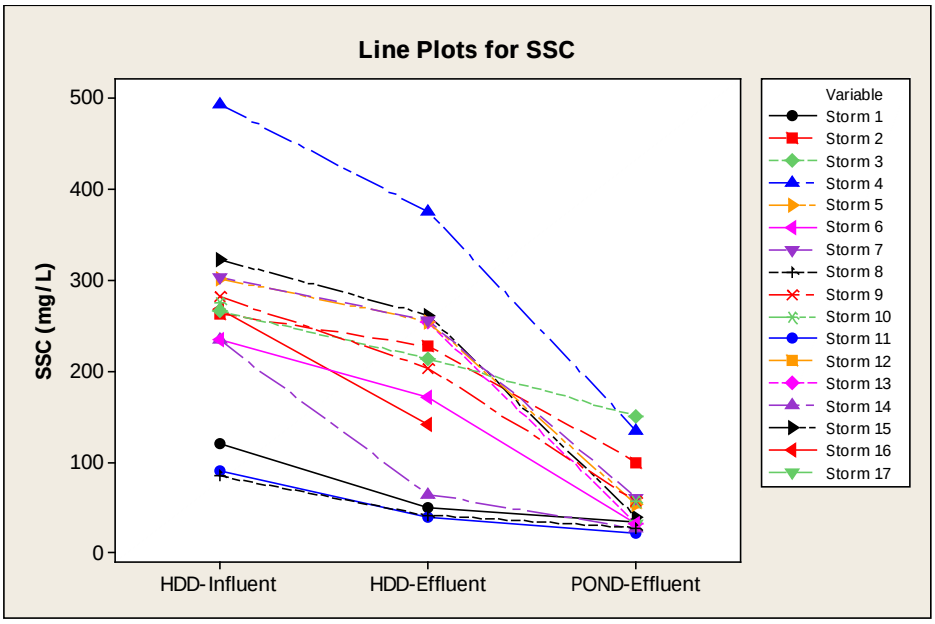

Figure 3-2 Line plots of SSC for influent and effluent samples of HDD and dry pond

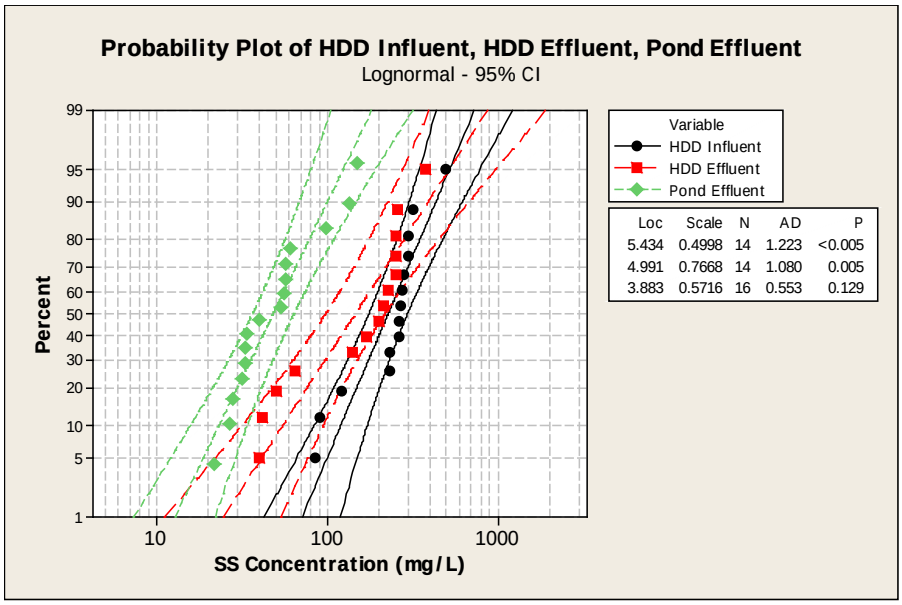

Figure 3-3 Probability plots of SSC for influent and effluent samples of HDD and dry pond

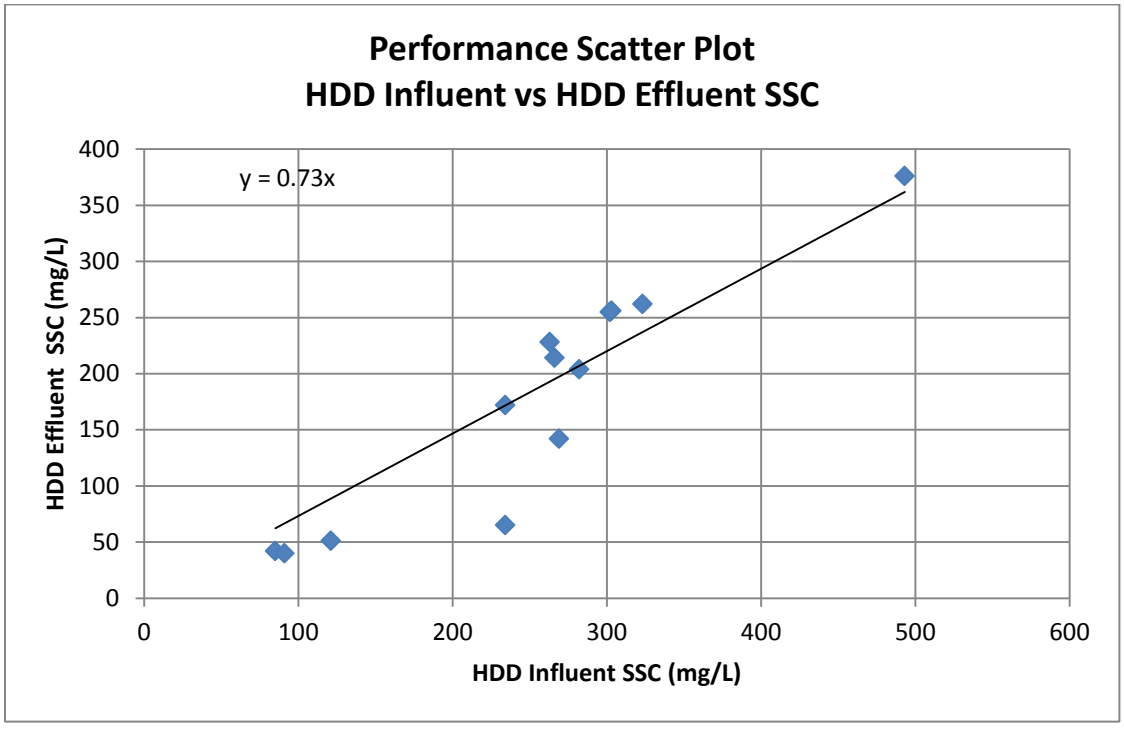

Figure 3-4 Scatter plot of SSC for HDD influent vs effluent (showing significant regression equation)

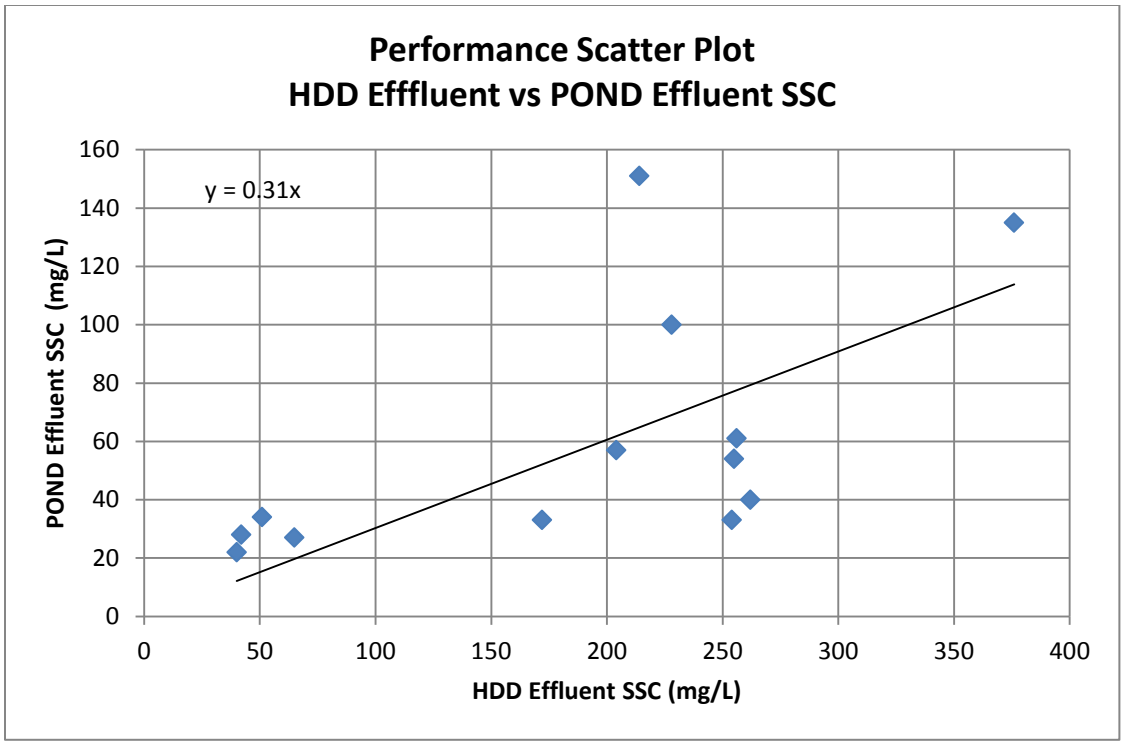

Figure 3-5 Scatter plot of dry pond influent vs effluent (showing significant regression equation)

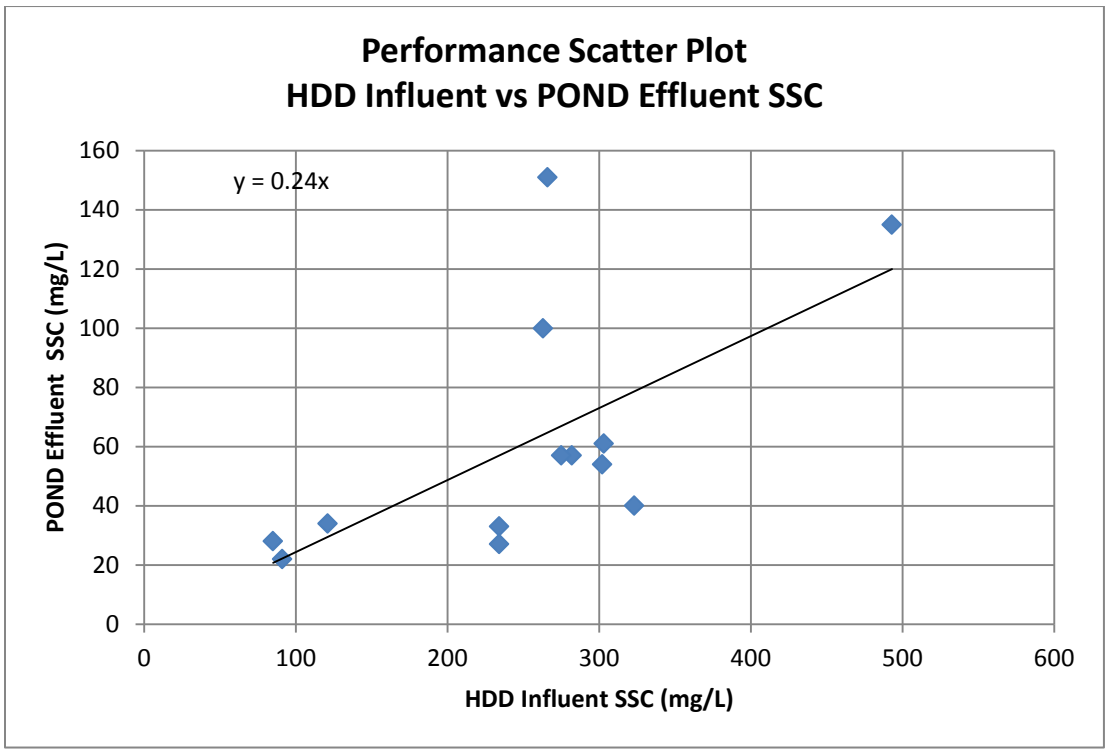

Figure 3-6 Scatter plot of HDD influent vs dry pond effluent (complete treatment train) (showing significant regression equation)

Regression analyses for HDD influent and effluent and pond influent and effluent are shown below (the HDD effluent is the pond influent). All the equations indicate significant regressions, also with significant p-values for the slope terms, while the intercept terms were not significant (the regression equations therefore had zero intercepts). Figures 3-7 through 3-9 show the corresponding residual plots of SSC values for all the monitored storms. Residual plots were inspected to check if the error term in the regression model satisfied the four assumptions (constant variance, zero mean, must be independent, and be normally distributed). The Anderson-Darling statistic was calculated to check for normality. Normal plots of the residuals (Figures 3-7 through 3-9) show p-values greater than 0.05 indicating normality of the residuals. Descriptive statistics and graphs of residuals vs. fitted value and residuals vs. observation order were also examined to check for the assumption of zero mean and independence of observations. The residuals were normally distributed, had zero mean and were independent of each other.

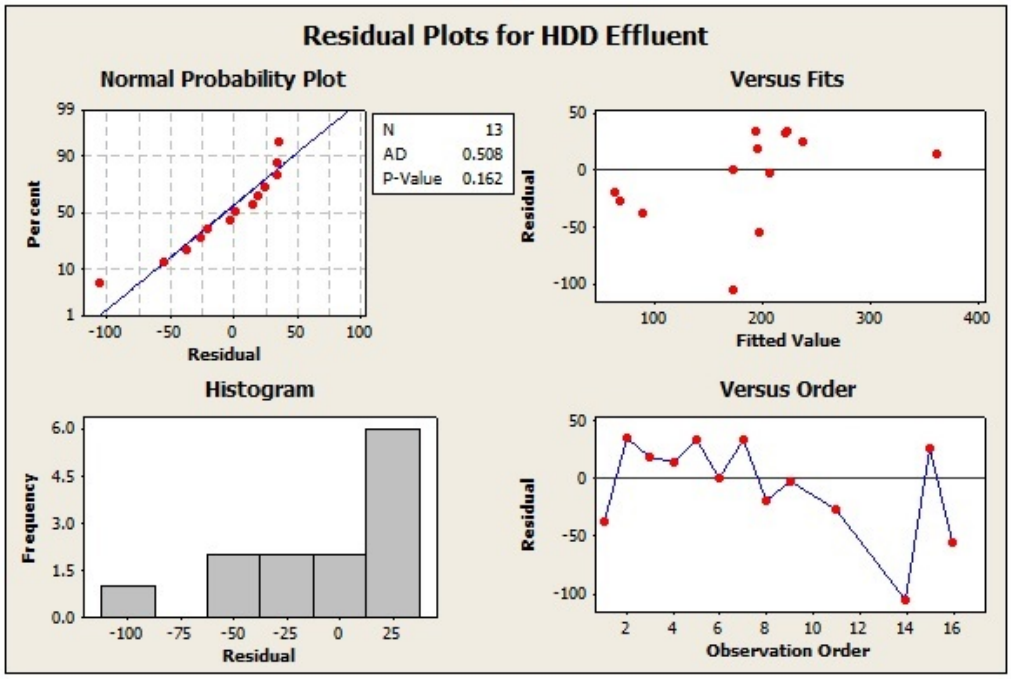

Figure 3-7 Residual plots for HDD influent vs. effluent

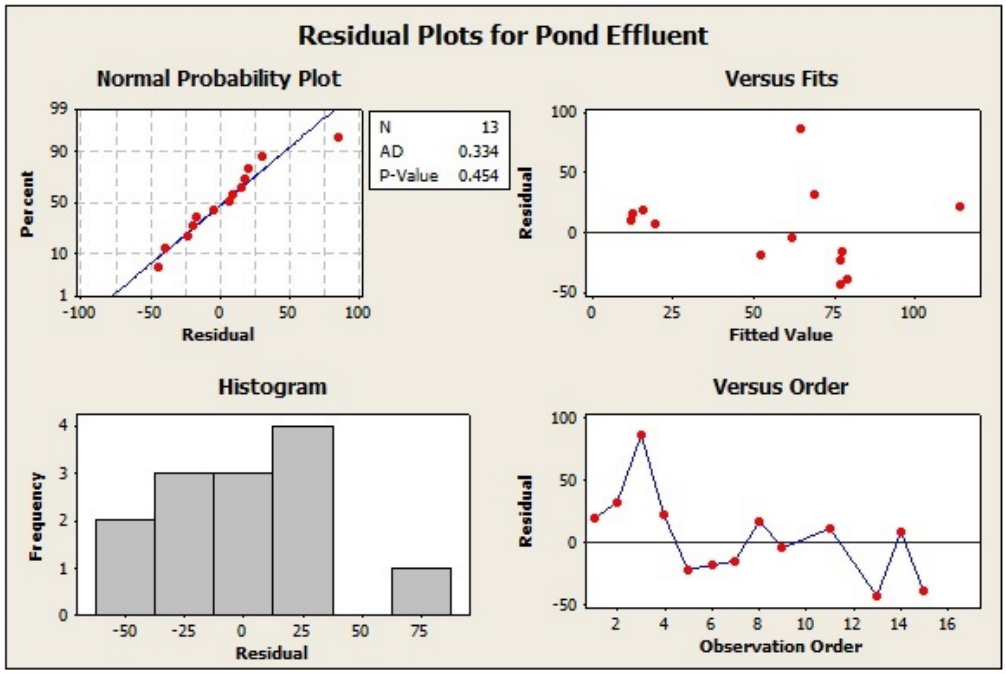

Figure 3-8 Residual plots for dry pond influent vs. effluent

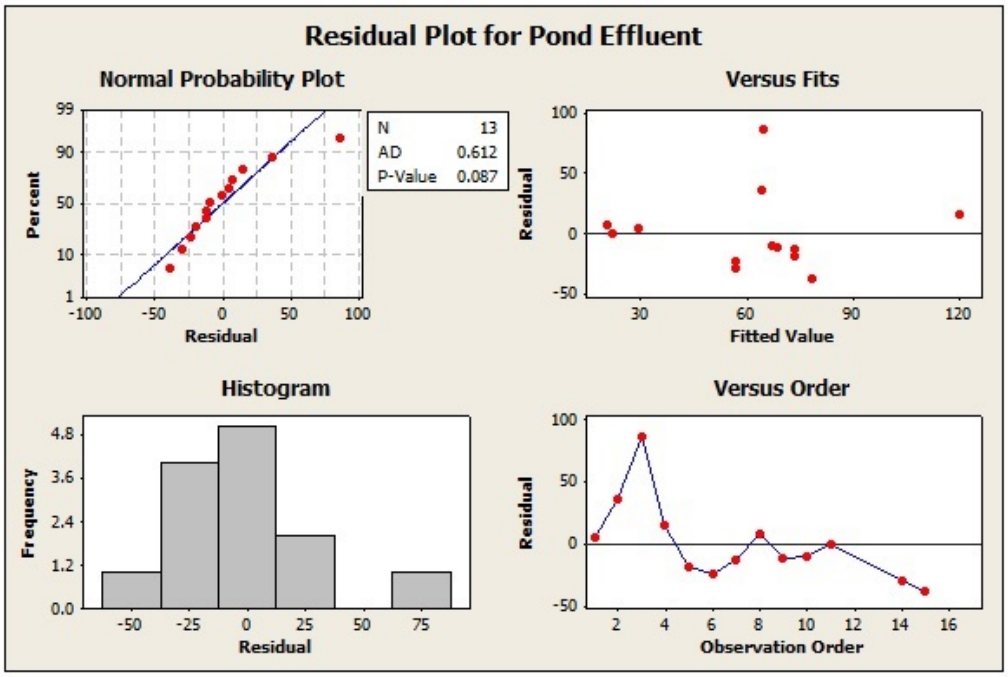

Figure 3-9 Residual plots for HDD influent vs. pond effluent (complete treatment train)

Regression Analysis and ANOVA: HDD Effluent versus HDD Influent

```
The regression equation is
HDD Effluent = 0.734 HDD Influent

Predictor        Coef  SE Coef      T      P
Noconstant
HDD Influent  0.73402  0.04334  16.94  0.000

S = 42.5031

Analysis of Variance

Source          DF      SS      MS       F      P
Regression       1  518237  518237  286.87  0.000
Residual Error  12   21678    1807
Total           13  539915
```

Regression Analysis and ANOVA: Pond Effluent versus HDD Effluent

```
The regression equation is
Pond Effluent = 0.303 HDD Effluent

Predictor        Coef  SE Coef     T      P
Noconstant
HDD Effluent  0.30289  0.04507  6.72  0.000

S = 34.4475
```

```
Analysis of Variance

Source          DF     SS     MS      F      P
Regression       1  53603  53603  45.17  0.000
Residual Error  12  14240   1187
Total           13  67843
```

Regression Analysis and ANOVA: Pond Effluent versus HDD Influent

```
The regression equation is
Pond Effluent = 0.244 HDD Influent

Predictor        Coef  SE Coef     T      P
Noconstant
HDD Influent  0.24351  0.03321  7.33  0.000

S = 32.6268

Analysis of Variance

Source          DF     SS     MS      F      P
Regression       1  57229  57229  53.76  0.000
Residual Error  12  12774   1065
Total           13  70003
```

Table 3-1 Performance summary of SSC concentration reductions for each monitored storm event

Storm Event	HDD Influent SSC (mg/L)	HDD Effluent SSC (mg/L)	HDD % SSC Reduction	Pond Effluent SSC (mg/L)	Pond % SSC Reduction	Overall System % SSC Concentration Reduction
1	121	51	57.9	34	33.3	71.9
2	263	228	13.3	100	56.1	62
3	266	214	19.5	151	29.4	43.2
4	493	376	23.7	135	64.1	72.6
5	302	255	15.6	54	78.8	82.1
6	234	172	26.5	33	80.8	85.9
7	303	256	15.5	61	76.2	79.9
8	85	42	50.6	28	33.3	67.1
9	282	204	27.7	57	72.1	79.8
10	275	n/a	n/a	57	n/a	79.3
11	91	40	56	22	45	75.8
12	n/a	n/a	n/a	56	n/a	n/a
13	n/a	254	n/a	33	87	n/a
14	234	65	72.2	27	58.5	88.5
15	323	262	18.9	40	84.7	87.6
16	269	142	47.2	n/a	n/a	n/a
17	n/a	n/a	n/a	32	n/a	n/a

Average	253	183	34.2	58	61.5	75.1

Table 2 lists summaries for the regression equations describing the performance of SSC for all the monitored storms.

Table 3-2 Summary of Regression and ANOVA of SSC for all the sampled storms

Constituent	Regression Equation	Variables (x,y)	p- value for the slope term	p- value for the intercept term	p-value for overall equation
SSC	y = 0.734x	HDD Influent, HDD Effluent	<0.001	>0.05*	<0.001
SSC	y = 0.303x	HDD Effluent, Pond Effluent	<0.001	>0.05	<0.001
SSC	y = 0.244x	HDD Influent, Pond Effluent	<0.001	>0.05	<0.001

* Not significant during the initial analyses so the intercept was removed for the final regression analyses

Table 3-3 Summary of non-parametric analyses for SSC

Constituent	Kruskal- Wallis p	Wilcoxon p for HDD (Influent =Effluent)	Wilcoxon p for Pond (Influent =Effluent)	Wilcoxon p for Overall system (Influent =Effluent)
SSC	p <0.001	p = 0.002	p = 0.002	p = 0.002

Figure 3-10 represents the line plots of how the particulate mass changed through the HDD, dry pond, and the complete treatment train. Table 3-4 is a descriptive performance summary of particulate mass reductions for all the sampled storms. As shown in the table and plots, the effluent particulate mass from the HDD and dry pond averaged about 590 lbs and 61 lbs, respectively compared to the average site untreated influent particulate mass of 747 lbs. The particulate mass reductions for the HDD averaged about 39%, with about 93% reductions for the pond. The overall treatment train mass reductions for particulate solids was about 95%.Results of

the regression and ANOVA analyses for mass reductions for particulate solids are summarized in Table 3-5.

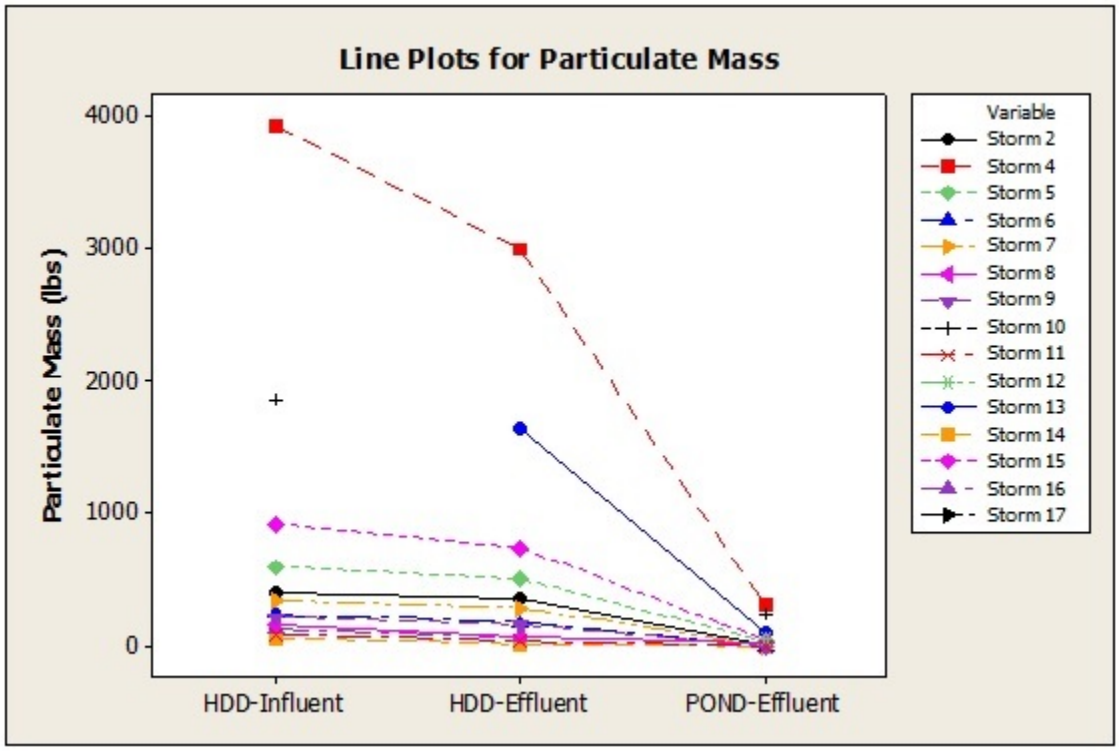

Figure 3-10 Line plots of particulate mass for influent and effluent samples of HDD and dry pond

Table 3-4 Performance summary of particulate mass for all the monitored storm events

Storm Event	HDD Influent Particulate Mass (lbs)	HDD Effluent Particulate Mass (lbs)	HDD % Particulate Mass Reduction	Pond Effluent Particulate Mass (lbs)	Pond % Particulate Mass Reduction	Overall System % Particulate Mass Reduction
2	412	357	13.4	13	96.3	97
4	3,925	2,993	23.7	321	89.3	91.8
5	599	506	15.5	39	92.3	93.5
6	242	178	26.3	4.3	97.6	98.2
7	349	294	15.6	4	98.7	99
8	155	77	50.6	20	73.7	87
9	221	159	27.7	4.8	97	98

10	1,868	n/a	n/a	241	n/a	87.1
11	88	39	56.2	2.7	93	97
12	n/a	n/a	n/a	50. 7	n/a	n/a
13	n/a	1,650	n/a	104	93.7	n/a
14	635	17	72.4	1.6	90.6	97.4
15	919	744	19	47	93.7	95
16	124	66	47	n/a	n/a	n/a
17	n/a	n/a	n/a	0.1	n/a	n/a
Average	747	590	39	61	93	95

Table 3-5 Summary of Regression and ANOVA of particulate mass for all the sampled storms

Constituent	Regression Equation	Variables (x,y)	p- value for the slope term	p- value for the intercept term	p-value for overall equation
Particulate Mass	y = 0.767x	HDD Influent, HDD Effluent	<0.001	>0.05*	<0.001
Particulate Mass	y = 0.094x	HDD Effluent, Pond Effluent	<0.001	>0.05	<0.001
Particulate Mass	y = 0.087x	HDD Influent, Pond Effluent	<0.001	>0.05	<0.001

* Not significant during the initial analyses so the intercept term was removed for the final regression analyses

Figures 3-11 and 3-12 summarize the particle size distributions for the HDD influent and effluent and dry pond samples for all sampled events. The HDD removed about 21% of the total particulate loading for all the sampled storms, with increasing removals for particle sizes greater than 30 μm. The dry infiltration pond removed about 92% of the total particulate loading for all particle sizes greater than 3 μm. The average median particle size of the HDD influent samples was about 20 μm, reducing to about 12 μm for both the HDD effluent and pond effluent samples, again indicating a preferential removal for the largest particles.

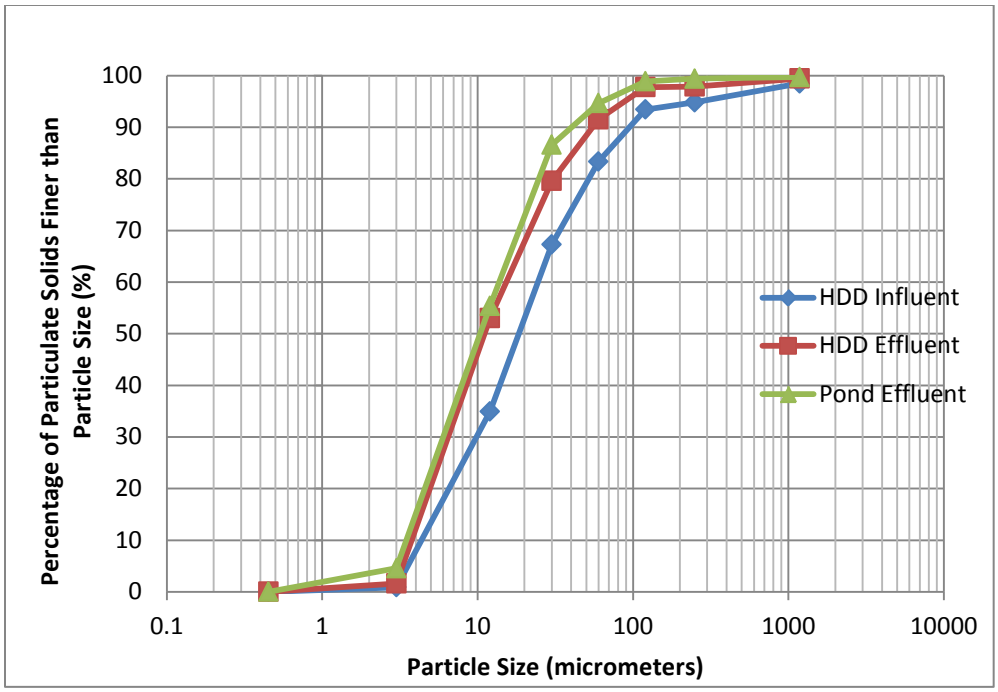

Figure 3-11 Accumulative particulate solids percentage distribution by particle size for all sampled events

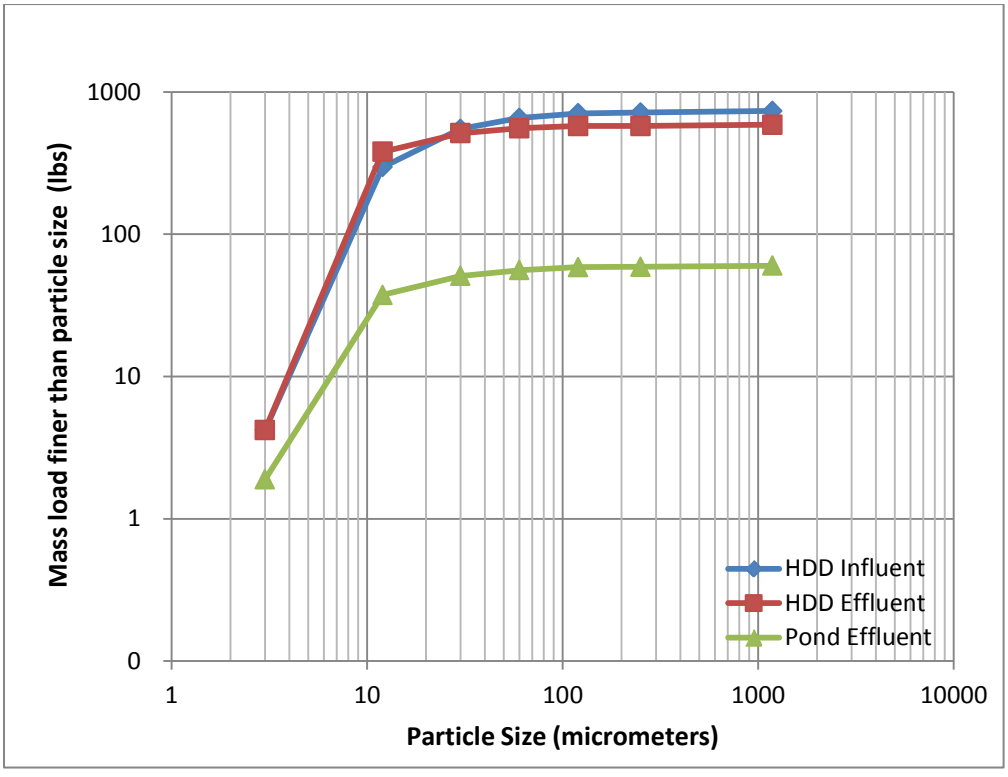

Figure 3-12 Accumulative Particulate Solids Mass Distribution by Particle Size for all sampled events

Figure 3-13 are the lines plots for the treatment showing the HDD influent and effluent and pond effluent concentrations for the eight particle size ranges studied. These plots present the overall removals of the HDD and dry pond for each specific particle size range. The plots show significant removals of suspended sediment concentrations for particle size range greater than 30 μm as expected due to preferential gravitational settling of larger particles. Few particles smaller than 30 μm were retained in the HDD, while the dry infiltration pond retained some particles as small as 3 μm.

Example probability plots for suspended sediment concentrations (SSC) for two particle size ranges (out of the eight particle sizes that were evaluated) for the three sampling locations (hydrodynamic device influent, hydrodynamic device effluent/dry pond influent, and dry pond effluent) are shown in Figures 3-14 and 3-15.

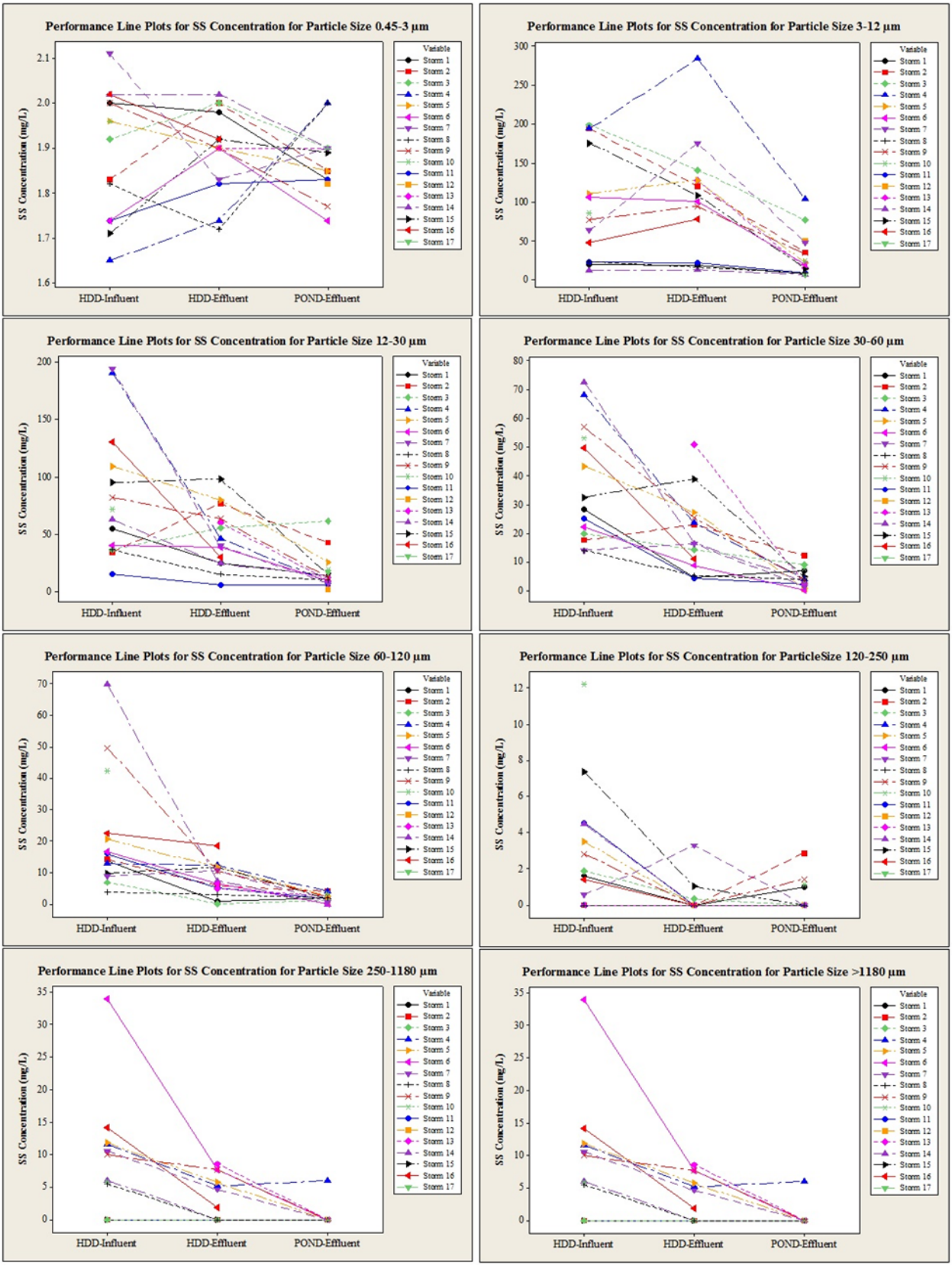

Figure 3-13 Line plots of SSC concentrations by particle size for influent and effluent samples of HDD and dry pond

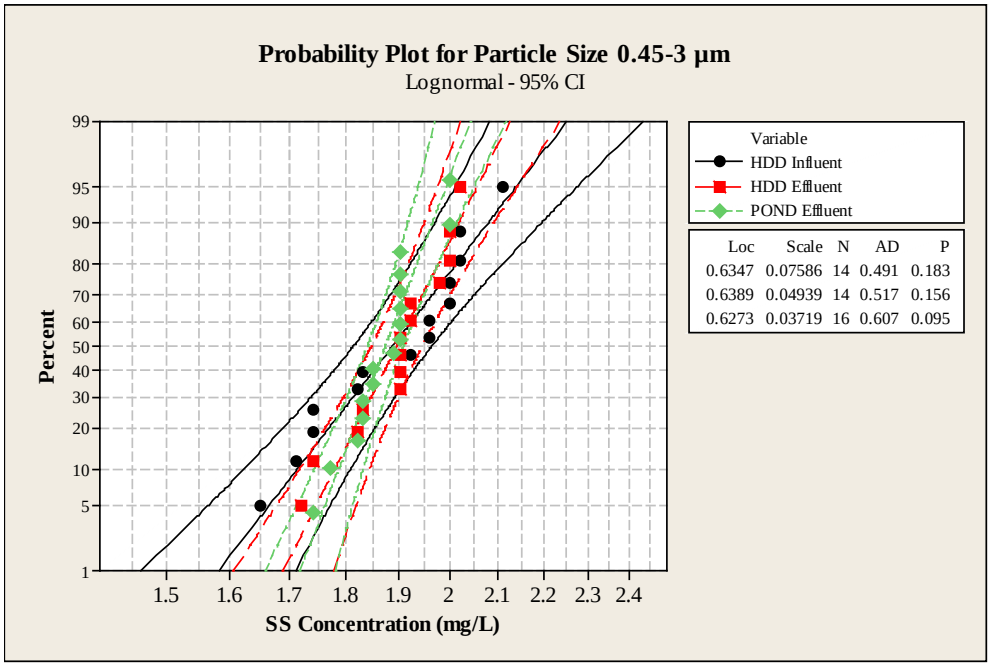

Figure 3-14 Probability plots of SSC for particle size (0.45-3µm) for influent and effluent samples of HDD and dry pond

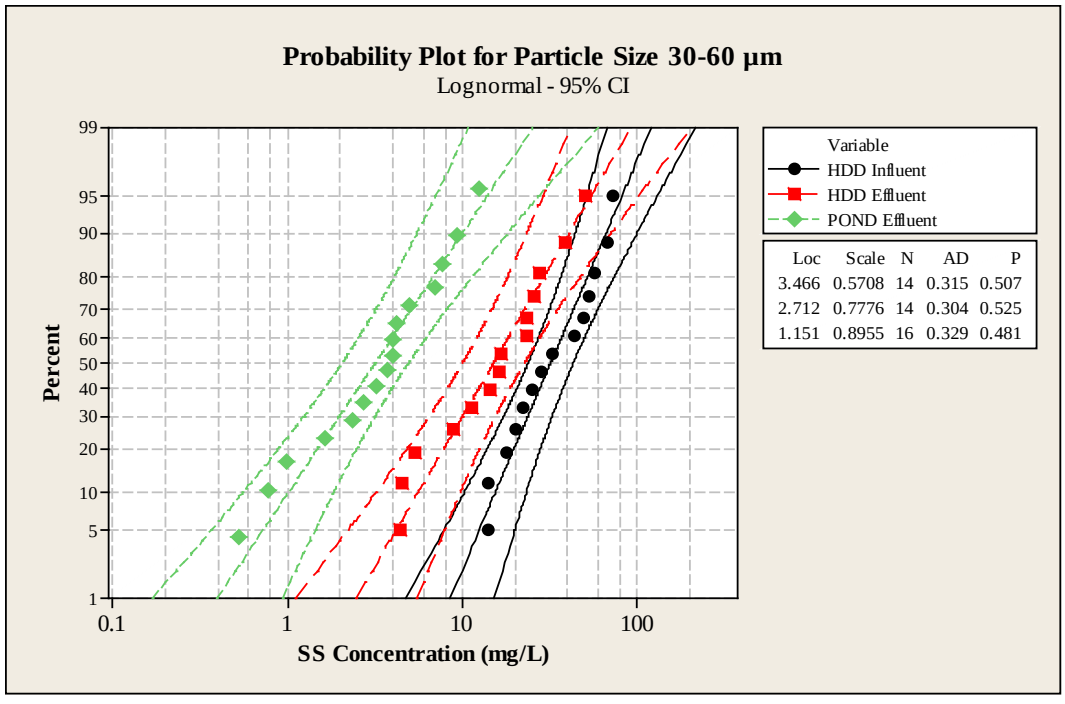

Figure 3-15 Probability plots of SSC for particle size (30-60µm) for influent and effluent samples of HDD and dry pond

The small particle size (0.45 to 3 µm) distributions did not indicate any significant concentration differences for the hydrodynamic device or the dry infiltrating pond. The plots' 95% confidence intervals overlap over much of the concentration range. However, the larger particle size range shown here (30 to 60 µm) indicated concentration differences for both the hydrodynamic device and the pond. The plots confidence intervals are clearly separate for the pond and less so for the hydrodynamic separator. Appendix XXXX contains similar plots for the other particle size ranges.

Results of the regression and ANOVA analyses for each of the particle size ranges for all the sampled events are summarized in Table 3-6. Similar statistical analyses were conducted for mass reductions of the particulate solids for all the particle size ranges with the results summarized in Table 3-7.

Table 3-6 Summary of Regression and ANOVA of particle concentrations for different particle size ranges for all the sampled storms

Regression and ANOVA for particulate concentrations (mg/L) for different particle sizes					
Particle size (µm)	Regression Equation	Variables (x,y)	p- value (X variable)	p- value (Intercept)	Significance factor of equation
0.45 to 3	y = x	HDD Influent, HDD Effluent	<0.001	>0.05*	<0.001
	y = 0.986x	HDD Effluent, Pond Effluent	<0.001	>0.05	<0.001
	y = 0.99x	HDD Influent, Pond Effluent	<0.001	>0.05	<0.001
3 to 12	y = 0.949x	HDD Influent, HDD Effluent	<0.001	>0.05	<0.001
	y = 0.314x	HDD Effluent, Pond Effluent	<0.001	>0.05	<0.001
	y = 0.310x	HDD Influent, Pond Effluent	<0.001	>0.05	<0.001
12 to 30	y = 0.409x	HDD Influent, HDD Effluent	0.001	>0.05	0.001
	y = 0.346x	HDD Effluent, Pond Effluent	0.001	>0.05	0.001
	y = 0.134x	HDD Influent, Pond Effluent	0.05	>0.05	0.05
30 to 60	y = 0.403x	HDD Influent, HDD Effluent	<0.001	>0.05	<0.001
	y = 0.149x	HDD Effluent, Pond Effluent	0.011	>0.05	0.011
	y = 0.096x	HDD Influent, Pond Effluent	0.008	>0.05	0.008
60 to 120	y = 0.248x	HDD Influent, HDD Effluent	0.004	>0.05	0.004
	y = 0.226x	HDD Effluent, Pond Effluent	0.001	>0.05	0.001
	y = 0.049x	HDD Influent, Pond Effluent	0.026	>0.05	0.026

120 to 250	y = 0.08x	HDD Influent, HDD Effluent	0.372	>0.05	0.372
	y = 0	HDD Effluent, Pond Effluent	1.000	>0.05	1.000
	y = 0.071x	HDD Influent, Pond Effluent	0.249	>0.05	0.249
250 to 1180	y = 0.283x	HDD Influent, HDD Effluent	<0.001	>0.05	<0.001
	y = 0.116x	HDD Effluent, Pond Effluent	0.269	>0.05	0.269
	y = 0.04x	HDD Influent, Pond Effluent	0.336	>0.05	0.336
>1180	y = 0.362x	HDD Influent, HDD Effluent	0.001	>0.05	0.001
	y = 0.097x	HDD Effluent, Pond Effluent	0.530	>0.05	0.430
	y = 0.151x	HDD Influent, Pond Effluent	0.015	>0.05	0.015

* Not significant during the initial analyses so the intercept term was removed for the final regression analyses

Table 3-7 Summary of Regression and ANOVA of Particulate Mass (lbs) for different particle size ranges for all the sampled storms

Regression and ANOVA for Particulate Mass (lbs) for different particle sizes					
Particle size (µm)	Regression Equation	Variables (x,y)	p- value (X variable)	p- value (Intercept)	Significance factor of equation
0.45 to 3	y = 1.05x	HDD Influent, HDD Effluent	<0.001	>0.05*	<0.001
	y = 0.386x	HDD Effluent, Pond Effluent	<0.001	>0.05	<0.001
	y = 0.455x	HDD Influent, Pond Effluent	<0.001	>0.05	<0.001
3 to 12	y = 1.05x	HDD Influent, HDD Effluent	<0.001	>0.05	<0.001
	y = 0.386x	HDD Effluent, Pond Effluent	<0.001	>0.05	<0.001
	y = 0.455x	HDD Influent, Pond Effluent	<0.001	>0.05	<0.001
12 to 30	y = 0.281x	HDD Influent, HDD Effluent	<0.001	>0.05	<0.001
	y = 0.065x	HDD Effluent, Pond Effluent	<0.001	>0.05	<0.001
	y = 0.03x	HDD Influent, Pond Effluent	0.057	>0.05	0.057
30 to 60	y = 0.380x	HDD Influent, HDD Effluent	<0.001	>0.05	<0.001
	y = 0.061x	HDD Effluent, Pond Effluent	<0.001	>0.05	<0.001
	y = 0.041x	HDD Influent, Pond Effluent	0.003	>0.05	0.003
60 to 120	y = 0.807x	HDD Influent, HDD Effluent	<0.001	>0.05	<0.001
	y = 0.105x	HDD Effluent, Pond Effluent	<0.001	>0.05	<0.001
	y = 0.053x	HDD Influent, Pond Effluent	<0.001	>0.05	<0.001
120 to 250	y = 0.122x	HDD Influent, HDD Effluent	0.047	>0.05	0.047
	y = 0	HDD Effluent, Pond Effluent	1.00	>0.05	1.00
	y = 0.052x	HDD Influent, Pond Effluent	<0.001	>0.05	<0.001
250 to 1180	y = 0.422x	HDD Influent, HDD Effluent	<0.001	>0.05	<0.001
	y = 0.117x	HDD Effluent, Pond Effluent	0.046	>0.05	0.046
	y = 0.108x	HDD Influent, Pond Effluent	0.001	>0.05	0.001
>1180	y = 0.142x	HDD Influent, HDD Effluent	<0.001	>0.05	<0.001
	y = 0.571x	HDD Effluent, Pond Effluent	0.001	>0.05	0.001
	y = 0.11x	HDD Influent, Pond Effluent	<0.001	>0.05	<0.001

* Not significant during the initial analyses so the intercept term was removed for the final regression analyses

Figure 3-16 present the performance concentration line plots for heavy metal removals for all the monitored storms. The overall performance indicates low reductions for the HDD and moderate to high reductions for the dry infiltrating pond. Table 3-8 is a descriptive performance summary of concentration and mass reductions of all the constituents for all the sampled storms. The hypothesis testing using the Wilcoxon signed ranked test indicates significant reductions for concentrations and mass for total Cu, Pb, Zn for the HDD and total Al, Cu, Fe, Pb, Zn for the dry infiltration pond. Similar results were shown by different studies conducted by Stanley et al 1996 (metal reductions up to 45% by dry pond, and Bay et al 2005 (low removals of metals in hydrodynamic devices). Higher removals in the dry pond can be related to higher reductions of particulate solids and associated particulate-bound pollutants in the pond due to its larger surface area for the same flow rate (as discussed later in relationship to the different surface overflow rates for the two devices) . Arsenic was not detected in the pond effluent (0.005 mg/L detection limit), so the average removal rate for total As was >29%. Regression and ANOVA analyses were conducted for concentrations and masses of heavy metals with the results shown in Tables 3-9and 3-10.

Table 3-8 Percentage reductions of all the constituents along with their significance based on Kruskal Wallis and Wilcoxon signed ranked tests

Constituent, and detection limit	Kruskal Wallis P	Average HDD Influent	Average HDD Effluent	Wilcoxon P for HDD (Influent = Effluent)	HDD % Reduction	Average Pond Effluent	Wilcoxon P for Pond (Influent = Effluent)	Pond % Reduction	Wilcoxon P for Overall System (Influent = Effluent)	Overall System %Reduction
SSC (mg/L), 1	**<001**	252.9	182.9	**0.002**	34.2	57.5	**0.002**	61.5	**0.002**	75.1
SS Mass (lbs)	**0.001**	747	590	**0.004**	39	61	**0.004**	93	**0.004**	95
0.45-3 µm SSC (mg/L)	0.835	1.9	1.9		0	1.9		N/A		N/A
0.45-3 µm SS Mass (lbs)	**0.008**	4.2	4.2	0.51	7.4	1.9	**0.004**	77.1	**0.004**	75.7
3-12 µm SSC (mg/L)	**0.014**	100	100	0.889	0	31	**0.002**	67	**0.002**	64.5
3-12 µm SS Mass (lbs)	**0.003**	310	310	0.625	0	36.5	**0.004**	94.2	**0.004**	92.0
12-30 µm SSC (mg/L)	**0.001**	82.4	47.2	**0.043**	31.5	17.3	**0.003**	57.7	**0.004**	62.8
12-30 µm SS Mass (lbs)	**0.001**	253.4	133.3	0.068	36.4	13.5	**0.004**	92.2	**0.004**	94.2
30-60 µm SSC (mg/L)	**<0.001**	37	19.4	**0.008**	47.5	4.3	**0.003**	65.0	**0.002**	82.8
30-60 µm SS Mass (lbs)	**<0.001**	107	42	**0.045**	46.0	4.9	**0.004**	92.7	**0.004**	96.3
60-120 µm SSC (mg/L)	**<0.001**	22.0	7.8	**0.008**	49.4	2.0	**0.004**	54	**0.002**	85.0
60-120 µm SS Mass (lbs)	**<0.001**	50.0	20.9	**0.029**	41.7	2.8	**0.004**	93.1	**0.004**	95.7
120-250 µm SSC (mg/L)	**0.02**	2.9	0.33	**0.033**	38.2	0.4	1.00	40.0	**0.025**	87.8
120-250 µm SS Mass (lbs)	0.052	10.0	0.55		36	0.37		99.0		99.0
250-1180 µm SSC (mg/L)	**0.019**	7.81	2.95	**0.014**	72.3	0.4	0.059	83.6	**0.014**	94.2
250-1180 µm SS Mass (lbs)	**0.035**	19.1	10.8	**0.014**	72.3	1.0	**0.036**	95.1	**0.014**	98.3
> 1180 µm SSC (mg/L)	0.129	3.07	1.0		74.5	0.3		66.0		92.4
> 1180 µm SS Mass (lbs)	0.181	11.1	2.2		74.6	0.8		71.4		97.7
Total Al Conc (mg/L), 0.005	**0.002**	4.3	3.7	0.06	12.9	1.2	**0.002**	63.4	**0.003**	65.6
Total Al Mass (lbs)	**0.003**	12.9	10.8	0.154	20.6	1.3	**0.004**	93.5	**0.006**	92.8
Total As Conc (mg/L), 0.005	NA	0.0062	0.0057		28.8	<DL		NA		NA
Total As Mass (lbs)	**0.007**	0.014	0.012	0.059	5.9	0.005	**0.004**	76.5	**0.006**	76.9
Total Cd Conc (mg/L), 0.001	NA	0.0043	0.0039		14.6	0.0016		58.8		64.4
Total Cd Mass (lbs)	**0.002**	0.05	0.05	0.636	18.6	0.001	**0.006**	88.4	**0.006**	90.8
Total Cu Conc (mg/L), 0.003	**0.001**	0.57	0.43	**0.009**	21.3	0.13	**0.002**	63.9	**0.003**	72.5
Total Cu Mass (lbs)	**0.001**	1.69	1.21	**0.018**	27.8	0.12	**0.004**	93.4	**0.006**	94.8
Total Fe Conc (mg/L), 0.041	**0.001**	14.7	12.2	0.055	15.4	3.4	**0.002**	67.6	**0.003**	71.4
Total Fe Mass (lbs)	**0.001**	43.8	34.7	0.103	21.4	3.6	**0.004**	94.1	**0.006**	94.0

Total Pb Conc (mg/L), 0.005	**0.001**	0.40	0.32	**0.025**	16.1	0.09	**0.002**	67.0	**0.003**	70.6
Total Pb Mass (lbs)	**0.001**	1.18	0.9	**0.025**	24.1	0.1	**0.004**	94.2	**0.006**	94.2
Total Mn Conc (mg/L), 0.003	0.826	0.27	0.24		9.3	0.11		47.7		48.4
Total Mn Mass (lbs)	**0.001**	2.8	3.1	0.415	17.1	0.9	**0.004**	90.3	**0.006**	90.4
Total Ni Conc (mg/L), 0.01	NA	0.029	0.028		10.8	0.013		58.7		61
Total Ni Mass (lbs)	**0.002**	0.08	0.06	0.058	11.0	0.01	**0.004**	86.5	**0.006**	88.3
Total Zn Conc (mg/L), 0.003	**0.002**	0.87	0.71	**0.029**	16.3	0.25	**0.002**	62.0	**0.003**	65.4
Total Zn Mass (lbs)	**0.001**	2.43	1.97	**0.025**	25.0	0.25	**0.004**	92.8	**0.006**	92.8
COD Conc (mg/L), 1.0	**0.035**	179.8	126.9	0.505	23.4	69.5	**0.014**	38.8	**0.009**	57.2
COD Mass (lbs)	**0.011**	555.8	345.2	0.76	31.0	83.5	**0.014**	90.6	**0.008**	92.3
Ammonia Conc (mg/L)	0.770	2.64	2.77		-89.9	1.53		48.4		-438.5
Ammonia Mass (lbs)	0.354	2.3	3.2		-87.5	2.0		94.0		-295
Nitrate Conc (mg/L)	0.842	0.6	0.9		-65.2	0.7		-8.6		-21.8
Nitrate Mass (lbs)	0.051	1.8	1.8		-50.0	0.8		75.6		72.4
Phosphate Conc (mg/L)	0.746	0.3	0.2		-85.0	0.2		-96.8		-19.9
Phosphate Mass (lbs)	0.08	0.86	0.33		34.3	0.2		62.4		85.4
Total N Conc (mg/L), 0.1	0.211	3.8	5.4		-74.4	2.4		1.4		28.2
Total N Mass (lbs)	**0.006**	6.9	8.4	0.476	-75.0	1.6	**0.009**	87.9	0.067	88.5
Total P Conc (mg/L), 0.01	0.222	0.3	0.6		-22.6	0.2		52.5		48.8
Total P Mass (lbs)	0.091	0.9	1.1		-9.5	0.2		93.7		86.7
Dissolved Cd Conc (mg/L), 0.001	NA	0.003	0.001		10.5	<DL		NA		NA
Dissolved As Conc (mg/L), 0.005	NA	<DL	<DL		NA	<DL		NA		NA
Dissolved Cu Conc (mg/L),0.003	0.8	0.037	0.022		10.6	0.026		-18.9		-24.8
Dissolved Cu Mass (lbs)	**0.021**	0.052	0.046	0.61	17.3	0.024	**0.004**	71.9	**0.032**	62.6
Dissolved Fe Conc (mg/L), 0.0041	NA	0.08	0.04		35.4	0.03		-9.7		NA
Dissolved Pb Conc (mg/L), 0.005	NA	0.02	<DL		NA	0.01		NA		NA
Dissolved Mn Conc (mg/L), 0.003	NA	0.038	0.038		-46.9	0.024		34.2		69.0
Dissolved Mn Mass (lbs)	0.026	0.038	0.042	0.726	-21.1	0.004	**0.004**	82.4	**0.009**	80.8
Dissolved Ni Conc (mg/L), 0.01	NA	<DL	<DL		NA	0.012		NA		NA

Dissolved Zn Conc (mg/L), 0.003	0.299	0.064	0.059		1.0	0.043		13.8		-3.8
Dissolved Zn Mass (lbs)	**0.007**	0.13	0.17	0.919	4.8	0.05	**0.004**	79.9	**0.008**	68.9
Dissolved N Conc (mg/L), 0.1	NA	3.2	2.9		-44.1	1.4		69.9		56.4
Dissolved N Mass (lbs)	0.826	1.71	2.6		-1100.0	1.1		-288.0		-266
Dissolved P Conc (mg/L), 0.01	NA	0.08	0.10		-42.50	0.19		-520.4		-196.4
Dissolved P Mass (lbs)	0.145	0.07	0.2		-441.7	0.02		48.2		12.7

(NA – too many samples have non-detectable concentrations to perform statistical analyses. Values in bold indicate the statistically significant p values ≤0.05). Be cautious when interpreting % reductions when the p-values are large

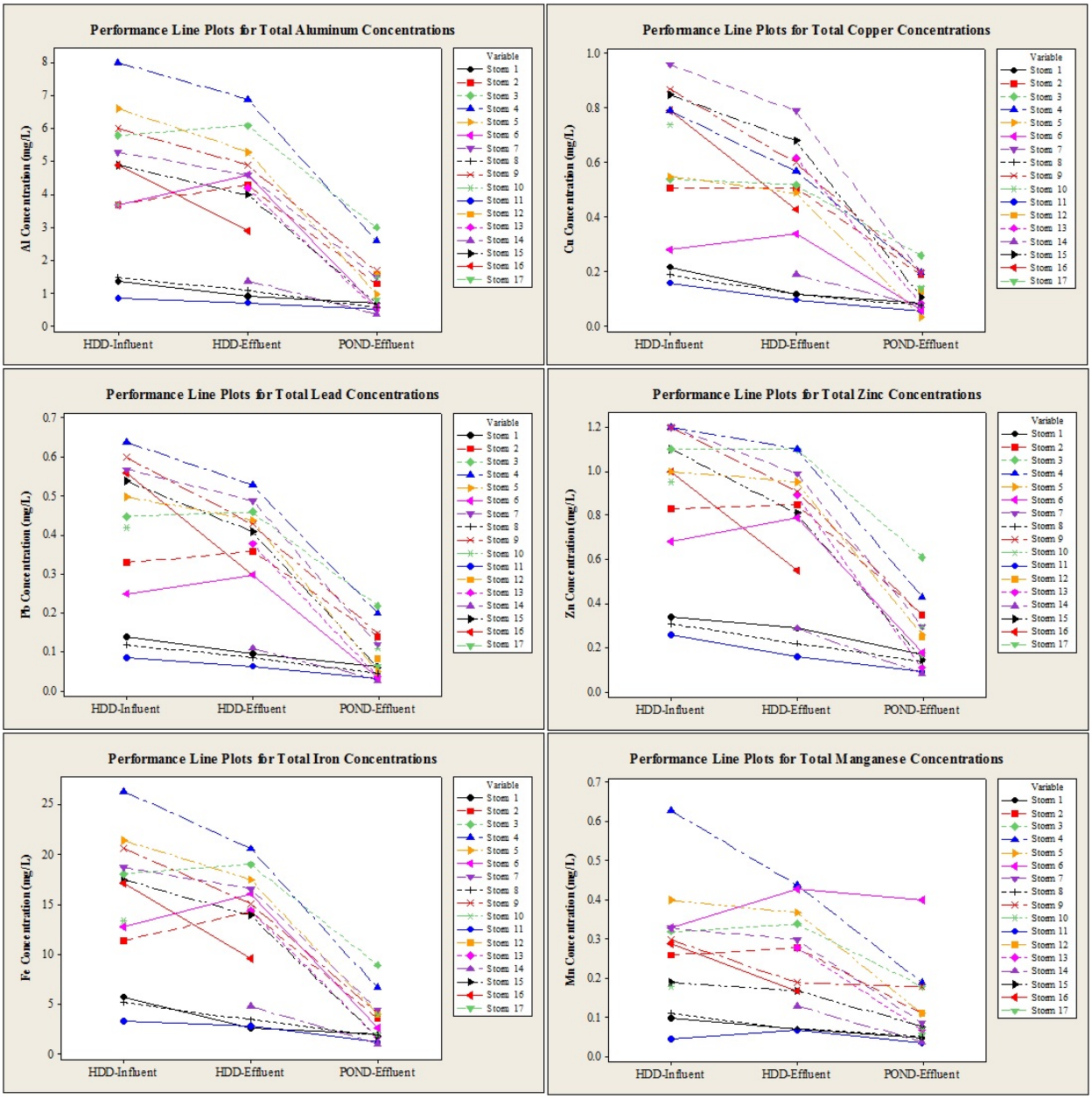

Figure 3-16 Line plots of total (unfiltered) metal concentrations for influent and effluent samples of the HDD and the dry pond

Table 3-9 Summary of Regression and ANOVA of total (unfiltered) and dissolved metal concentrations (mg/L) for all the sampled storms

Regression and ANOVA for total (unfiltered) metal concentrations (mg/L)					
Constituent	Regression Equation	Variables (x, y)	p- value (X variable)	p- value (Intercept)	Significance factor of equation
Total	y = 0.771x	HDD Influent, HDD Effluent	<0.001	>0.05*	<0.001

Copper Conc	y = 0.266x	HDD Effluent, Pond Effluent	<0.001	>0.05	<0.001
	y = 0.225x	HDD Influent, Pond Effluent	<0.001	>0.05	<0.001
Total Lead Conc	y = 0.81x	HDD Influent, HDD Effluent	<0.001	>0.05	<0.001
	y = 0.28x	HDD Effluent, Pond Effluent	<0.001	>0.05	<0.001
	y = 0.253x	HDD Influent, Pond Effluent	<0.001	>0.05	<0.001
Total Zinc Conc	y = 0.851x	HDD Influent, HDD Effluent	<0.001	>0.05	<0.001
	y = 0.341x	HDD Effluent, Pond Effluent	<0.001	>0.05	<0.001
	y = 0.319x	HDD Influent, Pond Effluent	<0.001	>0.05	<0.001
Total Iron Conc	y = 0.84x	HDD Influent, HDD Effluent	<0.001	>0.05	<0.001
	y = 0.273x	HDD Effluent, Pond Effluent	<0.001	>0.05	<0.001
	y = 0.253x	HDD Influent, Pond Effluent	<0.001	>0.05	<0.001
Total Manganese Conc	y = 0.852x	HDD Influent, HDD Effluent	<0.001	>0.05	<0.001
	y = 0.508x	HDD Effluent, Pond Effluent	<0.001	>0.05	<0.001
	y = 0.447x	HDD Influent, Pond Effluent	<0.001	>0.05	<0.001
Total Aluminum Conc	y = 0.874x	HDD Influent, HDD Effluent	<0.001	>0.05	<0.001
	y = 0.307x	HDD Effluent, Pond Effluent	<0.001	>0.05	<0.001
	y = 0.295x	HDD Influent, Pond Effluent	<0.001	>0.05	<0.001
Dissolved Copper Conc	y = 0.211x	HDD Influent, HDD Effluent	0.018	>0.05	0.018
	y = 1.11x	HDD Effluent, Pond Effluent	<0.001	>0.05	<0.001
	y = 0.198x	HDD Influent, Pond Effluent	0.076	>0.05	0.076
Dissolved Zinc Conc	y = 0.636x	HDD Influent, HDD Effluent	<0.001	>0.05	<0.001
	y = 0.556x	HDD Effluent, Pond Effluent	<0.001	>0.05	<0.001
	y = 0.5x	HDD Influent, Pond Effluent	0.002	>0.05	0.002

Table 3-10 Summary of Regression and ANOVA of total (unfiltered) and filtered metal masses (lbs) for all the sampled storms

Regression and ANOVA for total (unfiltered) metal masses (lbs)					
Constituent	Regression Equation	Variables (x, y)	p- value (X variable)	p- value (Intercept)	Significance factor of equation
Total Copper Mass	y = 0.741x	HDD Influent, HDD Effluent	<0.001	>0.05	<0.001
	y = 0.082x	HDD Effluent, Pond Effluent	<0.001	>0.05	<0.001
	y = 0.086x	HDD Influent, Pond Effluent	<0.001	>0.05	<0.001
Total Lead Mass	y = 0.826x	HDD Influent, HDD Effluent	<0.001	>0.05	<0.001
	y = 0.091x	HDD Effluent, Pond Effluent	<0.001	>0.05	<0.001
	y = 0.102x	HDD Influent, Pond Effluent	<0.001	>0.05	<0.001
Total Zinc Mass	y = 0.9x	HDD Influent, HDD Effluent	<0.001	>0.05	<0.001
	y = 0.096x	HDD Effluent, Pond Effluent	<0.001	>0.05	<0.001
	y = 0.125x	HDD Influent, Pond Effluent	<0.001	>0.05	<0.001
Total Iron Mass	y = 0.79x	HDD Influent, HDD Effluent	<0.001	>0.05	<0.001
	y = 0.084x	HDD Effluent, Pond Effluent	<0.001	>0.05	<0.001
	y = 0.09x	HDD Influent, Pond Effluent	<0.001	>0.05	<0.001

Total Manganese Mass	y = 1.40x	HDD Influent, HDD Effluent	<0.001	>0.05	<0.001
	y = 0.0025x	HDD Effluent, Pond Effluent	0.655	>0.05	0.655
	y = 0.0064x	HDD Influent, Pond Effluent	0.474	>0.05	0.474
Total Aluminum Mass	y = 0.861x	HDD Influent, HDD Effluent	<0.001	>0.05	<0.001
	y = 0.099x	HDD Effluent, Pond Effluent	<0.001	>0.05	<0.001
	y = 0.112x	HDD Influent, Pond Effluent	<0.001	>0.05	<0.001
Dissolved Copper Mass	y = 0.312x	HDD Influent, HDD Effluent	0.044	>0.05	0.044
	y = 0.456x	HDD Effluent, Pond Effluent	<0.001	>0.05	<0.001
	y = 0.235x	HDD Influent, Pond Effluent	0.11	>0.05	0.11
Dissolved Zinc Mass	y = 0.813x	HDD Influent, HDD Effluent	0.002	>0.05	0.002
	y = 0.136x	HDD Effluent, Pond Effluent	0.001	>0.05	0.001
	y = 0.418x	HDD Influent, Pond Effluent	0.001	>0.05	0.001

Figure 3-17 and Table 3-11 present the performance concentration line plots and descriptive summaries of statistics for COD and nutrients for all the monitored storms. The overall performance indicates low reductions of COD concentrations for the HDD and moderate reductions for the dry infiltration pond. The dry pond showed moderate reductions for ammonia and total phosphorous concentrations and higher mass reductions (> 90%) due to the infiltration losses. Statistical analyses were also conducted for mass of COD and nutrients with the results shown in Table 3-12.

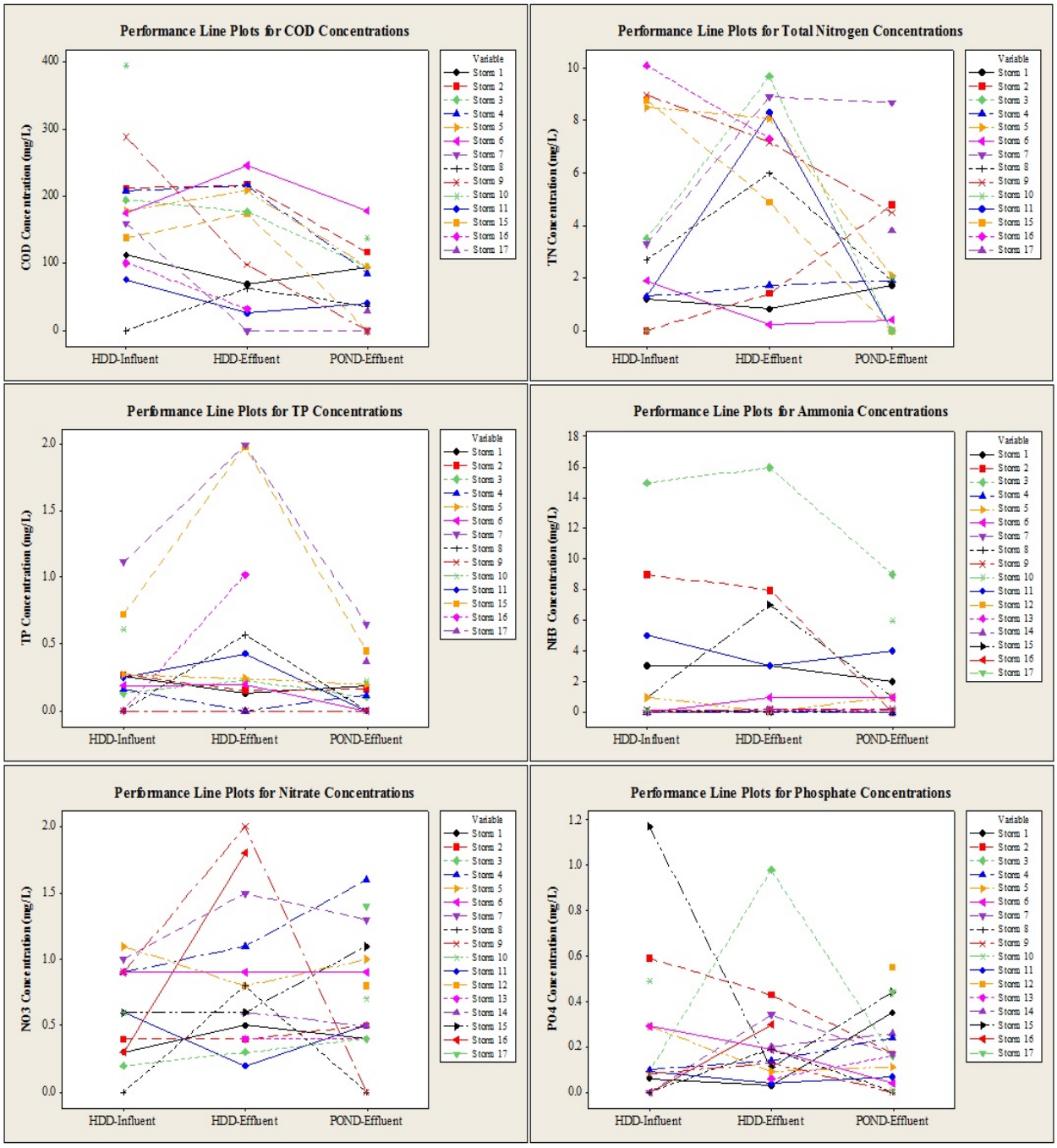

Figure 3-17 Line plots of COD and nutrient concentrations for influent and effluent samples of HDD and dry pond

Table 3-11 Summary of Regression and ANOVA of COD and nutrient concentrations (mg/L) for all the sampled storms

Regression and ANOVA for COD and nutrient concentrations (mg/L)					
Constituent	Regression Equation	Variables (x,y)	p- value (X variable)	p- value (Intercept)	Significance factor of equation

COD Conc	y = 0.787x	HDD Influent, HDD Effluent	<0.001	>0.05	<0.001
	y = 0.48x	HDD Effluent, Pond Effluent	<0.001	>0.05	<0.001
	y = 0.361x	HDD Influent, Pond Effluent	0.001	>0.05	0.001
Total Nitrogen Conc	y = 0.927x	HDD Influent, HDD Effluent	0.001	>0.05	0.001
	y = 0.352x	HDD Effluent, Pond Effluent	0.029	>0.05	0.029
	y = 0.362x	HDD Influent, Pond Effluent	0.078	>0.05	0.078
Total Phosphorous Conc	y = 1.88x	HDD Influent, HDD Effluent	<0.001	>0.05	<0.001
	y = 0.268x	HDD Effluent, Pond Effluent	<0.001	>0.05	<0.001
	y = 0.547x	HDD Influent, Pond Effluent	<0.001	>0.05	<0.001
Ammonia Conc	y = x	HDD Influent, HDD Effluent	<0.001	>0.05	<0.001
	y = 0.438x	HDD Effluent, Pond Effluent	<0.001	>0.05	<0.001
	y = 0.479x	HDD Influent, Pond Effluent	0.003	>0.05	0.003
Nitrate Conc	y = 1.28x	HDD Influent, HDD Effluent	<0.001	>0.05	<0.001
	y = 0.644x	HDD Effluent, Pond Effluent	0.003	>0.05	0.003
	y = 1.07x	HDD Influent, Pond Effluent	<0.001	>0.05	<0.001
Phosphate Conc	y = 0.303x	HDD Influent, HDD Effluent	0.249	>0.05	0.249
	y = 0.322x	HDD Effluent, Pond Effluent	0.062	>0.05	0.062
	y = 0.337x	HDD Influent, Pond Effluent	0.006	>0.05	0.006

Table 3-12 Summary of Regression and ANOVA of COD and nutrient mass (lbs) for all the sampled storms

Regression and ANOVA for COD and nutrient masses (lbs)					
Constituent	Regression Equation	Variables (x,y)	p- value (X variable)	p- value (Intercept)	Significance factor of equation
COD Mass	y = 1.04x	HDD Influent, HDD Effluent	<0.001	>0.05	<0.001
	y = 0.109x	HDD Effluent, Pond Effluent	<0.001	>0.05	<0.001
	y = 0.184x	HDD Influent, Pond Effluent	<0.001	>0.05	<0.001
Total Nitrogen Mass	y = 0.50x + 4.6	HDD Influent, HDD Effluent	0.017	0.032	0.02
	y = 0.114x	HDD Effluent, Pond Effluent	0.029	>0.05	0.029
	y = 0.076x	HDD Influent, Pond Effluent	0.447	>0.05	0.447
Total Phosphorous Mass	y = 1.87x	HDD Influent, HDD Effluent	0.001	>0.05	<0.001
	y = 0.083x	HDD Effluent, Pond Effluent	0.004	>0.05	<0.001
	y = 0.216x	HDD Influent, Pond Effluent	<0.001	>0.05	<0.001
Ammonia Mass	y = 1.06x	HDD Influent, HDD Effluent	0.021	>0.05	0.021
	y = 0.045x	HDD Effluent, Pond Effluent	0.009	>0.05	0.009
	y = 0.134x	HDD Influent, Pond Effluent	0.814	>0.05	0.814
Nitrate Mass	y = 1.18x	HDD Influent, HDD Effluent	<0.001	>0.05	<0.001
	y = 0.412x	HDD Effluent, Pond Effluent	<0.001	>0.05	<0.001
	y = 0.549x	HDD Influent, Pond Effluent	<0.001	>0.05	<0.001
Phosphate	y = 0.209x	HDD Influent, HDD Effluent	0.107	>0.05	0.107

Mass	y = 0.447x	HDD Effluent, Pond Effluent	0.007	>0.05	0.007
	y = 0.01x	HDD Influent, Pond Effluent	0.039	>0.05	0.039

The HDD resulted in significant removals for SSC and for particle sizes greater than 12 μm. The removals for particle sizes increased with increases in particle size. Removals for particulates ranged from 35% to about 75% for particles with size ranges greater than 250 μm. The dry infiltration pond and the system as a whole showed moderate to high reductions for total SSC and for all the particle size ranges analyzed. The dry pond and the overall system showed high removals for particulate and dissolved masses which can be associated with major reductions of runoff volume by the dry infiltration pond.

The HDD indicated significant removals for metals, but at lower removal rates compared to the particulate solids (due to the filtered metal components that are poorly removed in the HDD). The average reductions of metal concentrations ranged from 8% to 30% in the HDD. The dry infiltration pond and the overall system showed medium to high levels of removals for heavy metal (> 45%) concentrations and high removals for total masses of the metals. Only filtered copper and zinc could be statistically evaluated as the other filtered metal concentrations were not detected in more than 80% of the samples. The dry infiltration pond showed mass removal rates larger than 60% for dissolved copper and zinc. No significant reductions were observed for nutrients. Significant (based on non-parametric Wilcoxon signed rank tests) concentration and mass percentage removal summaries for all the constituents for the HDD, the dry pond, and the overall treatment train system are shown for low, moderate and high percentage removals in Tables 3-13 through 3-17. The largest particle size ranges (>120 μm) likely also have almost complete concentration removals in the HDD and the pond, but are not shown due to the lack of

these large particles in many of the samples resulting in few quantifiable results available for reliable statistical analyses. However, the mass reductions of these large particles in the pond were able to be evaluated due to the large runoff volume reductions.

Table 3-13 HDD significant % concentration removals

Constituent	Low Removals (< 40 % Removal)
SSC	34.2
12-30 µm SSC	31.5
120-250 µm SSC	38.2
Total Cu Concentration	21.3
Total Pb Concentration	16.1
Total Zn Concentration	16.3
	Moderate Removals (40-70% Removal)
30-60 µm SSC	47.8
60-120 µm SSC	49.4

Table 3-14 Dry pond significant % concentration removals

Constituent	Low Removals (< 40 % Removal)
COD	38.8
	Moderate Removals (40-70 % Removal)
SSC	61.5
3-12 µm SSC	67.0
12-30 µm SSC	57.7
30-60 µm SSC	65.0
60-120 µm SSC	54.0
Total Al Concentration	63.4
Total Cu Concentration	63.9
Total Fe Concentration	67.6
Total Pb Concentration	67.0
Total Zn Concentration	62.0

Table 3-15 Dry pond significant % mass removals

Constituent	High Removals (> 70% Removal)
SS Mass	93.0
0.45-3 µm SS Mass	77.1
3-12 µm SS Mass	94.2
12-30 µm SS Mass	92.2
30-60 µm SS Mass	92.7

60-120 µm SS Mass	93.1
250-1180 µm SS Mass	95.1
Total Al Mass	93.5
Total As Mass	76.5
Total Cd Mass	88.4
Total Cu Mass	93.4
Total Fe Mass	94.1
Total Pb Mass	94.2
Total Mn Mass	90.3
Total Ni Mass	86.5
Total Zn Mass	92.8
COD Mass	90.6
Total N Mass	87.9
Dissolved Cu Mass	71.9
Dissolved Mn Mass	82.4
Dissolved Zn Mass	79.9

Table 3-16 Overall system significant % concentration removals

Constituent	Moderate Removals (40-70 % Removal)
3-12 µm SSC	64.5
12-30 µm SSC	62.8
Total Al Concentration	65.6
Total Zn Concentration	65.4
COD	57.2
	High Removals (> 70 % Removal)
SSC	75.1
30-60 µm SSC	82.8
60-120 µm SSC	85.0
120-250 µm SSC	87.8
250-1180 µm SSC	94.2
Total Cu Concentration	72.5
Total Fe Concentration	71.4
Total Pb Concentration	70.6

Table 3-17 Overall system significant % mass removals

Constituent	Moderate Removals (40-70 % Removal)
Dissolved Cu Mass	62.6
Dissolved Zn Mass	68.9
	High Removals (> 70 % Removal)
SS Mass	95.0

0.45-3 µm SS Mass	75.7
3-12 µm SS Mass	92.0
12-30 µm SS Mass	94.2
30-60 µm SS Mass	96.3
60-120 µm SS Mass	95.7
250-1180 µm SS Mass	98.3
Total Al Mass	92.8
Total As Mass	76.9
Total Cd Mass	90.8
Total Cu Mass	94.8
Total Fe Mass	94.0
Total Pb Mass	94.2
Total Mn Mass	90.4
Total Ni Mass	88.3
Total Zn Mass	92.8
COD Mass	92.3
Dissolved Mn Mass	80.8

3.3.6 Prediction of Sedimentation Removal of Particulate Pollutants by the Surface Overflow Rate (SOR) Method

In order to make solids removal predictions based on settling equations, the hydrograph and influent particle distribution (as well as specific gravity of the particles) need to be known, along with the physical and hydrodynamic features of the stormwater control device. Critical parameters that define the dimensions of a settling unit include the surface overflow rate (SOR) and the hydraulic loading rate. The surface overflow rate is expressed as a factor of flow per surface area (Clark et al 2009, Bolognesi et al 2012). As per Stokes' Law, all the particles with settling velocities greater than the SOR are assumed to be captured in the device (ignoring short-circuiting, hindered settling, and other detrimental elements) (Clark et al 2009).

$$SOR = \frac{Q}{A_E} \qquad \text{(Equation 1)}$$

Where Q = average flow rate of the runoff through the device, and

A_E = effective surface area of the device.

Settling velocities for the fine particles can be calculated according to the Stokes' Law (Yang et al 1996):

$$V_s = \frac{1}{18} * \left(\frac{\rho_s - \rho}{\rho}\right) * g * \left(\frac{d^2}{v}\right) \qquad \text{(Equation 2)}$$

Where,

V_s = settling velocity of the particle;

ρ_s = density of the solid particle;

ρ = density of the liquid;

g = gravitational acceleration;

d = diameter of the particle; and

v = kinematic viscosity of the liquid.

Since sedimentation is the main phenomenon for removal of particulates from runoff, both the HDD and the dry infiltration pond observed performance were evaluated in terms of its SOR (Figures 3-18 and 3-19).

Average surface over flow rates for each of the individual events were calculated using Equation 1. The average flow rate was obtained from the flow meter data recorded for each individual event. The effective surface area for the HDD is calculated by multiplying the length with the width of the device which was the same for all events (vertical sides). The effective surface area for the dry pond was calculated based on the average depth of flow in the dry pond during each individual event. SOR is then calculated as the ratio of the average flow rate to the effective surface area. Percentage removals for each event were calculated based on the observed SSC values from the HDD influent, HDD effluent and dry pond effluent as per equation 3.

$$\%\ SSC\ Removal = \left(\frac{Influent\ SSC - Effluent\ SSC}{Influent\ SSC} * 100\right) \qquad \text{(Equation 3)}$$

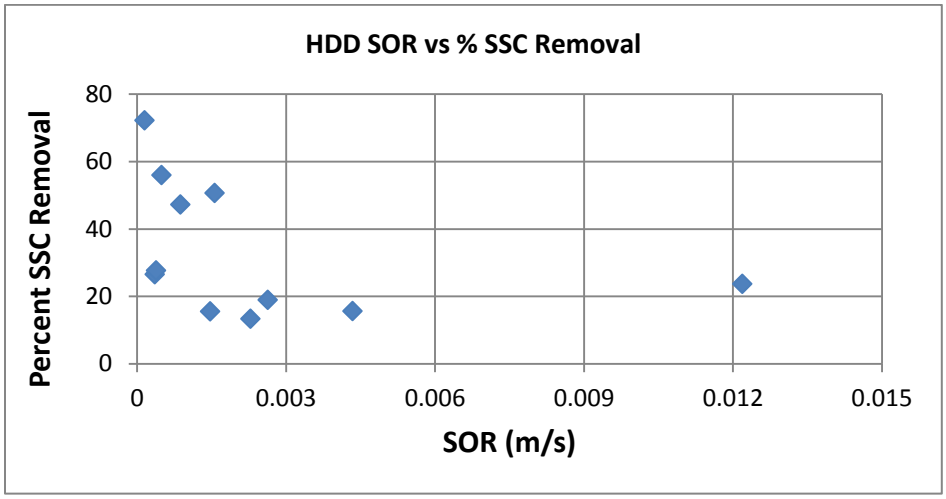

Figure 3-18 Percent removal of SSC by HDD based on measured influent SSC concentrations

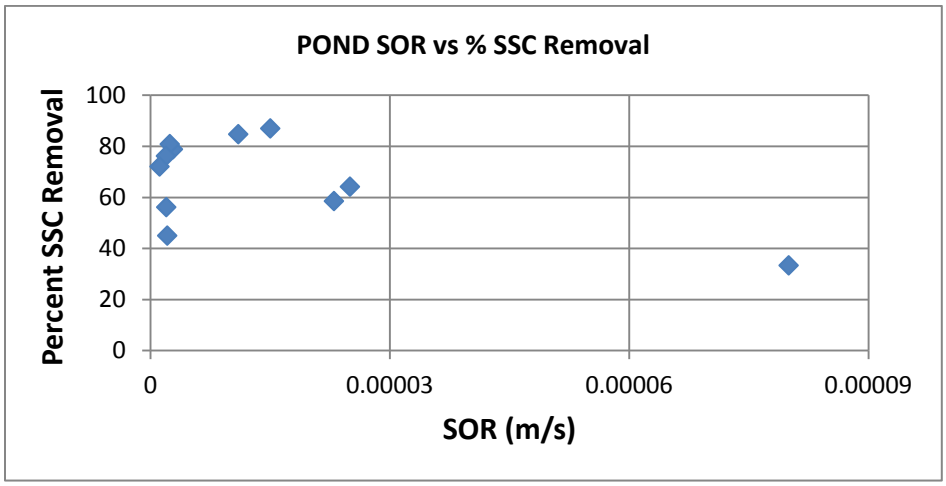

Figure 3-19 Percent removal of SSC by dry pond based on measured influent concentrations

As predicted by Stokes' Law, the performance of both the HDD and the pond decreased with increasing SOR. The critical particle sizes increases with increases in the SOR. The critical particle size (having a settling velocity equal to the SOR) is the theoretical maximum particle size remaining in the runoff, with larger particles trapped in the treatment device. Critical particles sizes were calculated according to Stokes' Law (Yang et al 1996, Guo et al 2005) based

on the particle settling velocities, as shown on Tables 3-15 and 3-16. The values ranged from 10 to 158 µm for the HDD and 0.6 to 24.4 µm for the dry pond. Based on PSD analyses, the HDD was capable of reducing the median particle size from 20 µm to 12 µm. The calculated and predicted removal rates for the HDD and dry pond are also shown on Tables 3-18 and 3-19.

Table 3-18 Predicted and calculated SSC removals for HDD

Hydrodynamic Separator Device						
Event Date	Average flow rate (cfs)	Surface Area (ft^2)	SOR (m/s)	Observed % SSC Reduction	Critical particle size (Calculated based on SOR)	% of particles > critical particle size (expected % SSC reduction)
1/10/2014	2.1	280	0.002286	13.3	42	9
2/20/2014	11.19	280	0.01219	23.7	158	5
2/25/2014	3.99	280	0.00434	15.6	65	11.5
3/4/2014	0.33	280	0.00036	26.5	13.4	53
4/4/2014	1.35	280	0.00147	15.5	116	7
4/7/2014	1.435	280	0.00156	50.6	45.2	18
4/8/2014	0.35	280	0.00038	27.7	10	75
4/18/2014	0.45	280	0.00049	56	20.2	73
5/14/2014	0.14	280	0.00015	72.2	7.5	95
5/28/2014	2.415	280	0.00263	18.9	73	5
6/13/2014	0.8	280	0.00087	47.2	35	29

Table 3-19 Predicted and calculated SSC removals for dry pond

Dry Infiltration Pond						
Event Date	Average flow rate (cfs)	Surface Area (ft^2)	SOR (m/s)	Observed % SSC Reduction	Critical particle size (Calculated based on SOR)	% of particles > critical particle size (expected % SSC reduction)
1/10/2014	0.105	16100	0.00000199	56.1	2	99
2/20/2014	1.49	18152	0.000025	64.1	5.1	73
2/25/2014	0.153	16668	0.0000028	78.8	2	99
3/4/2014	0.13	16507	0.0000024	80.8	1.6	99
4/4/2014	0.104	16362	0.00000194	76.2	24.4	18
4/7/2014	0.43	16434	0.00008	33.3	22.1	33
4/8/2014	0.06	16187	0.00000113	72.1	1.1	99.5
4/18/2014	0.11	16238	0.0000021	45	0.6	99.5
5/9/2014	0.81	16560	0.000015	87	10	46

5/14/2014	0.12	16174	0.000023	58.5	2.7	97
5/28/2014	0.585	16477	0.000011	84.7	5	84

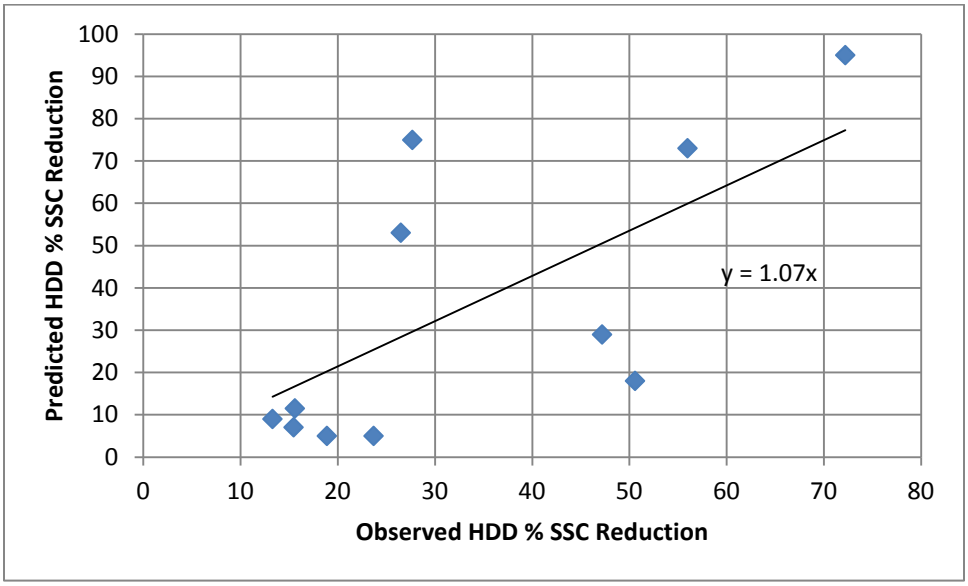

Figure 3-20 Scatterplot of observed vs. predicted SSC reductions for HDD (showing significant regression equation)

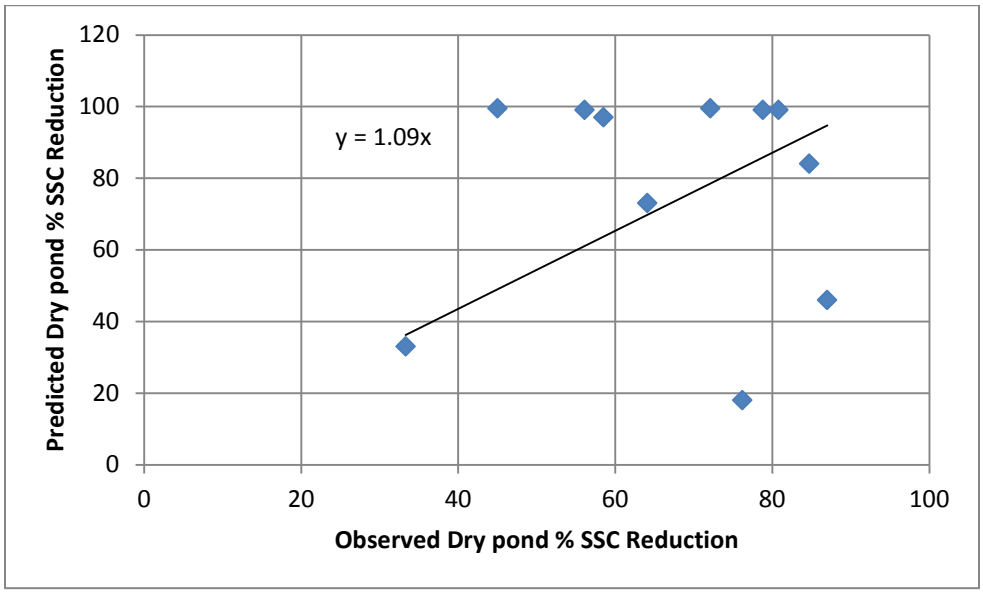

Figure 3-21 Scatterplot of observed vs. predicted SSC reduction for dry pond (showing significant regression equation)

Figures 3-20 and 3-21 show the scatterplots for observed vs. predicted SSC reductions The plots show a lot of variability as the predicted SSC reductions were based on an entire storm event, while the observed reductions only account for SSC reductions during the sample period for each event (about 70 – 80% of each event). The scatter for the pond is greater than for the HDD because the flow rate varied throughout the pond due to infiltration, while the HDD had constant flows. The pond effluent was used in the pond's SOR calculations, as is traditional. Overall, the differences between the average calculated removals and the observed removals for both devices were less than 10% (based on the significant slope term of the regression term). In addition, the non- parametric Wilcoxon signed rank test indicated no significant differences ($p > 0.05$) between the calculated and observed removal rates (for the amount of data available).

3.3.7 Analysis of sediment captured in the Hydrodynamic Separator Device

The hydrodynamic device and the inlet screens were intended to pretreat the water by capturing floatables and larger particles before the runoff enters the dry infiltration pond. The HDD was cleaned of all accumulated sediment at the beginning monitoring program. At the end of the monitoring period, sediment grab samples were collected each of the 4 chambers of the HDD. No sediment was found in the fourth chamber (outlet). The sediment from the first three chambers (inlet, oil & grease, and settleable solids chambers) was dark colored and coarse sandy in texture. During the sediment sampling oil sheens were observed in chambers 2 and 3. At the end of the monitoring period, several inches of sediment was observed in chambers 2 and 3. If the sediment was six inches deep, this would correspond to about 140 ft^3. Based on a dry bulk density value range of 1.5 g/cc to 2.5 g/cc for the sediment of material, this corresponds to about 13,000 to 22,000 lbs of sediment, if six inches of sediment had accumulated. About 25% of the

total monitoring period sediment was assumed to be associated with the 11 monitored storms, based on the ratio of the total runoff volume during the monitored storms to the expected runoff volume for all of the storms during the monitoring period.

The sediment samples from the three chambers was heated in a drying oven at 103 to 105^{o}C for 48 hours, dried and further processed to separate into different particle sizes. Sieve analysis was performed using eight sieves ranging from 45 μm to 4760 μm in aperture. The results of the sieve analysis are shown in Table 3-20 and Figure 3-22. These results represent the characteristics of the sediment captured during the entire monitoring period in each chamber.

Table 3-20 Mass distribution of sediment by particle size range in HDD chambers

	Chamber 1		Chamber 2		Chamber 3	
Particle size	Weight of sample* (gm)	% distribution in chamber 1	Weight of sample* (gm)	% distribution in chamber 2	Weight of sample* (gm)	% distribution in chamber 3
<45	12.07	6.74	35.3	11.16	16.6	3.97
45 - 106	11.48	6.41	26.9	8.50	28.19	6.74
106 - 250	40.23	22.46	102.89	32.52	143.72	34.34
250 - 425	33.96	18.96	56.6	17.89	100.71	24.06
425 - 850	33.4	18.65	75.12	23.74	94.95	22.69
850 - 1180	12.08	6.74	9.52	3.01	21.38	5.11
1180 - 4760	27.36	15.28	8.87	2.80	9.59	2.29
>4760	8.53	4.76	1.18	0.37	3.37	0.81
	179.11	100.0	316.38	100.0	418.51	100.0

*Weight of sample, not mass in the HDD chamber

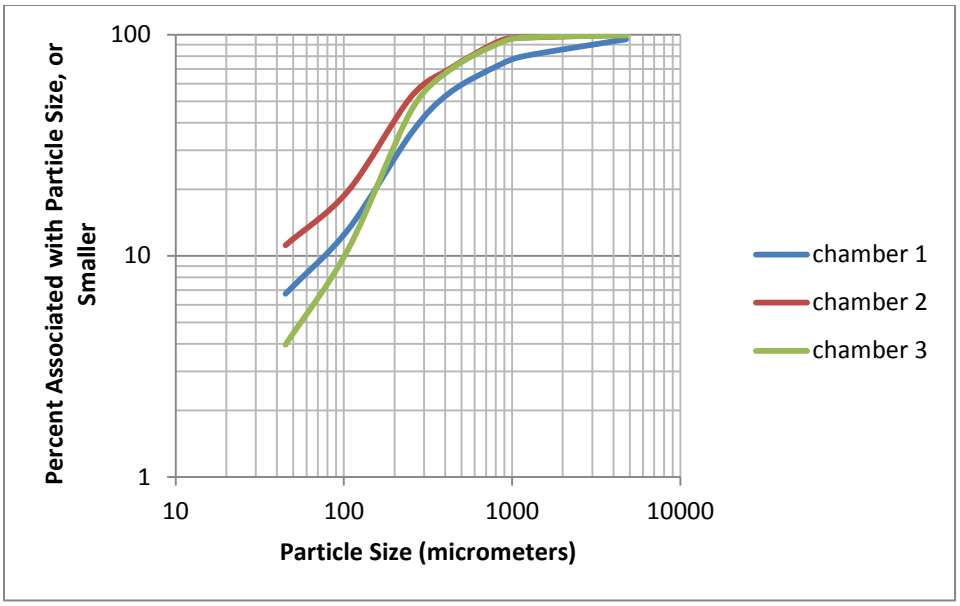

Figure 3-22 Accumulative particulate solids percentage distribution by particle size for HDD sediment by chamber

Table 3-21 shows the particle size calculations and Figure 3-22 shows the PSD for the sediment collected at the end of the monitoring period. For the overall sum of loads calculations, the total mass was calculated by scaling up the calculations with a factor (4.23 for HDD, and 3.28 for dry pond corresponding to the total sediment associated with the overall monitoring period (using a calibrated WinSLAMM analysis) compared to the total sediment mass associated with the monitoring period. The overall sum of loads calculations based on the scaling factors as calculated to be retained by automatic samplers are as shown in Table 3-21. Based on the dry bulk density value range of 1.5 g/cc to 2.5 g/cc this results in a range of 45 to 75 ft^3 of sediment material corresponding to 2 to 3 inches of sediment depth for HDD. Similarly for dry pond, the amount of sediment retained ranges from 135 to 226 ft^3 corresponding to 0.05 to 0.08 inches of sediment depth over the larger area (although most would accumulate near the pond entrance and long the main channel behind the rock check dams).

Table 3-21 Overall mass balance of sediment accumulation for the entire monitoring period

	Influent mass for sampled storms (lbs)	Effluent mass for sampled storms (lbs)	Amount retained for Monitored Events (lbs)	Scaling factor (sediment in runoff during complete monitoring period/sediment during sampled events)	Total Mass for Monitoring Period (lbs)
HDD	7,097	5,431	1,666	4.23	7,046
Dry pond	7,015	561	6,454	328	21,181

Most of the sediment captured in the chambers was greater than 45 um (less than 10% of the mass was less than this size), and the maximum size observed was about 5,000 μm,

The median particle sizes were 275 μm and 245 μm for the oil & grease and settleable solids chambers (the second and third chambers respectively). About 80% of the particles captured in the oil & grease chamber 2 and 90% of the particles captured in the settleable solids chamber 3 are larger than 100 μm indicating retention of the larger size particles in the HDD. This is typical for hydrodynamic devices as smaller particles require more time to settle and are more susceptible to scour.

Chemical analyses were performed on the sediment for the different particle sizes (Al, As, Cd, Cu, Fe, Pb, Mn, Ni, and Zn) and the results were as shown in Figures 3-23 through 3-31 . Accumulative mass percentage distribution plots show that about 80% of the metal mass is distributed between the particle size ranges of 45 to 1180 μm. Heavy metal associations tend to be higher on very fine particles (due to large surface areas) and organic material (due to organic bonds). As shown in these figures. Only small portions of the mass are associated with the smaller particle sizes in the HDD; most (about 75+%) of the metals by mass are associated with the particle sizes from about 100 to 1,000 μm.

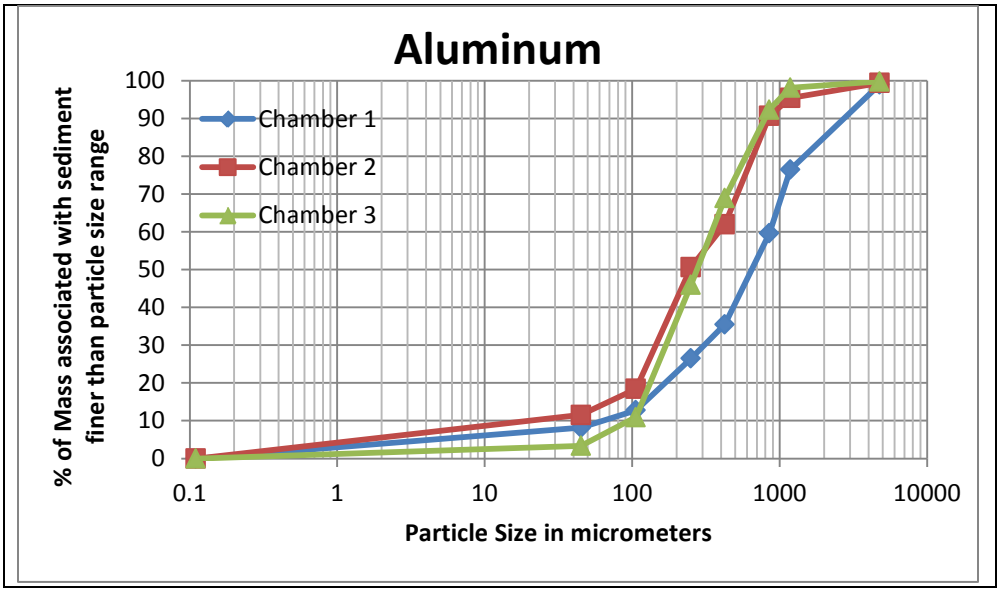

Figure 3-23 Accumulative mass distribution of aluminum by particle size in HDD sediments

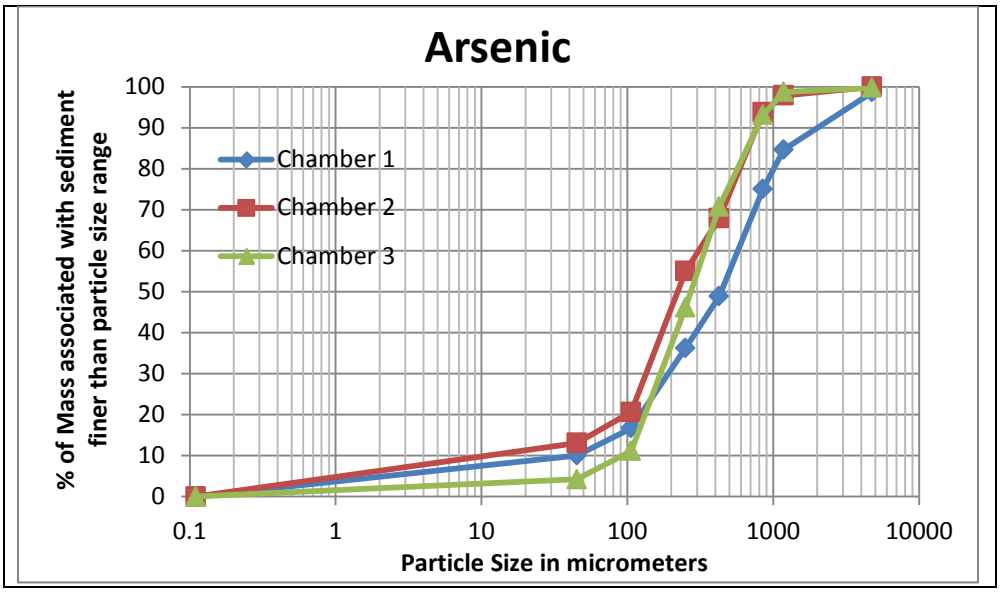

Figure 3-24 Accumulative mass distribution of arsenic by particle size in HDD sediments

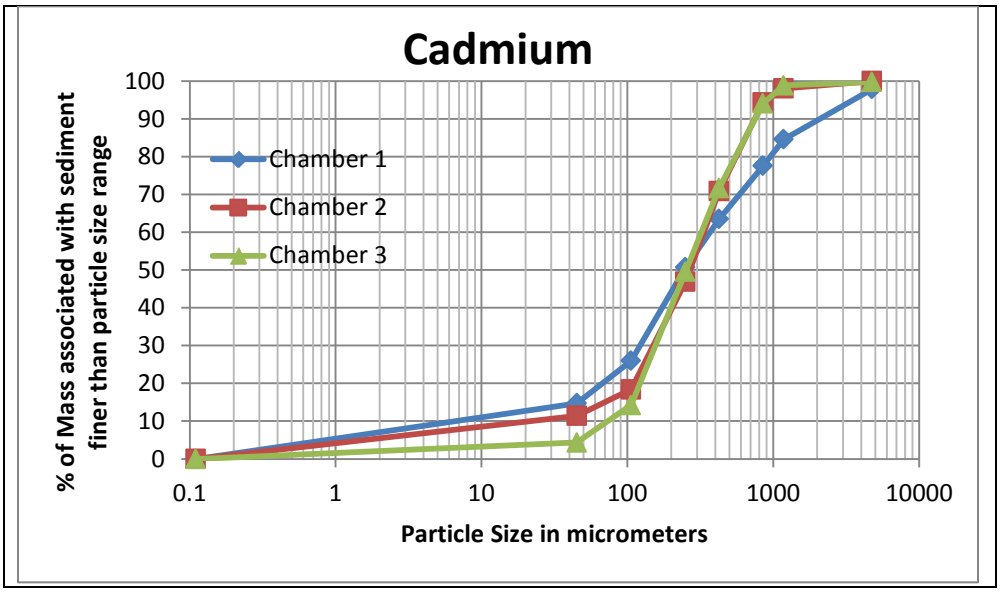

Figure 3-25 Accumulative mass distribution of cadmium by particle size in HDD sediments

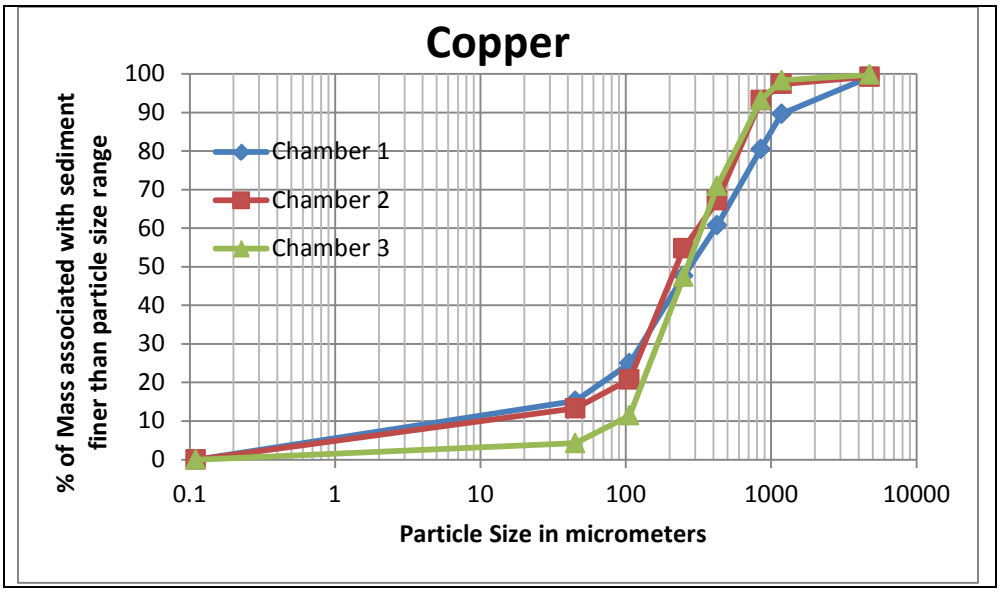

Figure 3-26 Accumulative mass distribution of copper by particle size in HDD sediments

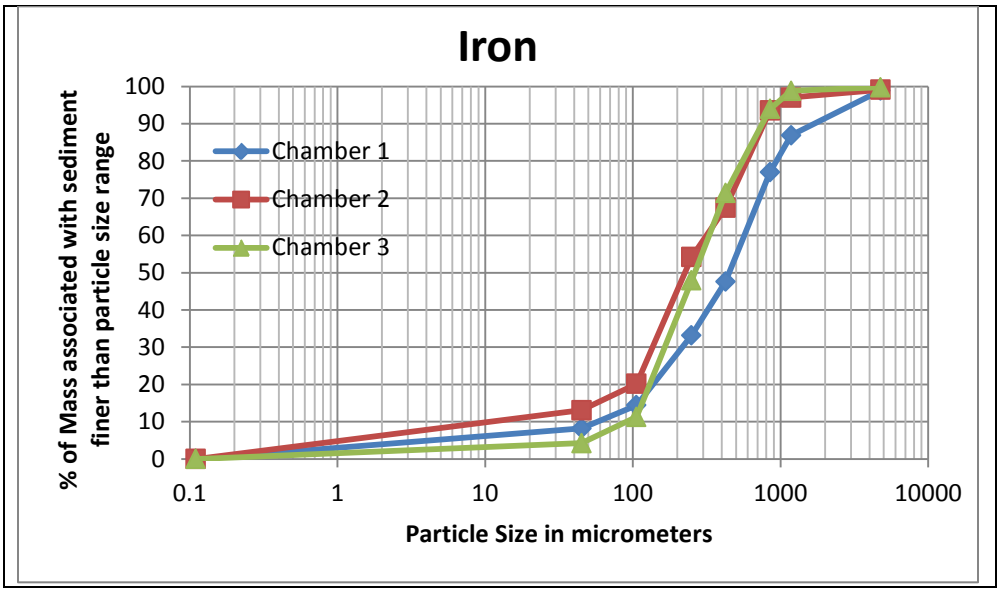

Figure 3-27 Accumulative mass distribution of iron by particle size in HDD sediments

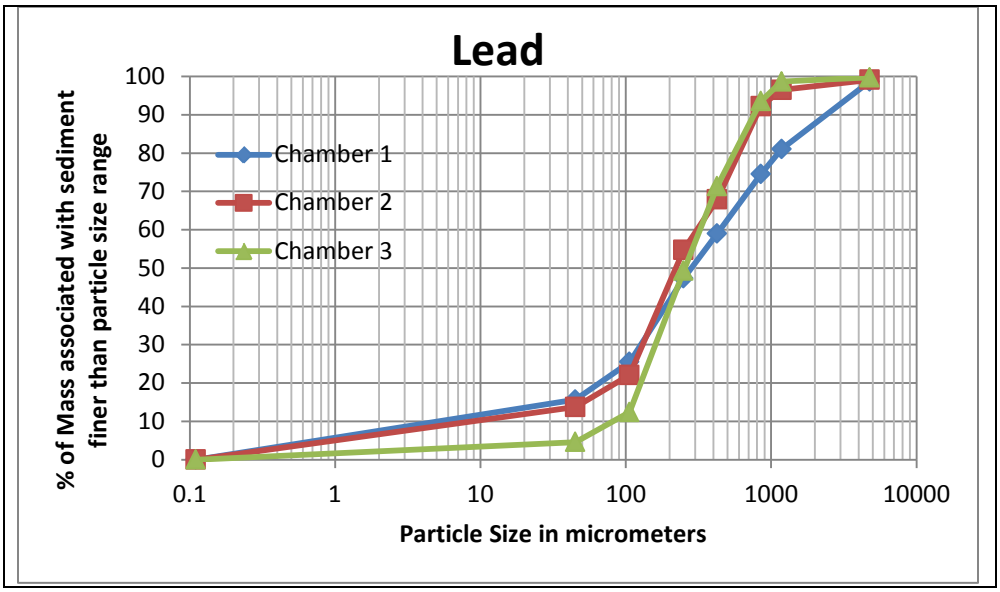

Figure 3-28 Accumulative mass distribution of lead by particle size in HDD sediments

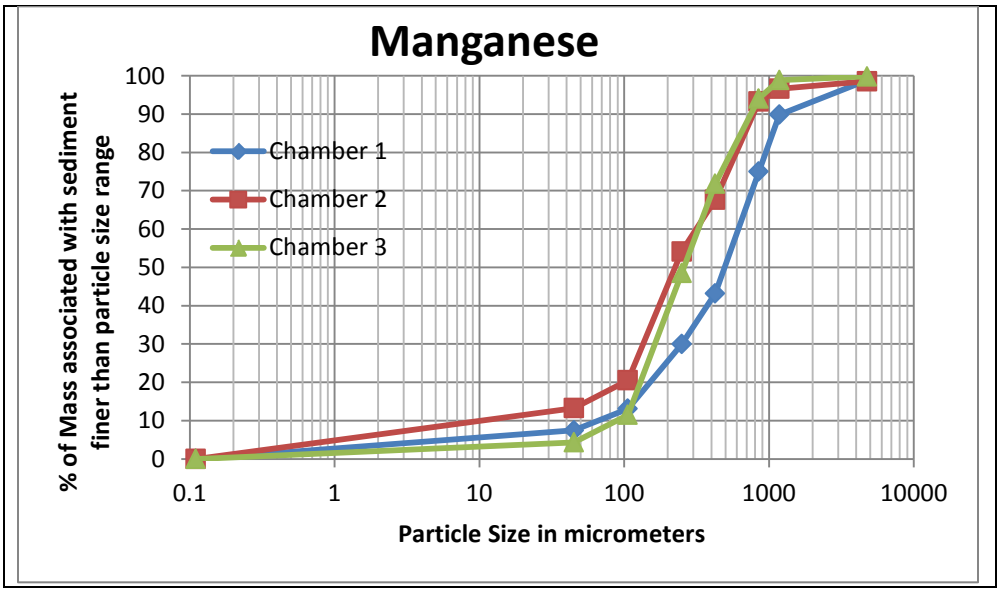

Figure 3-29 Accumulative mass distribution of manganese by particle size in HDD sediments

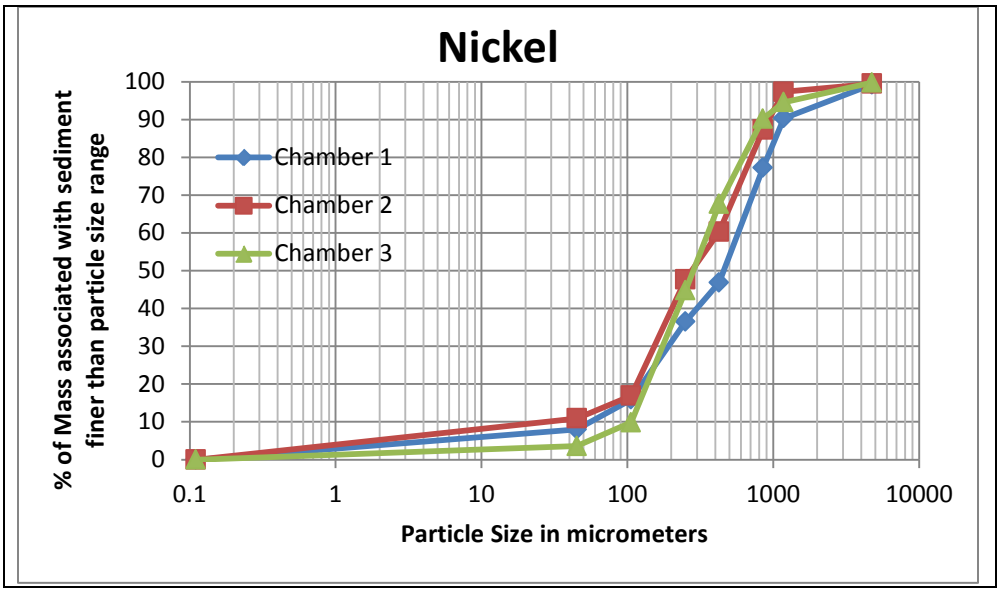

Figure 3-30 Accumulative mass distribution of nickel by particle size in HDD sediments

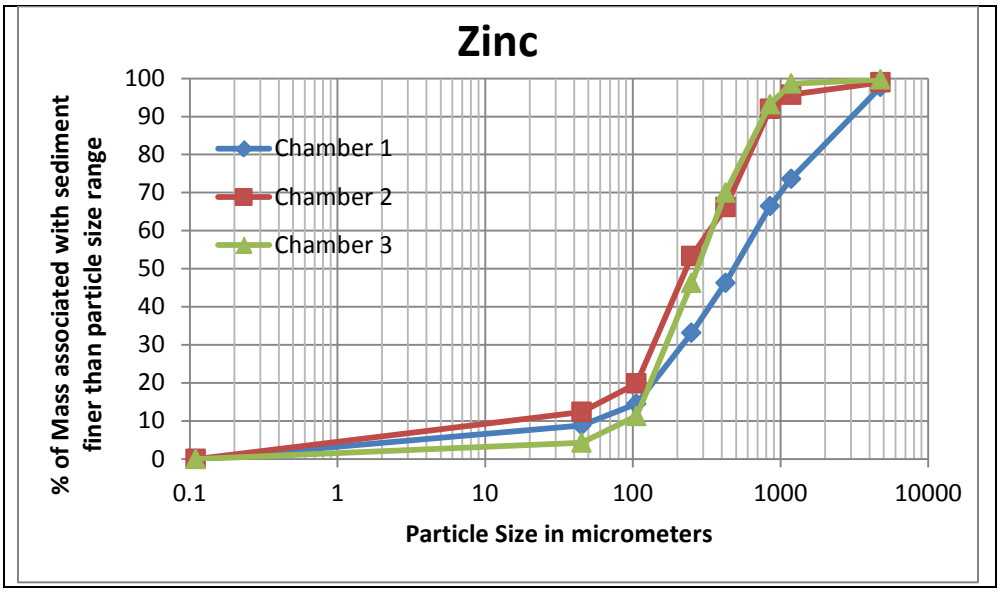

Figure 3-31 Accumulative mass distribution of zinc by particle size in HDD sediments

Figures 3-32 through 3-40 show the metal concentrations associated with stormwater particulates and concentrations of the sediment captured in the HDD for different particle sizes. The stormwater samples have more resolution for the smaller particles, as particles smaller than 45 µm are not plentiful in the HDD sediments and were therefore combined into one size category. Similarly, the HDD sediments have more of the large sediments compared to the stormwater and particles larger than 105 µm in the HDD were therefore separated into several size ranges. The stormwater particle size strengths increased as the particle sizes increased, while the HDD sediments had more uniform particulate strengths over the larger range of sizes. Overall, the strengths for each constituent were similar in both sample categories, considering the overlapping size ranges.

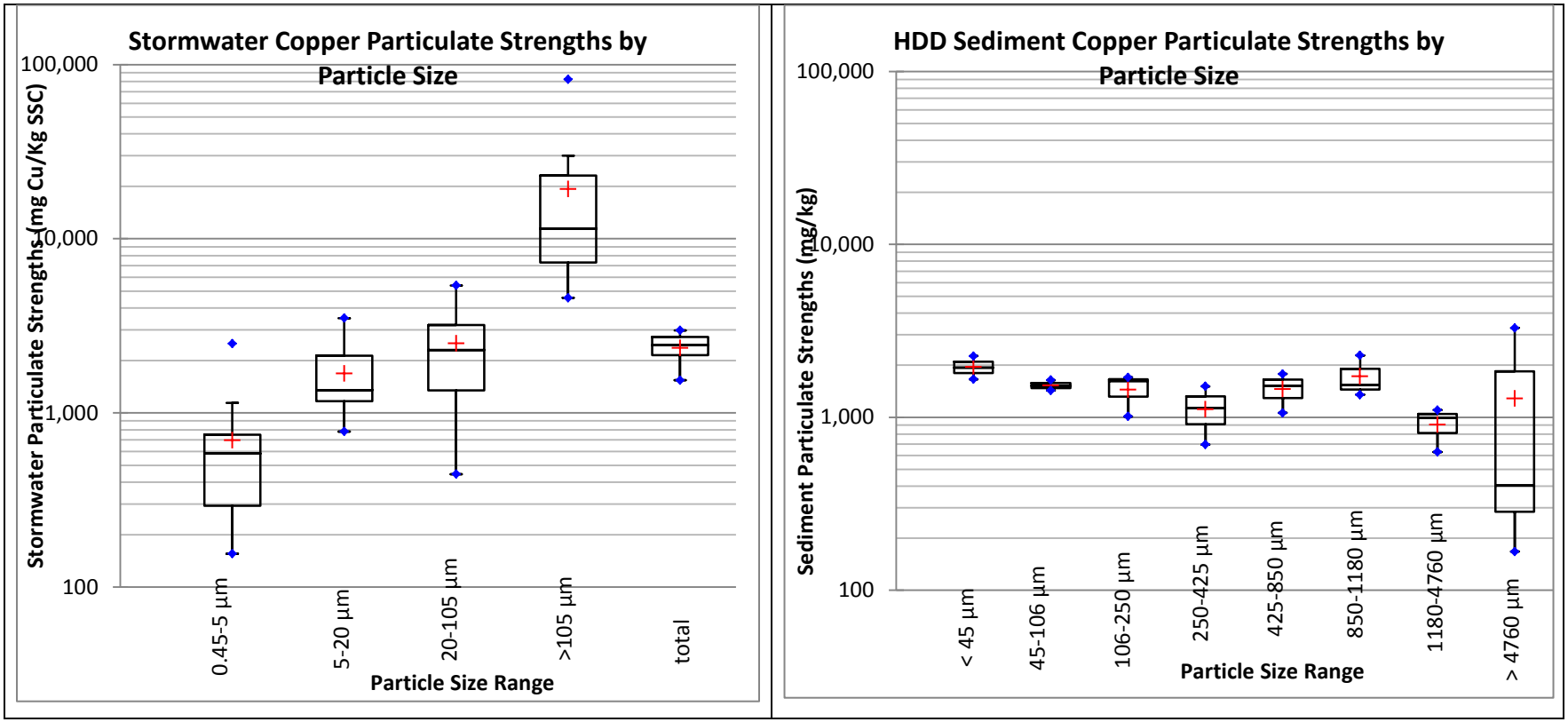

Figure 3-32 Stormwater copper particulate strengths compared to HDD copper sediment particle strengths by particle size

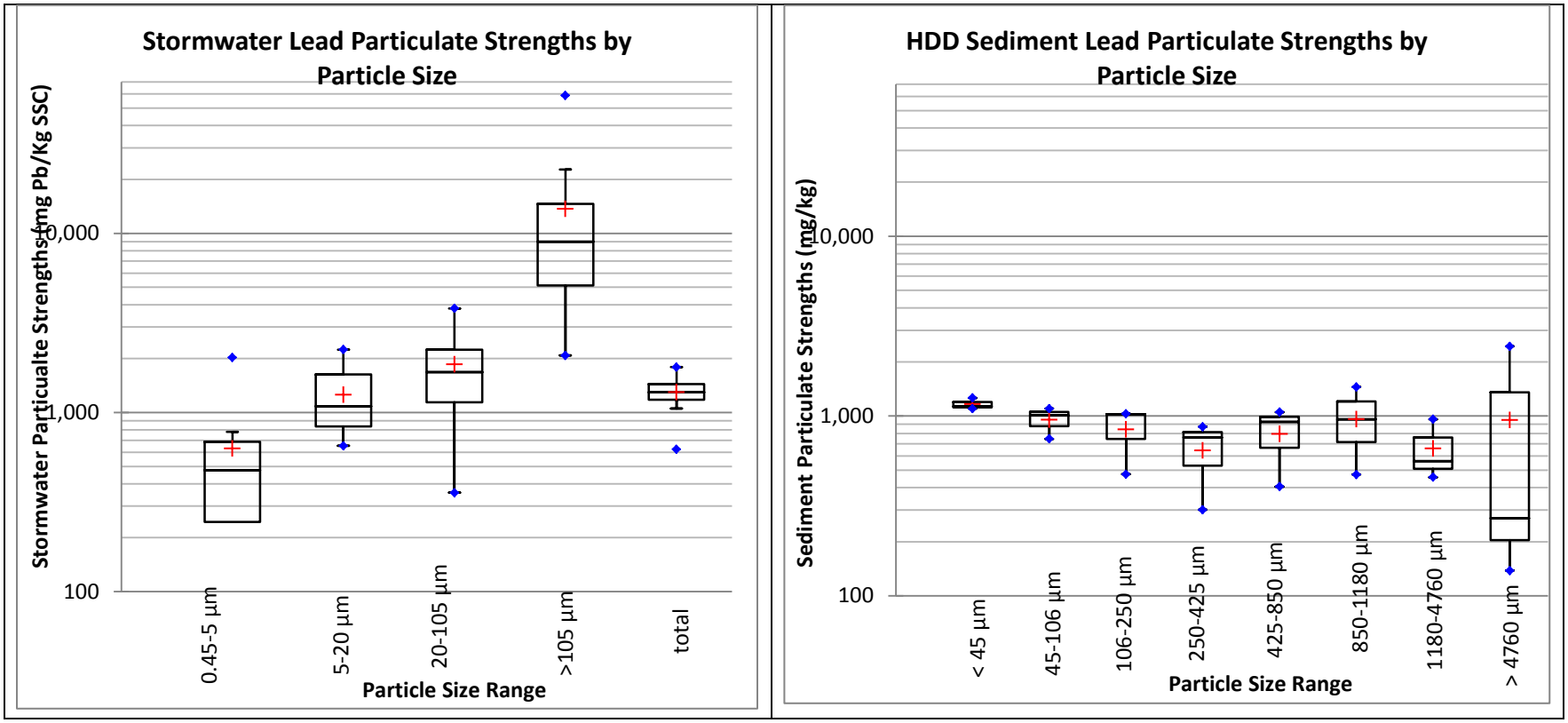

Figure 3-33 Stormwater lead particulate strengths compared to HDD lead sediment particle strengths by particle size

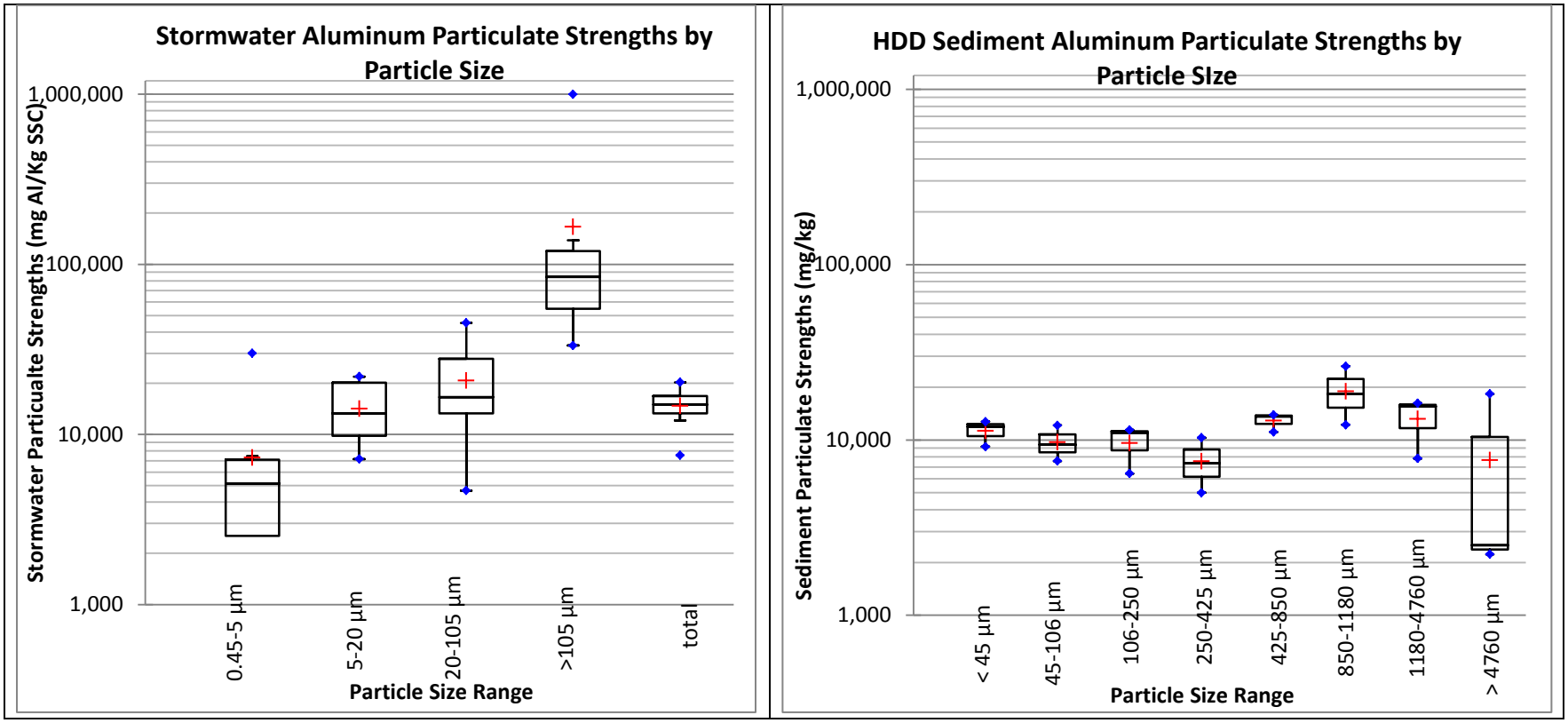

Figure 3-34 Stormwater aluminum particulate strengths compared to HDD aluminum sediment particle strengths by particle size

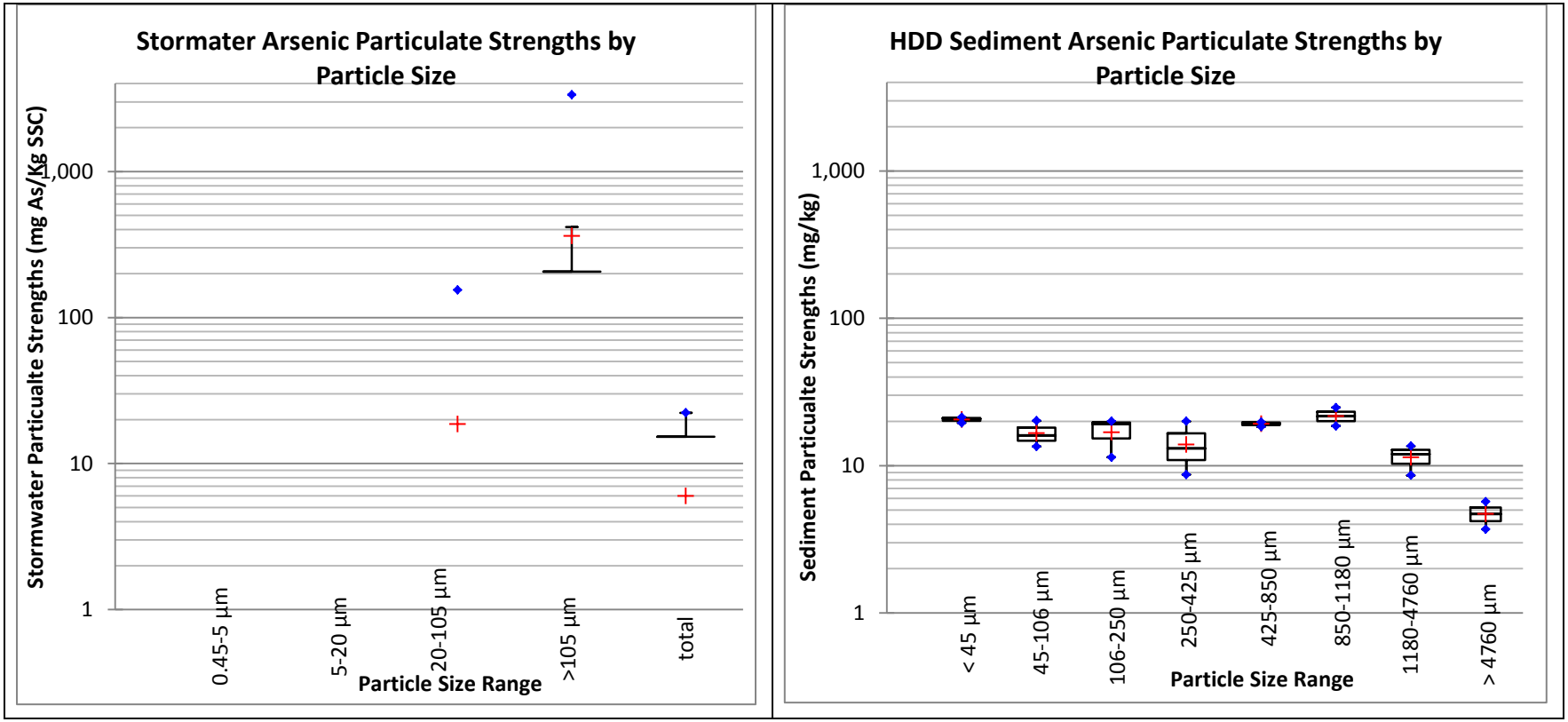

Figure 3-35 Stormwater arsenic particulate strengths compared to HDD arsenic sediment particle strengths by particle size

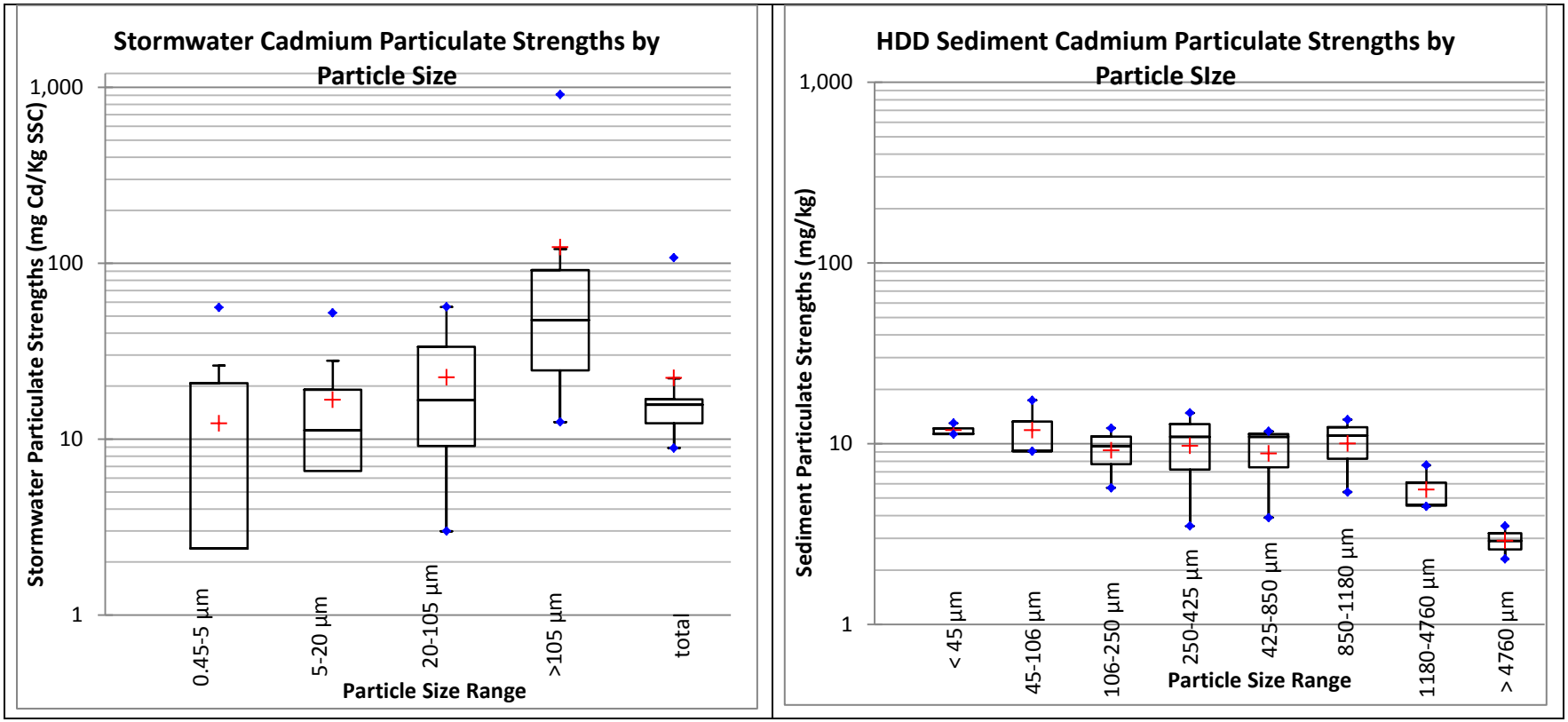

Figure 3-36 Stormwater cadmium particulate strengths compared to HDD cadmium sediment particle strengths by particle size

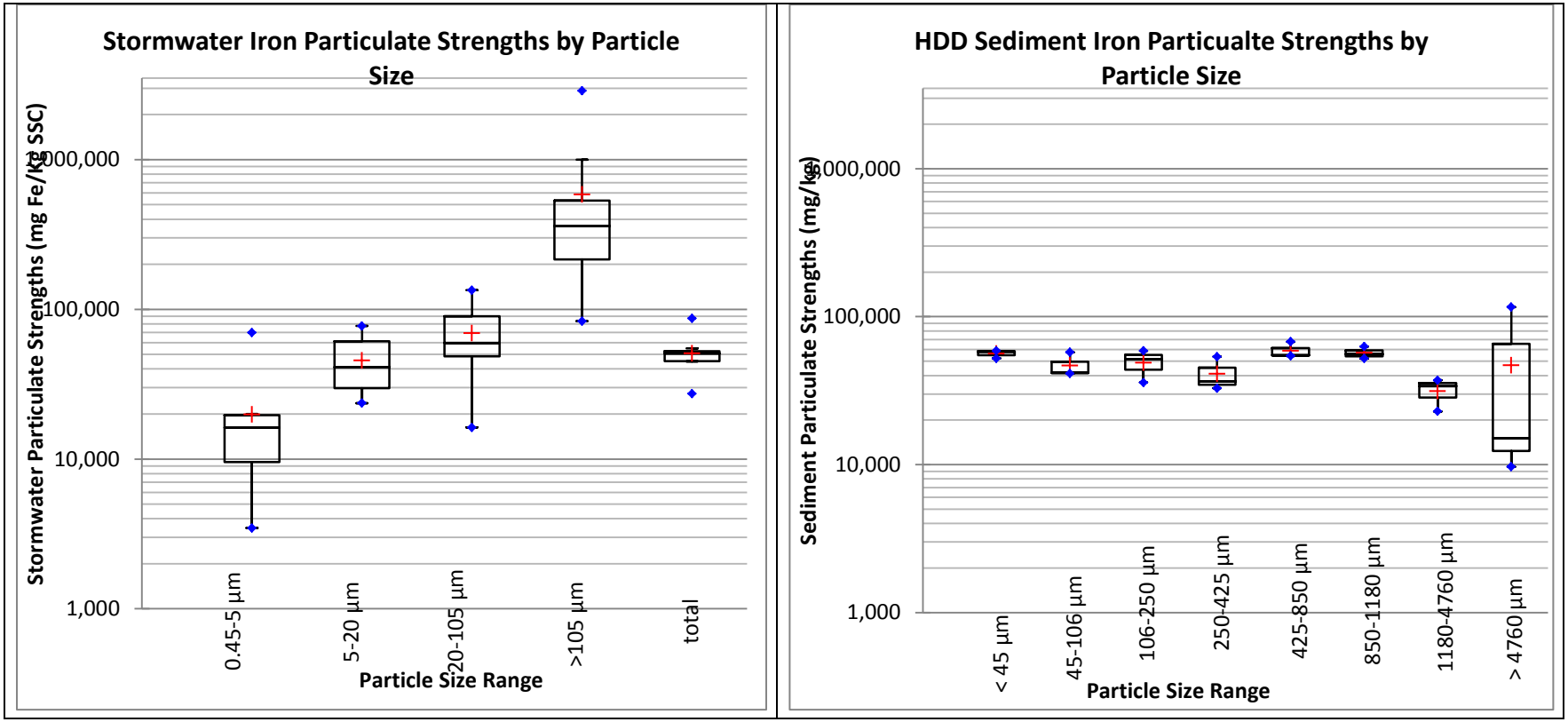

Figure 3-37 Stormwater iron particulate strengths compared to HDD iron sediment particle strengths by particle size

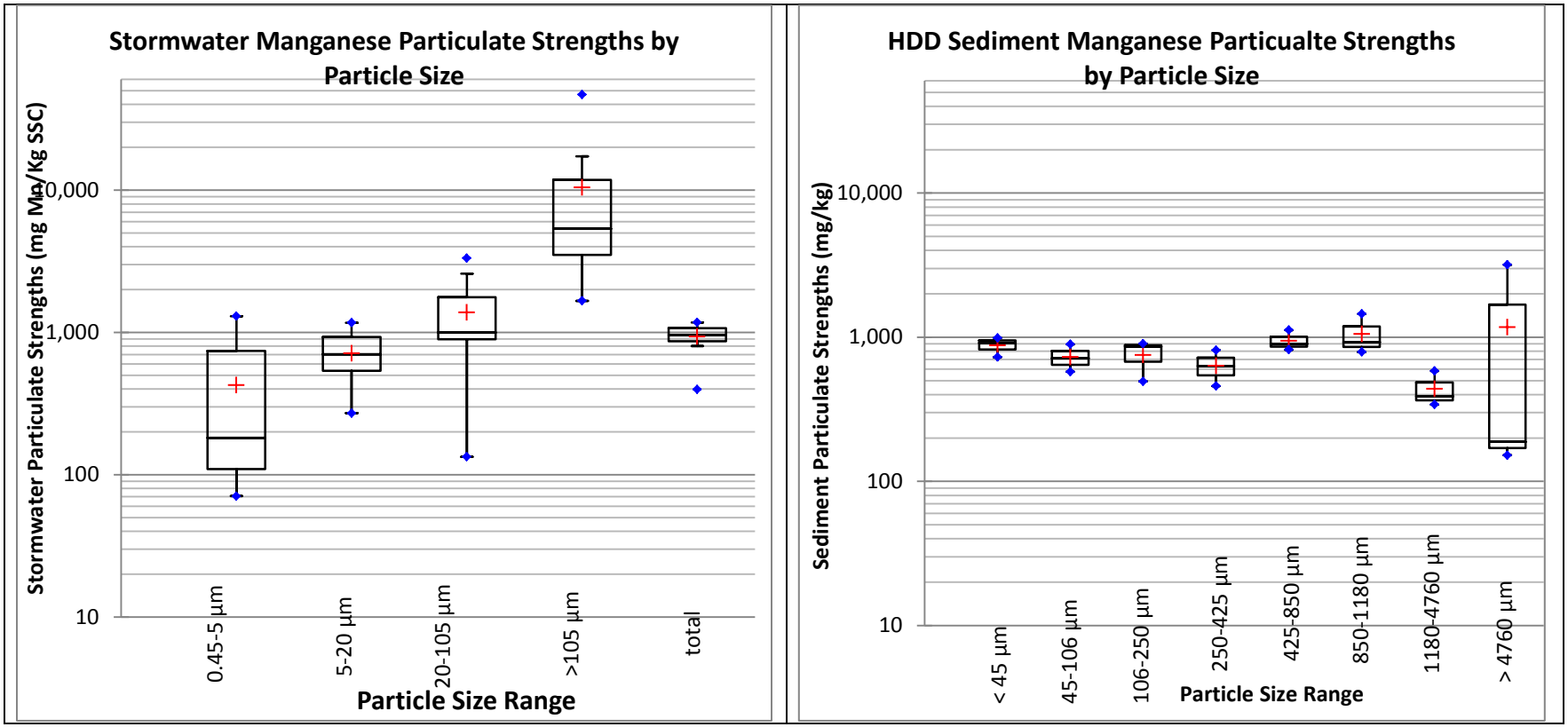

Figure 3-38 Stormwater manganese particulate strengths compared to HDD manganese sediment particle strengths by particle size

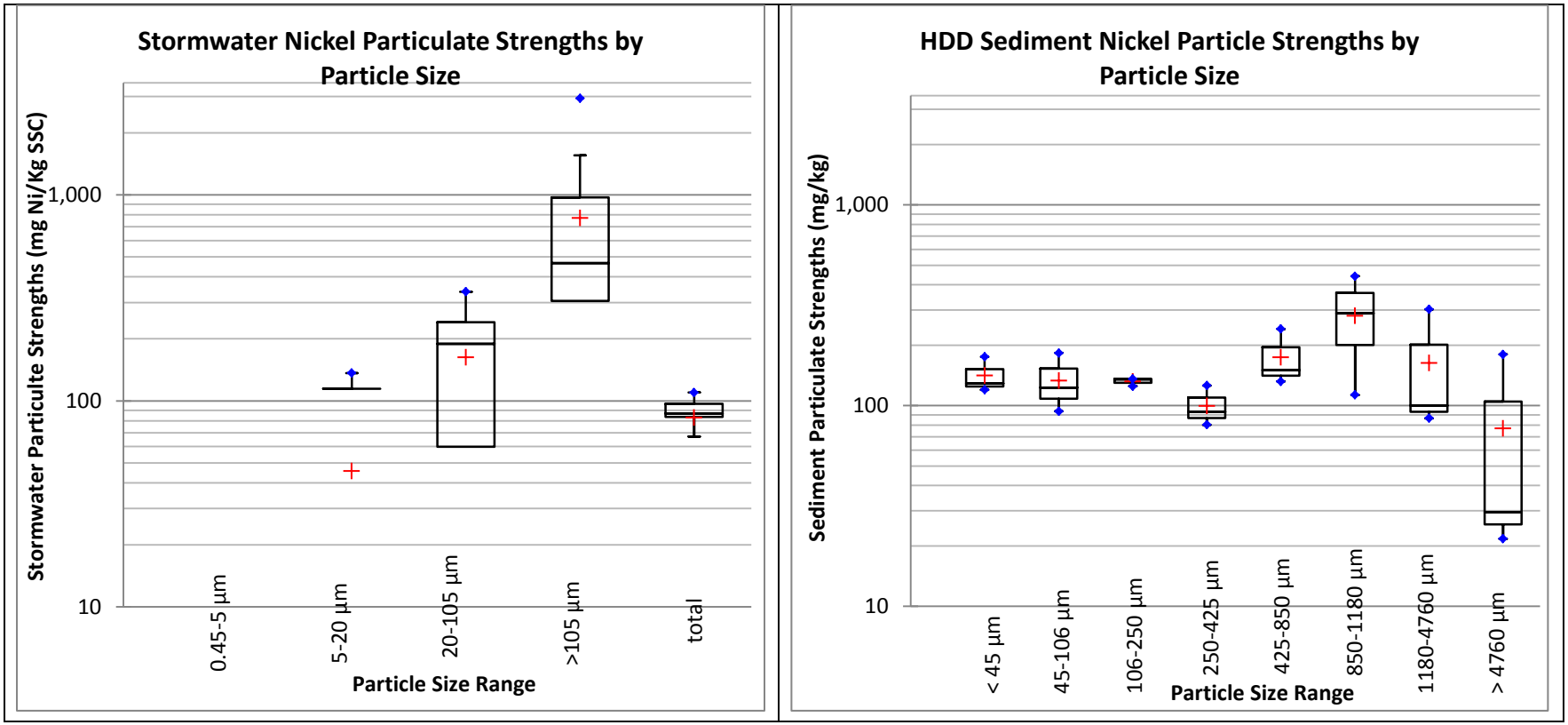

Figure 3-39 Stormwater nickel particulate strengths compared to HDD nickel sediment particle strengths by particle size

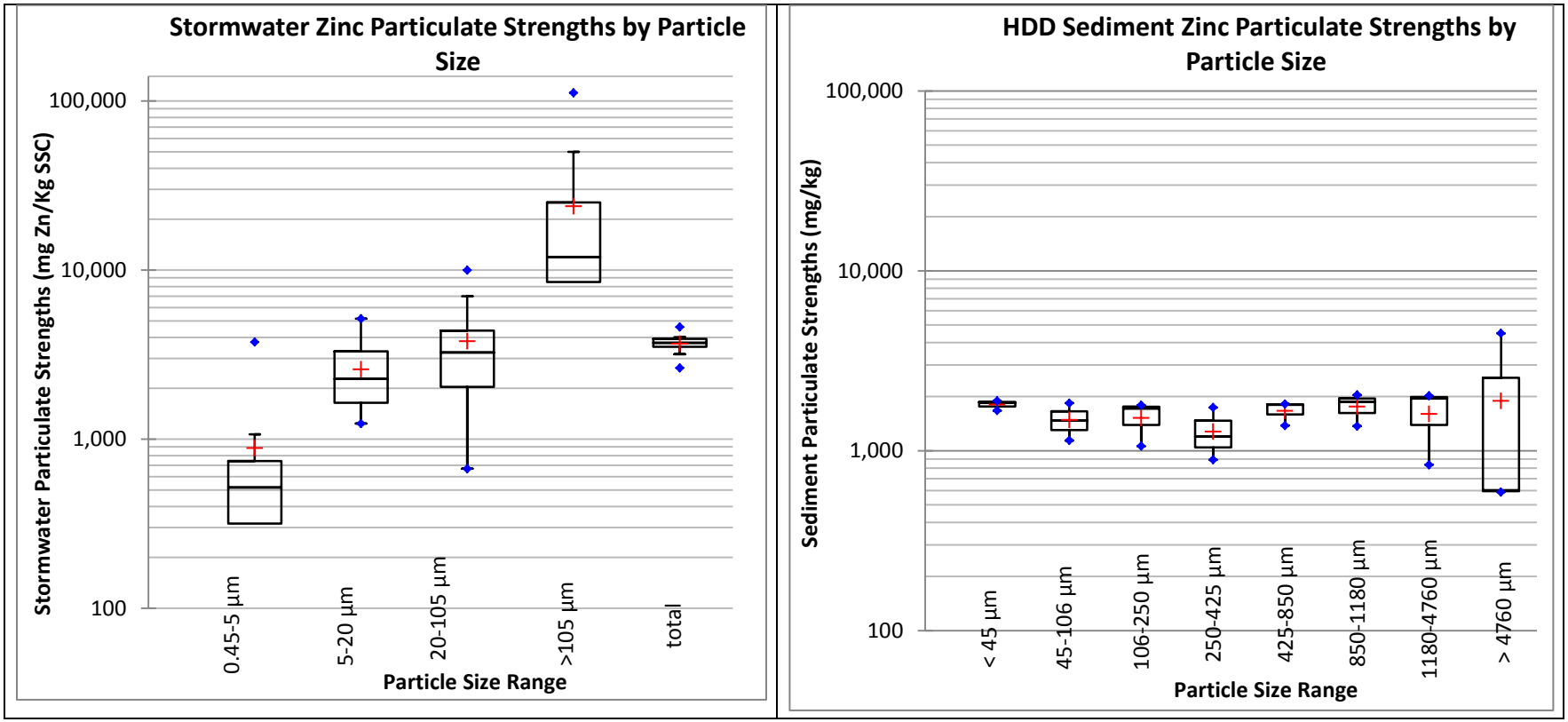

Figure 3-40 Stormwater zinc particulate strengths compared to HDD zinc sediment particle strengths by particle size

3.3.8 Infiltration Pond Characteristics

Field infiltration tests were conducted at six different locations in the pond to determine the dry pond infiltration characteristics. Turf-Tec infiltrometers were used to measure the infiltration rates in the dry pond (Figure 3-41). Infiltration tests were conducted using three infiltrometers placed within about 1m from each other to measure the variability of infiltration rates in close proximity. Water was added to the inner ring and allowed to overflow to fill up the outer ring. The decrease in the water level in the inner ring was measured for a period of 1 to 2 hours until a constant infiltration rate was observed. Additional water was added as the water level in the inner ring dropped to less than an inch of the ground surface to maintain continuous pooling of water. The infiltration rate was calculated as the rate of decline of the water level in the inner chamber. The rate of infiltration depends on several factors including hydraulic conductivity, soil structure, rain intensity, chemical nature of soils, depth to groundwater , etc. (Horton et al 1940, Chow et al 1998).

Figure 3-41 Photographs showing infiltrometer test setup

The values obtained during the infiltration tests were fit to the Horton infiltration equation to obtain the saturated final infiltration rate which is similar to the rate in the pond during actual rain conditions (Horton 1939, and Turner et al 2006).

Figure 3-42 Dry pond infiltration test locations

Horton's infiltration equation is:

$$f = f_c + (f_o - f_c)e^{-kt} \qquad \text{(Equation 4)}$$

Where,

f_o = initial infiltration rate (in/hr)

f_c = final infiltration rate (in/hr)

k = decay constant (t^{-1})

f = infiltration rate at time t (in/hr)

The values measured in the field were plotted and they were found to follow an exponential decay, the general shape of a Horton infiltration rate curve. Figure 3-43 is an example plot for one of the test locations in the pond showing the results from the three infiltrometers. The average initial infiltration rate, decay constant, and final infiltration rates obtained from the field tests are shown in Table 3-22.

Table 3-22 Field infiltration test data measured by double ring infiltrometers

Averaged Horton's Parameters			
Location	f_o (in/hr)	f_c (in/hr)	k(hr^{-1})
1	36.25	13.31	11.10
2	7.50	2.29	4.45
3	51.25	39.35	10.54
4	5.02	0.46	4.60
5	41.25	31.16	13.90
6	25.00	16.72	9.10

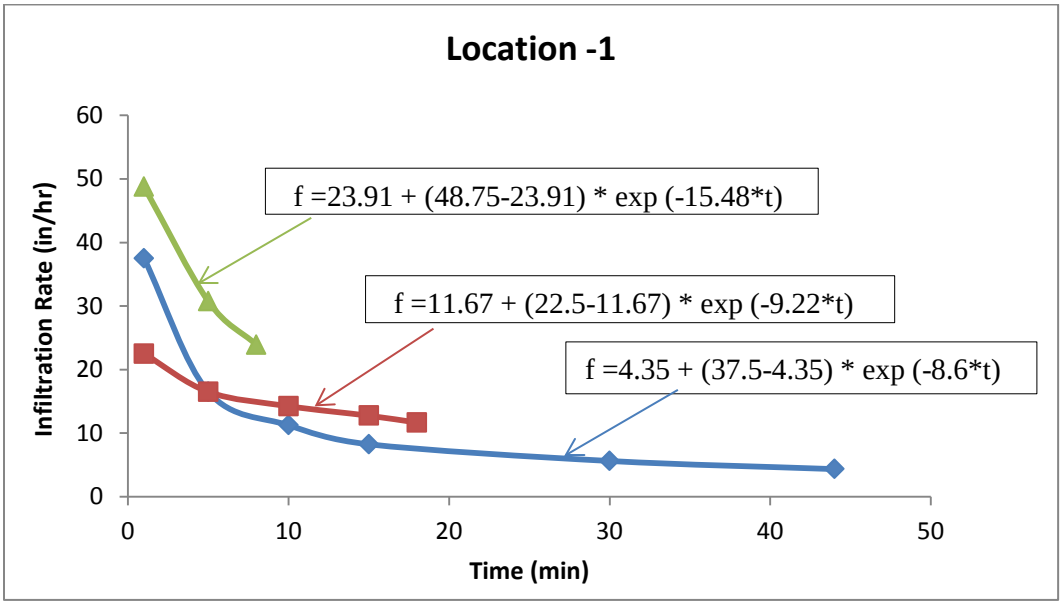

Figure 3-43 Example infiltration measurement fitted with Horton equation

Variations of final infiltration rates were observed in the infiltrometers placed about within a meter from each other at different locations. Also, different locations resulted in final infiltration rates occurring at different times and different rates. Higher infiltration rates were observed at Locations 1, 3 (located towards pond side slopes) and 5 (outlet location of the pond). The dry pond system was not completely saturated during the infiltration tests and the measured infiltration rates only indicated the more favorable surface conditions. However, the soils in the pond showed moderate to high infiltration capacities and the measured runoff volume losses during the storm monitoring supported high infiltration rates in the pond. The average final infiltration rates ranged from 0.5 in/hr to 39 in/hr with an average of about 17.2 in/hr.

Rain and runoff depths (total runoff volume divided by the site drainage area) for the monitored events are shown in Table 3-23. Figures 3-44 and 3-45 show example hydrographs for pond inflow and outflow for small (0.55 in) and a large (2.36 in) rain events.

Table 3-23 Rain and runoff depths for the monitored storm events along with associated dry pond flow reductions

		Runoff Depth		
Storm Event #	Rain Depth (in)	Dry Pond Inlet (in)	Dry Pond Outlet (in)	% Runoff Volume Reductions
2	0.55	0.48	0.038	92.1
4	2.52	2.42	0.7	71.1
5	0.75	0.61	0.21	65.6
6	0.39	0.32	0.04	87.5
7	0.47	0.36	0.02	94.4
8	0.6	0.56	0.21	62.5
9	0.3	0.24	0.02	91.7
10	2.36	2.1	1.24	41
11	0.39	0.3	0.04	86.7
12	1.48	1.31	0.28	78.6
13	2.28	2.0	0.91	54.5
14	0.12	0.08	0.02	75
15	0.95	0.88	0.35	60.2
16	0.23	0.14	0.04	71.4
17	0.1	0.04	0.00	100

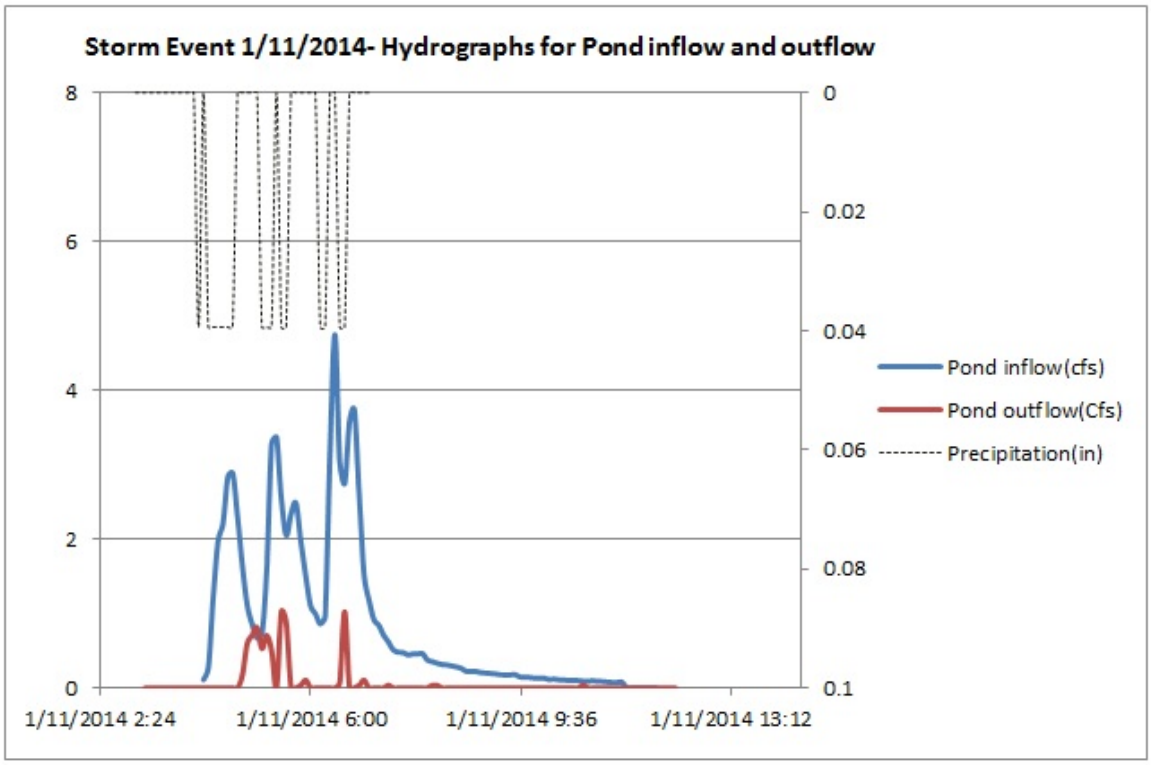

Figure 3-44 Example hydrograph of a monitored small event (0.55 inch rain depth)

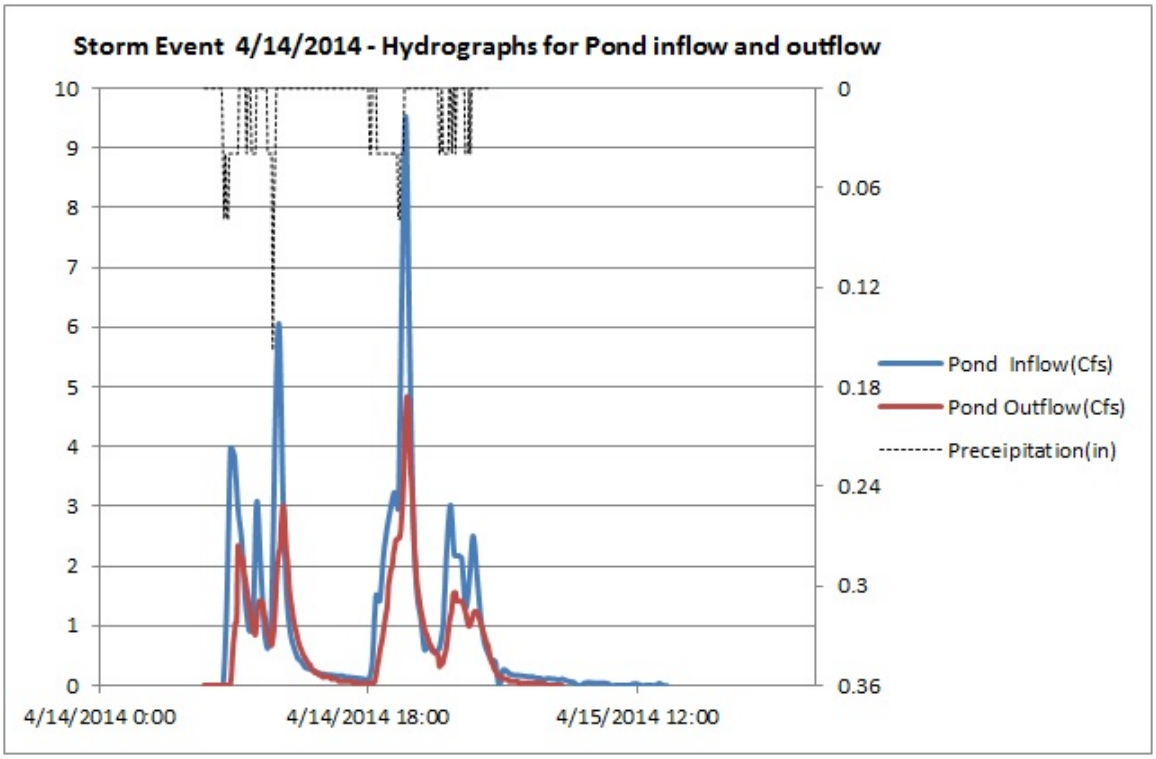

Figure 3-45 Example hydrograph of a monitored larger event (2.36 inch rain depth)

These data show that the dry infiltration pond is highly capable in attenuating (runoff reductions from 75% up to 100%) runoff from storm events less than 1.5 inches and had moderate reductions of about 50% for events greater than 1.5 inches (Figure 3-46). Large mass reductions of pollutants in the dry pond were mostly attributed to the infiltration of stormwater through the bottom of the pond, although the particulate-bound constituents also had significant concentration reductions.

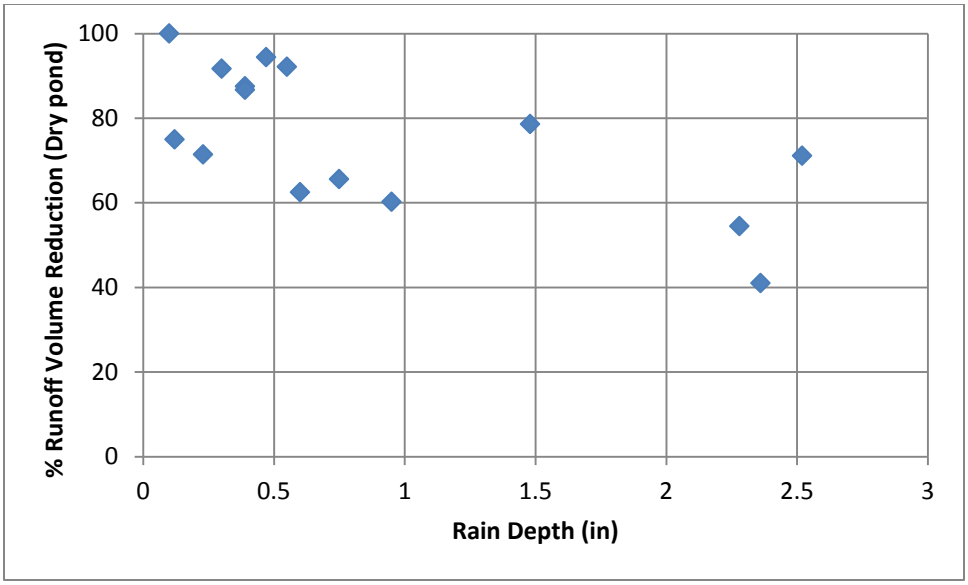

Figure 3-46 Rain depth vs % flow attenuation for dry pond

3.4 Summary

Treatment performance evaluations for a hydrodynamic separator device/dry infiltration pond treatment train were conducted at a heavy industrial site in the southeastern US. The HDD had low to moderate reduction (34%) for SSC and low reductions for heavy metals (the same for both concentrations and mass as there are no runoff volume reductions in the HDD). Moderate (35 to 45%) reductions were observed for particle sizes greater than 12 µm in the HDD, with minimal (not significant) removals for smaller particles. The dry infiltration pond showed moderate to high reductions for sediment concentrations for all particle sizes greater than 3µm. Moderate to high reductions (50 to 95%) of concentrations and mass were observed for total forms of the metals and COD in the dry infiltrating pond. No significant concentration reductions were observed in the HDD and dry pond for nutrients. The dry pond was most effective in flow

reductions during storm events with rain depths less than 1.5 inches, along with high removals of pollutant masses for all constituents.

References

Barrett, M. E. (2003). Performance, cost, and maintenance requirements of Austin sand filters. Journal of water resources planning and management, 129(3), 234-242

Bay, S., Brown, J. (2005). Evaluation of Best Management Practice (BMP) Effectiveness. Final Report. California State Water Resources Control Board

Birch, G. F., Fazeli, M. S., & Matthai, C. (2005). Efficiency of an infiltration basin in removing contaminants from urban stormwater. Environmental Monitoring and Assessment, 101(1-3), 23-38

Bolognesi, A., Ciccarello, A., Maglionico, M., Kim, J. Y., Artina, S., & Sansalone, J. (2011). Can Surface Overflow Rate Predict Particulate Matter Load Capture for Common Urban Drainage Appurtenances?. *Journal of Environmental Engineering*, *138*(7), 723-733

Chow, V.T., D.R. Maidment, and L.W. Mays. (1988). Applied Hydrology. McGraw-Hill, Inc

Chys, M., Depuydt, V., Boeckaert, C., & Van Hulle, S. W. H. (2013). Treatment of rainwater runoff in recovery and recycling companies: Lab and pilot-scale testing. Journal of Environmental Science and Health, Part A, 48(4), 446-452

Clark, S. E., Roenning, C. D., Elligson, J. C., & Mikula, J. B. (2009). Inclined plate settlers to treat storm-water solids. *Journal of Environmental Engineering*, *135*(8), 621-626

Guo, Q. (2005). Development of adjustment and scaling factors for measured suspended solids removal performance of stormwater hydrodynamic treatment devices. In *Proceedings of the World Water and Environmental Resources Congress 2005* (pp. 15-19).

Guo, Q. (2007). Research to support certification of TSS removal efficiency of stormwater manufactured treatment devices. In Proceedings of ASCE/EWRI World Environmental and Water Resources Congress (Vol. 9, No. 9, pp. 9-10)

Horton, R.E. (1939). Analysis of runoff plat experiments with varying infiltration capacity, Transactions – American Geophysical Union 20: 693-711

Horton, R.E. (1940). An Approach toward physical Interpretation of infiltration –capacity. Soil Science Society of America proceeding 5: 399-417

Kellems, B. L., Randall Johnson, P. E., & Sanchez, F. (2003). Design of emerging technologies for control and removal of stormwater pollutants. Bridges, 10(40685), 277

Kim, J. Y., & Sansalone, J. (2008). Particulate matter particle size distributions transported in urban runoff. In *World Environmental and Water Resources Congress 2008@ sAhupua'A* (pp. 1-10). ASCE.

MPCA 2011, Industrial Stormwater Best Management Practices Guidebook. Minnesota Pollution Control Agency

Nelson, E. A., & Gladden, J. B. (2008). Full-scale treatment wetlands for metal removal from industrial wastewater. Environmental Geosciences, 15(1), 39-48

Stanley, D. W. (1996). Pollutant removal by a stormwater dry detention pond. Water Environment Research, 1076-1083

Turner, Ellen. (2006). Comparison of Infiltration Equations and Their Field Validation with Rainfall Simulation. Master Thesis, University of Maryland College Park

Wilson, M. A., Mohseni, O., Gulliver, J. S., Hozalski, R. M., & Stefan, H. G. (2009). Assessment of hydrodynamic separators for storm-water treatment. Journal of Hydraulic Engineering, 135(5), 383-392

Yang, C. T. (1996). *Sediment transport: theory and practice* (pp. 19-48). New York: McGraw-Hill.

CHAPTER 4 THE IMPACT OF INDUSTRIAL RUNOFF ON A DRY INFILTRATION POND: ASSESSMENT OF SOIL CONTAMINATION AND GROUNDWATER CONTAMINATION POTENTIAL

4.1 Introduction

Infiltration facilities have been used to reduce flooding and to reduce stormwater discharges to surface receiving waters, although there are concerns about the potential contamination of underlying soils and groundwater (Mikkelsen, et al. 1996; Barraud, et al. 1999; Pitt, et al. 1999). Heavy metal contamination of topsoil at infiltration facilities has been reported in many studies (Deschne et al 2003, Hossain et al 2009), although very little or no information is available on infiltration facilities at industrial facilities (Winiarski et al 2006). This research focused on the groundwater and soil contamination potential of heavy metals at a heavy industrial facility in the southeast US. Soil profiles were evaluated for heavy metals to determine metal concentrations in the soils with depth and a groundwater fate model was used to determine the potential migration of soluble forms of the metals beneath an infiltrating dry detention pond after pre-treatment by a hydrodynamic separator device.

The assessment of the fate of metals in soil systems is affected by particulate forms of the metals being captured through filtration actions and the dissolved forms potentially retained by the soil through several processes including soil surface association, precipitation, adsorption to metal oxides, complexation with organic matter , etc. (Evans et al 1989, Pitt et al 1999). Much of the heavy metals in stormwater are usually associated with particulates and can be retained in the

soil column by physical filtration while the stormwater is being infiltration into the soil, with little potential for deeper groundwater contamination by these particulate-bound contaminants (Pitt et al 1995, Sansalone et al 1996). However, past work has focused on stormwater from residential and commercial areas with little information available for infiltration at industrial facilities.

The mobility of heavy metals in soil is affected by several stormwater, site and soil factors including soil acidity, pH, CEC, organic matter, etc. The interaction of heavy metals and their binding to soil matrices can be evaluated to understand the mobility of metals through the soil and vadose zones and their potential in reaching underlying groundwater. The interactions between heavy metals and soil components have been evaluated in different studies (Evans et al 1989, Yong et al 1992, Taylor et al 1995, Lee et al 1996). CEC has been reported as an important characteristic showing good associations of metals to soil adsorption (Tyler et al 1982, Christensen 1984, King et al 1988, Deschne et al 2003).

The groundwater contamination potential can be evaluated based on the pollutant abundance in stormwater (not a problem if not present), pollutant mobility in vadose zone (not a problem if it can't reach the groundwater), the treatability of pollutants (not a problem if pre-treated to low concentrations), and the infiltration procedure used (to take advantage of these hindrances) (Pitt et al 1999). The infiltration techniques that are most commonly used for stormwater include a variety of "low impact development" devices, such as biofilters/bioinfiltration practices, along with older approaches such as French drains, porous pavements, infiltration wells, percolating sewerage drainage, and dry percolating basins. The general causes of concern that indicate probable groundwater contamination potential are: high mobility in vadose zone, high abundance

in stormwater, and high soluble fractions in stormwater, along with sandy soils having low organic content (Pitt et al 1999).

The effect of stormwater infiltration through a dry pond on the underlying soil matrix was studied at a heavy industrial site in southeastern US during this research. The distribution of various soil characteristics including pH, acidity, CEC, organic matter, heavy metal content, in a 2 ft vertical profile, were evaluated. The migration of contaminants in the vadose zone was modeled using a simulation model; SESOIL (Environmental Software Consultants Inc), a one-dimensional, unsaturated zone model was selected to predict soluble pollutant movement in the vadose zone.

The main objectives of this study were as follows:

1) To investigate the movement of the metals and capture with soils at different soil depths and assess the level and extent of soil contamination by particulate forms of the heavy metals
2) To investigate the long-term potential migration of soluble contaminants in the vadose zone under the infiltrating dry pond.

4.2 Methodology

4.2.1 Site description and dry pond characteristics

The test site is a heavy industrial facility located in the southeastern United States. The facility is approximately 21 acres in size, mostly covered with concrete, roofs, and severely compacted soils. As per the survey and based on site drainage network, approximately 15 acres are served by a stormwater collection system that drains towards inlets having filter fabric bags, a hydrodynamic device, and finally to a dry infiltration pond. The dry pond has been in operation

since 2010 The pond has an area of 0.75 acres and has a 1 foot wide shallow concrete channel for flow conveyance. Several rock check dams are present along this channel for flow rate attenuation (Figures 4-1 and 4-2).

Figure 4-1 Dry pond with rock check dams showing channel and grass cover

Figure 4-2 Dry pond after period of very intense rain showing partial flooding of pond

The county soil map shows the underlying soil as Bassfield-Urban land complex (NRCS Web Soil Survey available online at http://websoilsurvey.nrcs.usda.gov/) and is composed of

loamy soil over sandy alluvium deposits. The typical soil profile is comprised of fine sandy loam (0 to 10 inches), sandy loam (10 to 41 inches) and loamy sand (41 to 70 inches).The depth to the water table is reported to be more than 6.5 ft by the soil map. Infiltration tests were performed during this research and the long-term infiltration rates in the pond and averaged about 17 in/hr, ranging from 0.5 to 39 in/hr. The results of the infiltration measurements are shown in Figures 4-3 through 4-8 fitted to the Horton equation. The stormwater is pre-treated by a hydrodynamic device before draining to the infiltrating dry pond.

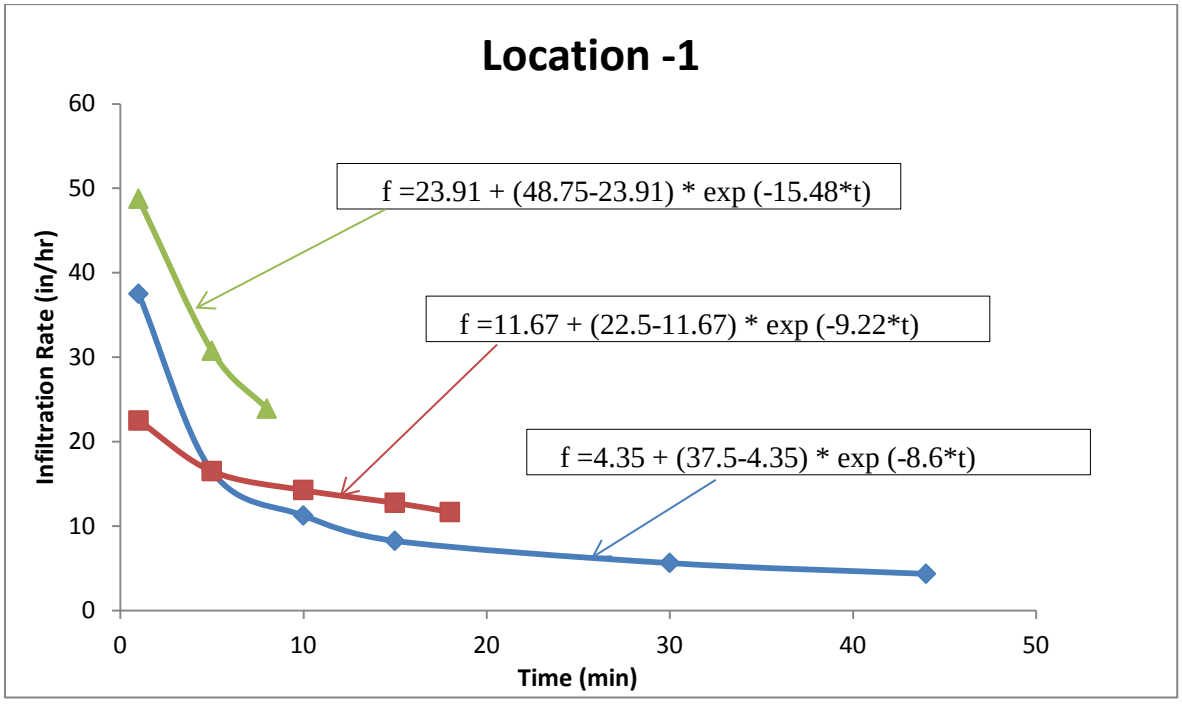

Figure 4-3 Infiltration Measurements at Location 1 fitted with the Horton Equation

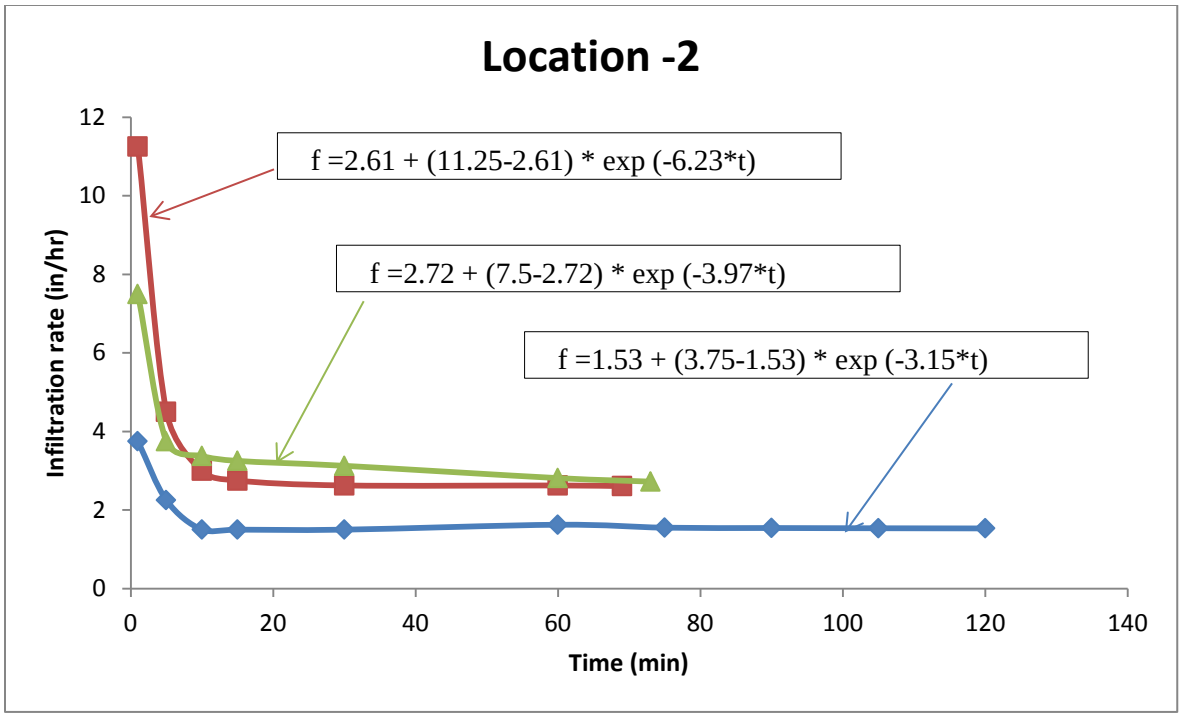

Figure 4-4 Infiltration Measurements at Location 2 fitted with the Horton Equation

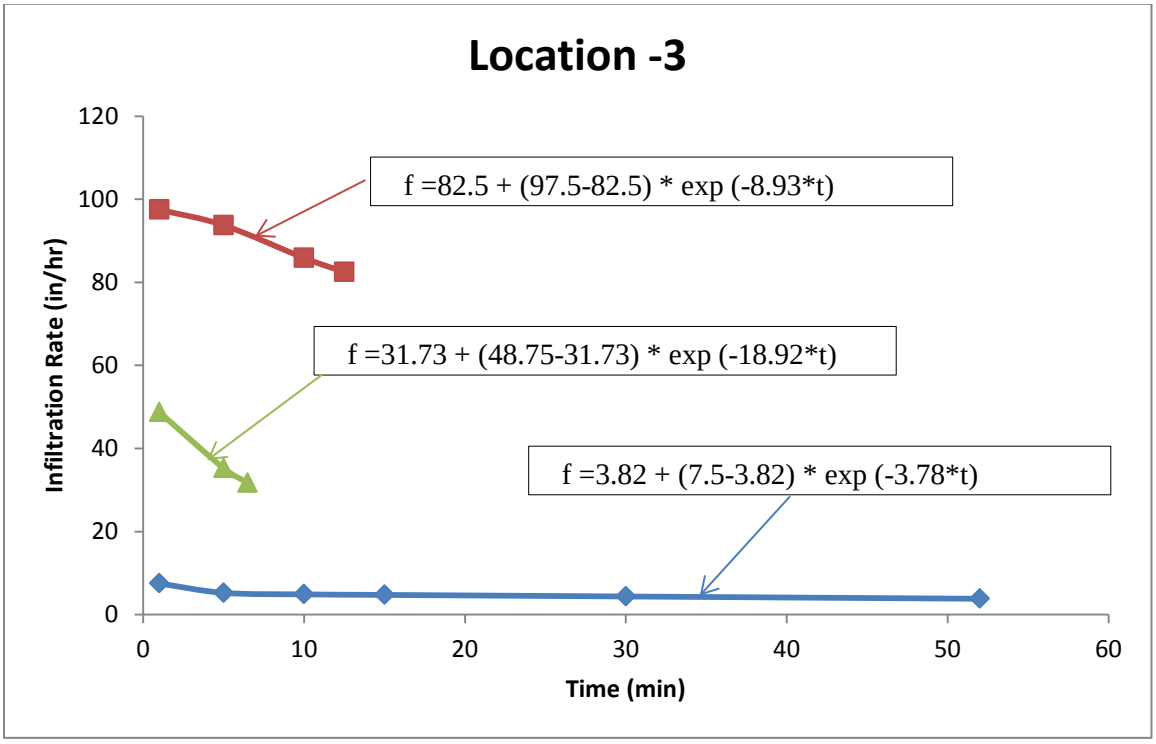

Figure 4-5 Infiltration Measurements at Location 3 fitted with the Horton Equation

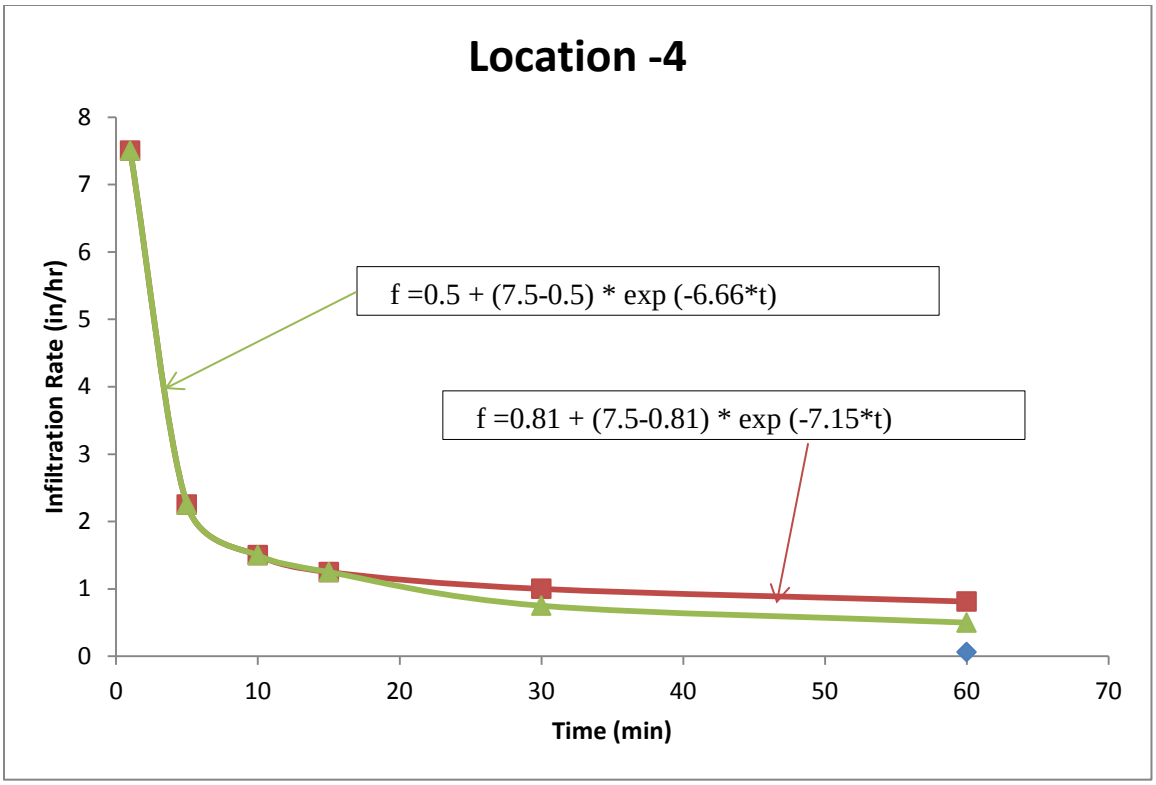

Figure 4-6 Infiltration Measurements at Location 4 fitted with the Horton Equation

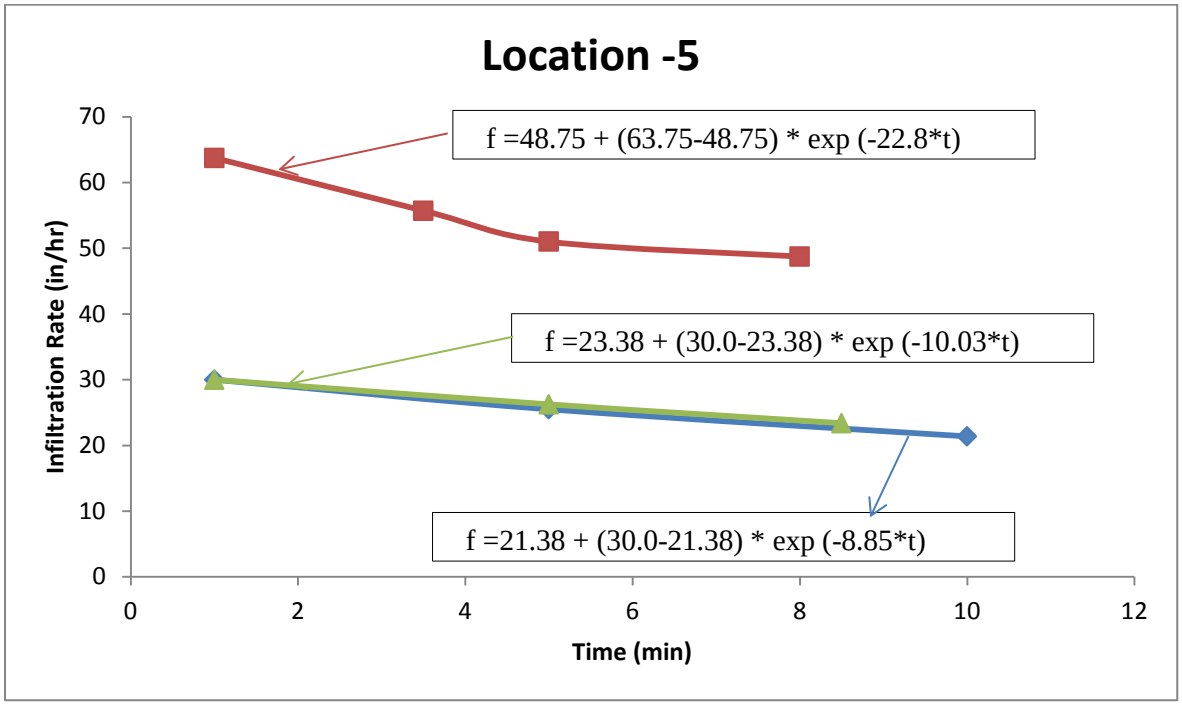

Figure 4-7 Infiltration Measurements at Location 5 fitted with the Horton Equation

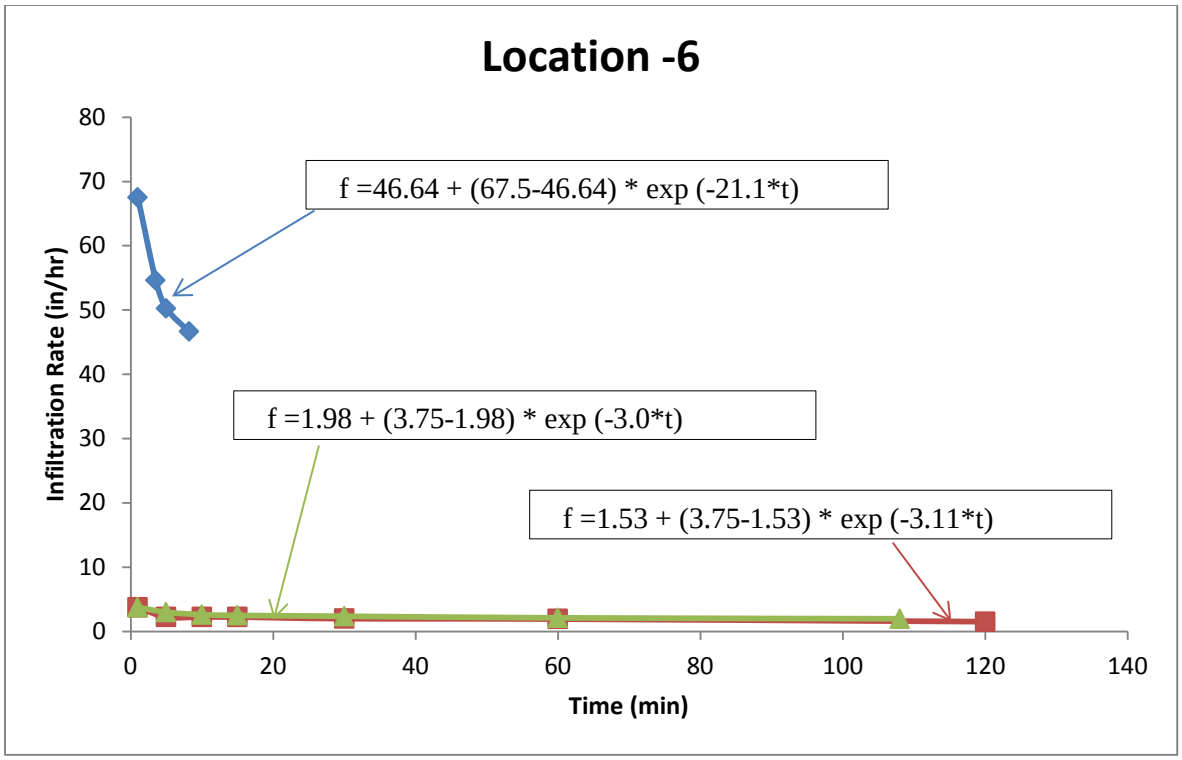

Figure 4-8 Infiltration Measurements at Location 6 fitted with the Horton Equation

The soils in the dry pond showed moderate to high infiltration capacities. Variations of the final infiltration rates were observed in the infiltrometers placed about within a meter from each other and at different locations. This spatial variability in the dry pond was loosely correlated with the water path through the pond. Higher infiltration rates were observed at Locations 1, 3 (located towards pond side slopes) and 5 (outlet location of the pond). The dry pond system was not completely saturated during the infiltration tests and the measured infiltration rates only indicated the more favorable surface conditions. However, the pond infiltration rates were still high, and confirmed by runoff water losses monitored during actual rain conditions. In contrast, an infiltration test was attempted on the site's surface soils, but the compaction was extreme and no infiltration was observed.

4.2.2 Soil sampling

Soil sampling was conducted in June 2014. Samples were collected within the pond at six locations at different depths: surface soil (level 1), 4" to 6" (level 2), and 1' to 2' (level 3). The surface soil samples were collected using a small trowel and a post hole digger was used for the deeper depths (levels 2 and 3). Sampling locations are shown in Figure 4-9. Locations 5 (near the discharge location) and 6 (midway along channel) were located close to the main flow path through the pond, while locations 2 and 4 were adjacent to the channel, several feet from the flow pathway, and locations 1 and 3 were on the pond periphery farthest from the main channel. A total of 18 soil samples were collected in the pond area for analyses. The surface soil samples were brownish in color and the samples obtained from levels 2 and 3 were sandy. The collected samples were sealed in polyethylene- linear low density (LLDPE) Ziploc bags and sent to the soils lab for analyses.

Figure 4-9 Sampling locations in dry pond

4.2.3 Chemical Analyses of Soil Samples

Chemical analyses of the collected soil samples included: pH, acidity, cation exchange capacity (CEC), phosphorous, nitrogen, carbon, sulfur, potassium, magnesium, calcium, heavy metals (Al, As, Zn, Cu, Cd, Mn, Fe, Ni, Pb), and organic matter (OM). The metals in the soils were analyzed using two different methods: Mehlich 3 method (a less aggressive digestion method indicating plant availability of the constituents) and EPA method 3050B acid digestion method (complete chemical content).

4.2.4 Migration of pollutants in vadose zone

Stormwater infiltration is a stormwater control practice used to reduce discharges to surface waters and to enhance shallow groundwater recharge. However, it may also facilitate transport of pollutants to the groundwater. In recent years, there have been extensive studies (Fischer et al 2003, Jacques et al 2008, Zubair et al 2010, Mikula et al 2011) on the fate and transport of various organic and inorganic pollutants associated with stormwater infiltration in the saturated and unsaturated (vadose) layers of the soil. Various computer models have been developed to determine the movement of pollutants through the subsurface. The Seasonal Soil Compartment Model (SESOIL) Version 7.1 (Environmental Software Consultants Inc.) was selected as a suitable model to evaluate these processes and predict the potential fate and transport rate of these contaminants as a result of wet-weather flow infiltration in this dry pond.

4.2.5 An Overview on SESOIL

SESOIL is an integrated screening-level soil compartment model which is used to model the water transport, sediment transport, and the fate of the pollutants in the subsurface beneath infiltration facilities. It simulates contaminant transport and fate based on diffusion, adsorption, volatilization, biodegradation, and hydrolysis processes. Arthur D. Little, Inc (ADL), developed the model for the EPA's Office of Water and Office of Toxic Substances in 1981, and, in 1984, a fourth soil layer was added to enhance the original three soil layer model. At the end of the 1980s, it was integrated with the Graphical Exposure Modeling System for the PC (PCGEMS) that was later named RISKPRO.

Modeling Capabilities

SESOIL uses soil, chemical, and meteorological values as input information. The data requirements for SESOIL are generally less (Mikula, *et al*. 2011) than needed for most other similar models. As it accepts time varying pollutant loadings, it has a capability of simulating variable and seasonal chemical releases into the soil from various sources pollutant sources, such as seasonal stormwater discharges.

Methodology

The various processes modeled by SESOIL are subdivided into three cycles: the hydrologic cycle, the sediment cycle and the pollutant fate cycle. The hydrologic cycle focuses on moisture movement, the sediment cycle deals with runoff from the soil surface, and the pollutant fate cycle deals with the movement of the pollutants through the soil.

Hydrologic Cycle

The hydrological cycle is simulated by one-dimensional vertical movement of the moisture through the soil compartments based on the water balance dynamics theory of Eagleson (1978). The water balance dynamics theory is based on interactions of hydraulic processes, including climate, soil and vegetation. The water balance equations used in this theory are:

$$P-E-MR = S+G =Y$$

$$I = P-S$$

Where,

Yield (Y) is the sum of recharge (G) and surface runoff (S). Yield can be also calculated as a function of moisture retention (MR), precipitation (P), and Evapotranspiration (E). Infiltration is

represented as the difference between precipitation and surface runoff. The results obtained from the hydrological cycle are passed into the sediment washload cycle.

Monthly Load

The monthly input pollutant loads (mass per unit area) for the pollutants are calculated based on the filtered pollutant loads of the pollutants in the runoff entering the study site per unit area. The monthly pollutant load is based on observed filtered concentration for a particular month, total runoff and area of the study site. The calculation for monthly load is based on the following equation:

Monthly load = (Observed average filtered concentration for the month*Total runoff for the month)/ (Area of interest)

Pollutant Fate Cycle

The pollutant fate cycle uses the output obtained from the hydrologic cycle and the inputted monthly pollutant load data to stimulate the fate and transport of the specified pollutants in the subsurface. Pollutant fate cycle involves contaminant transport and transformation process that occur in the soil. Transformation process involved in pollutant fate includes partition of the contaminant into soil air, soil moisture, and soil solids phases. Different types of transformation may include biodegradation through microbial activity, photodegradation, and hydrolysis Equilibrium is assumed between the three phases and concentration of contaminant in one phase is used to calculate the concentrations in the other two phases.

Modified Henry's law is used to calculate the concentration of pollutant in the soil air and the concentration of pollutant adsorbed to the soil is estimated by Freundlich isotherm as per the following equations:

$C_{sa} = cH/R\ (T + 273)$

Where

C_{sa} = pollutant concentration in soil air (μg/mL);

c = pollutant concentration in soil water (μg/mL);

H = Henry's law constant (m^3atm/mol);

R = Universal gas constant; and

T = soil temperature (^oC)

$s = K_d c^{1/n}$

Where,

s = pollutant adsorbed concentration (μg/g);

n = Freundlich exponent;

K_d = pollutant partitioning coefficient (μg/g)/ (μg/mL);

c = pollutant concentration in soil water (μg/mL).

The total concentration of the pollutant in the soil is calculated as:

$C_o = f_a * C_{sa} + \theta * C + \rho_b S$

Where,

C_o = overall (total) pollutant concentration ($\mu g/cm^3$);

$f_a = f - \theta$ = the air-filled porosity (mL/mL);

f = soil porosity (mL/mL);

θ = soil water content (mL/mL);

ρ_b = soil bulk density (g/cm^3)

4.2.6 SESOIL Inputs

As mentioned earlier, the runoff from the industrial site is pretreated by a hydrodynamic separator located upstream of the pond. The monitored effluent from this separator (the influent to the infiltrating dry pond) was therefore used to describe the pollutant loads available for infiltration. Rainfall hydrologic parameters were selected from SESOIL's climatic database for the selected study area. Soil parameters were selected from SESOIL's soil database derived from the soil information for the site obtained from the NRCS soil database (NRCS Web Soil Survey available online at http://websoilsurvey.nrcs.usda.gov/).

The pollutant load parameters were calculated based on the filtered concentrations of effluent (Table 4-1) sampled at the outlet point of the hydrodynamic device and were loaded into the model as a monthly load, based on the monthly average concentrations entering the pond (Table 4-2). A soil profile of four meters was selected and the migrations of pollutants were simulated for a period of 50 years as a semi-continuous release.

Table 4-1 Summary of total and filtered concentrations of pond influent

Constituent	Min	Max	Average	COV	Detection Limit

					(DL)
Al Total (mg/L)	0.73	6.9	3.71	0.54	0.05
Al filtered (mg/L)	<DL	<DL	<DL	n/a	0.05
As Total (mg/L)	<DL	0.0063	0.0038	0.78	0.005
As filtered (mg/L)	<DL	<DL	<DL	n/a	0.005
Cd Total (mg/L)	<DL	0.0077	0.0039	0.41	0.001
Cd filtered (mg/L)	<DL	0.001	<DL	n/a	0.001
Cu Total (mg/L)	0.1	0.79	0.43	0.52	0.005
Cu filtered (mg/L)	0.0062	0.039	0.022	0.48	0.005
Fe Total (mg/L)	2.7	20.6	12.2	0.51	0.03
Fe filtered (mg/L)	<DL	0.056	0.045	0.23	0.03
Pb Total (mg/L)	0.066	0.53	0.32	0.51	0.003
Pb filtered (mg/L)	<DL	<DL	<DL	n/a	0.003
Mn Total (mg/L)	0.068	0.44	0.24	0.55	0.0025
Mn filtered (mg/L)	<DL	0.22	0.038	1.8	0.0025
Ni Total (mg/L)	<DL	0.038	0.023	0.51	0.01
Ni filtered (mg/L)	<DL	<DL	<DL	n/a	0.01
Zn Total (mg/L)	0.16	1.1	0.71	0.48	0.01
Zn filtered (mg/L)	0.026	0.16	0.059	0.56	0.01
Nitrate (mg/L)	<DL	1.4	0.78	0.49	0.1
Phosphate (mg/L)	<DL	0.45	0.12	0.95	0.01
Filtered N as N (mg/L)	<DL	9.9	2.9	1.38	0.1
Filtered P as P (mg/L)	<DL	0.64	0.1		0.01

The pollutants modeled included filtered copper, filtered zinc, filtered iron, filtered manganese, and nitrate, as sufficient data were available for these constituents (having few non-detects) and they represent the most likely pollutants of most potential concern for the site. The monthly input loads for these pollutants are shown in Table 4-2.

Monthly pollutant load Calculations

The monthly input pollutant loads (mass per unit area) for the pollutants are calculated based on the filtered pollutant loads of the pollutants in the runoff entering the dry pond per unit area of the pond.

The monthly loads are calculated as:

(Observed average filtered concentration for the month*Total runoff for the month)/ (Area of dry pond)

An example calculation for the monthly load of filtered copper for January is shown below:

Observed average concentration of filtered copper for month of January: 22.5 µg/L

Total inflow of runoff to the dry pond for January: 1,512,686 liters

Total Area of the dry pond: 14,957,389 cm^2

Monthly load of filtered copper for January = (22.5*1,512,686)/(14,957,389) = 2.3 $\mu g/cm^2$

Table 4-2 SESOIL monthly pollutant load inputs for modeled pollutants

	Monthly Load ($\mu g/cm^2$)				
Month	Filtered Copper	Filtered Zinc	Filtered Iron	Filtered Manganese	Nitrate
Jan	2.3	6.2	4.8	2.1	35.4
Feb	5.0	22.8	19.2	3.7	618
Mar	3.0	21.0	13.6	96.3	394
Apr	10.8	26.2	26.8	21.0	537
May	17.5	42.5	6.8	2.7	242
Jun	4.3	4.8	2.8	1.1	332
Jul	5.7	5.4	3.5	1.1	351
Aug	6.1	5.0	5.0	1.2	406
Sep	1.8	5.0	3.9	2.2	31.4
Oct	1.9	6.0	4.9	1.7	67.8
Nov	2.2	5.1	4.1	3.9	47.5
Dec	7.3	17.7	13.7	7.5	121

4.3 Results

4.3.1 Distribution of pollutants in vertical soil profiles

The characteristics of the soils at different depths and associated pollutant concentrations analyzed using the two different sample digestion methods are shown in Tables 4-3 and 4-4 (only copper and zinc were analyzed using both methods), and the soil profile plots are shown in Figures 4-11 through 4-29.

Table 4-3 Soil characteristics and heavy metal concentrations at different depths (Mehlich 3 digestion, Method 1)

	Location - 1			Location - 2			Location - 3			Location - 4			Location - 5			Location - 6		
	TS*	4" - 6"	1' - 2'	TS	4" - 6"	1' - 2'	TS	4" - 6"	1' - 2'	TS	4" - 6"	1' - 2'	TS	4" - 6"	1' - 2'	TS	4" - 6"	1' - 2'
Soil pH	7.3	6.2	7.4	7.3	7.3	7.6	5.2	4.8	4.9	7.3	5.4	6.7	7.3	7.6	7.6	7.7	8.2	8
P (mg/kg)	38	15	30	6	14	14	29	9	10	12	6	5	5	2	5	6	1	4
K (mg/kg)	89	53	50	91	36	38	30	31	31	96	35	18	73	15	14	48	17	8
Mg (mg/kg)	98	48	75	203	43	40	48	42	49	321	64	61	222	14	17	134	17	17
Ca (mg/kg)	2,434	1,498	2,449	2,867	341	423	433	258	336	7,389	579	636	5,580	108	162	3,245	144	154
Zn (mg/kg)	152.7	15.2	42.2	218.5	1.5	5	9.1	2.1	2.5	264.5	33.8	15.6	321.3	2.8	11.9	151.2	2.6	4.5
Cu (mg/kg)	49.8	6.4	28.1	194.1	1.2	3.9	6	0.7	1.1	169.7	12	7.5	158.8	1.9	6.8	109.4	2.2	4.3
S (mg/kg)	19.3	21.5	21	59.4	10.9	10.1	12.4	34.6	39.9	40.1	99	18.8	22.7	5.2	4	18	3	4.3
% Nitrogen	0.19	0.06	0.09	0.16	0.02	0.02	0.04	0.03	0.04	0.3	0.05	0.05	0.36	0.07	0.03	0.07	0.02	0.02
% Carbon	3.87	0.73	1.88	2.77	0.04	0.06	0.23	0.07	0.1	0.3	0.05	0.05	0.36	0.07	0.03	0.07	0.02	0.02
% Org Matter	2.2	0.7	1.5	2.9	0	0	0.2	0.1	0.2	5.2	0.8	0.6	7	0	0	0.5	0	0
Acidity (meq/100g)	0	2.8	0	0	0	0	2	3.9	4.5	0	2.8	2	0	0	0	0	0	0
CEC (meq/100g)	13.2	10.8	13	16.3	2.2	2.5	4.6	5.6	4.5	17.9	6.3	5.7	17	0.7	1	16.2	0.9	0.9

* surface soil sample

Table 4-4 Heavy metal concentrations at different depths (EPA acid digestion, Method 2)

	Location - 1			Location - 2			Location - 3			Location - 4			Location - 5			Location - 6		
	TS*	4" - 6"	1' - 2'	TS	4" - 6"	1' - 2'	TS	4" - 6"	1' - 2'	TS	4" - 6"	1' - 2'	TS	4" - 6"	1' - 2'	TS	4" - 6"	1' - 2'
Al (mg/kg)	2,650	2,740	2,610	3,990	989	1,330	1,710	1,750	2,320	7,490	3,780	2,470	8,970	601	412	4,210	308	477
As (mg/kg)	7.4	ND	3	6.7	ND	ND	2.5	ND	2.4	14.5	2.2	ND	15.9	ND	ND	5.3	ND	ND
Cd (mg/kg)	1.9	ND	ND	2.4	ND	ND	ND	ND	ND	5.5	ND	ND	6.1	ND	ND	2	ND	ND
Cu (mg/kg)	124	12.3	32	305	ND	ND	9.6	ND	ND	600	18.1	7.7	596	3.1	11.5	291	ND	7.4
Fe (mg/kg)	18,600	2,430	6,400	15,400	194	403	4,050	2,570	3440	32,300	6,220	3,080	32,900	762	859	12,700	604	1,040
Pb (mg/kg)	247	31.8	111	322	ND	ND	10.1	ND	3.1	672	40.1	14.5	841	5.1	15.2	267	ND	8.7
Mn (mg/kg)	169	28.3	49.6	261	6.7	21.1	48.2	14.6	32.9	558	102	133	484	4.2	8.6	200	2.8	14.2
Ni (mg/kg)	20.3	2.5	4.8	26	ND	ND	ND	ND	ND	58.2	5.4	2.3	68	ND	ND	23.2	ND	ND
Zn (mg/kg)	417	45.4	79.3	573	2.2	3.4	20.6	3.9	5.7	1,110	76.4	29.8	1,260	8.3	29.2	490	2.9	14.7

ND = not detected or below detection limit, * surface soil sample

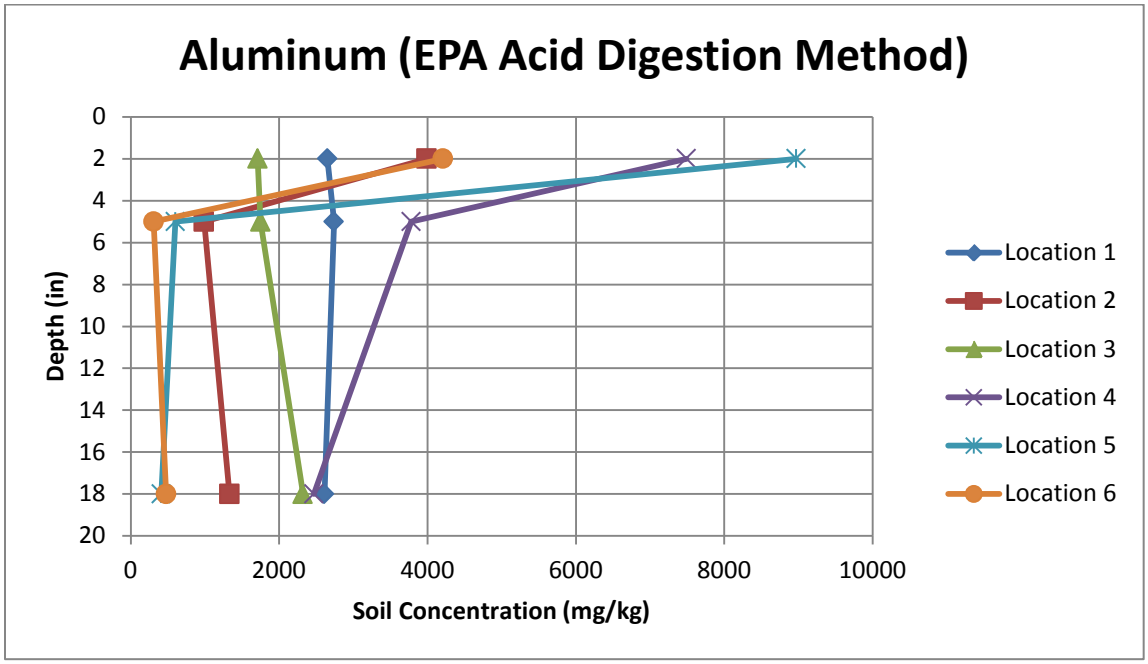

Figure 4-10 Soil accumulation of Aluminum (EPA acid digestion method)

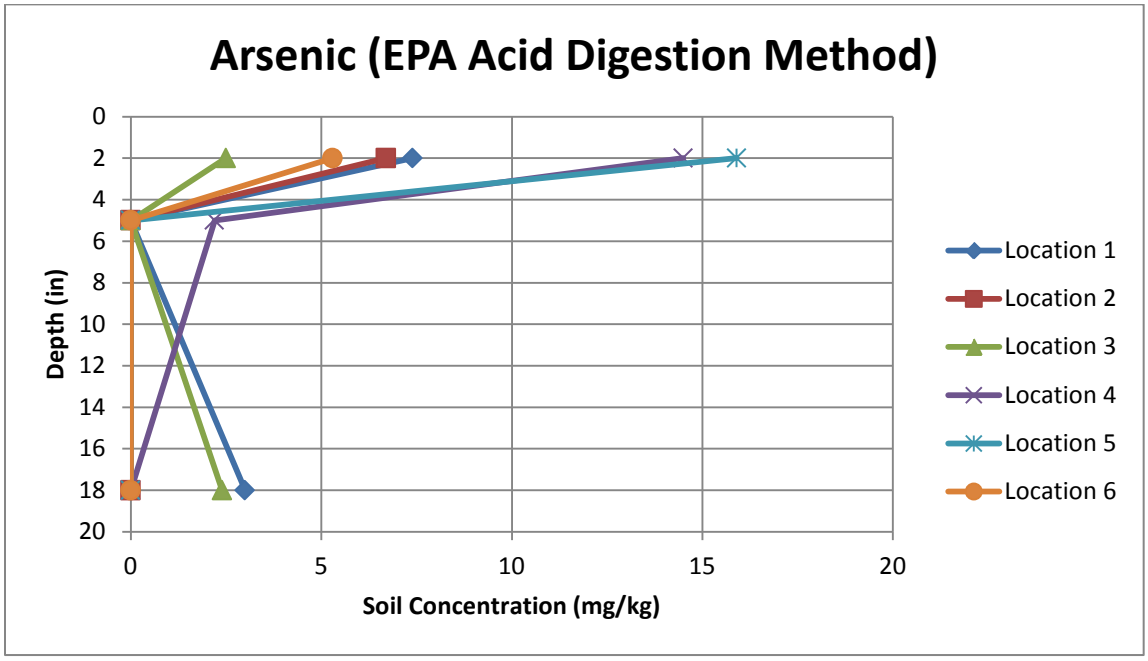

Figure 4-11 Soil accumulation of Arsenic (EPA acid digestion method)

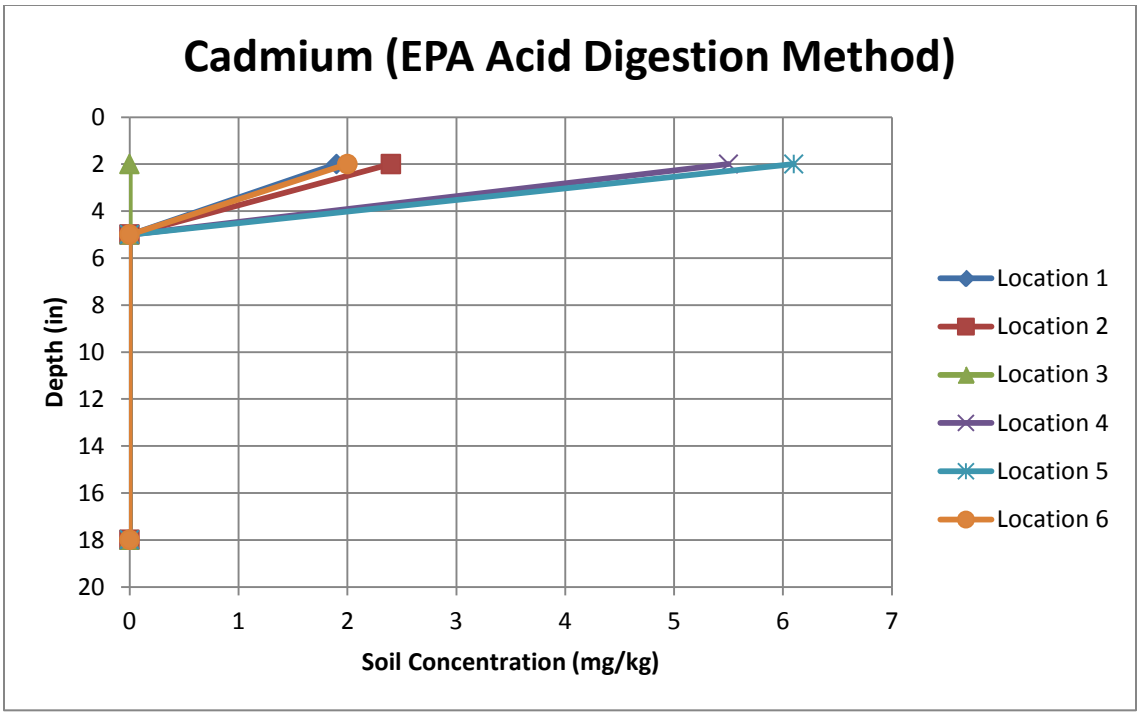

Figure 4-12 Soil accumulation of Cadmium (EPA acid digestion method)

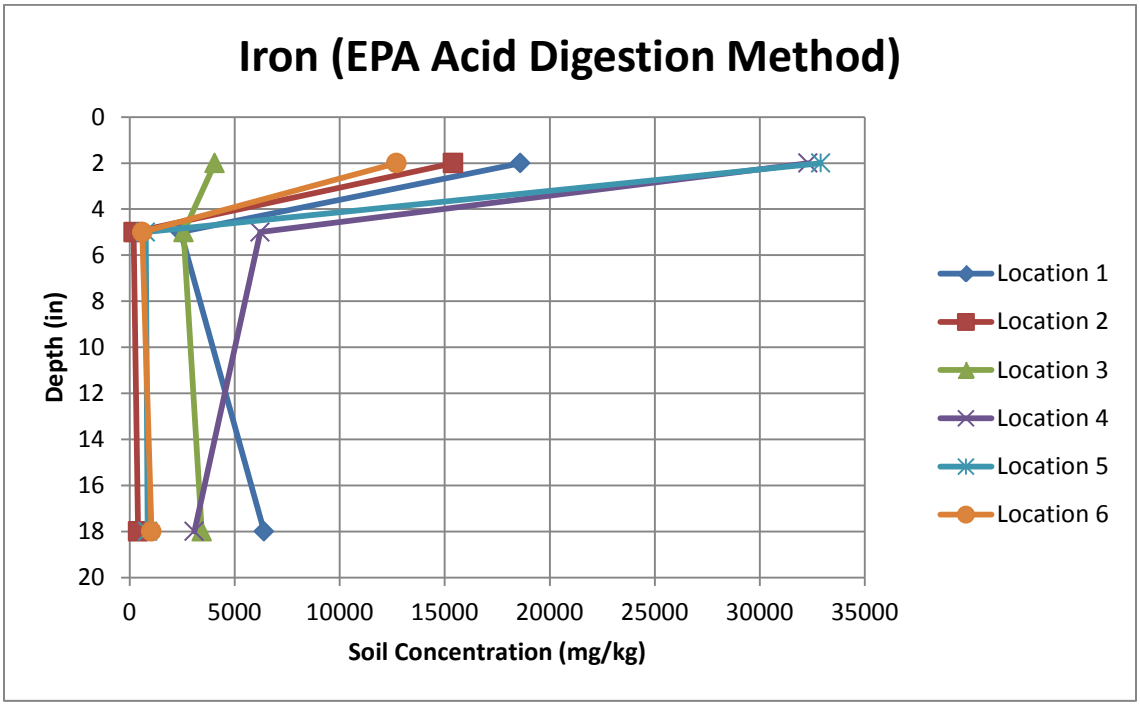

Figure 4-13 Soil accumulation of Iron (EPA acid digestion method)

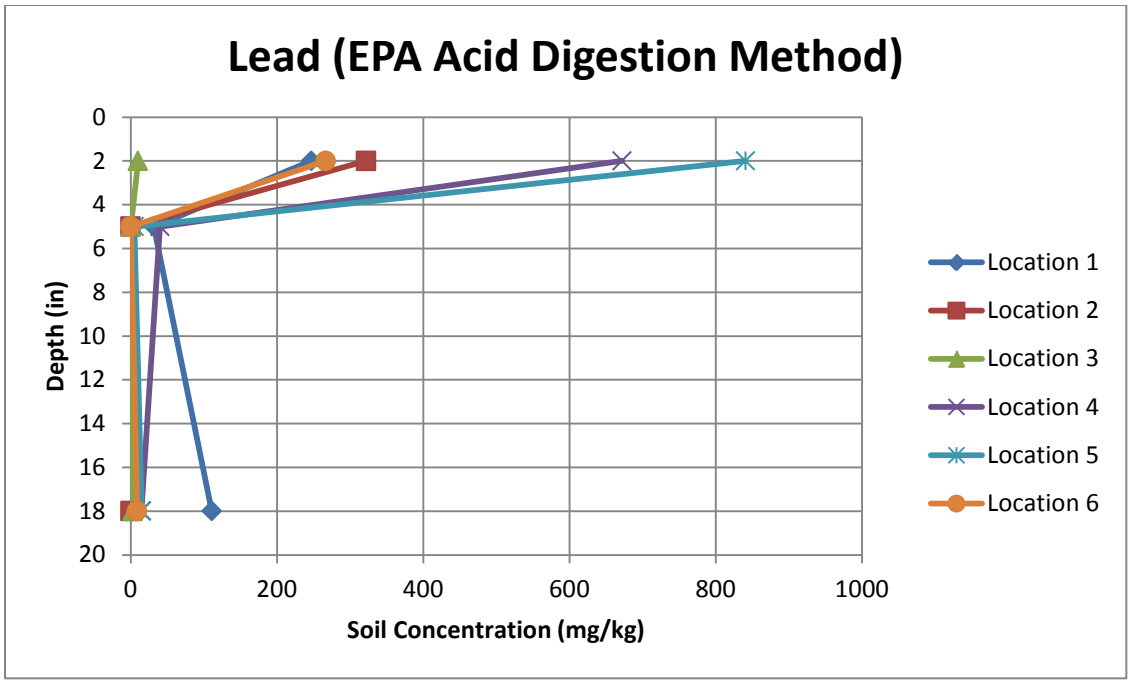

Figure 4-14 Soil accumulation of Lead (EPA acid digestion method)

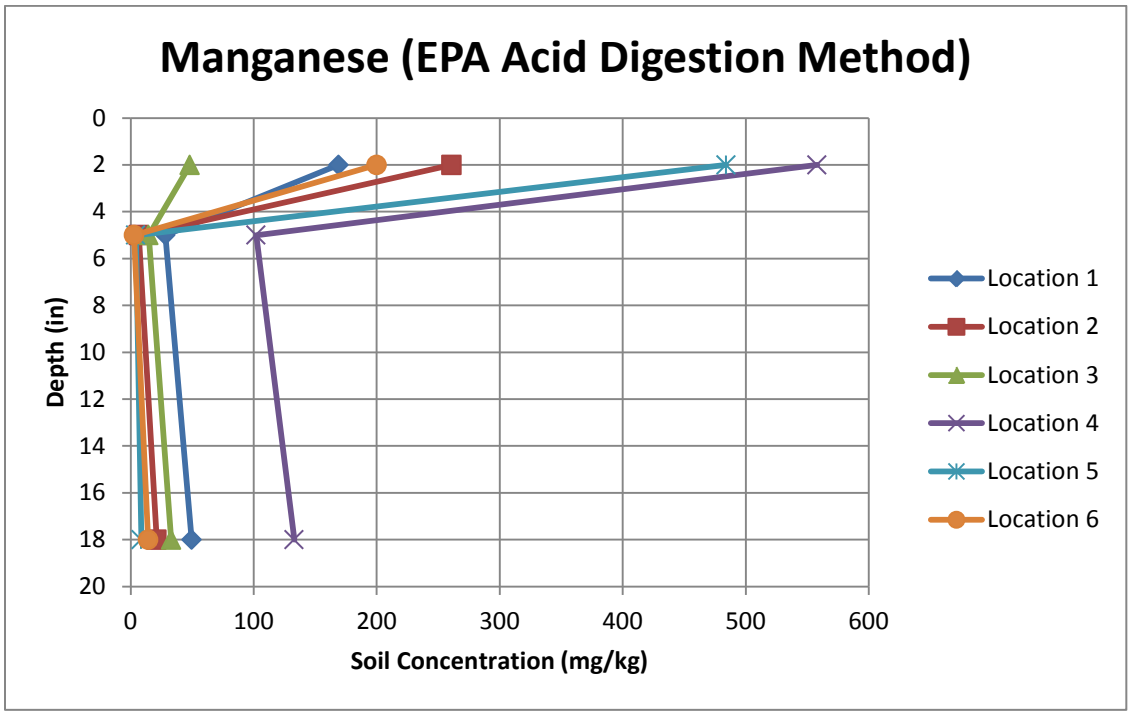

Figure 4-15 Soil accumulation of Manganese (EPA acid digestion method)

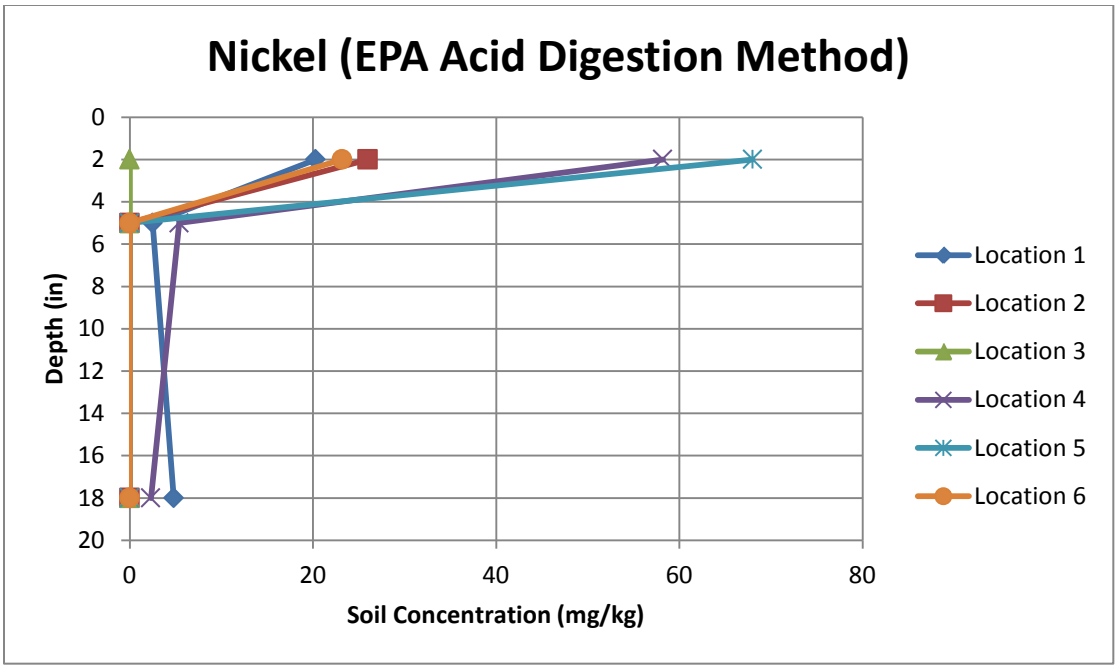

Figure 4-16 Soil accumulation of Nickel (EPA acid digestion method)

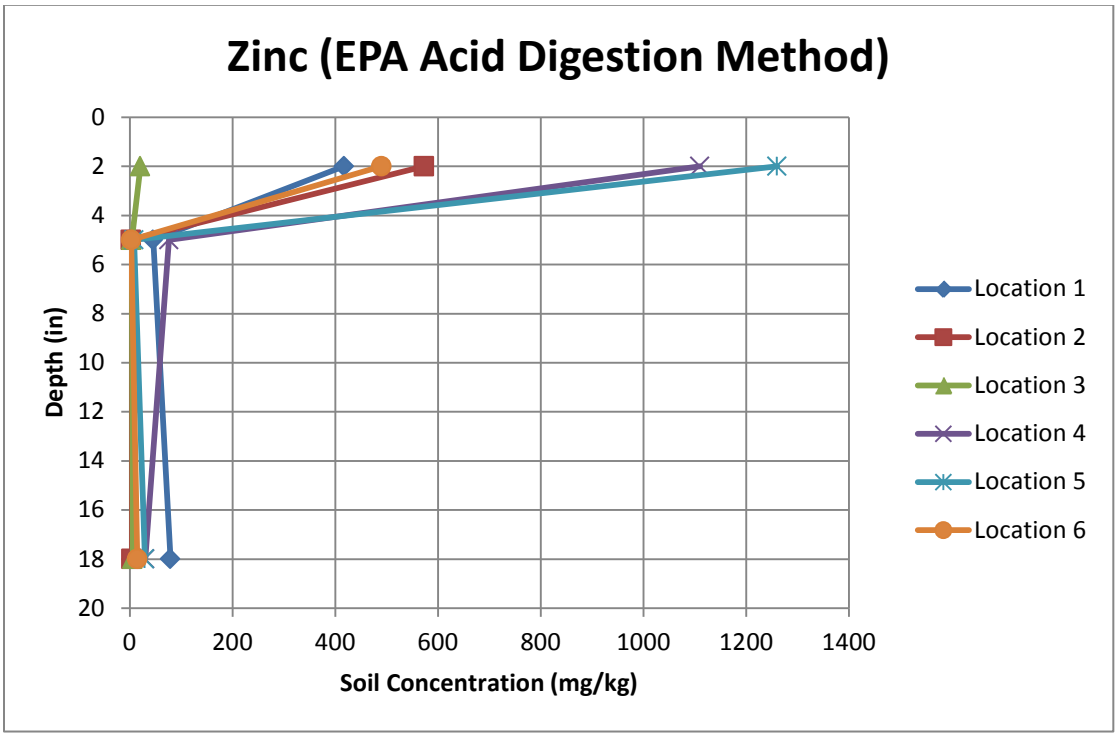

Figure 4-17 Soil accumulation of Zinc (EPA acid digestion method)

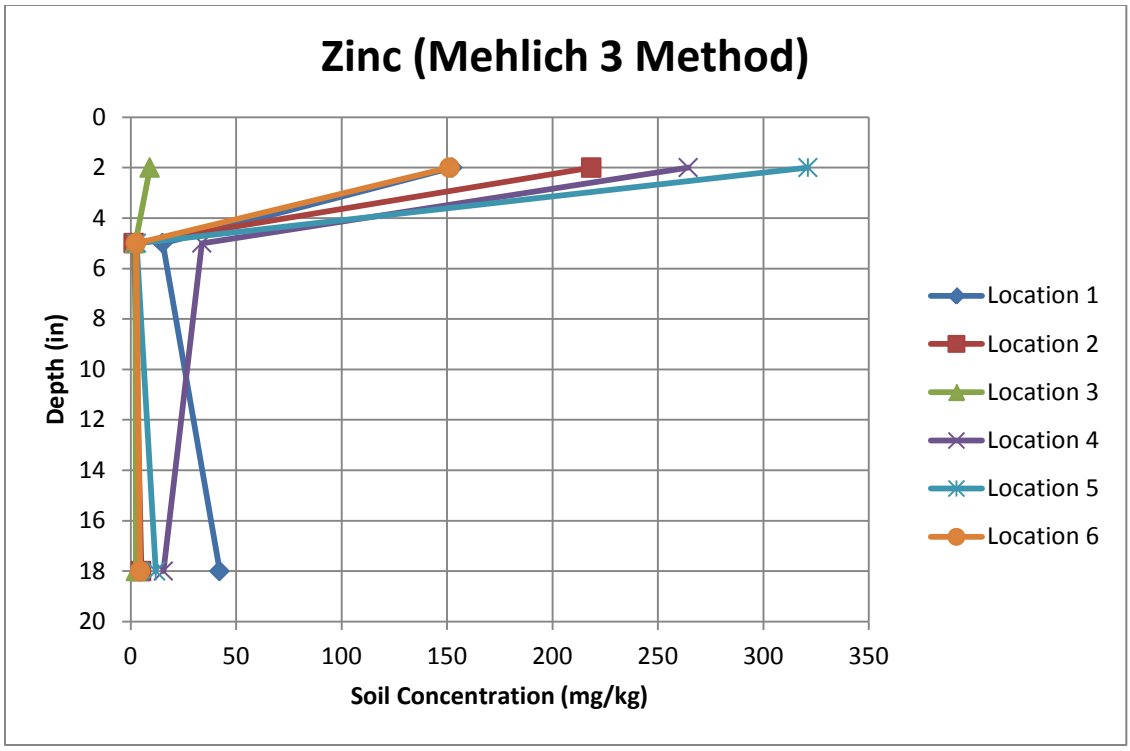

Figure 4-18 Soil accumulation of Zinc (Mehlich 3 method)

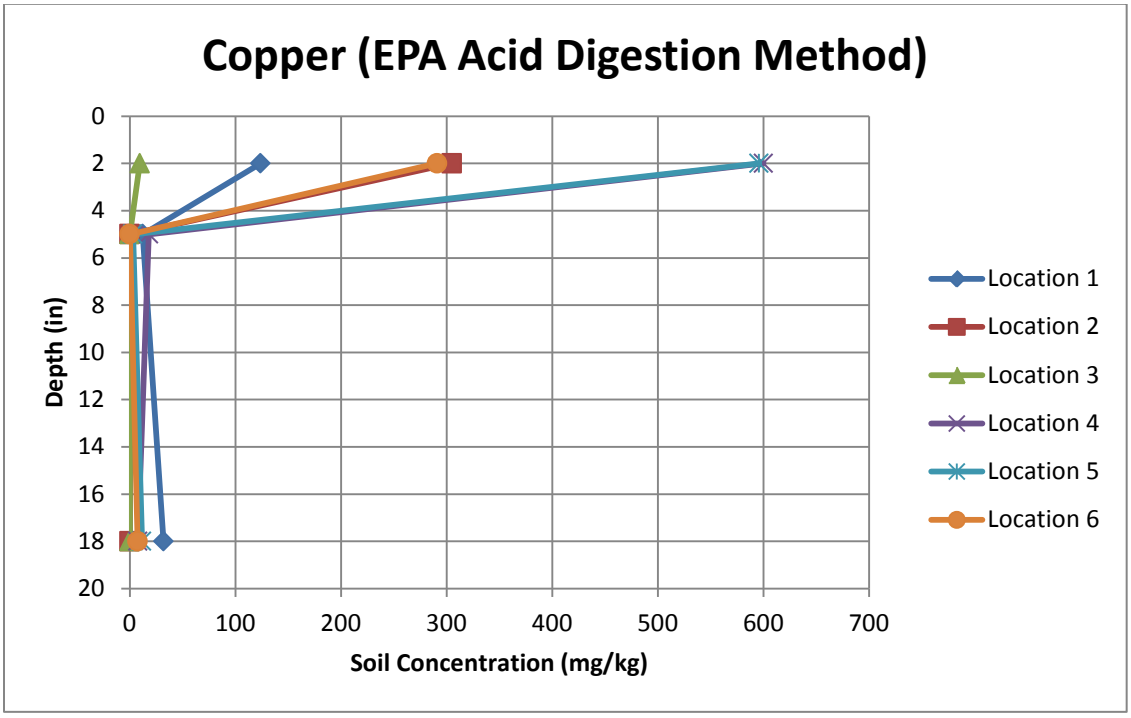

Figure 4-19 Soil accumulation of Copper (EPA acid digestion method)

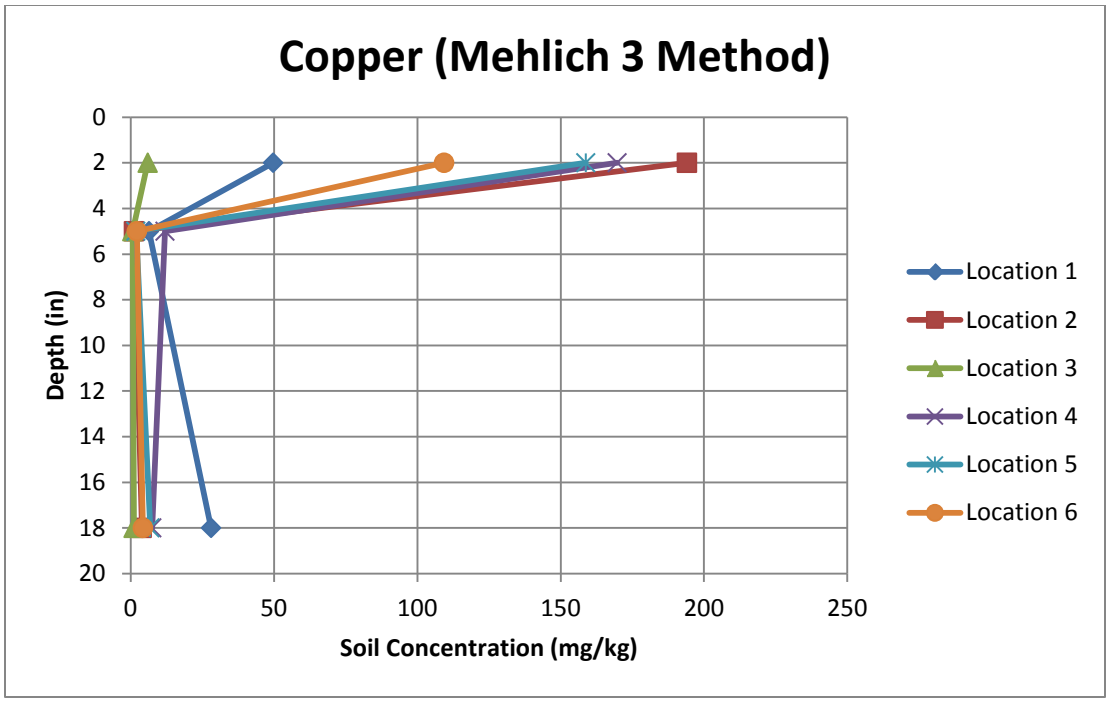

Figure 4-20 Soil accumulation of Copper (Mehlich 3 method)

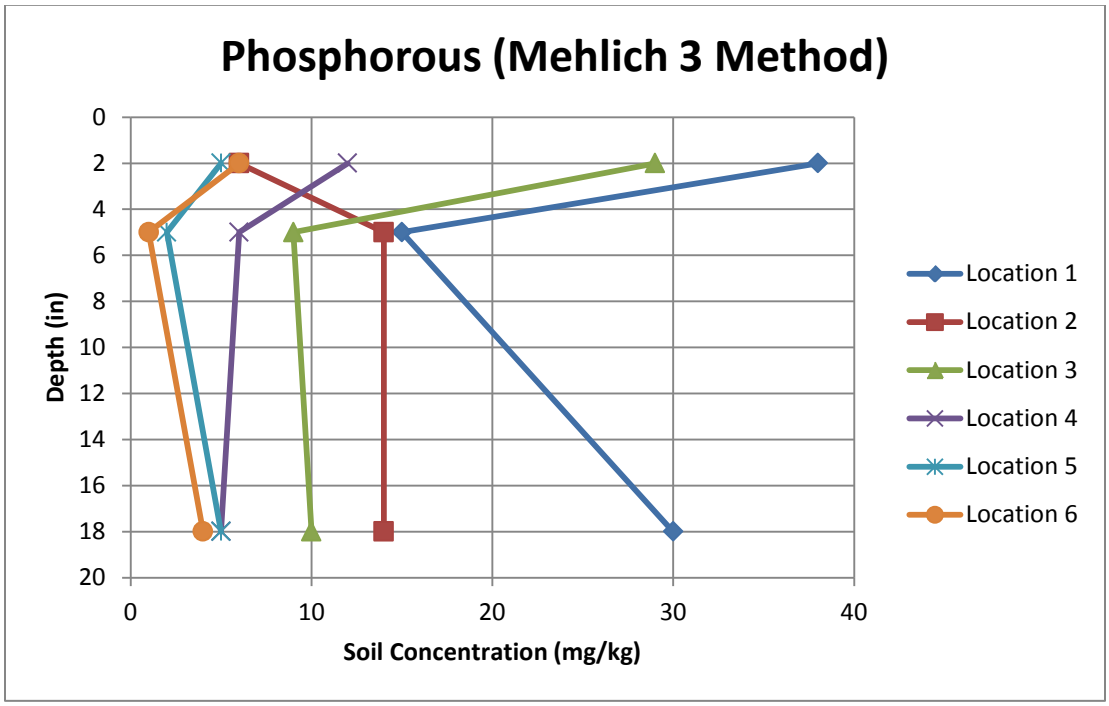

Figure 4-21 Soil accumulation of Phosphorous (Mehlich 3 method)

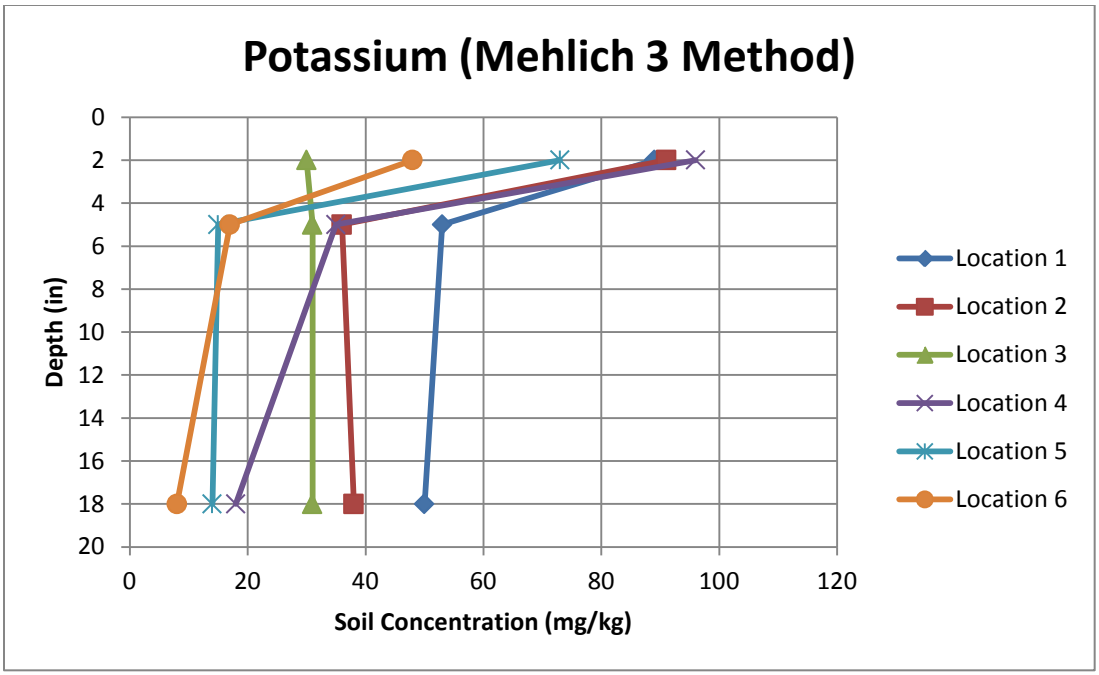

Figure 4-22 Soil accumulation of Potassium (Mehlich 3 method)

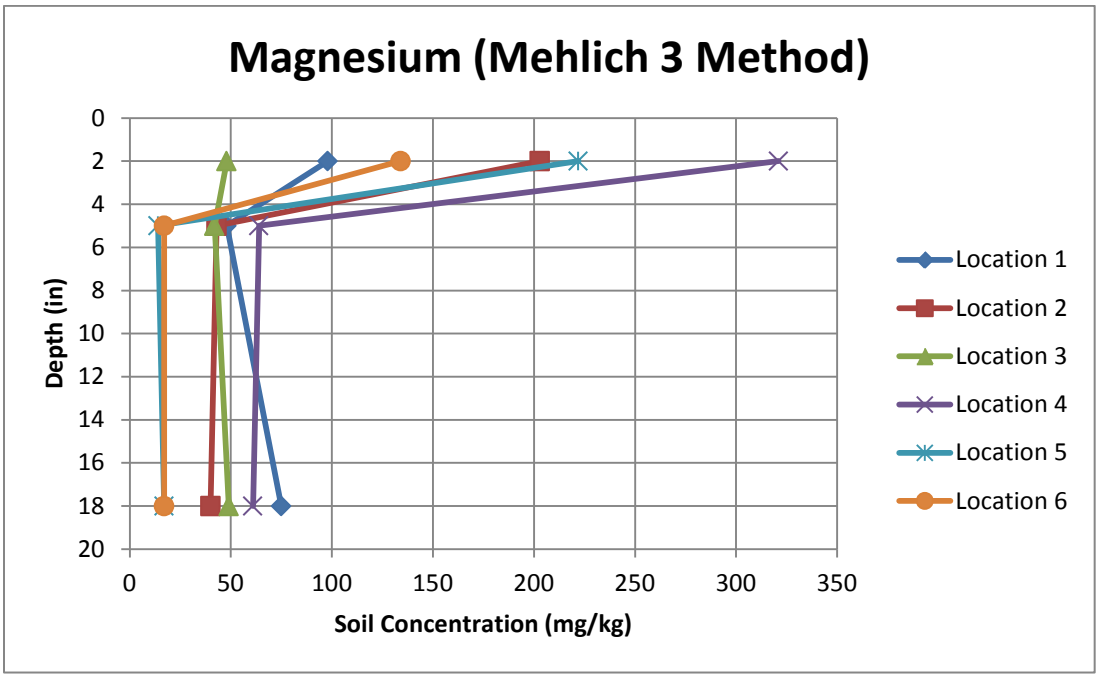

Figure 4-23 Soil accumulation of Magnesium (Mehlich 3 method)

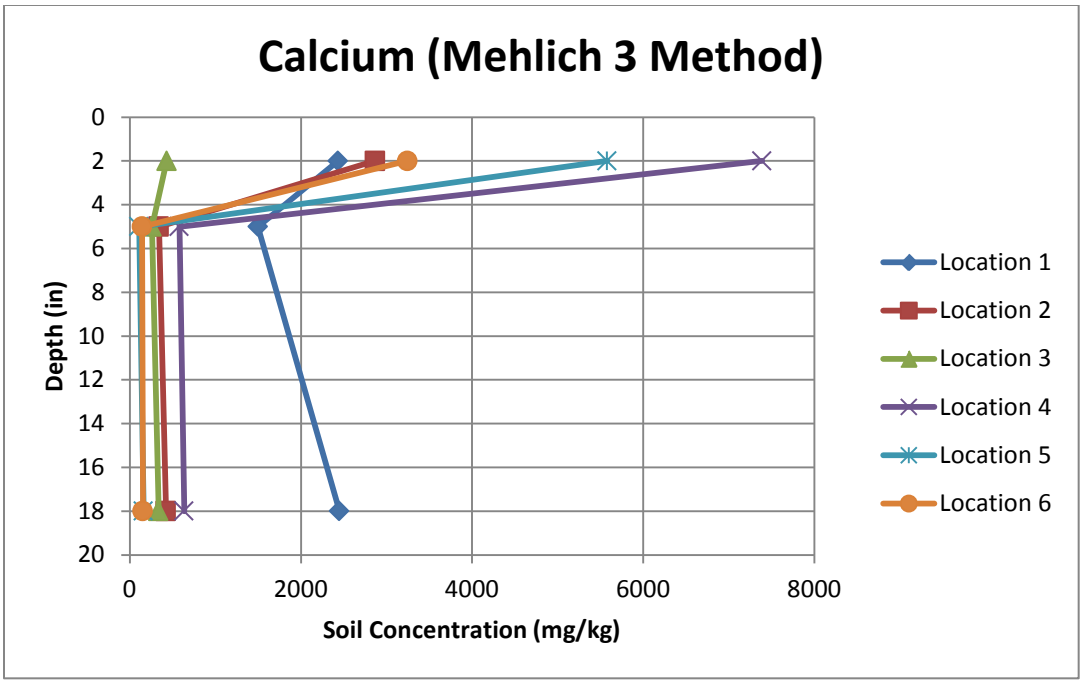

Figure 4-24 Soil accumulation of Calcium (Mehlich 3 method)

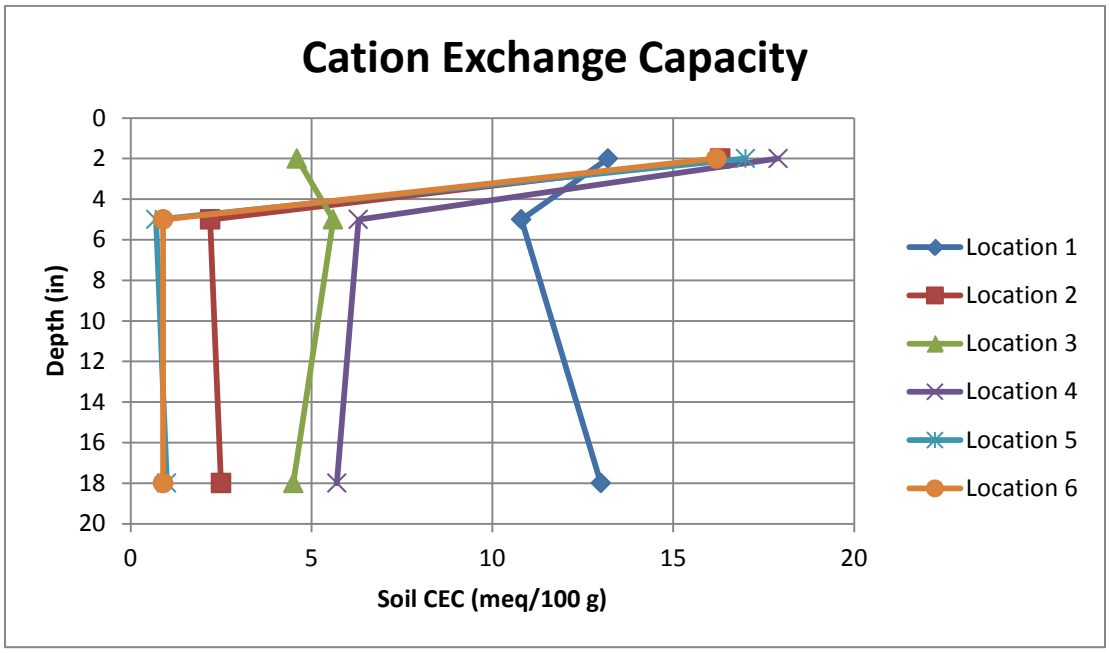

Figure 4-25 CEC profile with soil depth

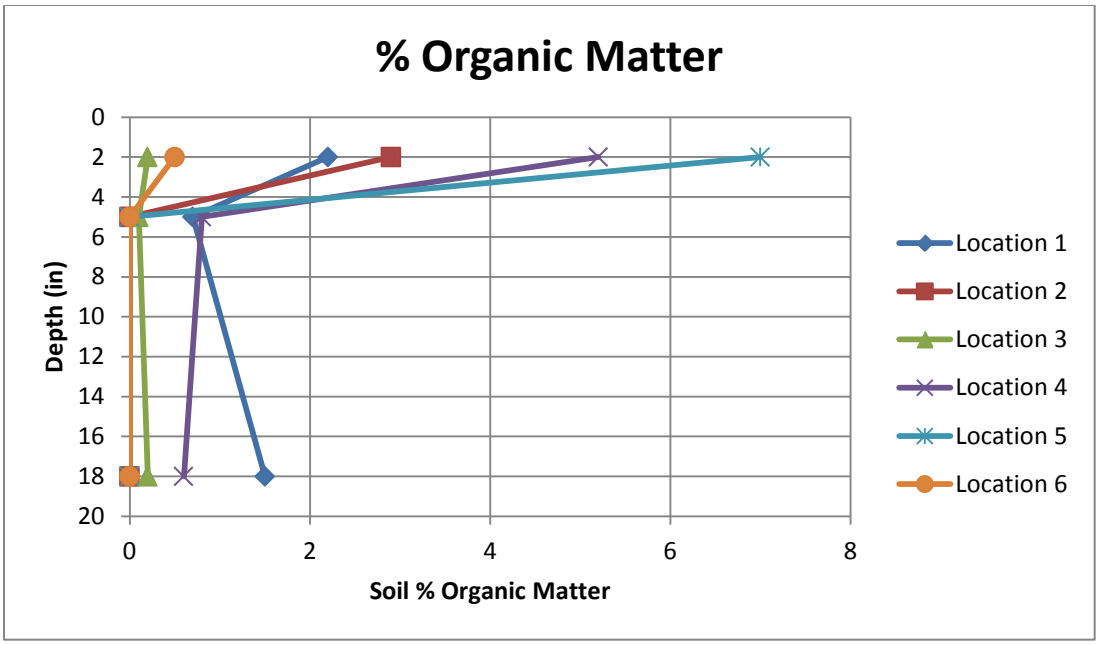

Figure 4-26 Organic matter profile with soil depth

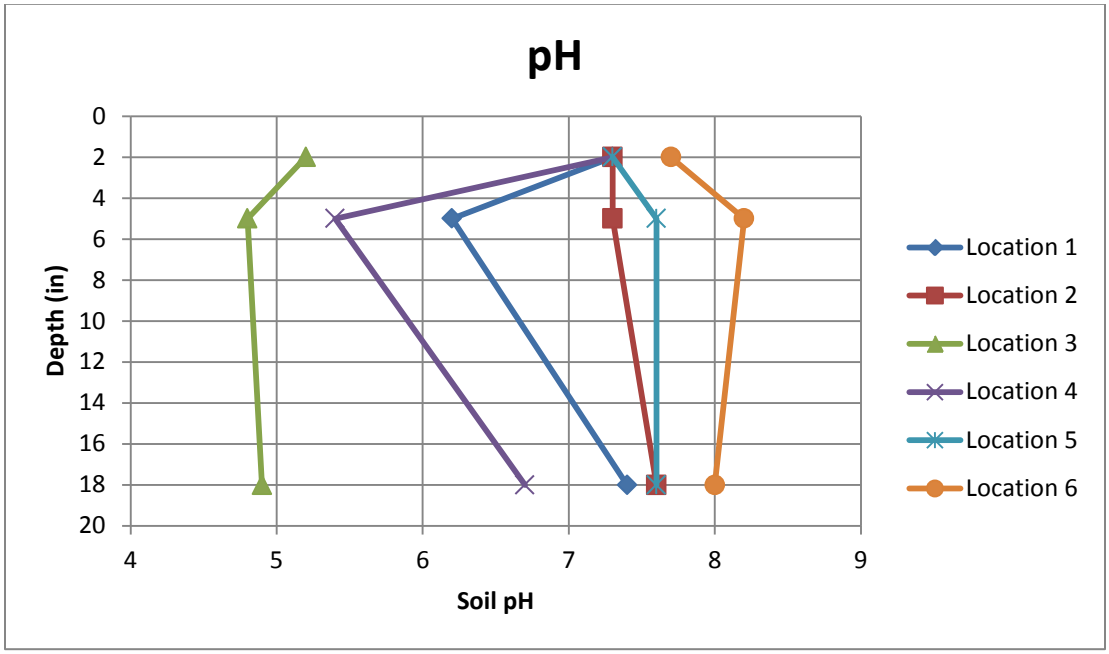

Figure 4-27 pH profile with soil depth

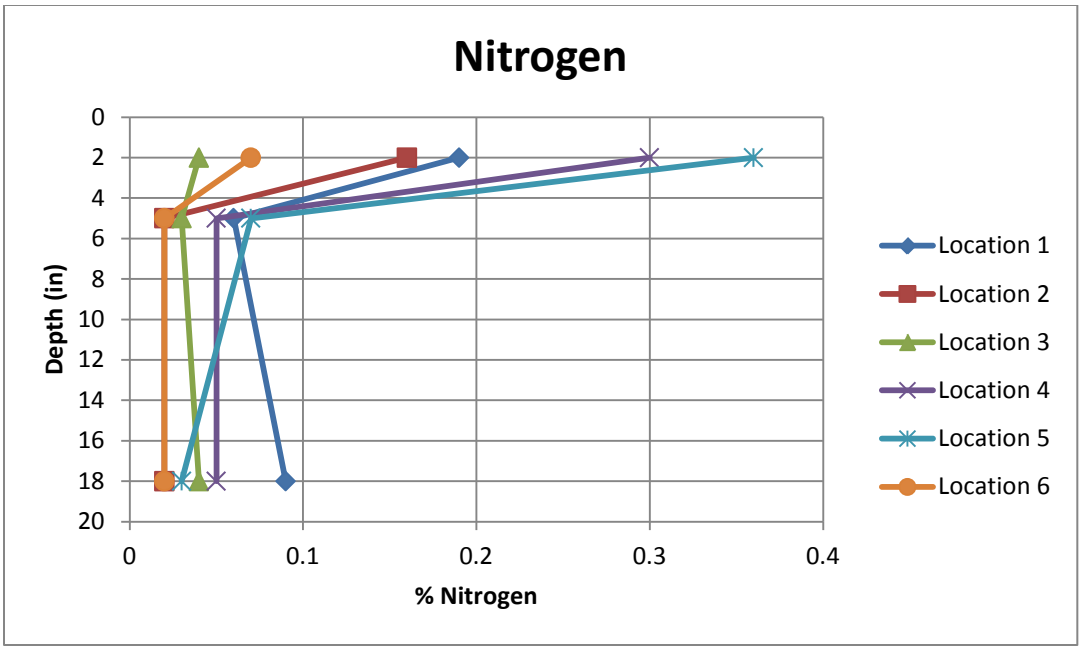

Figure 4-28 Nitrogen profile with soil depth

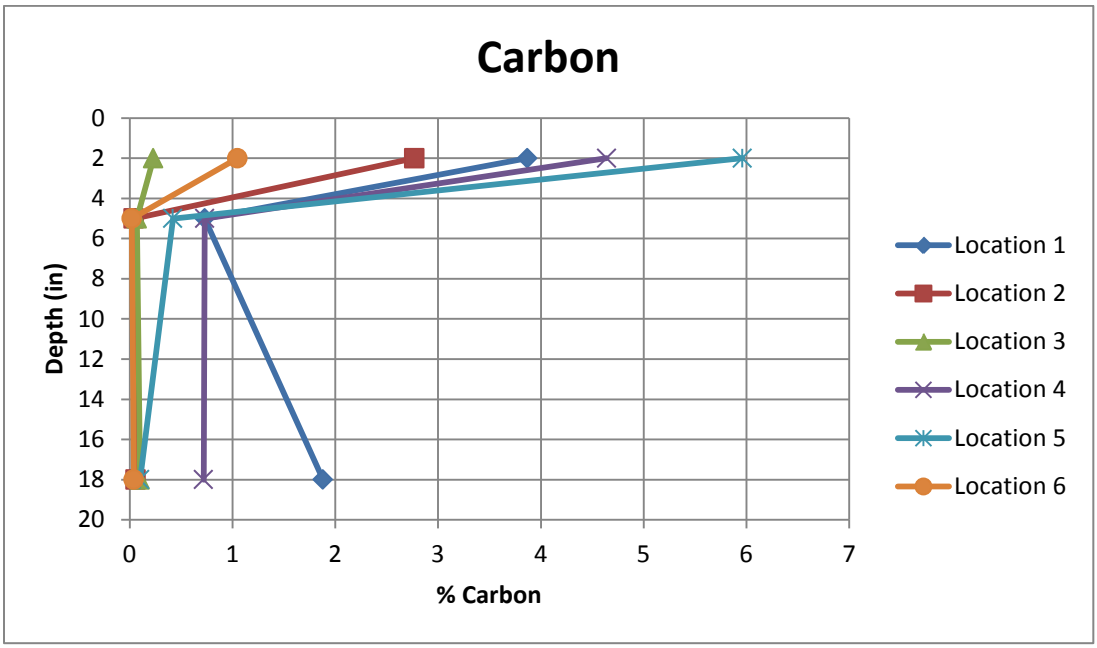

Figure 4-29 Carbon profile with soil depth

The results show a significant decrease in metal and nutrient concentrations between the surface soil and lower level samples for all of these constituents. The surface soils also have more organic matter content and CEC concentrations than the underlying soils for most of the

locations, as expected. The surface soil layer also had a distinct brown color. Basic filtering of the particulate-bound metals near the soil surface is an important capture mechanism, and the higher organic matter and CEC also likely play an important role in adsorption of filtered metals near the surface soils.

Figure 4-30 Infiltration test and soil sampling at location 5 showing typical brown colored surface soil color

As shown on Figure 4-30, the surface soil is brownish in color indicating higher organic matter content at location 5 near the pond outlet. Soils from all the locations, except location 3 (located on pond side slopes), exhibited brownish surface soil and fine sand at deeper depths. It was also observed that surface soils were silty and the deeper soils were sandy in texture. The pH values also stayed mostly in the basic range, except for location 3.

For all the sampling locations, pollutant concentrations increased somewhat between level 2 to level 3 (but not as much as the decrease from level 1 to level 2). The pH increased while there was a slight increase in organic matter content, and CEC. The increase in metal concentrations, although slight, was generally consistent, and may be associated with the increase in CEC and

organic matter content values in level 3, as metal retention is promoted by an increase in CEC and organic matter content (Deschne et al 2004, Winiarski et al 2006) Iron has the highest level of concentrations among all the constituents analyzed, followed by aluminum. Higher concentrations of iron and aluminum can be related to their higher concentrations in the stormwater entering the pond compared to the other metals.

All of the metals followed a similar pattern with location. The lowest concentrations were observed in locations 1 and 3 which are located towards the pond side slopes. A decrease in concentrations was also observed from location 4 to location 6. The metal concentrations increased with the increase in distance of the location from the conveyance channel which flows through the center of the pond. Higher concentrations were observed at location 5 which is the effluent location of the dry pond where water ponded before discharge. Location 5 has the highest organic carbon content and CEC values relating to more metallic ions binding to the soil. This shows the infiltrating dry pond does not operate in the same pattern across its entire surface, but indicates higher concentrations of some pollutants in the surface soils in areas where the water may pool for extended periods and where the water preferentially flows (the pond seldom fills and floods most of the area; during most events, there is only limited pooling near the central channel and near the outlet).

Figures 4-31 and 4-32 are scatterplots for zinc and copper soil concentrations analyzed by Mehlich 3 and EPA digestion methods. The scatterplots show a strong correlation between the two methods (R^2 = 0.96 for Zn, and R^2 = 0.86 for Cu). The concentrations observed by the EPA digestion method are 3 to 4 times that of the Mehlich method 3; the Mehlich 3 method is a weaker method (indicating plant availability) in comparison to EPA Acid digestion method (total metal content). The plots indicate Mehlich 3 may be useful as a screening method for plant

effects of metal contaminated soils as it is available at low cost at state agricultural soil testing laboratories. In this example, the total zinc and copper accumulations may be about 30% available for plants growing in the pond (which would then be released as soluble metals when the plant dies and decomposes), with the remaining incorporated into the pond surface soils.

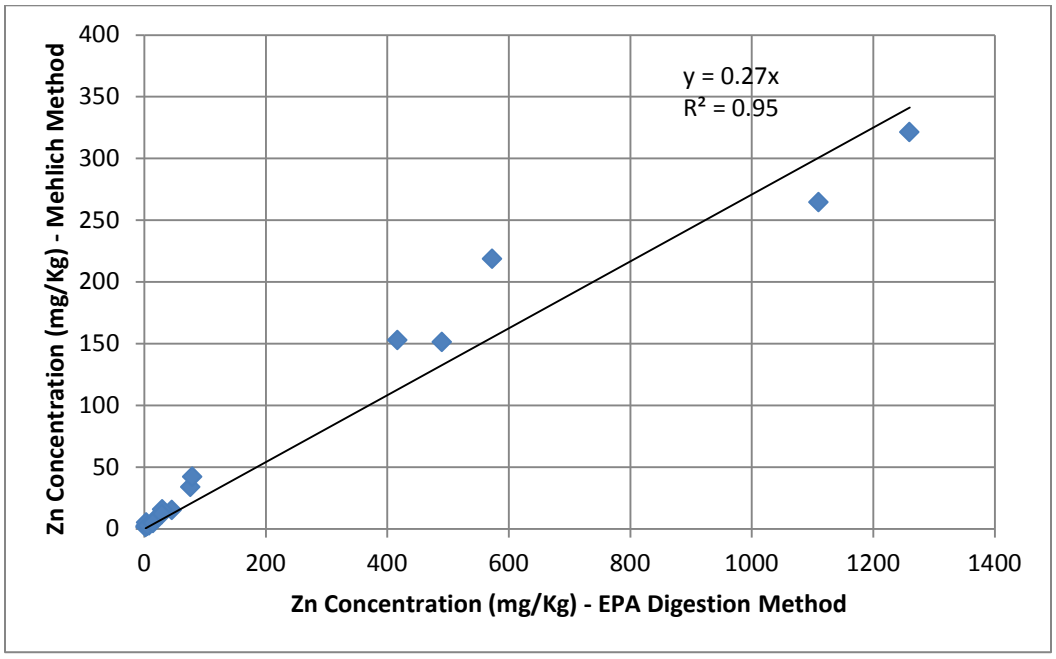

Figure 4-31 Scatter plot of Zinc concentration as measured by Mehlich 3 and EPA acid digestion methods

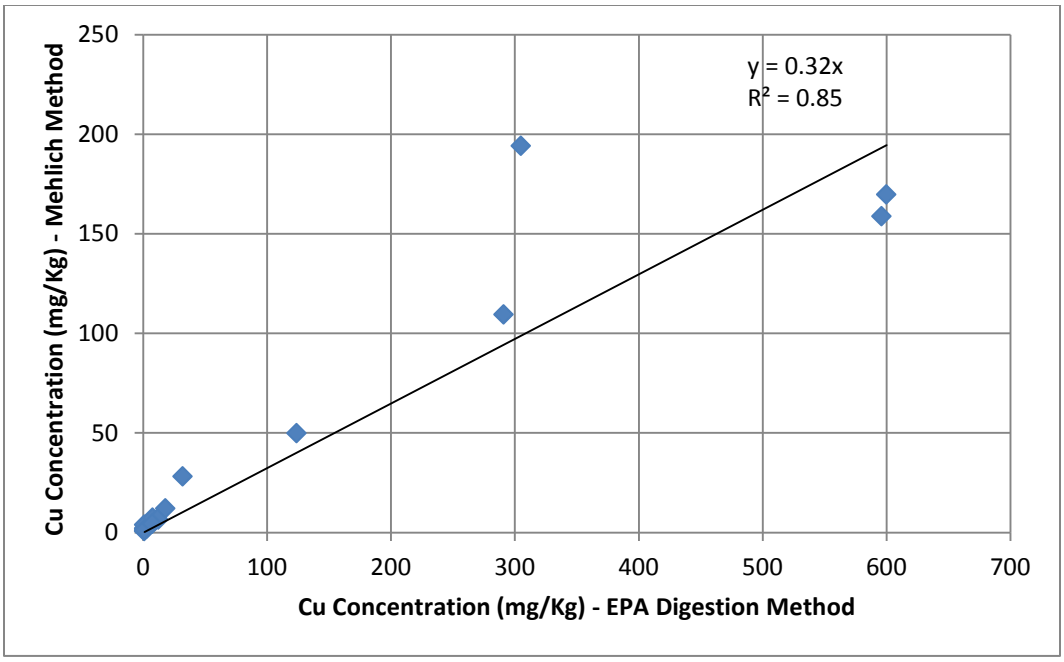

Figure 4-32 Scatter plot of Copper concentration as measured by Mehlich 3 and EPA acid digestion methods

4.3.2 Multivariate Analyses of Soil Contaminant Data

Multivariate analyses were conducted to study the relationships between different soil parameters and pollutant concentrations involved in the study and to identify group memberships. The different analyses performed include Pearson correlation analyses, cluster analyses, and principal component analyses. Pearson correlation analyses were performed to determine simple linear associations between different pairs of parameters, while cluster analyses were performed to identify more complex relationships between the parameters. Principal component analyses were performed to identify groupings of parameters with similar characteristics, to explain the variability in the data. Statistical software XLSAT 2015 was used to conduct these analyses.

4.3.3 Pearson Correlation Analyses of Soil Contaminant Data

Pearson correlation is one of the most common measure of correlation. The Pearson's correlation coefficient measures the strength of the association (stronger or weaker) between two variables (Johnson et al 2007). Values of the Pearson's correlation coefficient range between –1 (negative correlation) and +1 (positive correlation), while a value of 0 indicates no correlation. The linear relationships between pairs of variables are examined with scatterplots. The strength of association between the variables is assessed by the distance of the scatter of points to a straight line, the nearest the scatter points are to the straight line, the higher is the strength of the association between the variables. Pearson correlation analyses were performed to investigate relationships between different soil parameters including pollutant concentrations from the soil profiles. Parameters examined included pH, CEC, percent organic matter, acidity, phosphorous, calcium, potassium, and metal concentrations in the soil. The results of the Pearson correlation analyses are shown in Table 4-5 with highlighted values in bold indicating significant Pearson correlation coefficients (p value ≤ 0.05).

4.3.4 Regression Analyses

Regression analyses were used to determine associations between variables (independent and a dependent variable). Regression analyses help illustrate relationships between variables. Simple linear regression is the most common type and requires that the dependent variable has a linear relationship with the independent variable and for each value of the independent variable. The probability distributions of the independent and dependent variables also need to have the same standard deviation. Linear regression analyses were used to predict the relationships

between hydrological and water quality parameters included in the study. The results of the linear regressions were supplemented with ANOVA and residual analyses to ensure that regression assumptions are valid.

4.3.5 Analysis of Variance

ANOVA was conducted to test the significance of the regression coefficients (slope and intercept terms), which are highly dependent on the number of data observations. When an observed data set has only a few observations, it is difficult for the important relationships to have significant calculated coefficients. An ANOVA table presents the variability of the responses and distinguishes what can be explained by regression and what remains as error. The F critical value is the value that would result in a p-value equal to 0.05. A large F value (and correspondingly low p value) suggests that there is a significant linear relationship between the observed and predictor variables. Statistical software Minitab (Version 17) was used to perform these data analyses, including associated residual analyses to verify the regression assumptions.

4.3.6 Relationships among different soil parameters

Strong correlations were observed between different metal concentrations retained in the soil. All the pollutant concentrations were strongly correlated with each other except for sulfur and phosphorous. The strongest correlation was observed between nickel and zinc concentrations ($p < 0.05$, $R^2 = 0.996$) (Figure 31). As expected, pH showed a strong negative correlation with acidity (Figure 28). All the parameters included in the study showed weak correlations with pH.

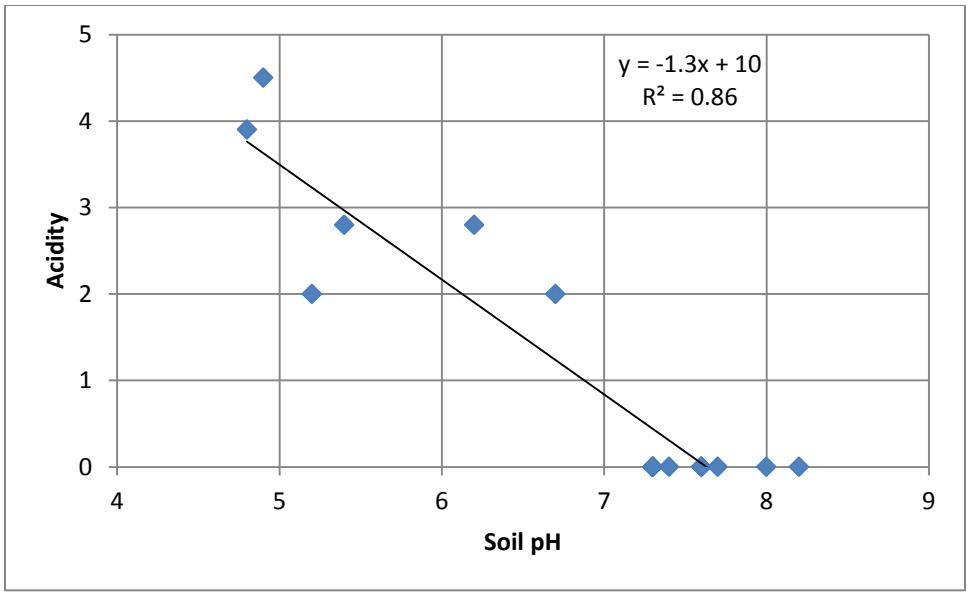

Figure 4-33 Scatterplot of Soil pH vs. Acidity (Pearson coefficient = -0.930, p = <0.0001

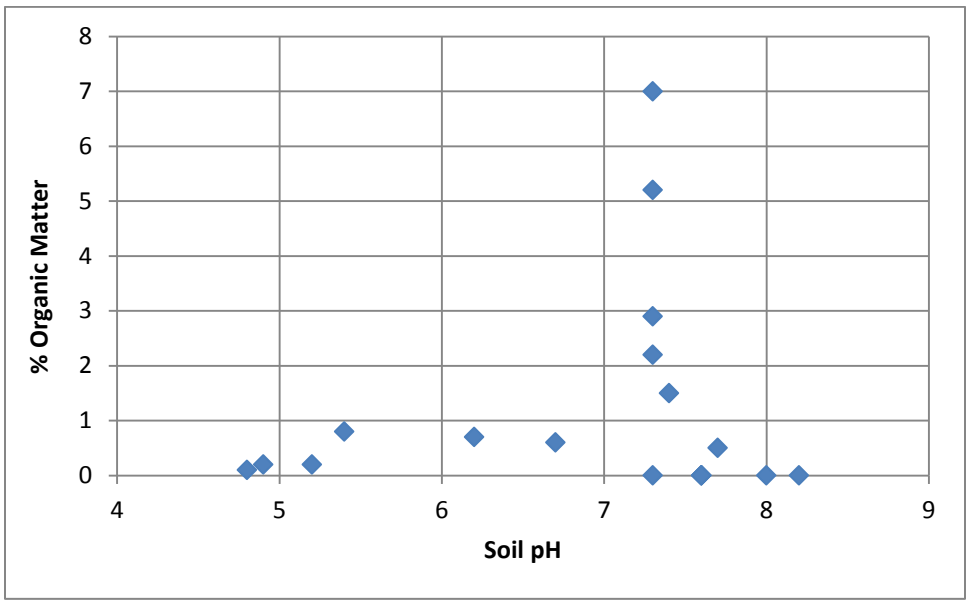

Figure 4-34 Scatterplot of Soil pH vs. % Organic matter (Pearson coefficient = 0.16, p = 0.5)

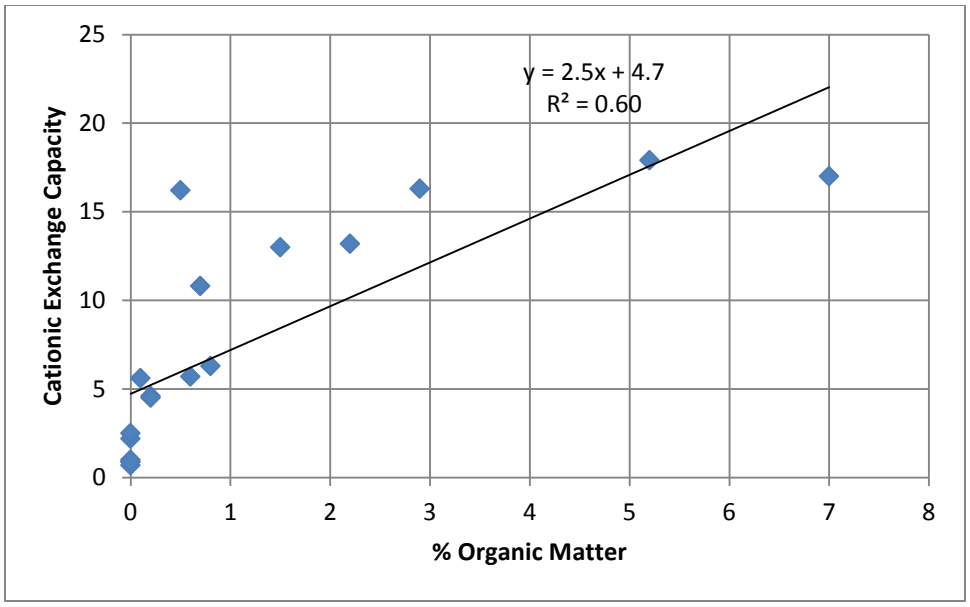

Figure 4-35 Scatterplot of % Organic matter vs Cation exchange capacity (Pearson coefficient = 0.78, p = <0.001)

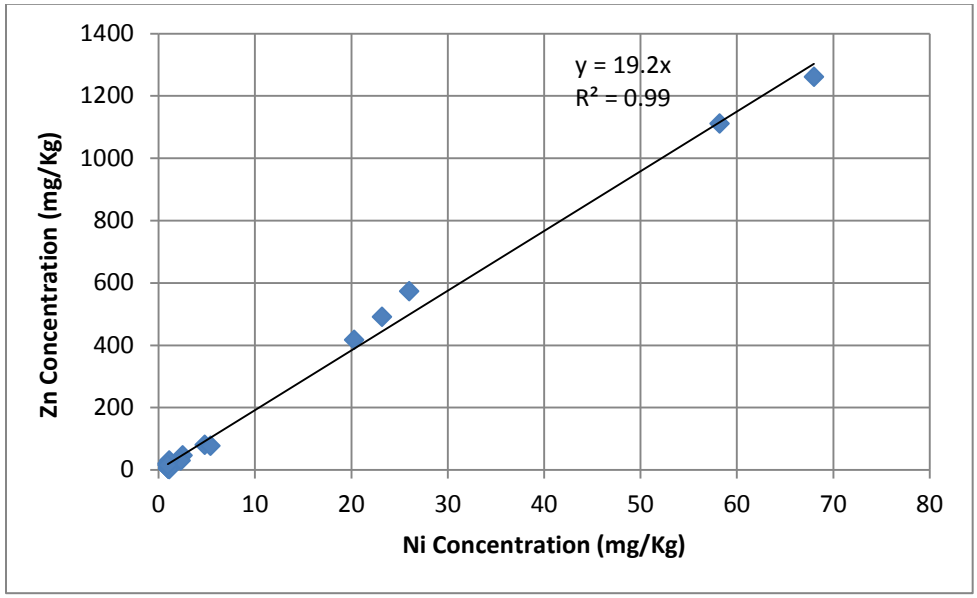

Figure 4-36 Scatterplot of Ni vs Zn soil concentrations (Pearson coefficient = 0.998, p = <0.0001)

Phosphorous concentrations had negative correlations with the metals included in the study. CEC and organic matter content showed strong correlations (Pearson's coefficients > 0.7) with potassium, calcium, magnesium, nitrogen, carbon and the metal concentrations (Figure 4-32). This depicts the increase in metal retention to soils with increases in organic matter content and

CEC, as expected. Similar results of metal retention associations with organic matter and CEC were also reported by other researchers (Deschne et al 2004, Winiarski et al 2006). Metallic pollution, organic matter content, and CEC are all inter-dependent. Figures 4-33 through 4-37 show the scatterplots for some of the weaker (Figure 4-34) and stronger correlations (Figure 4-35 through 4-37) based on the Pearson correlation analyses. Scatterplots for all the soil parameters are included in Appendix XX.

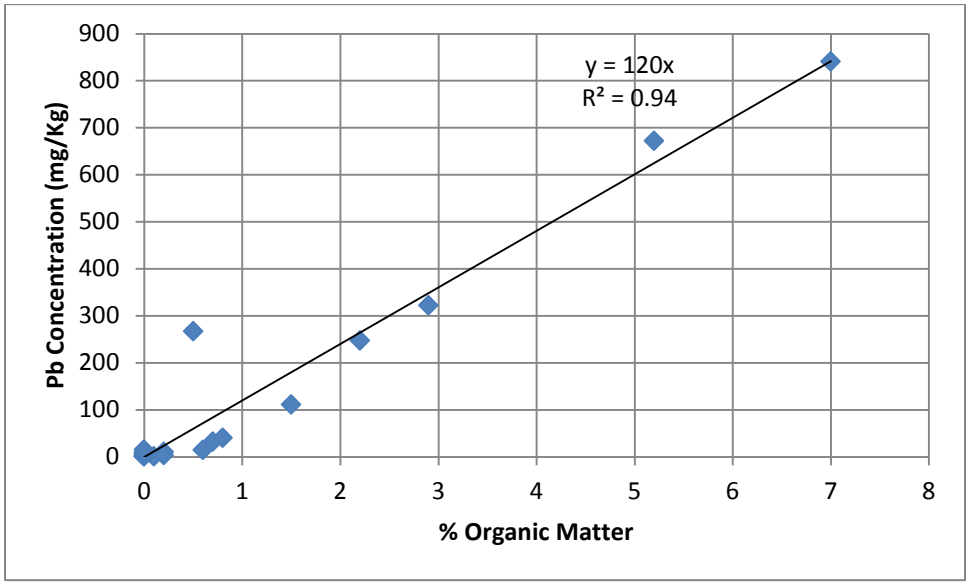

Figure 4-37 Scatterplot of % Organic matter vs soil lead concentration (Pearson coefficient = 0.97, p = <0.0001)

Table 4-5 Pearson correlation matrix for all the parameters included in the study

Variables	Soil pH	P (mg/kg)	K (mg/kg)	Ca (mg/kg)	% Org Matter	% Nitrogen	% Carbon	Acidity (meq/100g)	CEC (meq/100g)	S (mg/kg)	Mg (mg/kg)	Al (mg/kg)	As (mg/kg)	Cd (mg/kg)	Cu (mg/kg)	Fe (mg/kg)	Pb (mg/kg)	Mn (mg/kg)	Ni (mg/kg)	Zn (mg/kg)
Soil pH	1	-0.17	0.08	0.23	0.16	0.19	0.22	-0.93	0.06	-0.51	0.14	-0.03	0.17	0.23	0.24	0.15	0.24	0.16	0.22	0.24
P (mg/kg)	-0.17	1	0.39	0.10	0.05	0.11	0.21	-0.01	0.26	-0.08	0.02	-0.02	0.08	-0.05	-0.10	0.12	-0.01	-0.04	-0.04	-0.03
K (mg/kg)	0.08	0.39	1	0.82	0.77	0.80	0.84	-0.23	0.88	0.36	0.84	0.74	0.79	0.75	0.75	0.83	0.76	0.77	0.75	0.78
Ca (mg/kg)	0.23	0.10	0.82	1	0.90	0.91	0.90	-0.34	0.88	0.21	0.96	0.91	0.94	0.94	0.95	0.95	0.94	0.95	0.94	0.95
% Org Matter	0.16	0.05	0.77	0.90	1	0.98	0.97	-0.28	0.78	0.25	0.89	0.92	0.96	0.95	0.92	0.95	0.97	0.93	0.96	0.95
% Nitrogen	0.19	0.11	0.80	0.91	0.98	1	0.98	-0.32	0.78	0.20	0.88	0.89	0.98	0.96	0.92	0.97	0.97	0.93	0.96	0.96
% Carbon	0.22	0.21	0.84	0.90	0.97	0.98	1	-0.35	0.82	0.21	0.86	0.87	0.95	0.92	0.88	0.96	0.94	0.90	0.93	0.93
Acidity (meq/100g)	-0.93	-0.01	-0.23	-0.34	-0.28	-0.32	-0.35	1	-0.17	0.43	-0.27	-0.08	-0.32	-0.35	-0.36	-0.29	-0.36	-0.28	-0.34	-0.36
CEC (meq/100g)	0.06	0.26	0.88	0.88	0.78	0.78	0.82	-0.17	1	0.36	0.86	0.84	0.79	0.76	0.80	0.84	0.80	0.81	0.79	0.81
S (mg/kg)	-0.51	-0.08	0.36	0.21	0.25	0.20	0.21	0.43	0.36	1	0.36	0.42	0.21	0.17	0.20	0.27	0.18	0.30	0.20	0.21
Mg (mg/kg)	0.14	0.02	0.84	0.96	0.89	0.88	0.86	-0.27	0.86	0.36	1	0.90	0.92	0.92	0.95	0.93	0.92	0.97	0.93	0.94
Al (mg/kg)	-0.03	-0.02	0.74	0.91	0.92	0.89	0.87	-0.08	0.84	0.42	0.90	1	0.92	0.91	0.92	0.92	0.93	0.94	0.93	0.93
As (mg/kg)	0.17	0.08	0.79	0.94	0.96	0.98	0.95	-0.32	0.79	0.21	0.92	0.92	1	0.99	0.96	0.99	0.99	0.96	0.99	0.99
Cd (mg/kg)	0.23	-0.05	0.75	0.94	0.95	0.96	0.92	-0.35	0.76	0.17	0.92	0.91	0.99	1	0.99	0.97	0.99	0.97	1.00	0.99
Cu (mg/kg)	0.24	-0.10	0.75	0.95	0.92	0.92	0.88	-0.36	0.80	0.20	0.95	0.92	0.96	0.99	1	0.95	0.98	0.97	0.99	0.99
Fe (mg/kg)	0.15	0.12	0.83	0.95	0.95	0.97	0.96	-0.29	0.84	0.27	0.93	0.92	0.99	0.97	0.95	1	0.98	0.97	0.98	0.98
Pb (mg/kg)	0.24	-0.01	0.76	0.94	0.97	0.97	0.94	-0.36	0.80	0.18	0.92	0.93	0.99	0.99	0.98	0.98	1	0.96	1.00	1.00
Mn (mg/kg)	0.16	-0.04	0.77	0.95	0.93	0.93	0.90	-0.28	0.81	0.30	0.97	0.94	0.96	0.97	0.97	0.97	0.96	1	0.97	0.97
Ni (mg/kg)	0.22	-0.04	0.75	0.94	0.96	0.96	0.93	-0.34	0.79	0.20	0.93	0.93	0.99	1.00	0.99	0.98	1.00	0.97	1	1.00
Zn (mg/kg)	0.24	-0.03	0.78	0.95	0.95	0.96	0.93	-0.36	0.81	0.21	0.94	0.93	0.99	0.99	0.99	0.98	1.00	0.97	1.00	1

Values in bold are correlation coefficients with a 95% CI ($p<0.05$)

4.3.7 Cluster Analyses of Soil Contaminant Data

Cluster analysis is a statistical technique used to organize large sets of data into meaningful groups or clusters (Johnson et al 2007). Cluster analyses identifies significant inter-relationship between variables, maximizing the similarity of variables within each cluster. Cluster analyses divide the objects into groups based on similarity distances. Cluster analyses consider each variable as a separate cluster, and then combines the clusters sequentially, reducing the number of clusters based on distances or dissimilarities. The output of the Cluster analyses is presented graphically using a hierarchical tree-like diagram called a dendogram representing the similarity distances at which the clusters are joined. Cluster analyses were performed to examine associations between different soil parameters included in the study.

The cluster analyses in this study included soil parameters, phosphorous, potassium, calcium, sulfur, nitrogen, carbon and heavy metal concentrations in soil. The resulting dendogram is shown in Figure 4-38. The analyses resulted in three different clusters. All the metal concentrations were closely identified as a single cluster. Nickel was closely associated with cadmium, zinc and lead. Acidity and sulfur were identified as different clusters. Phosphorous was identified as a separate cluster. Potassium was closely associated with CEC. Concentrations for all the metals were strongly associated with organic matter content and CEC (similarity > 0.80). These analyses also showed close correlations of metal concentrations with organic matter content and CEC, as did the Pearson correlations, supporting the weight of evidence of the importance of CEC and organic matter on metal retention in the soil.

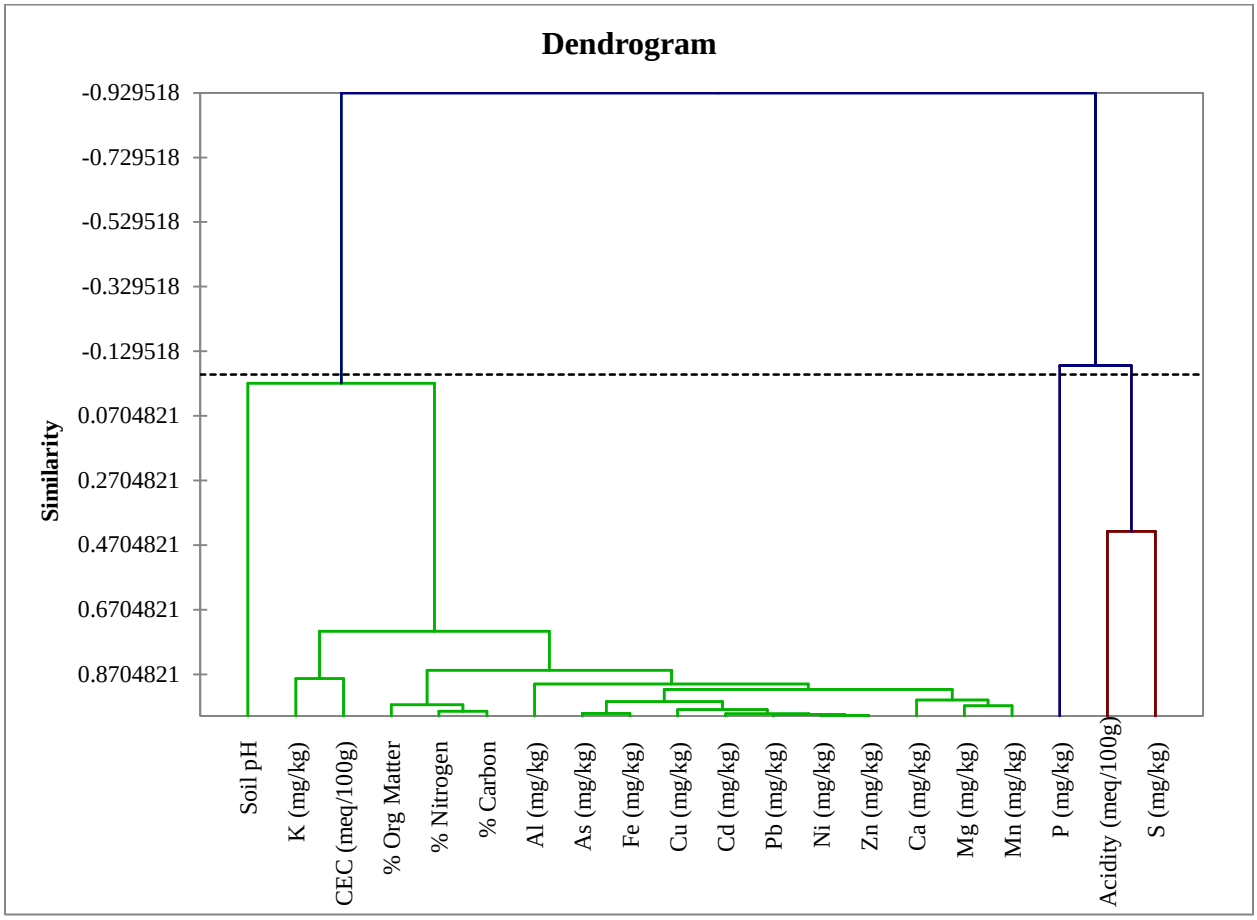

Figure 4-38 Dendogram for Cluster analysis for soil parameters and pollutants

4.3.8 Principal Component Analyses of Soil Contaminant Data

Principal Component Analysis (PCA) is a statistical tool that reduces a large set of data variables into smaller sets explaining the variance-covariance structure of the variables through

linear combinations (Johnson et al 2007). Principal components are derived from the original data sets which retain most of the variance in the data. The maximum fraction of the variance is contained in the first component with successive components accounting for the remaining (and lesser fractions) of the variance. The variance of the data is expressed in terms of eigen vectors and eigenvalues which exist in pairs. Eigen vectors represent the direction of the variance and eigenvalues represent how much variance is exhibited in that direction. Principal component analyses were used to identify groupings of parameters with similarities, specifically in how they explained the variability in the data. PCA was conducted on all the soil parameters and pollutant concentrations included in the study. Table 6 presents the variability explained by the first four principal components (explaining about 96% of the total variability) and the loadings of all the first ten principal components are shown in Table 4-7.

Table 4-6 Percentage of total variance explained by first four principal components

	F1	F2	F3	F4
Eigenvalue	14.1	2.4	1.9	0.7
Variability (%)	70.6	11.8	9.7	3.5
Cumulative %	70.6	82.4	92.1	95.6

Table 4-7 Loadings of first ten principal components

	F1	F2	F3	F4	F5	F6	F7	F8	F9	F10
Soil pH	0.199	-0.932	-0.021	0.265	-0.016	0.092	-0.005	0.068	-0.052	0.064
P (mg/kg)	0.062	0.144	0.970	-0.103	-0.060	-0.090	-0.108	0.003	-0.001	0.017
K (mg/kg)	0.838	0.152	0.380	0.249	0.043	0.000	0.246	-0.028	0.040	0.051
Ca (mg/kg)	0.968	-0.028	0.052	0.028	0.171	-0.037	-0.070	0.108	-0.004	0.059
% Org Matter	0.966	0.018	-0.028	-0.104	-0.167	0.088	0.010	0.069	0.107	-0.020
% Nitrogen	0.970	-0.021	0.045	-0.126	-0.161	0.066	0.059	0.048	-0.011	-0.029
% Carbon	0.957	-0.026	0.158	-0.050	-0.183	0.127	0.031	0.037	-0.043	-0.040
Acidity (meq/100g)	-0.329	0.876	-0.129	-0.259	0.113	0.091	0.083	0.069	-0.059	0.052
CEC	0.861	0.178	0.236	0.208	0.272	0.211	-0.056	-0.050	-0.021	-0.064

(meq/100g)										
S (mg/kg)	0.262	0.752	-0.187	0.518	-0.235	-0.037	-0.073	-0.010	-0.019	0.016
Mg (mg/kg)	0.956	0.080	-0.041	0.138	0.143	-0.159	0.045	0.082	0.035	-0.053
Al (mg/kg)	0.939	0.235	-0.124	-0.040	0.040	0.083	-0.155	0.000	0.067	0.059
As (mg/kg)	0.986	-0.011	-0.001	-0.115	-0.066	-0.059	-0.005	-0.038	-0.039	0.022
Cd (mg/kg)	0.980	-0.074	-0.120	-0.115	-0.010	-0.054	0.033	-0.040	-0.001	0.028
Cu (mg/kg)	0.975	-0.069	-0.155	-0.013	0.105	-0.070	-0.001	-0.060	0.012	-0.008
Fe (mg/kg)	0.990	0.038	0.039	-0.047	-0.046	-0.033	-0.009	-0.026	-0.104	-0.003
Pb (mg/kg)	0.988	-0.066	-0.079	-0.090	-0.023	0.028	-0.024	-0.052	0.024	0.011
Mn (mg/kg)	0.976	0.035	-0.121	-0.002	0.035	-0.104	-0.028	0.084	-0.042	-0.046
Ni (mg/kg)	0.986	-0.053	-0.113	-0.085	-0.016	-0.013	-0.010	-0.051	0.000	0.029
Zn (mg/kg)	0.989	-0.059	-0.094	-0.047	0.011	-0.016	0.013	-0.073	-0.015	0.002

* High-lighted loadings are the largest values for each constituent indicating their most important principle component

Most (about 75%) of the variance in the data is contained in the first principal component. The principal loadings in the first four principal components account for about 96% of the variance in the data. Organic matter content, CEC, potassium, calcium, nitrogen, carbon and the heavy metals have high loadings in the first principal component and explain most of the variance in the data sets. pH, acidity, and sulfur have their highest loadings in the second component, while phosphorous has its highest loading in the third component (Table 4-7).

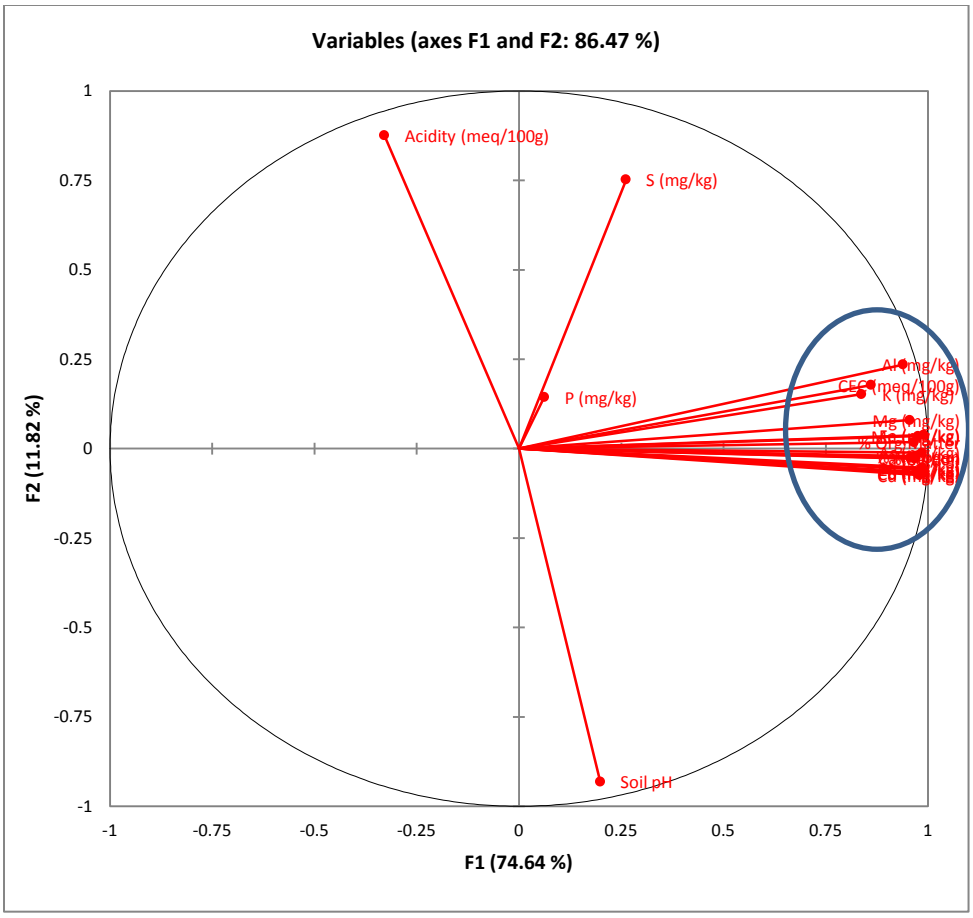

Figure 4-39 Principal component loadings for all the parameters in first two principal components

In the loading plot (Figure 4-39), Axis F1 represents 75% of the total variance, with strong contributions from heavy metals, potassium, calcium, magnesium, nitrogen, carbon, CEC, and organic matter content. The loadings of these parameters are situated close to each other indicating high correlations between these variables, in agreement with other researchers who have found strong associations of metal concentrations with CEC and organic matter content (Deschne et al 2004, Winiarski et al 2006).

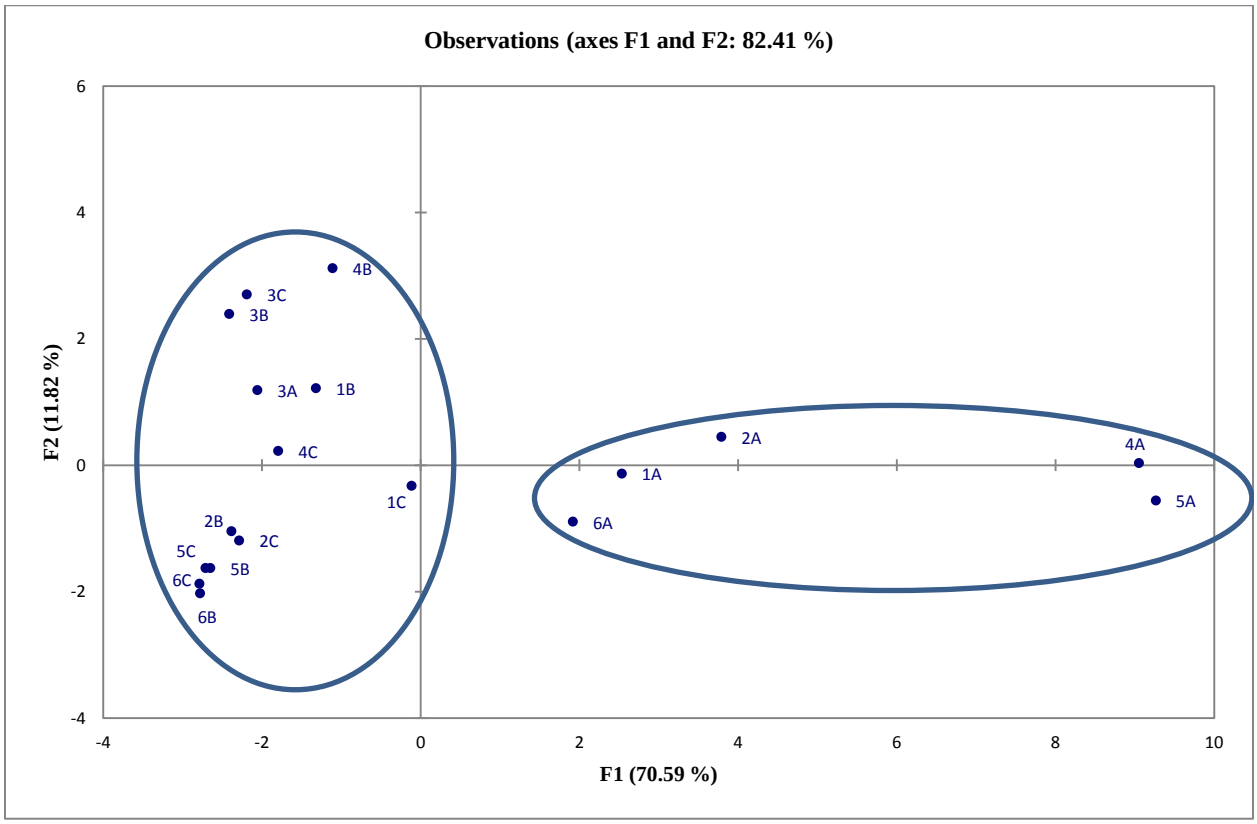

Figure 4-40 Observations plot for principal component analysis of soil samples

Figure 4-40 represents soil samples according to different depths. The level A samples (surface soil samples) are spread out on the F1 axis, mostly influenced by high pollutant concentrations (with the exception of site 3A located on the pond side slopes and having much lower metal concentrations in the surface soils compared to the other locations more affected by the stormwater flows). All the other samples form a different group indicating lower pollution concentrations of groups B and C in comparison to group A. Based on the PCA, organic matter content, CEC, potassium, calcium, and heavy metals were identified as a similar group.

4.3.9 Variability in Soil Contaminant Concentrations

A Two-Way ANOVA was conducted to test the variability in pollutant concentrations within the pond at different locations, depths, and their interaction. The results of Two-Way ANOVA are summarized in Table 8, with the significant relationships ($p \leq 0.05$) high-lighted.

Table 4-8 Two-Way ANOVA p values for pollutant concentrations

Constituent	P Value		
	Location	Depth	Location*Depth
Phosphorous	0.008	0.14	>>0.05
Potassium	0.050	0.001	>>0.05
Calcium	0.47	0.009	>>0.05
Aluminum	0.43	0.021	>>0.05
Arsenic	0.51	0.003	>>0.05
Cadmium	0.46	0.006	>>0.05
Copper	0.46	0.004	>>0.05
Iron	0.77	0.13	>>0.05
Lead	0.46	0.006	>>0.05
Manganese	0.16	0.002	>>0.05
Nickel	0.42	0.006	>>0.05
Zinc	0.42	0.003	>>0.05
Sulfur	0.58	0.093	>>0.05
Magnesium	0.02	0.74	>>0.05

This analysis showed that potassium, calcium, and all the metal concentrations, except iron, were found to be affected by depth (low P values), while phosphorous, magnesium and potassium concentrations were affected by location. Iron and sulfur concentrations were not affected by either location or depth. No interactions of location and depth were observed for all the pollutants included in the study.

4.3.10 Migration of Pollutants in Vadose Zone under Infiltrating Dry Pond

The SESOIL model was used to predict the migration potential of the filtered constituents in the vadose zone underneath the dry pond. The different soil parameters included in the modeling are listed in Table 4-9.

Table 4-9 Summary of soil parameters used in SESOIL model

Parameter	Value
pH	7
% Organic matter	3
Intrinsic permeability	10^{-8} cm^2
Bulk density	1.7 g/cm^3

The results of the simulations are shown in Figures 4-41 through 4-45. These figures represent the mass fate and contaminant plots of the pollutants simulated in the study. Mass fate plots display the distribution of the contaminant and the total mass distributed into the soil and leachate phases in the SESOIL column over time. The leachate concentration expressed as groundwater total (GND WTR TOTAL) depicts the concentration of pollutant leaving the bottom of the soil column. Contaminant depth plots indicate the depth (in cm) to which pollutants migrate during the simulation period. It also presents the initial and final depths of the pollutant migration.

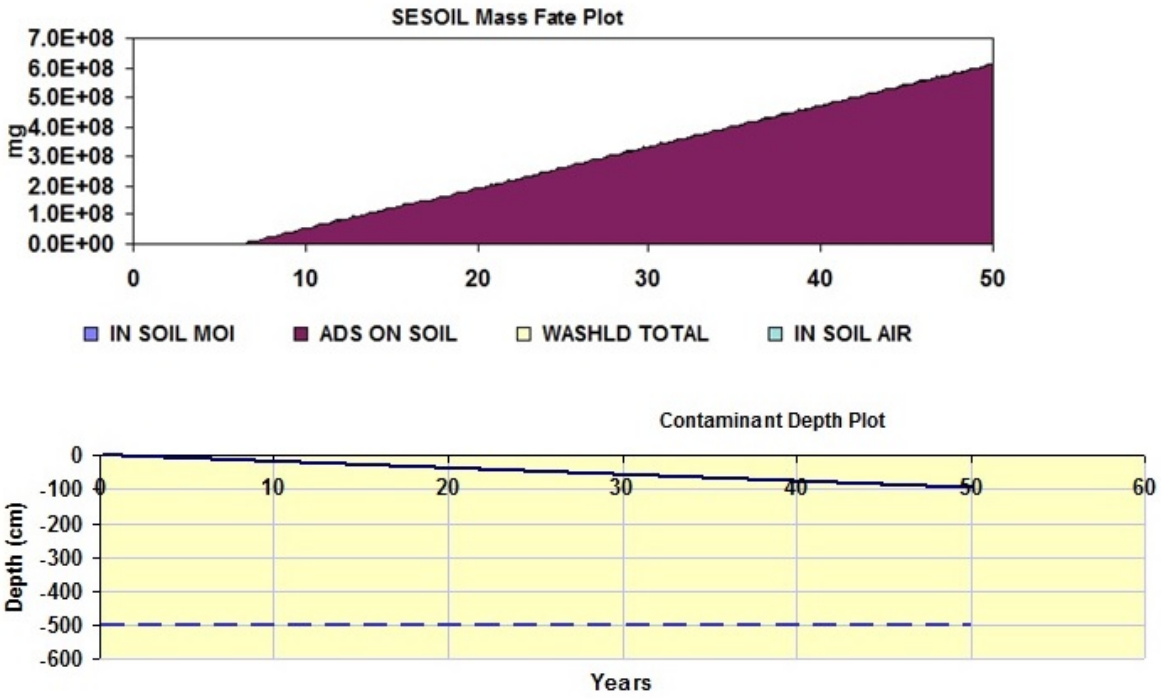

Figure 4-41 Mass fate and contaminant depth plots for Copper

The mass fate plots indicate high retention of the filtered metals to the soil as the water percolates vertically through the soil column. The maximum migration depths of the metals for a simulation period of 50 years were as follows: 96 cm for copper, 72 cm for iron, 110 cm for manganese, and 134 cm for zinc. These results indicate slightly higher migration potential for zinc compared to other three metals included in the study. Nitrate, as noted in the literature, is highly soluble and has high mobility (Pitt et al 1999). The model analyses indicate that nitrate can reach the maximum simulated depth of 5 m within about 3 years, with a much greater potential of reaching the groundwater compared to the metals.

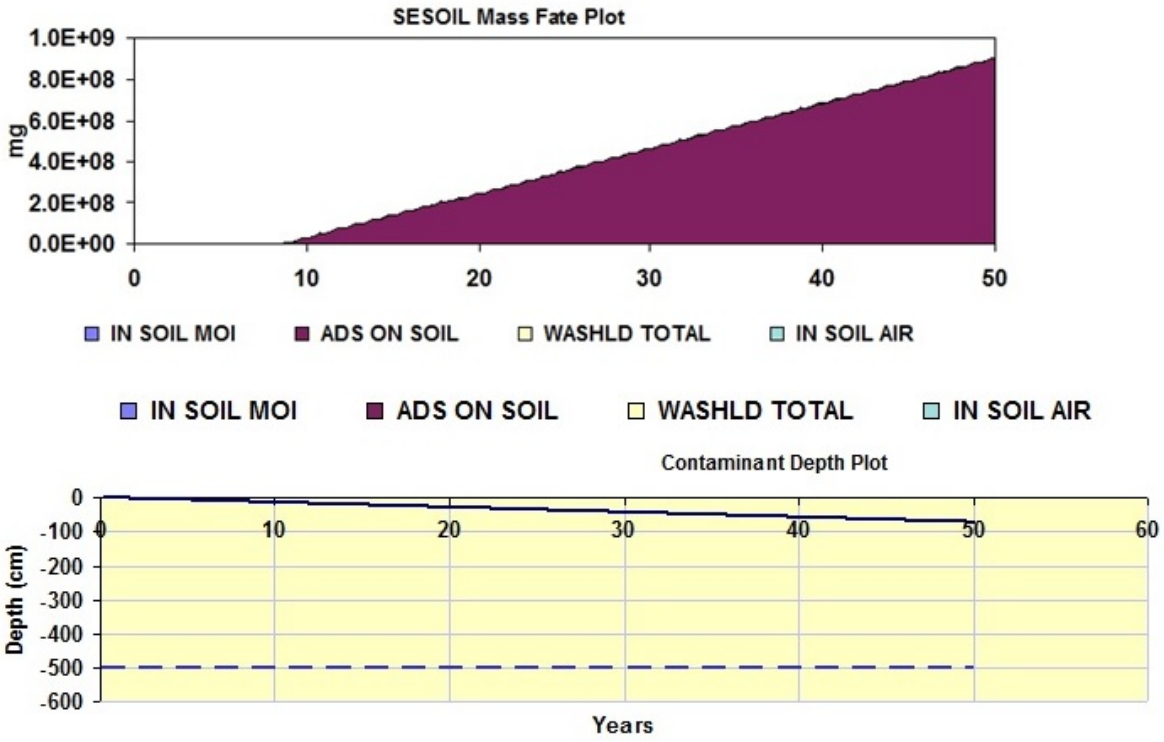

Figure 4-42 Mass fate and contaminant depth plots for Iron

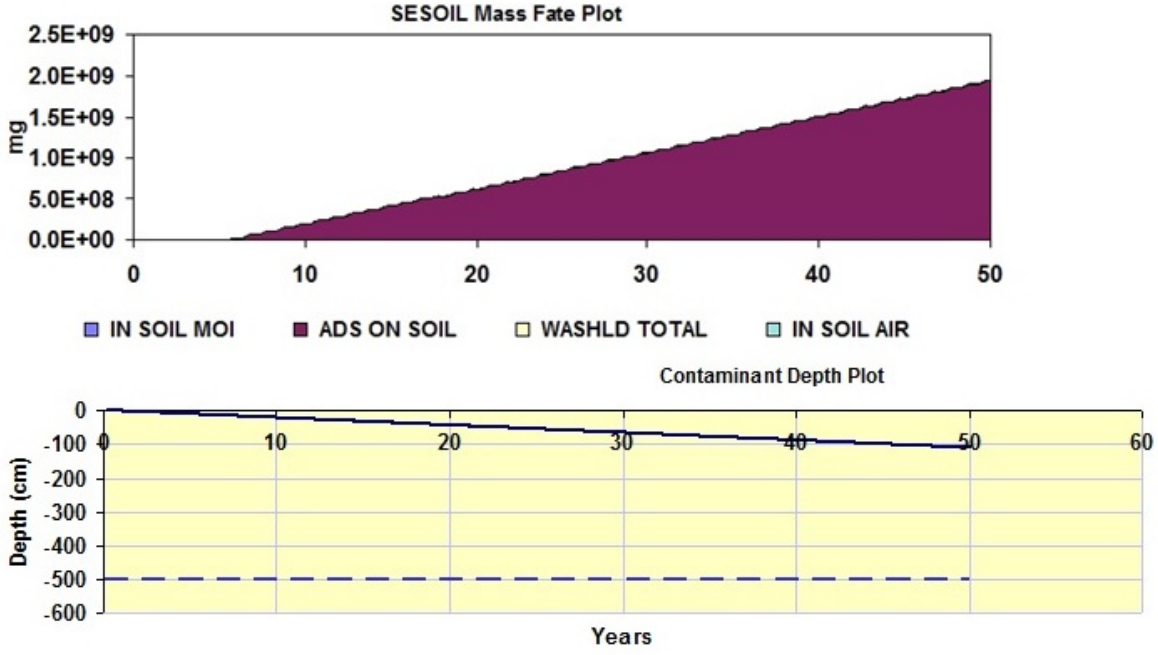

Figure 4-43 Mass fate and contaminant depth plots for Manganese

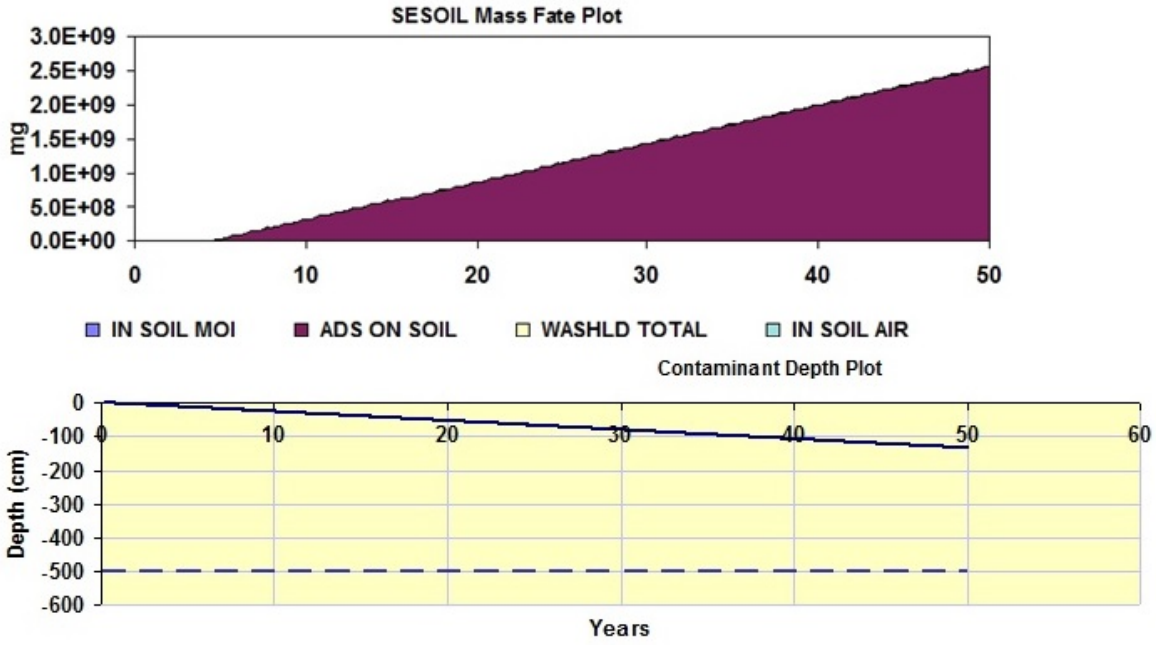

Figure 4-44 Mass fate and contaminant depth plots for Zinc

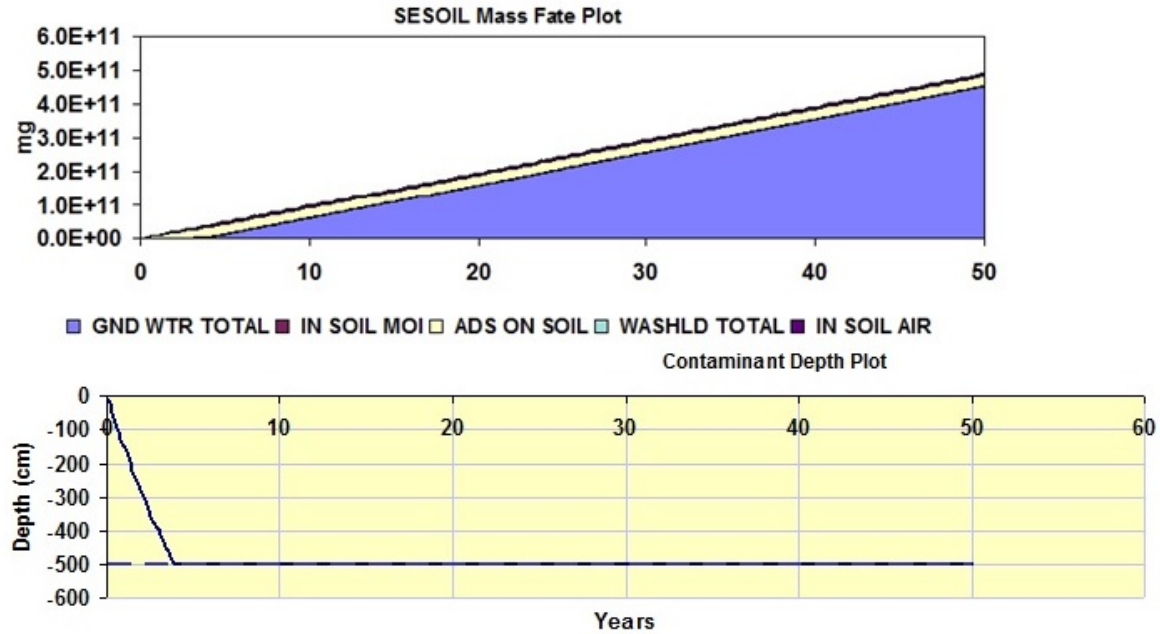

Figure 4-45 Mass fate and contaminant depth plots for Nitrate

The results observed from the SESOIL modeling of the filtered constituents support the observed retention of the metals to the soils. The migration depths of metals stayed under 150 cm for a simulation period of 50 years which is well above the water table for the selected study site, indicating the additional retention of soluble metals in the surface soil profile, in addition to the filtered capture of particulate-bound metals in the surface soils. The mobility for the metals, while low, was ranked as follows: Zn > Mn > Cu > Fe. This mobility ranking of the metals is similar to the mobility classes described in the literature (Pitt et al 1999), with zinc being the most mobile and Fe being the least mobile of the four metals examined.

Further analyses were conducted to evaluate site conditions that may affect subsurface pollutant migration, especially associated with a drainage area directing runoff into an infiltration area resulting in much more water in the infiltration area than the direct rainfall.

4.3.11 Variations in pollutant migration with different site conditions

To assess the variations of pollutant migrations with different site conditions, the SESOIL simulations were conducted for sites having different rainfall, intrinsic permeability, and organic matter content. Values for high and low factors of these components were selected from different locations in the Unites States.

4.3.12 Full Factorial Analyses

Full factorial analyses were performed for zinc (most mobile among the four metals modeled as a worst case example) to examine the effects of rainfall, intrinsic permeability, organic matter content, and their interactions on migration depth. Nitrate was not examined as it was previously shown to be highly mobile with minimal decreases in migration depth timing for most site conditions (will "always" be a concern if the nitrate concentrations are high in the infiltrating water, as shown by Pitt, et al. 1999). A full factorial analysis (Box, et al 1978) was used to understand the effect of the independent site variables on a dependent variable (migration depth). The factorial design identifies the effects of individual variables and their interaction on the dependent variable of interest (migration depth). The effects of different variables are calculated using a table of contrasts, with the averages of the differences between the sums of the migration depth (or any dependent variable of interest) when the factor is at its maximum value and at its minimum value. Probability plots of the calculated effects for the individual factors high-lighting unusual factors (abnormal factors affecting the results). High and low values for rainfall and soil parameters were selected from the NRCS database included in SESOIL and are shown in Table 10.The significant factors were identified by probability distributions of the results by observing which were not associated with the normal distribution for calculated values. Factorial analyses were performed using the statistical software package Minitab (Version 17).

Analyses used a full 2^4 factorial design on zinc migration depth to examine the effects of concentration, rainfall, intrinsic permeability, organic matter content, and their interactions. The high and low values for zinc were selected from the NSQD data base (International BMP

Database at BMPdatabase.org) for residential and industrial land uses. High and low values for rainfall and soil parameters are selected from NRCS database included in SESOIL.

Table 4-10 High and low factors for 2^4 factorial analyses

Factor	High (+)	Low (-)
Zinc concentration (μg/L) (A)	500	50
Rainfall (cm/yr) (B)	154 (West Palm Beach, FL)	19.9 (Phoenix, AZ)
Intrinsic permeability (cm^2) (C)	1.00E-07	1.00E-10
% Organic matter (D)	3	0.5

The effects of concentration, rainfall and intrinsic permeability on migration depth were analyzed and the results are shown in Appendix XX. Probability factors of the effects of the factors on zinc migration depth and shown in Figure 4-46. It is observed that concentration, rainfall, and intrinsic permeability, and their interactions are showing significant effects on zinc migration in vadose zone, again with no significant effect associated with organic matter.

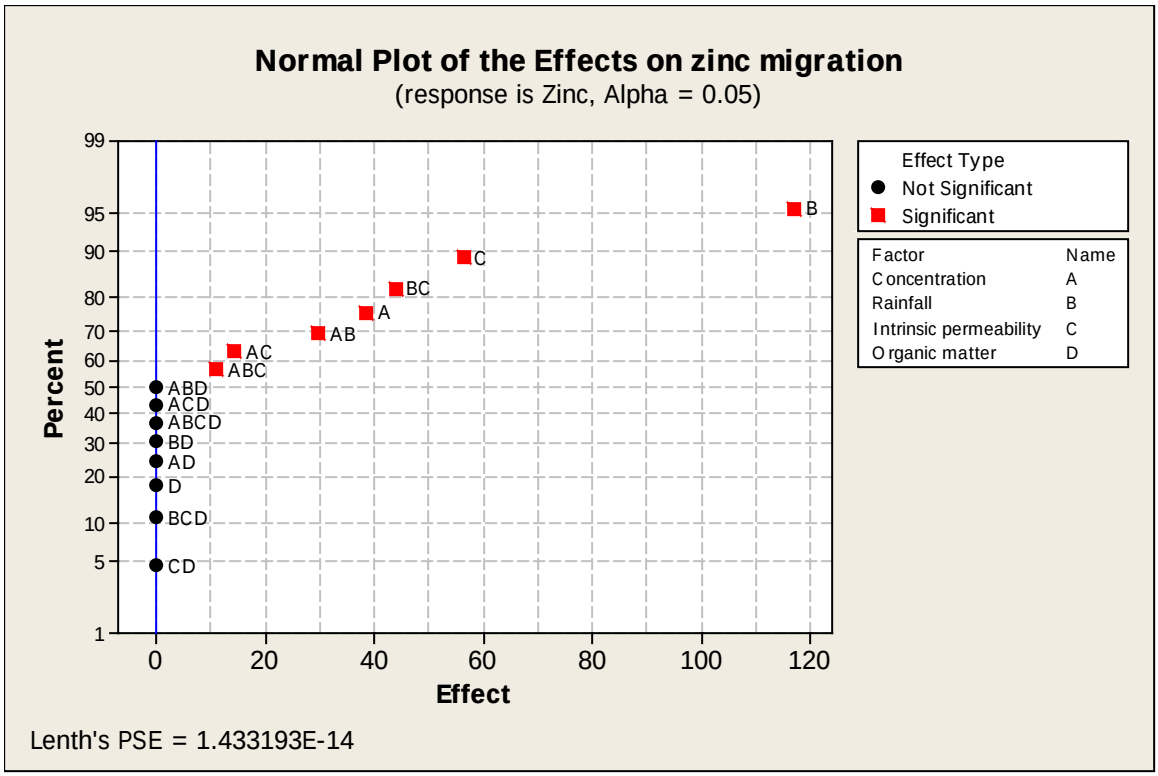

Figure 4-46 Normal plots of the effects of zinc concentration, rainfall, intrinsic permeability, and organic matter on zinc migration

4.3.13 Response surface plots

The results of the factorial analyses indicated that rainfall, concentration, and intrinsic permeability are the significant factors that affect the migration depth of zinc. Significant interactions terms are, rainfall and concentration, concentration and intrinsic permeability, rainfall and intrinsic permeability, and rainfall, concentration and intrinsic permeability. Rainfall had the greatest effect followed by intrinsic permeability, interaction of rainfall and intrinsic permeability and concentration. 3D response surface plots were therefore produced to follow-up the factorial analyses for multiple levels of these factors to enable more accurate evaluations of

other site conditions. Response surface plots are an advanced design of experiment technique that help in optimization and better understanding of response (Minitab).

Table 4-11 factors with high and low ranges for response surface analyses

Factor	Range of values (low to high)				
Rainfall (location)	19.6 (Phoenix, AZ)	47.2 (Boulder, CO)	87.5 (Toledo, OH)	116.9 (Chapel Hill, NC)	154.3 (West Palm Beach, FL)
Intrinsic permeability (soil type)	1.00E-11 (Silty clay)	1.00E-10 (medium fine clay)	1.00E-09 (Sandy loam)	1.00E-08 (Sand)	1.00E-07 (Loamy sand)

Five sets of rainfall conditions and intrinsic permeabilities were considered for this analyses as listed in Table 4-11, resulting in 25 combinations of rain and permeability. Analyses were conducted for the low zinc concentration (50 µg/L) and for the high zinc concentration (500 µg/L). Figures 4-47 and 4-48 are the resulting response surface plots for these two concentrations showing the combined effects of rainfall and intrinsic permeability on the maximum migration depth after 50 years of infiltration operation.

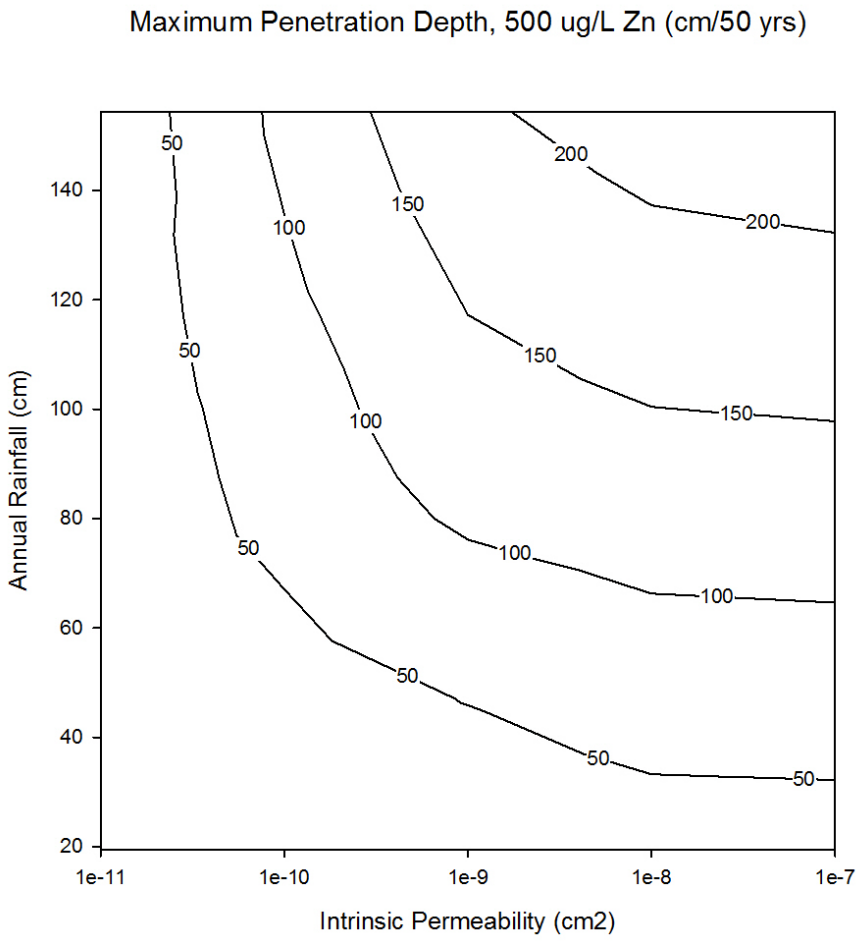

Figure 4-47 Response surface plot for rainfall and intrinsic permeability vs. migration depth (50 years) for high zinc concentration (500 µg/L)

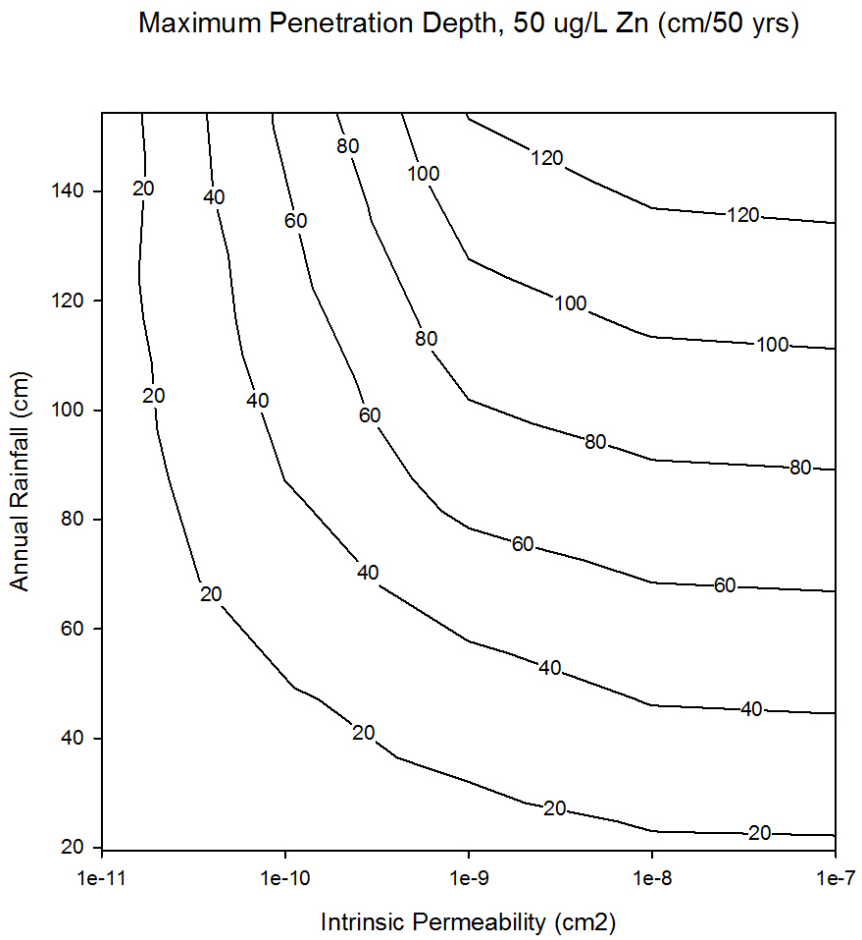

Figure 4-48 Response surface plot for rainfall and intrinsic permeability vs. migration depth (50 years) for low zinc concentration (50 µg/L)

It is clear that the amount of rain (or added runoff) greatly affects the migration depth. At the heavy industrial site, 15 acres of the site drain into the 0.75 acre pond. Site runoff responses during the monitored rains indicates an Rv of about 0.65 for the site (about 65% of the rain occurs as runoff). Therefore, the amount of runoff to the infiltration pond is about 13 times more than the direct rainfall considered during the SESOIL analysis, resulting in a much great maximum migration depth of the zinc. Instead of about 130 cm maximum migration depth, the

actual migration depth would be several times this depth (doubling the rain depth results in somewhat less than doubling the migration depth for the same permeability and concentration).

4.4 Conclusions

Soil contamination and groundwater contamination potential of heavy metals was examined at a dry infiltration pond treatment system at a heavy industrial site in the southeastern US. The results indicated a high retention capacity of both particulate-bound and filtered metals in the surface soils in the pond. The concentrations of pollutants in the soil dramatically decreased with depth indicating high retention of heavy metals in the surface soil.. In addition to the physical filtering of particulate-bound metals near the surface, , CEC, and organic matter were shown to be significant factors in retention of soluble pollutants to the surface layers of the soil. Concentration variations of pollutants in the pond indicated increased surface concentrations in areas along the main flow pathway and where the water pooled (the pond seldom flooded to large depths). Vadose zone chemical fate modeling showed retention of metals to the soils at depths (maximum of about 100 cm after 50 years of pond operation) well above the water table indicating minimal groundwater contamination potential from metals over the 50 year simulation period. This depth may increase by about ten times when the additional site runoff directed to the pond is considered. However, nitrates could reach the watertable in a short period of time. The current site conditions closely represent the worst case conditions for the pollutant concentrations originating from the study site Rainfall, intrinsic permeability, concentration and their interactions were found to be significant factors for mobility of zinc in vadose zone.

References

Barraud, S., Gautier, A., Bardin, J. P., & Riou, V. (1999). The impact of intentional stormwater infiltration on soil and groundwater. *Water Science and Technology*, *39*(2), 185-192.

Dechesne, Magali, Sylvie Barraud, and Jean-Pascal Bardin. "Spatial distribution of pollution in an urban stormwater infiltration basin." *Journal of contaminant Hydrology* 72.1 (2004): 189-205.

Eagleson, P. A (1978). Climate, Soil, and vegetation. Water Resources Research 14(5): 705-776.

Evans, L. J. (1989). Chemistry of metal retention by soils. *Environmental Science & Technology*, *23*(9), 1046-1056.

Fischer, D., Charles, E. G., & Baehr, A. L. (2003). Effects of stormwater infiltration on quality of groundwater beneath retention and detention basins.*Journal of Environmental Engineering*, *129*(5), 464-471.

Hossain, M. A., Furumai, H., & Nakajima, F. (2009). Competitive adsorption of heavy metals in soil underlying an infiltration facility installed in an urban area.*Water Science and Technology*, *59*(2), 303.

Jacques, D., Šimůnek, J., Mallants, D., & Van Genuchten, M. T. (2008). Modelling coupled water flow, solute transport and geochemical reactions affecting heavy metal migration in a podzol soil. *Geoderma*, *145*(3), 449-461.

Johnson, R. A., and Winchern, D. W. (2007). Applied Multivariate Statistical Analysis. 6th Edition. Prentice Hall, Upper Saddle River, NJ.

Lee, S. Z., Allen, H. E., Huang, C. P., Sparks, D. L., Sanders, P. F., & Peijnenburg, W. J. (1996). Predicting soil-water partition coefficients for cadmium. *Environmental science & technology*, *30*(12), 3418-3424.

Mikkelsen, P. S., Häfliger, M., Ochs, M., Tjell, J. C., Jacobsen, P., & Boller, M. (1996). Experimental assessment of soil and groundwater contamination from two old infiltration systems for road run-off in Switzerland. *Science of the total environment*, *189*, 341-347.

Mikula, J. B., Clark, S. E., & Baker, K. H. (2010, January). Modeling Zinc And Sodium Chloride Migration In Vadose Zone Soils Beneath Stormwater Infiltration Devices. In *Proceedings of the Annual International Conference on Soils, Sediments, Water and Energy* (Vol. 11, No. 1, p. 2).

Pitt, R., Field, R., Lalor, M., & Brown, M. (1995). Urban stormwater toxic pollutants: assessment, sources, and treatability. *Water Environment Research*, *67*(3), 260-275.

Pitt, R. E. and S. Clark. (1996). *Groundwater contamination from stormwater infiltration*. CRC Press.

Pitt, R., Clark, S., & Field, R. (1999). Groundwater contamination potential from stormwater infiltration practices. *Urban water*, *1*(3), 217-236.

Sansalone, J. J., Buchberger, S. G., & Al-Abed, S. R. (1996). Fractionation of heavy metals in pavement runoff. *Science of the Total Environment, 189*, 371-378.

Taylor, R. W., Hassan, K., Mehadi, A. A., & Shuford, J. W. (1995). Zinc sorption by some Alabama soils. *Communications in Soil Science & Plant Analysis*, *26*(7-8), 993-1008.

Tyler, L. D., & McBRIDE, M. B. (1982). Mobility and extractability of cadmium, copper, nickel, and zinc in organic and mineral soil columns. *Soil Science*,*134*(3), 198-205.Winiarski, T., Bedell, J. P., Delolme, C., & Perrodin, Y. (2006). The impact of stormwater on a soil profile in an infiltration basin. *Hydrogeology Journal*, *14*(7), 1244-1251.Yong, R. N., Mohamed, A. M. O., & Warkentin, B. P. (1992). *Principles of contaminant transport in soils*. Elsevier Science Publishers.

Zubair, A., Hussain, A., Farooq, M. A., & Abbasi, H. N. (2010). Impact of storm water on groundwater quality below retention/detention basins. *Environmental monitoring and assessment*, *162*(1-4), 427-437.

CHAPTER 5 CONCLUSIONS

As discussed in Chapter 1, limited information is available in the literature concerning the treatability characteristics of stormwater pollutants from heavy industrial sites. Stormwater discharges from industrial activities may contain a wide variety of pollutants that may need to be reduced before discharge. The most basic information needed relates to the filtered fraction of the pollutants and the association of the pollutants with different particle sizes. The main activities of this research was therefore to obtain this stormwater information for a heavy industrial site and demonstrate how this information affects its treatment.

5.1 Evaluation of Hypotheses

Dissertation Research Hypothesis 1: Pre-treatment hydrodynamic devices are effective in removing large particles but less effective for smaller particles

The effectiveness of a hydrodynamic separator device (HDD) was quantified for different particle sizes based on influent and effluent stormwater monitoring and detailed laboratory analyses. Exploratory data analyses included probability plots that were used to compare the distributions of influent and effluent pollutant concentrations and mass for the hydrodynamic device. The 95% confidence intervals of the influent and effluent concentrations overlapped for

particle sizes from 0.45μm to 12 μm. However, larger particle sizes (> 12 μm) indicated differences in concentrations and mass. Probability plots also indicated that the particulate concentrations and mass for HDD influent and effluent were not normally distributed in most cases, indicating the need for non-parametric statistical comparison tests.

Particle size distribution analyses indicated the average median particle size of the HDD influent samples were about 20 μm, while the effluent sample median particle sizes were about 12 μm, indicating preferential removal for larger particles. Line plots of influent and effluent concentrations for several particle size ranges further indicated significant removals of particulate concentrations for particle size concentrations greater than 12 μm. Results of non-parametric Wilcoxon signed rank tests indicated significant removals for concentrations and mass for SSC and for particle sizes greater than 12 μm. The removals of particulate concentrations and mass increased with increases in particle size with removals up to 75% for particle sizes greater than 250 μm.

At the end of the monitoring period, a full mass balance of sediment captured in the hydrodynamic device was performed. Sediment samples were collected and analyzed for particle size distribution. Median particle size of the sediment captured in the HDD was about 250 μm, with 90% of the sediment mass greater than 45 μm, and the maximum size observed about 5,000 μm. About 80% of the sediment mass captured in the HDD was greater than 100 μm, indicating retention of larger size particles.

Overall, testing of hypothesis 1 through particle size distribution and exploratory data analyses techniques such as probability plots and non-parametric comparison tests strongly

demonstrated the significant removals for SSC and larger particulates (> 12µm) by the hydrodynamic device. Therefore, hypothesis 1 can be accepted.

Dissertation Research Hypothesis 2: The dry infiltration pond is very effective in reducing the runoff volumes for monitored storm events, along with associated pollutant mass reductions, along with small to moderate pollutant concentration reductions.

The effectiveness of the dry infiltration pond was quantified by evaluating inflow and outflow pond hydrographs along with particle size distributions of particulates from monitored influent and effluent locations of the dry pond. The hydrographs indicated high runoff reductions (75 to 100%) for storm events less than 1.5 inches, and moderate reductions (about 50%) for events greater than 1.5 inches.

The dry infiltration pond was found to have very good to excellent removals for particulate solids concentrations and mass, medium to high removals for heavy metal concentrations (>45%) and high removals for masses of the metals (>90%). Observed suspended sediment mass reductions were about 95% during the seventeen monitored events. Performance line plots showed significant removals of SSC for even small particle sizes (as small as 3 µm). Statistically significant removals (based on Wilcoxon signed ranked tests) were found for concentrations and masses for particle sizes greater than 3 µm, COD, and unfiltered heavy metals, while filtered heavy metals and some of the nutrients had too few detectable concentration results to indicate significant differences for the amount of available quantifiable data.

The sedimentation removal of particulate pollutants was also compared to the Surface Overflow Rate (SOR) method. The performance of both the HDD and the dry pond decreased

with increases in SOR (associated with increasing flowrates), as expected. The percentage removals of particulates for each event were calculated based on the observed sediment concentrations from the HDD influent, HDD effluent, and dry pond effluent and compared to the predicted removals (based on SOR). The average predicted removals for both the HDD and dry pond were within 10% of the observed removals. Non-parametric Wilcoxon signed rank tests indicated no significant differences between the observed and predicted removals.

Overall, testing of hypothesis 2 through runoff hydrographs, particle size distributions, and exploratory data analyses techniques, such as probability plots and non-parametric comparison tests, strongly demonstrated the significant and large reductions in runoff volume associated with infiltration in the dry infiltration pond, along with high pollutant mass removals and moderate pollutant reductions. Therefore, hypothesis 2 can be accepted.

5.2 Additional Conclusions from Research

Chapter 1 outlined the research hypotheses and experimental design for this research. Runoff samples were collected from a heavy industrial site in the southeastern Unites States (site specifics are client confidential). Rainfall, runoff volumes, and flow rates were continuously monitored using rain gages and area-velocity flow sensors. Runoff samples were collected from influent and effluent locations from a pre-treatment hydrodynamic separator device and a dry infiltration pond. Performance of treatment controls were evaluated using summary statistics and exploratory data analyses methods such as box and whisker plots and probability plots. Statistical tests such as probability plots, followed by Kruskal-Wallis and Wilcoxon sign ranked tests were

performed to identify the significant differences in pollutant concentrations and mass to evaluate the treatability of the runoff and performance of treatment processes. Cluster analyses and principal component analyses were also used to identify complex relationships between site conditions and runoff characteristics, and between the different monitored constituents.

Chapter 2 described the site characteristics, pollutants associated with the industrial activity, monitoring activities, and description of the laboratory analytical procedures used during this research. Influent sample analyses (site characterization) showed that suspended sediment concentrations (SSC), COD, nutrients, and heavy metals were commonly found in the runoff, some at potentially problematic levels. Iron and aluminum had the highest metal concentrations due to their high occurrence in natural soils and possible exposure to site materials. Zinc and copper were detected in unfiltered and filtered forms during all of the events monitored, again, likely due to exposure to site materials.

Correlations between different hydrological and pollutant constituents were studied. Pearson correlation analyses were conducted to determine the relationships between hydrologic and pollutant constituents. These analyses showed strong correlations between the different hydrologic parameters (rain intensity, runoff rates, etc.). Scatterplots illustrated possible linearity between parameters. Regression analyses were used to determine associations between variables, supplemented with ANOVA and residual analyses to ensure that regression analyses were valid.

No significant relationships were observed between different hydrologic parameters and pollutants constituents (no “first flush” effects or higher concentrations associated with longer interevent periods). Erosion of the compacted site soils was not found to be a significant factor in

the runoff characteristics. The supply of sediment on the site was variable and related to the changing site activities and material storage. The rainfall intensity, depth, and interevent period parameters were not significant in affecting the SSC in the runoff. The median particle sizes showed negative correlations with hydrologic and other water quality parameters. Strong correlations were observed between suspended sediment and heavy metal concentrations relating to high affinity of metals with particulates. COD, Total N and Total P did not indicate any significant relationships with other parameters or constituents.

Cluster analyses were conducted to identify more complex relationships between the parameters. These indicated close associations between the hydrologic parameters (such as rainfall and runoff depth). Nitrate concentrations were found to be correlated with bicarbonate and total alkalinity. Cluster analyses also confirmed close associations between SSC and the metal concentrations. All the metals were also strongly associated with each other indicating possible similar sources of all the metals (through exposure to site materials).

Principal component analyses (PCA) were conducted to identify complex groupings of parameters with similar characteristics (through reducing variance). The first four principal components accounted for about 80% of the total variance. Rain intensity, SSC, and metals had high loadings associated with the first principal component. The second principal component had high loadings associated with rain depth, runoff depth, inter-event time, and phosphate. Runoff depth and average rain intensity had high loadings associated with the third principal component, while COD and medina particle size had high loadings associated with the fourth principal component. The principal component analyses confirmed that the hydrological parameters were of a similar group, and that SSC and metal concentrations were also of a similar group.

Full 2^2 factorial analyses were conducted on median particle size, SSC, and metals to further examine the effects of rain depth, peak rain intensity, and their interactions, on these constituents. No significant effects were observed relating these factors or their interaction to these pollutant concentrations.

The median particle sizes for the SSC in the site runoff before treatment for all monitored events ranged from 7.5 to 45 μm, with an average median particle size of 21 μm. About 80% of the SSC was distributed in the particle size range of 3 to 120 μm. Cumulative pollutant concentrations associated with different particle sizes indicated that the majority of the pollutant concentrations and masses were associated with particle sizes between 10 and 100 μm. Particulate pollutant strengths of the stormwater particulates (such as mg pollutant/kg particulate solids) were calculated and analyzed. The particulate strengths increased with increases in particle size, in contrast to preferential adsorption to smaller particle sizes due to larger surface areas. The higher particulate strengths associated with larger particulates may be related to the nature of the runoff particulates that has large metal components from this specific industrial site. However, most of the mass of the pollutants were found to be associated with moderate particle sizes as the amount of the large particles was limited in the runoff.

Performance evaluations of the treatment controls were discussed in Chapter 3. As part of these analyses, the fate of the captured pollutants in the site stormwater controls, especially the dry infiltration pond, were further evaluated. Metal retention in the soils under the pond and the movement of the metals in the vadose zone under the dry infiltration pond are discussed in Chapter 4. Replicated infiltrometers tests were conducted at six locations in the dry pond to measure the variability of the infiltration potential of the soils lining the pond. Most of the

locations in the pond had very high infiltration capacities, with long-term saturated infiltration rates averaging about 17 in/hr (ranging from 0.5 to 39 in/hr). Soil samples were collected at different depths at six locations in the dry pond and were analyzed for pollutant concentrations in the pond soil profile. The chemical analyses indicated significant decreases in metal and nutrient concentrations between the surface soil and lower level samples. The surface soils had greater organic matter content and CEC concentrations than the deeper soils. Multivariate analyses (Pearson correlation analyses, cluster analyses, and principal component analyses) indicated strong associations of metal concentrations with CEC and organic matter content, as reported in the literature. Vadose zone water chemistry modeling examined the movement of filtered metals through the soils at depths. The results indicated maximum penetration depths of the heavy metals to be within a meter of the surface over 50 year simulation period, when considering the additional stormwater entering the pond. However, nitrates are expected to migrate through the soils at a much more rapid rate, potentially reaching the water table in a few years. The nitrate concentrations in the site stormwater however, are low, resulting is reduced contamination potential.

5.3 Further Research Needs

The current study was limited to seven months of monitoring due to available resources and time line of the project. Further investigations would benefit by increasing the duration of study allowing for variations of pollutant concentrations on a seasonal basis (wet and dry weather), and site activities.

Runoff originating from industrial activity contains many types of contaminants of concern, including floatables, metals, oil and grease, organic toxicants (such as PAHs), chemical oxygen demand, nutrients, and suspended sediment. Different treatment controls may be needed to effectively remove the different contaminant categories. Further research would benefit by evaluating additional treatment control technologies (such as media filtration techniques to treat filtered fractions of pollutants and nutrients). This site had a simple treatment train including screened inlets, a hydrodynamic separator, and a dry infiltration pond. A more complex system may be needed for a wider range of contaminants of concern, or if groundwater contamination potential was a greater concern.

This research illustrated the benefit of examining the treatability of solids, metals and nutrients. Further research of pollutant associations for various particle sizes should be conducted for other pollutant categories such as PCBs, dioxins, and hydrocarbons, for other industries having these contaminants to enable the effective design of treatment controls.